STUDIES OF THE INTERACTION OF GEMINI SURFACTANTS WITH POLYMERS AND TRIBLOCK COPOLYMERS

A Thesis Submitted to the College of Graduate Studies and Research

in Partial Fulfillment of the Requirements for the

Degree of Doctor of Philosophy

in the Department of Chemistry, University of Saskatchewan

Saskatoon, Saskatchewan, Canada

By Shawn D. Wettig

Fall 2000

PERMISSION TO USE

In presenting this thesis in partial fulfillment for the requirements for a Postgraduate degree from the University of Saskatchewan, I agree that the Libraries of this University may make it freely available for inspection. I further agree that permission for copying this thesis in any manner, in whole or in part, for scholarly purposes may be granted by the professor or professors who supervised my thesis work or, in their absence, by the Head of the Department or the Dean of the College in which my thesis work was done. It is understood that any copying or publication or use of this thesis or parts thereof for financial gain shall not be allowed without my written permission. It is also understood that due recognition shall be given to me and to the University of Saskatchewan in any scholarly use which may be made of any material in my thesis.

Requests for permission to copy or make any other use of material in this thesis in whole or in part should be addressed to:

Head of the Department of Chemistry

University of Saskatchewan

110 Science Place

Saskatoon, Saskatchewan

Canada S7N 5C9

ABSTRACT

A systematic study was carried out to investigate the aqueous solution behavior of two homologous series of N,N'-bis(alkyldimethyl)-α,ω-alkanediammonium dibromide surfactants, known as m-s-m gemini surfactants; one having a constant spacer s (=3) with m = 8, 10, 12, and 16 and the other having a constant alkyl chain length m (=12) with variable spacer length $2 \leq s \leq 16$, using specific conductance, surface tension, fluorescence, and densimetry techniques. A surfactant with m = 12 and a *p*-xylyl (ϕ) spacer also was studied to assess the effect of rigidity in the spacer group on gemini interfacial properties. The interaction of two members of these series of surfactants, namely the 12-3-12 and 12-6-12 homologues, with aqueous solutions of neutral polymers, specifically polyethylene oxide (PEO), polypropylene oxide (PPO), and polyethylene oxide-polypropylene oxide-polyethylene oxide (PEO-PPO-PEO) triblock copolymers, has been investigated using specific conductance, surface tension, NMR, fluorescence, densimetry and equilibrium dialysis techniques. Properties such as the critical micelle concentration (cmc), the surfactant head group area (a_0), the surfactant mean aggregation number (N_{agg}), the I_1/I_3 vibronic intensity ratio of pyrene, and the apparent molar volume were used to characterize the aqueous solution behavior of the gemini surfactants, and the nature of the interaction of these surfactant with neutral polymers in aqueous solution. It was found that the interaction of the gemini surfactants with the triblock copolymers in aqueous solution was markedly different from that typically observed in surfactant-polymer systems, and is similar in nature to a solubilization or mixed micelle formation process.

The results obtained for the critical micelle concentrations and head group areas for the binary surfactant-water systems are in reasonable agreement with those obtained in previous investigations. The mean aggregation number of the surfactants decreases with increasing spacer chain length up to s = 8, after which the aggregation number increases. The decrease results from a decrease in the surface area available to a surfactant monomer as the area taken up by the spacer group is increased. Geometric considerations require that in order to maintain a spherical aggregate the aggregation number must decrease. The observed increase in the aggregation number corresponds to a transition from micelles to vesicles as the spacer group becomes incorporated into the core of the surfactant aggregate.

Experimental apparent molar volume data have been modeled assuming both a mass-action model (8-3-8, only) and a pseudo-phase model. Predicted values for the apparent molar volume of the surfactant at the cmc ($V_{\phi,cmc}$) obtained from the pseudo-phase model have been compared to infinite dilution volumes (V^0) calculated from two additivity methods, one based on the contribution of the corresponding mono-quaternary ammonium surfactant and the other based upon the contribution of the corresponding bolaform cation. Poor agreement was obtained with the first method, while good agreement was obtained with the second. The observed variation in the volume change due to micelle formation, $\Delta V_{\phi,M}$, is consistent with variations in the head group area and critical micelle concentrations, and can be rationalized in terms of possible spacer conformations in the aqueous and micellar phases. Results obtained for the 12-ϕ-12 surfactant indicate that rigidity of the spacer has no measurable effect on the micellization process for shorter spacer lengths.

The interaction of the gemini surfactants with the triblock copolymers in aqueous solution was markedly different from that typically observed in surfactant-polymer systems, and is similar in nature to a solubilization or mixed micelle formation process. The results obtained indicate that the interaction occurs primarily with the PPO segment of the triblock copolymer through a replacement of hydration water by polymer at the micellar surface. The solubility of the surfactant monomer (i.e., the CMC) may be increased through specific interactions between the surfactant and polymeric microdomains in solution. The results of a temperature dependent study indicate that the aggregation state of the copolymer in solution has a significant effect on the interaction with gemini surfactants. For systems where conditions (specifically the combination of polymer concentration and temperature) are such that self-aggregation of the copolymer can occur, two distinct type of aggregates are hypothesized; 1) polymer dominated, similar in nature to copolymer micelles, and 2) surfactant dominated, similar to regular gemini surfactant micelles.

ACKNOWLEDGMENTS

First, I would like to express my gratitude to my supervisor, Professor Ron E. Verrall. His guidance and advice during the course of this work has been invaluable and are an indication of his deep understanding of his field of research, as well as of his students. Through his efforts he has made this experience a truly rewarding one, and it is deeply appreciated.

I would like to also express my appreciation to the members of my supervisory committee: Dr. D. MacDonald; Dr. M.S. Pedras; Dr. R.S. Reid; and Dr. W.L. Waltz, for their advice during the course of this work. By the same token I would like to express my thanks to my colleagues, former members of Dr. Verrall's research group: Dr. H. Huang; Dr. L. Wilson; Dr. X. Wen; D. Hart; and K. Jenkins. These individuals provided many constructive discussions regarding this project and their input was invaluable.

I would also like to thank the Department of Chemistry and the University of Saskatchewan for the award of Graduate Teaching Fellowships and Teaching Assistantships as a means of financial support for this work. Financial assistance from the Natural Sciences and Engineering Research Council was also greatly appreciated.

Finally I would like to thank my parents, my wife April, and my children, Thomas and Zachary, for their loving support, patience and understanding throughout the course of my studies. These people have sacrificed a great deal so that I might pursue this endeavor.

DEDICATION

This work is dedicated to my father

Morley H. Wettig

You are always remembered.

TABLE OF CONTENTS

LIST OF TABLES

LIST OF FIGURES

NOMENCLATURE

8-3-8	N,N'-bis(dimethyloctyl)-1,3-propanediammonium dibromide
10-3-10	N,N'-bis(decyldimethyl)-1,3-propanediammonium dibromide
16-3-16	N,N'-bis(hexadecyldimethyl)-1,3-propanediammonium dibromide
12-2-12	N,N'-bis(dimethyldodecyl)-1,2-ethanediammonium dibromide
12-3-12	N,N'-bis(dimethyldodecyl)-1,2-propanediammonium dibromide
12-4-12	N,N'-bis(dimethyldodecyl)-1,4-butanediammonium dibromide
12-6-12	N,N'-bis(dimethyldodecyl)-1,6-hexanediammonium dibromide
12-8-12	N,N'-bis(dimethyldodecyl)-1,8-octanediammonium dibromide
12-10-12	N,N'-bis(dimethyldodecyl)-1,10-decanediammonium dibromide
12-12-12	N,N'-bis(dimethyldodecyl)-1,12-dodecanediammonium dibromide
12-16-12	N,N'-bis(dimethyldodecyl)-1,16-hexadecanediammonium dibromide
12-ϕ-12	(p-Phenylenedimethylene)-bis(dimethyldodecylammonium bromide)
A_2, A_3, A_4	Fluorescence decay parameters
A, B	Constants describing the behavior of the cmc as a function of alkyl tail length *or*
	Instrument constants for the vibrating tube densimeter
a, b	Constants describing the behavior of the cmc as a function of total counterion concentration
A', B'	Constants describing the behavior of the cmc as a function of the number of ethylene oxide groups (y) in the surfactant molecule
A_V	Debye-Hückel limiting slope for volumes
a_0	Experimental surfactant head group area
a, a_p, a_h	Area of the surfactant at the micelle interface, cross-sectional area of the head group, and cross sectional area of the hydrocarbon chain, respectively
a_s, a_{pol}	Area per surfactant molecule shielded by water, and by polymer, respectively
α	Degree of micelle ionization
α_0	Fraction of surfactant monomer in the aqueous phase
B_V	Pair-wise interaction parameter for surfactant monomers
β	Binding ratio of surfactant to polymer

C_2 or T_2	Concentration of surfactant at which free micelles begin to form in ternary surfactant-polymer-water systems
$C_{10}(EO)_8$	Octaethylene glycol monodecyl ether
$C_{14}(EO)_8$	Octaethylene glycol monotetradecyl ether
CAC, C_1 or T_1	Critical aggregation concentration
$[C^+]$, [complex], $[S^-]$	Equilibrium concentrations of counterion, surfactant-polymer complex, and surfactant, respectively
C_C	Total counterion concentration
cmc, cmc_S	Critical micelle concentration
cmt	Critical micelle temperature
CTAB	Cetyltrimethylammonium bromide
C_mTAB	Alkyltrimethylammonium bromide surfactant with alkyl tail length equal to m
C_P, c_P	Polymer concentration
CPyCl	Cetylpyridinium chloride
cryo-TEM	Cryogenic Transmission Electron Micrography
C_S	Surfactant concentration
$C_{S,f}$	Surfactant monomer concentration
C_V	Pair-wise interaction parameter for surfactant micelles
δ_{obs}, δ_M, $\Delta\delta$	Observed chemical shift, the chemical shift of the surfactant in the micellar form, and the change in chemical shift due to micelle formation, respectively
d, d_0	Densities of the solution, and the solvent, respectively
DLS	Dynamic Light Scattering
DTAB	Dodecyltrimethylammonium bromide
EO	Ethylene oxide
ϕ	Solution property
g, g_b	Aggregation numbers of free and polymer bound surfactant micelles
ΔG^{HI}	Gibbs energy for the hydrophobic interaction
$\Delta G°_E$, $\Delta G°_M$	Standard Gibbs energies of solution for ethane and methane, respectively
$\Delta G°_m$	Standard Gibbs energy for the transfer of an ionic surfactant from the aqueous phase into a polymer bound aggregate of size m

ΔG°_{mic}, $\Delta\mu^\circ_g$	Standard Gibbs energy of micelle formation
$\Delta G^\circ_{mic}(CH_2)$	Standard Gibbs energy for micelle formation per methylene unit
ΔG°_{tr}	Standard Gibbs energy of transfer
γ	Surface tension
Γ_i	Gibbs surface excess of component i
ΔH°_{mic}	Standard enthalpy of micelle formation
ΔH°_{tr}	Standard enthalpy of transfer
HPC	Hydroxypropylcellulose
I, I_0	Intensity of fluorescence at time t, and at t = 0, respectively
k_0, k_q	Rate constant for the decay of an excited probe in the absence of quencher, and the rate constant of fluorescence quenching, respectively
K, K_M	Equilibrium constant for micelle formation
K_b	Equilibrium constant for the formation of polymer bound micelles
K_D	Distribution constant for the distribution of an additive between the aqueous and micellar phases
κ, κ'	Specific conductance of the aqueous surfactant and the aqueous surfactant-polymer solutions, respectively
l_{max}, l_{hc}	Length of a fully extended hydrocarbon chain
μ_S, μ_M	Chemical potential of the surfactant in its monomer and micellar states, respectively
μ°_S, μ°_1	Standard chemical potential of the surfactant in its monomer state
μ°_M, μ°_g	Standard chemical potential of the surfactant in its micellar state
$\Delta\mu^\circ_{HC/W}$	Chemical potential change for the transfer of the alkyl tail of a surfactant from water to a liquid hydrocarbon environment
$\Delta\mu^\circ_C$	Chemical potential change corresponding to a decrease in conformational freedom of an alkyl chain as a result of restricting the polar head group to the micellar surface
$\Delta\mu^\circ_{elec}$	Chemical potential change arising from electrostatic interactions in the micelle formation process
M, [M]	Micelle, and concentration of micelles, respectively
M_2	Molar mass of the solute
MeC	Methylcellulose

m-s-m	N,N'-bis(alkyldodecyl)-α,ω-alkanediammonium dibromide surfactant with alkyl tail length = m and alkyl spacer length = s
m_b	Molality of additive bound in the micellar phase
m_S	Surfactant molality
N_{agg}, n	Mean aggregation number of a surfactant micelle
n_C	Number of carbons in an alkyl chain
n_i	Number of moles of component i (S = surfactant, H_2O and w = water)
[P]	Concentration of polymer
$[P_0]$	Concentration of active polymer sites
P	Surfactant packing parameter
PEO	Polyethylene oxide
PGSE-NMR	Pulsed-gradient spin-echo NMR
PO	Propylene oxide
PPO	Polypropylene oxide
PVAc	Polyvinyl acetate
PVOH	Polyvinyl alcohol
PVP	Polyvinyl pyrrolidone
PEO-PPO-PEO	Polyethylene oxide-polypropylene oxide-polyethylene oxide triblock copolymers or Pluronics
[Q]	Concentration of quencher
$\Delta S°_{tr}$	Standard entropy of transfer
S, [S]	Surfactant monomer, and concentration of surfactant monomers, respectively
SDS	Sodium dodecylsulfate
σ	Interfacial tension
$\Delta\sigma$	Change in interfacial tension between the hydrocarbon core and water
$\Delta\sigma_p$	Change in interfacial tension between the head groups and water
t	Time
τ_0	Fluorescence lifetime of the unquenched probe *or*
	The period of vibration for the solvent
τ	The period of vibration for the solution
V, $\overline{V}_i$	Total volume, and partial molar volume of component i, respectively

V_{core}	Volume of the hydrophobic core of a micelle
V_{hc}	Volume of a hydrocarbon chain
ΔV°_{mic}, ΔV_M	Standard volume change due to micelle formation
ΔV_{mic}, $\Delta V_{\phi,M}$	Volume change due to micelle formation based on apparent molar volume
ΔV_{ion}, ΔV_{CH_2}	contributions of an ionic head group and a methylene group to the volume change due to micelle formation, respectively
$\Delta V_{\phi}(W \rightarrow W+P)$	Transfer volume of the surfactant from aqueous (W) to aqueous polymer (W+P) solution
V_{ϕ}	Apparent molar volume
$V_{\phi,\ specific}$	Apparent specific volume
V^0	Partial molar volume of the surfactant at infinite dilution
V^M	Partial molar volume of the surfactant in its micellar form
$V_{\phi,S}$, $V_{\phi,M}$, $V_{\phi,cmc}$	Apparent molar volume of the surfactant, of the surfactant at the cmc, and of the surfactant in the micellar phase, respectively
V_b, V_f	Standard partial molar volumes of an additive in the micellar and aqueous phases, respectively
w, w_0	Weight ratio of the solute and solvent, respectively
x_S, x_{cmc}, x_M	Mole fraction of surfactant, the cmc in mole fraction units, and the mole fraction of micelles, respectively
X_1, X_t	Mole fraction of surfactant monomer, and total surfactant, respectively
y	Experimental binding ratio of surfactant to polymer

1 INTRODUCTION

1.1 Rationale for study

The widespread application of mixed surfactant/polymer systems in industry has generally been a result of the observed enhancement of solution properties (related to the application of interest) brought about by the combination of the surfactant and polymer. Applications of surfactant/polymer mixtures can be found in nearly any aspect of daily life ranging from the formulation of industrial products (including detergents, cosmetics, paints and coatings, adhesives, lubricants, and food and pharmaceutical products) to biological systems (e.g., the structure and functioning of membranes, and lipid transport).[1] In such mixed systems the surfactant provides control over interfacial tension, emulsification capacity, and colloidal stability, while the polymer provides control of the rheological properties as well as colloidal stability.[2] In addition, the combination may also increase the solubility of one or the other component (a specific example of this is the observed increase in the cloud point of polymers in the presence of added surfactant), or an added third component, making such systems highly attractive in applications such as enhanced oil recovery, detergent formulations, and drug transport. Some specific examples of the application of such systems include the formation of gels, i.e., solutions of very high viscosity, as a result of the polyelectrolyte effect (repulsion between charged centers along the polymer chain causes the polyelectrolyte to adopt an extended conformation thus increasing solution viscosity).[1] Such gels are of particular interest in the food and pharmaceutical industries; however, current patent literature indicates an increase in their use in the cosmetic and detergent industries. The addition of either a neutral polymer or an oppositely charged polyelectrolyte is observed to cause a reduction in the critical micelle

concentration of ionic surfactants. This also results in a reduction in the surfactant monomer concentration, a factor associated with the reduction of skin irritation due to surfactants.[3] Therefore, such combinations have significant implications for the development of "milder" skin-care product formulations. The addition of surfactant (specifically sodium dodecylsulfate) to drug tablet formulations has been shown to prolong the time of release of a drug when the tablets contain the polymer hydroxypropylcellulose (HPC). The mechanism for the observed prolongation of release has been hypothesized to be the formation of a viscous gel layer, similar to the effect described above, around the tablet in an aqueous medium.[4] The possibility of tailoring systems, through the appropriate combination of surfactant and polymer, is of great scientific interest and points to the necessity of developing a clear understanding of the nature of surfactant-polymer interactions in aqueous solution under a variety of conditions. This understanding is of crucial importance with respect to any possible application, not simply drug delivery systems, in order to allow for some prediction of resulting solution properties.

Unfortunately, because of the complex nature of the surfactant / polymer systems, they are not yet well understood. The complexity of the problem arises from the similarities involved in the solubilization of polymers in water, and in the aggregation processes of surfactants in solution. The solubility of a neutral polymer in solution is governed primarily by the hydrophobicity of the polymer. The surfactant aggregation process is controlled through a delicate balance of hydrophilic, hydrophobic and ionic interactions. It is not surprising that the addition of a neutral polymer to a surfactant solution can have large effects on the overall properties of the solution.

The nature of the polymer and the surfactant both play an important role in the strength of the observed interaction. In the case of ionic polymers, strong electrostatic interactions are observed between polymers and surfactants of opposite charge, while little or no interaction is observed between polymers and surfactants having like charges. The primary electrostatic binding mechanism is further reinforced by the aggregation of the alkyl tails of the bound surfactant (hydrophobic interactions).[5] In the case of neutral polymers one must consider how the addition of the polymer affects the aggregation process of the surfactant in solution, a process also governed by a balance of interactions. In addition to attractive interactions, electrostatic repulsive interactions between the ionic head groups of the surfactant molecules as well as penetration of water into the hydrophobic core of the micelle occur. Any relief of these stresses due to the presence of the polymer will give rise to a net favorable interaction between the polymer and the surfactant. This interaction also will be influenced by such factors as temperature, the presence of additional components (e.g., salt, another surfactant), the structure and charge of the surfactant, as well as the size, concentration, and structure of the polymer. In addition, any self-aggregation behavior of the polymer itself will be important.[6]

Anionic surfactants have been shown in a number of studies to interact with neutral polymers to a greater extent than cationic surfactants. In many cases only a weak interaction (if any) is observed between cationic surfactants and hydrophilic polymers. Anionic surfactants interact with both hydrophilic and hydrophobic polymers.[7-10] The reason for this difference is not well understood; however, some authors have shown that the nature of both the head group of the surfactant as well as the counterion may play an important role in

determining whether or not a cationic surfactant will interact with a specific neutral polymer.[6] Due to the low mammalian toxicity of cationic surfactants in general, and quaternary ammonium surfactants in particular, cationic surfactants are used to a large extent in a number of pharmaceutical, biomedical and personal care product applications.[11] In many cases the formulations of these products also include polymeric compounds. It is for this reason that determining how and why cationic surfactants interact (or do not interact) with neutral polymers, as well as determining methods of enhancing such interactions is of great practical importance.

In order to gain a better understanding of how the nature of the head group of the surfactant influences the interaction, this work was initiated with the objective to study a new class of surfactants known as gemini surfactants. In particular, the choice of cationic gemini surfactants was made in an effort to determine if the interaction with neutral polymers can be enhanced as a result of the structure of the gemini surfactants. A gemini surfactant differs from a traditional surfactant in that two "monomer" surfactant molecules are linked chemically at or near the head group as shown in Figure 1.1-1. As will be discussed in section 1.3, it has been shown that both the size and composition of the spacer group that links the two head groups together greatly influences the shape of the aggregates formed in solution. In particular, micelles of the N,N'-bis(alkyldimethyl)-α,ω-alkanediammonium dibromide surfactants, studied in this work, show a rich array of morphologies extending from thread-like to spherical micelles to vesicles, depending on the length of the spacer group. It was anticipated that this range of morphologies might be exploited to enhance the interaction between cationic surfactants and neutral polymers.

Figure 1.1-1: Structure of the 12-s-12 (see pg. 14) series of cationic gemini surfactants

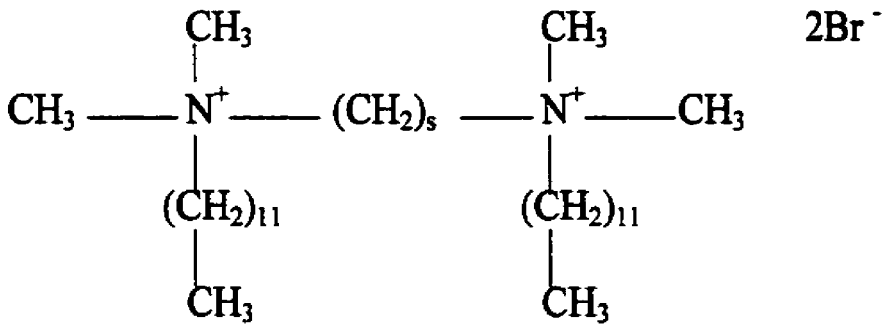

where s = 2,3,4,6,8,10,12, and 16

Figure 1.1-2: Schematic of the structure of the triblock copolymers used in this study (see also Table 3.1-1).

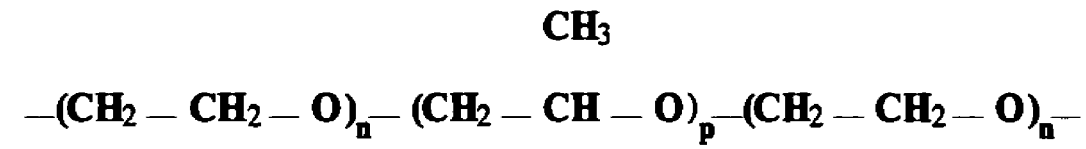

ethylene oxide (EO) propylene oxide (PO) ethylene oxide (EO)

where n is the number of ethylene oxide units (equal to N_{EO} in Table 3.1.1) and p is the number of propylene oxide units (equal to N_{PO} in Table 3.1.1)

The polymers used in this study are also a relatively new class of polymers known as triblock copolymers (or by the trade name Pluronics). Triblock copolymers consist of two hydrophilic segments (in this study polyethylene oxide or PEO) separated by a more hydrophobic segment (in this study polypropylene oxide or PPO). These polymers are unique compared to other polymers in their ability to form micellar aggregates in which the more hydrophobic propylene oxide segments form the core of the aggregate, with the more hydrophilic ethylene oxide segments forming what is known as the corona of the aggregate. It has been established that polymers that have been modified by the addition of hydrophobic groups interact with cationic surfactants more strongly than with the corresponding unmodified polymers.[12] Therefore the presence of the hydrophobic propylene oxide segment, coupled with the polymers unusual ability to self-aggregate, should make the triblock copolymers good candidates for the enhancement of the interaction of cationic surfactants with neutral polymers.

As was previously mentioned, the low toxicity of quaternary ammonium surfactants has led to their extensive use in numerous applications. In addition to low toxicity, quaternary ammonium surfactants exhibit a broad spectrum of antimicrobial activity including antibacterial, antifungal, and antiviral (including disinfection of the human immunodeficiency virus, type 1) properties.[13] The low toxicity of cationic surfactants is likely to be extended to the bis-quaternary ammonium gemini surfactants; however, to date no reference to toxicological studies of gemini surfactants has been published. The gemini surfactants have already been shown to have germicidal properties greater than those of traditional monoquaternary ammonium surfactants.[14] This fact coupled with the (probable)

low toxicity of such compounds, and the observed low critical micelle concentrations, suggest that the gemini surfactants may be an appropriate alternative to traditional quaternary ammonium compounds. The observation of lower critical micelle concentrations also has implications with respect to environmental considerations as less gemini surfactant is required to achieve the same surface activity, compared to a corresponding monoquaternary ammonium compound. Block copolymers also have low toxicity and have found application in a number of medical and pharmaceutical applications (in addition to non-biological applications).[15] These factors, coupled with the unique behavior of both the gemini surfactants and triblock copolymers in solution, individually, implicate the combination of the two as a potential system for many practical applications.

1.2 Role of water

The majority of chemical and biological applications of surfactants occur in the aqueous phase. As such it is useful to review some of the unique characteristics water possesses as a solvent. When one considers the low molar mass of water, one finds the melting and boiling points of water as well as the latent heat of vaporization to be unexpectedly high. Similar behavior is observed in other substances; however, these usually involve strong Coulombic interactions such as those in ionic solids and metals.[16] Also water possesses a number of other unusual characteristics such as the density maximum at 4°C, a relatively low compressibility, as well as its behavior both as a solute in organic solvents and as a solvent itself, which point to strong intermolecular interactions between water molecules. Computer simulations of water using models such as the ST2 model for water (in which charges of $+0.24e$, centered on each hydrogen center, and $-0.24e$, located on the opposite side of the oxygen center to account for the unshared electron pairs, are arranged in a tetrahedral arrangement) can account for many of the properties of water. Results show a preference for each water molecule to be tetrahedrally coordinated with four other water molecules in the solid state through a hydrogen-bonding network. The hydrogen bond arises due to the small size of the hydrogen atom, and its tendency to become positively polarized when bound to strongly electronegative atoms like O, N, F, and Cl. This allows for a strong interaction between the polarized hydrogen atom of one molecule with the strongly electronegative atom of a nearby molecule, forming an effective bond between the two molecules.[16] The strength of hydrogen bonds is in the range of 10 to 40 kJ mol^{-1}. This is relatively weak compared to covalent or ionic bond strengths of approximately 500 kJ mol^{-1}, but is significantly larger than those for typical van der Waals type interactions. In ice the intramolecular covalent O-

H bond distance is 1.00 Å, while that for the intermolecular O-H hydrogen bond is 1.76Å. This is significantly shorter than the sum of the van der Waals radii for two water molecules (2.6Å) indicating the presence of hydrogen bond formation. In liquid water the number of nearest neighbours is observed to increase to approximately 5, as molecules become more labile (hence the observed density maximum at 4°C), and the ice-like tetrahedral structure remains. However, the number of hydrogen bonds formed is observed to decrease from 4 to an average of 3.5 per molecule.[16] It is this tetrahedral coordination of water molecules that is critical to the unusual properties of water.

1.2.1 Hydrophobic hydration and the hydrophobic interaction

The term hydrophobic (water fearing) was introduced as a means of explaining the low solubility of apolar solutes in water. This term is somewhat misleading as the van der Waals interaction energies between apolar molecules and water molecules are in fact favorable (as can be seen by the large negative enthalpies for the transfer of an apolar solute into water).[17,18] However, it is useful to define hydrophobicity in terms of the thermodynamics of the transfer of an apolar solute from either its liquid state or a non-polar solvent into water. As illustrated in Table 1.2.1-1, those compounds which show a larger increase in the Gibbs energy of transfer to an aqueous phase are said to be more hydrophobic than those compounds which show a smaller increase in the Gibbs energy.

Two phenomena observed in the solubilization of apolar materials in water are hydrophobic hydration and the hydrophobic interaction. A great deal of confusion exists in

Table 1.2.1-1 Thermodynamic data for the transfer of small apolar compounds from the neat liquid to aqueous solution at 25°C

Compound	ΔG°_{tr} (kJ mol^{-1})	ΔH°_{tr} (kJ mol^{-1})	ΔS°_{tr} (J mol^{-1} K^{-1})
C_4H_{10}	25.0	-3.3	-96
C_5H_{12}	28.7	-2.1	-104
C_6H_{14}	32.4	0	-108
C_6H_6	19.2	2.1	-59
$C_6H_5CH_3$	22.6	1.7	-71
$C_6H_5C_2H_5$	25.9	2.0	-79
$C_6H_5C_3H_8$	28.8	2.3	-88
C_3H_7OH	6.6	-10.1	-56
C_4H_9OH	10.0	-9.4	-65
$C_5H_{11}OH$	13.5	-7.8	-71

from reference[19]

the literature when discussing these two phenomena and they are often grouped together under the heading of hydrophobic effects. The situation becomes even less clear as many authors refer to the combination of low solubility and the entropy dominated nature of the solvation energy of apolar solutes as the "hydrophobic effect".[16] An excellent review of the subject has been presented by Blokzijl and Engberts in which the terminology is clarified.[17]

The term hydrophobic hydration refers to the effect an apolar solute has on the local structure of water. The predication for water molecules to form hydrogen bonds with each other strongly influences the interaction of water with apolar solutes that do not form hydrogen bonds. Any apolar solute placed in water gives rise to an apparent problem; regardless of the orientation a water molecule adopts with respect to the solute molecule, some ability to hydrogen bond is lost by nature of the fact that either a hydrogen or oxygen center must point towards the solute. The extraordinary ability for tetrahedrally coordinated compounds to reorganize themselves around an inert compound without a loss of

coordination alleviates this problem.[16] Provided the solute molecule is small enough, water molecules surrounding it are able to reorganize themselves in such a fashion that there is no decrease in the number of hydrogen bonds formed. In some instances there may in fact be an increase in coordination of water molecules surrounding an apolar solute (from an average of 3.5 to 4), leading to an overall decrease in entropy as the water molecules become more ordered (as seen in Table 1.2.1-1). It is generally argued that this loss of entropy is the cause for the limited solubility of apolar compounds.[16,20] More recent arguments based upon results from scaled particle theories (SPT) indicate that this loss of entropy is more likely a result of a large number of water molecules being involved in the solubilization of a solute molecule, thus giving rise to a large number of water molecules in a small volume. This fact, coupled with the favorable enthalpic contribution to the Gibbs energy change for the solubilization of an apolar solute, suggests that hydrophobic hydration may in fact aid the dissolution of apolar solutes.[17] This implies that the interaction of apolar solutes in water through the hydrophobic interaction would require a disruption of the hydration shells and therefore hydrophobic hydration would not be the major contributing factor to the observed hydrophobic effect.

Hydrophobic interactions refer to the attractive interactions that occur between apolar solutes dissolved in water. An excellent example of the hydrophobic interaction has been given by Ben Naim[21] in which the association of two methane molecules is considered. The Gibbs energy for the hydrophobic interaction is evaluated by computing the differences between the thermodynamics parameters for the hydration of gaseous methane and ethane. From this treatment the following expression is obtained

$$\Delta G^{HI} = \Delta G^{\circ}_{E} - 2\Delta G^{\circ}_{M} \qquad 1.2.1\text{-}1$$

where ΔG°_{E} and ΔG°_{M} are the standard free energies of solution for ethane and methane, respectively. Hydrophobic interactions are unusually strong in aqueous solution and can be stronger than the interaction between two molecules in free space.[16] If we consider the example of two methane molecules, then the van der Waals interaction energy across free space is -2.5×10^{-21}J, while in water it is -14×10^{-21}J. Van der Waals theory for the interaction of molecules within a medium predicts a reduction in the interaction energy between the two particles, so we must ask: what is responsible for the unusual attraction between apolar solutes in water?

There have been relatively few direct measurements of the hydrophobic interaction because of the low solubility of apolar solutes. Values of –8.4 and -11.3 kJ mol^{-1} have been determined for the formation of dimers of benzene and cyclohexane, respectively.[22] Attempts have been made to determine the nature of the hydrophobic interaction through surface force measurements between hydrophobic surfaces, using the surface force apparatus (SFA) and atomic force microscopy (AFM). Israelachvili and Pashley have measured the attractive hydrophobic force between two macroscopic curved hydrophobized surfaces using the SFA and have found that, in the range of 0-10 nm, the force is observed to decay exponentially with distance, with a decay length of approximately 1.0 nm.[23] From these results it was proposed that for small molecules the Gibbs energy change for a pair-wise interaction could be obtained from

$$\Delta G \approx -40R \text{ in kJ mol}^{-1} \qquad 1.2.1\text{-}2$$

where R is the molecular radius in nm. This gives for cyclohexane a Gibbs energy change of -11.4 kJ mol^{-1} which is in good agreement with the experimental result given above.[16] More recent measurements have shown the force law for the attraction observed between macroscopic surfaces to be more complex and of a longer range than first predicted. The force law is now believed to consist of both a short and a long range contribution with decay lengths of 2.1 and 25 nm, respectively, indicating that the interaction occurs over a range equivalent to 300 water molecular diameters or larger.[24,25] Explanations for the observed long range decay are generally divided into three categories:

- an ordering of water molecules adjacent to the surface giving rise to a long range interaction through continued modifications of water structure
- Debye screened dipole-dipole correlations with an anomalously large amplitude
- the formation of vapor cavities between the surfaces

At this point none of the above theories have proven successful in explaining all of the observed results; however, the vapor cavitation model is currently the most accepted. The major conclusion that has been reached is that theories proposed to explain the observations for the interaction between microscopic surfaces are not likely to correlate to molecular interactions between apolar solutes in water.[24]

The hydrophobic interaction is known to play a crucial role in a number of biological processes (such as protein folding and host-guest recognition in enzymes)[17], as well as in many surface and self-assembly processes involving amphiphilic molecules. This fact will continue to drive research into the nature of the hydrophobic interactions in hopes of providing further insight into complex associative processes.

1.2.2 Hydrophilic hydration

In contrast to the above discussion for hydrophobic compounds there is no phenomenon known as the hydrophilic effect or the hydrophilic interaction. This does not imply that such interactions do not exist, indeed certain molecules are known to be water soluble and to strongly repel one another in aqueous solution, the opposite of that observed above for hydrophobic compounds.[16] Hydrophilic (water loving) groups show a strong preference to be in contact with water rather than each other. This desire for water contact may even go as far as the compound being hygroscopic in nature, i.e., absorbing water vapor.

As is the case with an apolar solute, the introduction of a hydrophilic solute will disrupt the local water structure and result in the creation of a hydration shell around the solute molecule. In the case of polar or ionic solutes, i.e., hydrophilic solutes, ion-dipole or dipole-dipole interactions between the solute and water molecules results in a re-orientation of the surrounding water molecules. Because of electrostatic effects, the re-orientation of the bulk water structure can be long-range giving rise to an overall disruption of the water structure, thus avoiding the entropic consequences for the creation of a hydration shell observed with hydrophobic solutes. For the case of ionic solutes the number of water molecules involved in the primary hydration shell is dictated by the size and shape of the ion. These molecules will be strongly polarized and oriented by the electrostatic field of the solute, with the effect diminishing as the distance from the solute is increased. For ions having a high charge density, such as Li^+, Na^+, and F^-, the resulting electrostatic field is strong enough to not only restrict the mobility of the water molecules immediately surrounding the ion, but also to orient the water molecules surrounding the primary hydration sphere. Such ions are referred

to as "structure-making ions". The effect of these ions in dilute solutions diminishes as the distance from the ion increases, though there may be an overlap of hydration spheres as the solute concentration is increased. Ions having a low charge density do not orient the water molecules in the primary hydration shell to the same degree resulting in a disordering of the surrounding regions. Such solutes are referred to as "structure-breaking".

As previously mentioned, hydrophilic solutes need not be ionic in nature. Polar non-electrolyte solutes interact with water through dipolar interactions that also serve to orient water molecules in the primary hydration shell. Depending upon the structure of the solute molecule, the possibility for the formation of new hydrogen bonds also exists. As in the case of ionic solutes, the effect of these solutes on water structure diminishes with increasing distance and the bulk water structure is eventually regained.

1.3 Gemini surfactants

In recent years considerable research has been carried out on gemini surfactants, both anionic[26-29] and cationic[14,30-56], using a variety of experimental methods. By far the most studied of the gemini surfactants are the N,N'-bis(alkyldimethyl)-α,ω-alkanediammonium dibromide surfactants, known as m-s-m gemini surfactants where m is the number of carbon atoms in the alkyl tails of the surfactant (m = 12 in Figure 1.1-1), and s is the number of carbon atoms in the unsubstituted alkyl spacer group. As it is this type of surfactant that has been used in this study, the remainder of this section will focus primarily on the properties of the m-s-m surfactants; however, the general observations are applicable to other types of gemini compounds.

As was stated in §1.1, gemini surfactants are unique in that they consist of two ionic head groups linked chemically at or near the head group. They can be visualized as two monomeric surfactants that are tethered by an alkyl chain. It is this tethering of monomer-like entities that provides some of the unusual solution properties observed in m-s-m gemini surfactants. Traditionally, in order to change the micellization properties of a surfactant to suit a specified application, one has the options of changing the head group, counterion or alkyl tail length. By directly linking two (or more) head groups together, the micellization properties are changed (as compared to the untethered surfactant monomers) and become dependent upon the nature of the spacer group.[57] This allows for additional control over the aggregation properties of the surfactant and possible applications are still being realized.

A number of surfactant properties such as the critical micelle concentration[33], head group area[35] and, as will be shown in this study, the mean aggregation number and apparent molar volumes show unusual behavior as the length of the alkyl spacer group is varied. The critical micelle concentration (cmc) is perhaps the most commonly known and extensively studied property of surfactant solutions and will be discussed in some detail in Chapter 2. Critical micelle concentrations obtained for the gemini surfactants are smaller than those of conventional single-tail surfactants by typically one order of magnitude or more. For example, the cmcs of the 12-2-12 gemini surfactant and dodecyltrimethylammonium bromide (DTAB) are 0.89 mM and 15mM, respectively. This decrease is one of the primary reasons for current interest in gemini surfactants and can be explained simply by considering that two alkyl chains (as opposed to one for conventional surfactants) are transferred at a time from the aqueous to the micellar phase. Indeed, relaxational studies have shown that

gemini surfactant monomers exchange between the bulk and the micellar phases as a unit as opposed to a two-step process in which the alkyl tails of the monomer enter the micelle separately.[36] This indicates the somewhat restricted motion of gemini surfactant monomers in solution and may provide experimental support for the argument that a preferential *cis* conformation exists for the surfactant monomers in solution. This argument was proposed to explain the unusual maximum observed in the cmc as the length of the spacer is increased. The cmc is observed to go through a maximum as the length of the spacer is increased in the range of s ≅ 5-6. This has been observed, independently, in two series of gemini surfactants, the 10-s-10 series[32] and the 12-s-12 series[33], and confirmed in this study. As indicated above, this maximum has been attributed to changes in conformation in which the spacer adopts a preferential *cis* conformation in the bulk solution to allow for intramolecular interactions between the two alkyl tails of the molecule.[33] This would increase the solubility of the monomer in the bulk, thus increasing the cmc. Beyond chain lengths of s = 10 the cmc begins to decrease in a linear fashion, similar to that observed for the lengthening of the alkyl chain of a conventional surfactant, and this behavior has been attributed to the penetration of the spacer into the core of the micelle.

From studies of the surface tension of the gemini surfactants, determinations of the head group area (a_0) at the air/water interface have been made. For the 12-s-12 series of surfactants a maximum is observed in a_0 as a function of increasing spacer length for s = 10-12. This maximum is attributed to an extension of the spacer group into the air side of the interface[35]; however, there is some speculation as to the reason for this. It was initially proposed by Alami et al.[35] that as the length of the polymethylene spacer is increased so does

the hydrophobicity of the spacer, and it is this increased hydrophobicity which results in expulsion of the spacer from the interface. Theoretical studies of the spacer chain conformation at the air/water interface have revealed that this is not the case, but rather there are three main factors that determine the variation of a_0 with s:[50,51]

i) geometric effects, i.e., larger spacers give rise to larger head group areas,

ii) interactions between gemini surfactant monomers which serve to decrease the head group area once the spacer has reached a certain length,

iii) conformational entropy of the spacer, which increases rapidly with increasing spacer length due to increased flexibility. This effect serves to enhance the second factor.

Therefore it is the competition between the first effect and the two others that gives rise to the observed maximum in a_0. This provides further evidence that the spacer lies fully extended at the air/water or micelle/water interface up to a certain length, after which folding of the spacer into the air or into the core of the micelle will occur as the two ammonium head groups attempt to achieve an equilibrium distance between each other, and with other molecules at the interface. It should be noted that the equilibrium distance between surfactant monomer head groups in a spherical or spheroidal micelle has been estimated to be approximately 7Å[34], and has been experimentally determined for CTAB to be 7.94 Å.[48] Therefore it is not surprising that the observed folding of the spacer does not occur for short spacer lengths.

Measurements of the mean aggregation number have shown that the size of the micelles increases more rapidly as a function of surfactant concentration for surfactants having short spacers (s = 2-4) as compared to those with longer spacers, indicating a tendency for micelle growth as s is decreased.[58] It has also been noted that the aggregation numbers converge to

an aggregation number of approximately 20-30 regardless of the size of m or s. This value correlates well with approximately 1/2 the mean aggregation number predicted for a minimum spherical micelle formed by conventional surfactants (c.f. §2.1.3) indicating that, at low concentrations, the micelles formed by gemini surfactants are spherical in nature. Observations made from cyrogenic transmission electron microscopy (cryo-TEM) show that in the case of short spacers, dimerization does result in the formation of aggregates of lower curvature than the corresponding monomeric surfactants. As the length of the spacer is increased, the observed geometries follow the pattern

elongated micelles → spheroidal micelles → vesicles

It is interesting to note that these structures can be predicted from the surfactant packing parameter (c.f. §2.1.3) which can be evaluated from head group areas and estimates of the hydrocarbon chain length and volume. Clearly the length, flexibility, and chemical composition of the spacer group of gemini surfactants will play a defining role in determining the shape of the aggregates formed in solution.

There have been attempts to examine the effect of rigidity in the spacer group through the introduction of aromatic rings or unsaturations in the spacer chain.[44,45,47,59] Results of these studies are somewhat inconclusive since the length of these spacers correspond to polymethylene chain lengths of 6 methylene units or less and results for the gemini surfactants with polymethylene spacers indicate that the spacer lies fully extended up to chain lengths of approximately 10 methylene units. This implies that the effect of rigidity in the spacer can only be evaluated if the effective length of the spacer is longer than a 10 – 12 carbon polymethylene chain. However, the major difficulty with such spacers is that the

compounds will have very low cmcs making experimental measurements of such surfactants problematic.

1.4 Triblock copolymers

Polyoxyalkylene block copolymers represent a diverse subset of non-ionic surfactants which derive their diversity from the broad range of structural possibilities available during synthesis. Triblock copolymers of the type poly(ethylene oxide)-poly(propylene oxide)-poly(ethylene oxide) (PEO-PPO-PEO) are members of this set of surfactants and are often referred to by the trade names Pluronic® (BASF) or Superonic® (ICI). Triblock copolymers have found widespread industrial and commercial application as emulsifying, wetting, thickening, coating, solubilizing, stabilizing, dispersing, lubricating, and foaming agents.[60] Industries which employ copolymers in a variety of formulations include (but are by no means limited to) medical and pharmaceutical, detergency, personal products, petrochemical, agricultural, corrosion prevention, and waste water treatment. An excellent review of the applications of copolymers is provided by Edens.[61] Such diverse application is primarily due to the broad range of solution properties which can be obtained through variation of not only the molecular mass of the polymer, but also through variation of its composition in terms of the PEO/PPO mass ratio.

Heat-induced micelle formation is one of the unique characteristics of triblock copolymers and, in addition to the usual critical micelle concentration, the definition of a critical micelle temperature (cmt) is also useful.[62] The temperature dependence of the self-assembly process for triblock copolymers is remarkably different from the dependence

observed for traditional polyoxyethylene nonionic ($C_m(EO)_n$) surfactants. A small increase in temperature of 10°C for a triblock copolymer (Pluronic) can bring about a reduction of the cmc by a factor of 10-100. Correspondingly, an increase in temperature of 25°C for the $C_{14}(EO)_8$ and $C_{10}(EO)_8$ surfactants yields a decrease of only 35-45% in the cmc, indicating a relatively weak temperature dependence.[60] The interconnection between the cmc and cmt for a given polymer allows for the investigation of these systems from two approaches, either by variation of temperature at a fixed concentration, or by variation of concentration at a fixed temperature. It is likely that the desired application will determine the most suitable means of study (i.e., as a function of temperature, or as a function of concentration) for a given system.

A number of generalizations can be made regarding the association of Pluronic triblocks in aqueous solution:

i) The PPO block is the most important factor in the formation of Pluronic micelles and the cmc is observed to decrease exponentially, and the cmt linearly with the PPO block length. An increase in the PEO block length causes a small increase in both the cmc and cmt.[60,63]

ii) Both the cmc and cmt decrease with increasing total molar mass of the polymer (for polymers having a constant EO/PO ratio). Additionally, the lower the relative EO content, the larger the influence of molar mass.[60]

iii) From measurements of the cmc as a function of temperature, the aggregation process is observed to be endothermic indicating that the micelle formation process is entropy driven in the case of Pluronic surfactants.[60,62] The entropy increase has been attributed to the the release of hydration water from the PPO blocks as the aggregation occurs.[63]

The size and structure of the micellar aggregates formed by Pluronics is most commonly studied using static light scattering methods;[60] however, determinations have also been

made using dynamic light scattering (DLS), pulsed-gradient spin-echo NMR (PGSE-NMR), and fluorescence quenching methods (particularly in the case of mixed ionic surfactant-Pluronic systems). It is generally accepted that the structure of the micelles formed of Pluronic surfactants consists of a hydrophobic core containing the PPO, and an outer corona consisting of a diffuse layer of PEO blocks and solvation water. Micelles formed from Pluronic surfactants are generally spherical in nature with the size of the micelle being determined by the size of the PPO block. The core of the micelle is generally considered to be free of water[60]; however, recent results obtained from fluorescent vibronic intensity ratios for pyrene suggest that the water content within the core may be as great as 30% in some cases.[64] From values of the aggregation number and the hydrodynamic radius of the aggregate (obtained from DLS or PGSE-NMR), determination of an approximate core size and thickness of the corona can be carried out. Aggregation numbers are typically in the range of 20-200 with hydrodynamic radii of the order of 8-12 nm.[60,62] The core radii are typically of the order 2-6 nm[60], indicating a coronal size which makes up approximately 50% of the Pluronic micelle. This is much larger than the hydrated surface layer of typical ionic surfactants, which generally comprises 10-20% of the aggregate volume. The aggregation number and, correspondingly, the core radius increase with increasing temperature; however, the overall hydrodynamic radius of the micelle is observed to remain constant. This effect can be understood when one considers that dehydration of the PEO blocks occurs as temperature increases and therefore these blocks begin to become part of the core resulting in a decrease of the coronal thickness. The aggregation number is also dependent upon the polymer composition, increasing with increasing length of the PPO block or decreasing

length of the PEO blocks; however, little dependence upon polymer concentration is observed (up to concentrations of 30% by mass).

The surface activity and adsorption behavior of block copolymers have been studied extensively by a number of research groups.[65,66] The surface tension profile for these surfactants is often complex, especially over broad ranges of concentration and temperature, exhibiting two break points in some cases. This has led to some confusion with regard to properties derived from surface tension measurements, such as the surface excess concentration and the surface area per molecule. The first of the two observed breaks has been attributed to a variety of possible phenomena; the formation of monomolecular micelles[67], the occurrence of a phase transition at the interface as the copolymer layer becomes more compact[66], and the presence of a broad distribution of polymer molar masses.[68] As in the case of the cmc and cmt for the triblock copolymers, some generalizations regarding their surface behavior can be made:[60]

i) For the condition of complete surface coverage, the area occupied by a copolymer molecule decreases with increasing temperature, indicating a more compact conformation is adopted as temperature is increased. This is similar to observations for the core radius of the micelle, described above.

ii) The area per molecule is observed to increase with the number of EO units and to decrease with an increase in the number of PO units

iii) For polymers exhibiting two breaks in the surface tension profile, the separation (as a function of concentration) is observed to decrease with increasing temperature, until only one break is observed at temperatures above 40°C. This is thought to be due to an increased tendency for micelle formation with a corresponding limited increase in surface adsorption.

As well, the surface tension, as in the case of all surfactants, is sensitive to the presence of surface active impurities. This is illustrated by a minimum in the surface tension versus log

concentration plot; however, with purification the minimum disappears. In contrast to the surface properties, purified and unpurified copolymers show little difference in their micellar properties in solution.

1.5 Surfactant – polymer interactions

As stated previously(§1.1), the broad application of surfactant-polymer mixtures has promoted a great deal of research interest in the aqueous solution behavior of these systems. While many types of surfactant-polymer interactions can occur depending upon the nature of both the surfactant (cationic, anionic, or non-ionic) and the polymer (neutral or polyelectrolyte), this discussion will focus on the type of interaction likely to arise in this study, namely that between ionic surfactants and neutral polymers. A number of excellent reviews and texts are available on the subject.[7,69-72] They indicate that the bulk of the research carried out in this field has focused on the interaction of anionic surfactants (usually sodium dodecylsulfate (SDS)) with a variety of polymers, and has involved a broad range of experimental methods. These include: measurements of surface tension, electrical conductivity, viscosity, cloud point, and solubility; binding studies using both dialysis and ion-specific electrodes; spectroscopic studies using fluorescence spectroscopy, NMR spectroscopy, light scattering, and small angle neutron scattering; and thermodynamic studies including calorimetry and volumetric methods.[6] Studies of the interaction of surfactants with water soluble polymers date back to the 1950's with the pioneering work of Saito.[6,72] However, it was a publication by Jones in 1967 which provided the conceptual framework to describe the interaction between surfactants and polymers that is still used today.[73] The

characteristics of the interaction between surfactants and polymers will be introduced in a general way in this section, and discussed in greater detail in Chapter 2.

The addition of a neutral polymer to an aqueous surfactant solution is generally observed to induce aggregate formation, with respect to the surfactant, at a concentration less than the cmc for the surfactant in aqueous solution. This concentration has been termed the critical aggregation or association concentration (CAC), although it is often referred to as T_1 or C_1 by some authors. As the concentration of the surfactant is increased, "binding" of surfactant molecules to the polymer continues until the activity of the surfactant reaches a point where any further increase in surfactant concentration results in the formation of regular surfactant micelles. This point, known as T_2 or C_2, is often referred to as the saturation concentration for the polymer. It is important to clarify, as some confusion exists regarding this issue, that C_2 does not correspond to the point at which the polymer becomes saturated with surfactant, rather it corresponds to the point at which any additional surfactant goes into the formation of regular micelles.[74] It may well be the case that the polymer never reaches a condition of saturation, indeed if the polymer were completely bound by surfactant it would likely result in restriction of the polymer motion giving rise to an entropically unfavorable situation.[7] It is also important to note that the term "binding", used by many authors to describe the nature of the surfactant-polymer interaction, may not be appropriate as it implies an interaction of the surfactant with specific sites on the polymer, as would be the case in a protein-surfactant interaction. It is generally accepted that the addition of the polymer to a surfactant solution results in a modification of the aggregation process and therefore association or aggregation better describes the interaction. The model presented by Jones was further modified by

Cabane based upon observations from NMR experiments using the SDS/PEO system.[75] In this model the polymer interacts at the micelle/water interface with approximately 10% of the polymer monomers being bound to the interface with the remainder of the polymer forming loops in solution, as shown in Figure 1.5.1. Carbon-13 chemical shifts for SDS indicate that the polymer does not penetrate into the core of this micelle, as variations were observed only for the first 3 methylene units of the hydrocarbon chain. This result also provides some insight as to the mechanism of the interaction. The possibilities are: either the polymer replaces hydration water around those methylene groups (in the hydrocarbon chain of the surfactant) near the surface of the micelle, or there is an electrostatic interaction between the polymer and the head group, or a combination of the two. The resulting complex is often referred to as the necklace or string of beads model. This refers to the manner in which the micelles form along the polymer chain and their resemblance to beads on a string or necklace.

Figure 1.5-1: Schematic representation of a surfactant-polymer complex in aqueous solution (taken from reference 76). The polymer represented here is significantly larger than those used in this study.

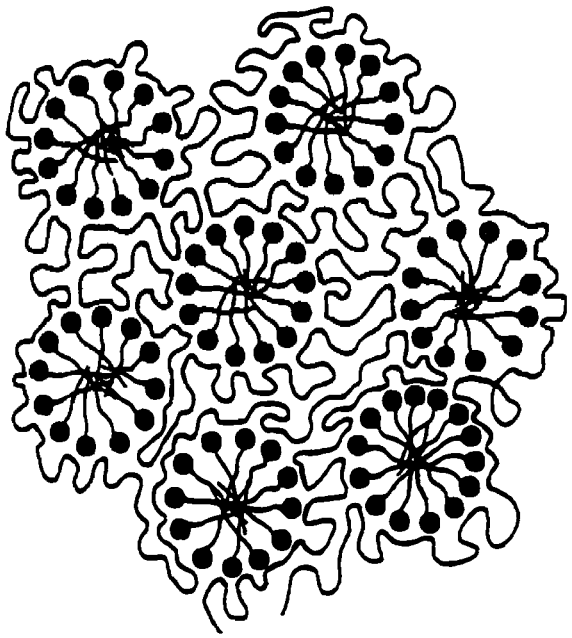

The formation of surfactant-polymer complexes, as for the case of regular micelle formation, is observed from equilibrium dialysis and ion specific electrode measurements to be a cooperative process, though not as strongly cooperative as micelle formation itself.[6] As is the case for regular micelle formation, the association of surfactants with nonionic polymers occurs through a balance of forces, dominated by electrostatic and hydrophobic interactions that include[77]:

i) hydrophobic interactions between polymer and surfactant molecules,
ii) hydrophobic interactions between surfactant molecules,
iii) hydrophobic interactions between polymer molecules,
iv) electrostatic interactions between polymer and surfactant molecules; these may be attractive or repulsive depending on the nature of the surfactant and the polymer,
v) electrostatic interactions between surfactant molecules; these interactions are repulsive in nature and therefore a modification of them due to the presence of the polymer may facilitate surfactant self-assembly, and
vi) electrostatic interactions between polymer molecules.

Obviously, for the case of neutral polymers, contributions from iv) and vi) will be weaker. Indeed the main driving force for association is still the hydrophobic interaction which occurs between surfactant molecules in solution, modified by interactions with the polymer in solution. The hydrophobicity of the polymer plays an important role as a result of this, with stronger interactions occurring for more hydrophobic polymers. For anionic surfactants the strength of the interaction increases in the order PVOH < PEO < MeC < PVAc ≤ PPO ~ PVP, where PVOH is polyvinyl alcohol, MeC is methycellulose, PVAc is polyvinyl acetate, and PVP is polyvinyl pyrrolidone.[72] The order is modified somewhat for cationic surfactants becoming PEO < PVP < PVOH < MeC <PVAc ~ PPO. The main difference is a much weaker interaction for PVP with cationic surfactants. A possible explanation for this difference is a shift of the dipole of the polymer such that the oxygen atom is protonated, leaving a small net positive charge on the nitrogen atom. This would result in an enhanced

interaction with anionic surfactants and a reduced interaction with cationics, as observed.[72] It has also been observed that cationic surfactants, in general, interact with nonionic polymers less strongly than anionic surfactants.[7,9,71,78] As stated previously, this difference has yet to be satisfactorily explained, but it has been attributed to the size of the head group, as well as differences in the structure of water surrounding the head groups.

In addition to the hydrophobicity, the actual structure of the polymer is also observed to play a crucial role in the interaction which occurs between surfactants and neutral polymers in aqueous solution. Polymers which are amphiphilic in nature, such as hydrophobically modified polymers (where alkyl chains are grafted to the polymer backbone) or block copolymers, are known to form hydrophobic microdomains in solution. As a result of this, non-cooperative binding of surfactant has been observed due to a "solubilization" of the surfactant molecule in the existing polymer microdomains. This is usually followed by a cooperative mixed micelle formation, different from the binding process which occurs with unmodified polymers. These interactions are characterized by a single critical micelle concentration as opposed to the two critical concentrations observed for the cooperative binding process described above.

From the above discussion it becomes clear that the nature of the association will be strongly influenced by the nature of the polymer, i.e., whether or not the polymer self-assembles in aqueous solution. For non-amphiphilic polymers, or homopolymers, the assembly process can be described as one in which the cooperative micelle formation process of the surfactant is facilitated by the polymer-micelle association.[19,69,79] The presence of the

polymer in solution results in a reduction of the surfactant chemical potential giving rise to surfactant self-assembly along the polymer chain. Free micelle formation begins when the chemical potential of the surfactant becomes equal to that for the case of micelle formation in aqueous solution, i.e., C_2, which will be dependent upon the polymer concentration. This aggregation process is well described by the "necklace model" of Cabane.[75] The thermodynamics of this process, as well as general observations of properties of surfactant-polymer solutions, will be described in more detail in Chapter 2.

In the case of amphiphilic or hydrophobically modified polymers, the association process becomes more complex. At low surfactant concentrations individual surfactant monomers can be solubilized or "bound" in the hydrophobic microdomains formed by the polymer. This has been observed as a non-cooperative binding in a number of studies.[80-84] As the surfactant concentration is increased the binding becomes anti-cooperative since the addition of a second ionic surfactant molecule to a polymeric microdomain is unfavorable. Finally, as the concentration is further increased, a cooperative binding is observed at a concentration equal to the CAC for the case of interaction with the corresponding unmodified polymer.[69] Alternatively, the process has been described in terms of a mixed micelle formation process where, at low surfactant concentrations, the micelles are dominated by polymer hydrophobes and at high surfactant concentrations the micelles will be dominated by the surfactant molecules.[79,85] In such a case the binding process, assuming ideal mixing and a pseudo-phase separation model of micelle formation, can be described[85] by

$$\beta = \frac{x_{S,b}}{1 - x_{S,b}} = \frac{\left(C_{S,f} / cmc_S\right)}{1 - \left(C_{S,f} / cmc_S\right)} \qquad 1.5\text{-}1$$

where β is the binding ratio of surfactant to polymer, $C_{S,f}$ is the concentration of free surfactant S, and cmc_S is the critical micelle concentration of S. At low surfactant concentrations, $\beta << 1$, the micelles will be similar in nature to those formed by the polymer alone, giving rise to similar solution properties. At high surfactant concentrations, $\beta >> 1$, the micelles and solution properties will be similar to those of a solution of surfactant alone. A transition region where $\beta \approx 1$ is observed at surfactant concentrations where $C_{S,f} \approx cmc_S/2$, i.e., a cooperative association will not be observed until the surfactant concentration is of the order of the cmc. In this transition region the aggregates shift from being polymer dominated to surfactant dominated, which may have important consequences with respect to macroscopic solution properties. An example of the effect of this transition is seen in the viscosity of hydrophobically modified polymer-surfactant systems as compared to that for regular polymer-surfactant systems. In the case of an unmodified polymer the viscosity of a mixed surfactant-polymer system shows little variation in viscosity with increased surfactant concentration, while for a modified polymer the viscosity shows a distinct maximum. The maximum is observed to occur at the CAC or cmc depending upon whether or not the parent unmodified polymer also interacts with the surfactant in question or not, respectively. While the increase in solution viscosity is not well understood[85] (it has been interpreted as an increase in cross-linking of polymers due to the addition of surfactant), the drop in viscosity is attributed to a disruption of the polymer cross-linking network as the micelles become surfactant dominated, i.e., as the surfactant concentration becomes large enough such that the probability of having more than one polymer hydrophobe present in a micelle is low.[69,79,85] It is important to note that in the case of hydrophobically modified polymers, for which the parent polymer shows an association with the surfactant, i.e., exhibits a CAC, the cooperative

process will begin at the CAC observed for the mixed surfactant-polymer system and not the cmc of the surfactant. The implication of this is that interactions may occur between surfactants and modified polymers whereas no interaction is observed between the surfactant and the corresponding un-modified or parent polymer.[85] In such a case the cooperative association process will occur at the surfactant cmc. This model of mixed micelle formation may also be useful in explaining the results of Brackman et al. who have experimentally observed surfactant-polymer interactions with no corresponding reduction of the cmc for the n-octyl thioglucoside/PPO system.[86]

The above discussion is of considerable importance with respect to the systems under investigation in this study. The Pluronics used in this study, as discussed previously, are known to self-assemble in aqueous solution and can be considered to be PEO polymers hydrophobically modified by the addition of a PPO segment. It is therefore possible that the microdomains formed in solution by these polymers may promote the association with cationic surfactants in general, and with the gemini surfactants in particular. There have been a limited number of studies of the interaction of SDS with Pluronics in aqueous solution, with the general conclusion being that the interaction occurs through the more hydrophobic PPO segment.[68,87] Determinations made by Almgren et al.[87] have shown that at low SDS concentrations the aggregates in solution are composed primarily of triblock copolymer molecules with small amounts of SDS and at high concentrations the aggregates are composed primarily of surfactant. These observations lend support for the model proposed by Piculell et al.[79,85] that the interaction of surfactants with hydrophobically modified polymers is analogous to mixed micelle formation.

2. CHARACTERISTICS AND MODELS OF AGGREGATE FORMATION

2.1 Characteristics of micelle formation

The amphiphilic nature of surfactants gives rise to unusual solution properties caused by the dual hydrophobic/hydrophilic character of the molecules. In dilute solutions ionic surfactants behave as typical strong electrolytes. As the concentration is increased the delicate balance of electrostatic and hydration interactions is disrupted and the hydrophobic portions of the molecules attempt to reorganize themselves in a manner which will allow for a reduction of the unfavorable hydrocarbon-water contact. The initial mechanism by which this is accomplished is through accumulation of amphiphilic molecules at an air/water or oil water interface, which allows for the extension of the hydrophobic moeities into the air or oil phase while allowing for the continued solubilization of the hydrophilic portion of the molecule. A consequence of this adsorption of amphiphiles at the interface is a reduction in surface (air/water) or interfacial (oil/water) tension. Once the surface becomes saturated with amphiphile alternative methods for reducing the Gibbs energy of the system must be found. One possible alternative mechanism is phase separation of the amphiphile from solution which would eliminate the unfavourable hydrocarbon-water contacts. The main difficulty with this approach is the removal of the hydrophilic portion of the molecule from water, which would also be energetically unfavourable. The formation of small aggregates, i.e., micelles, provides a compromise and can be thought of as forming discreet microphases in which the hydrophobic alkyl tails are isolated in the core of the aggregate, and the hydrophilic head groups comprise the shell of the aggregate allowing for continuous contact with water. A great deal of experimental evidence suggests that the mobility of the hydrocarbon chains in the micellar core resembles the mobility in a liquid hydrocarbon.

Therefore the isolation of the hydrophobic portion of the micelle does not restrict molecular motion which would result in additional unfavourable energy contributions.

The micelle formation process is a dynamic process in which aggregates of approximately similar size spontaneously begin to form over a narrow concentration range. The size of the micelles formed is governed by the not only the structure of the amphiphile molecule, but also by the solution conditions. The aggregates formed are in a dynamic equilibrium with dispersed monomer, a fact which distinguishes micelles from other association colloids. Once micelles are formed in solution they remain thermodynamically stable, with physicochemical properties distinct from those of the monomeric solution.[88]

The micellization process consists of a delicate balance of forces in the system and will depend upon such considerations as repulsion between head groups, the transfer of the hydrophobic moeties from water, as well as internal packing of the hydrocarbon chains. The Gibbs energy of micellization then can be considered to be comprised of three major contributions:[19]

- a favourable hydrophobic contribution arising from the transfer of the hydrophobic moeties from water into the core of the aggregate,
- a surface term which will account for the two opposing tendencies for the head groups to crowd together in order to minimize water contact with the core of the micelle, and to spread apart due to electrostatic repulsion, hydration, and steric considerations, and
- a packing term which requires water and hydrophilic head groups be excluded from the interior of the aggregate, which will ultimately limit the geometrically accessible forms available to the aggregate.

The surface term will play a major role in the energetics of the system and therefore minimization of this term through geometrical considerations is of crucial importance. For dilute solutions it will be shown in §2.1.3 that the geometry which arises for a given amphiphile can be predicted from the surfactant parameter. It should be noted that at high surfactant concentrations interactions between micellar aggregates can no longer be neglected and changes in aggregate morphology from spherical micelles to alternative morphologies can occur.

2.1.1 Critical micelle concentration

The critical micelle concentration (cmc) is perhaps the most commonly known and extensively studied property of micelle formation in aqueous solution. Several definitions of the cmc have been proposed (see §4.3 reference 88)however the definition provided by Philips[89] has been used the most. The cmc is defined as the surfactant concentration corresponding to the maximum change in a solution property gradient as a function of surfactant concentration, i.e.

$$\left(\frac{d^3\phi}{dC_t^3}\right)_{C_t=CMC} = 0 \qquad 2.1.1\text{-}1$$

where ϕ is the solution property of interest and can be separated into contributions due to the monomeric surfactant and micelles in solution according to

$$\phi = \alpha[S] + \beta[M] \qquad 2.1.1\text{-}2$$

with α and β being proportionality constants, and [S] and [M] are the concentrations of monomer surfactant and micelles, respectively. It is important to note that the cmc obtained from Equations 2.1.1-1 and 2.1.1-2 will be a function of the contribution factors α and β, and

is therefore dependent upon the solution property used in the determination. This means that the cmc for a given surfactant will not be a specific concentration, but rather will be a finite range of concentrations. In spite of this fact cmc values are often reported as a definite concentration in the literature. Experimentally, cmc values are usually determined as a transition or break in a plot of a physical solution property as a function of surfactant concentration (or in some cases log concentration) over a concentration range.

The value of the cmc is dependent upon a variety of parameters including the nature of the hydrophilic and hydrophobic groups, additives present in solution, and external influences such as temperature. The cmc of ionic surfactants has been shown to obey the following relation[90]

$$\log CMC = A - Bn_C \qquad 2.1.1\text{-}3$$

where A and B are constants for a homologous series, and n_C is the number of carbon atoms comprising the alkyl chain of the surfactant. The value for A has been shown to be approximately constant for a particular ionic group. Changing the head group has been shown to have only a small effect on the cmc; however, changes in the counterion, particularly in the valency of the counterion have been observed to have pronounced effects.[90,91] As a counterion is changed from a monovalent to a di- and trivalent the cmc is observed to decrease rapidly.[91] This is due primarily to the increased degree of counterion binding which results in decreased electrostatic repulsion between the ionic head groups. The size of the counterion will also be a determining factor in the value of the cmc, as it has been observed that the cmc increases with increasing hydrated radius of the counterion. This serves to increase ion separation, reducing the effectiveness of the counterion at minimizing

electrostatic repulsion. In addition to variations in the ionic head group or counterion, the cmc can also be influenced by the addition of a strong electrolyte into the solution. This serves to increase the degree of counterion binding, which has the effect of reducing head group repulsion between the ionic head groups, and thus decreases the cmc. This effect has been empirically quantified according to[92]

$$\log CMC = -a \log C_C + b \qquad 2.1.1\text{-}4$$

where a and b are constants for a specific ionic head group and C_C denotes the total counterion concentration. For non-ionic surfactants an increase in the size of the head group, i.e., an increase in the length of the polyethylene oxide segment, is observed to increase the cmc according to

$$\ln CMC = A' + B' y \qquad 2.1.1\text{-}5$$

where y is the number of ethyleneoxide segments comprising the head group, and A' and B' are constants specific to a given hydrophobic group. The addition of an electrolyte to solutions of non-ionic surfactants has a much reduced effect compared to the case for ionic surfactants and is primarily due to a "salting-in" or a "salting-out" of the surfactant.[91]

The value of B in Equation 2.1.1-3 has also been shown to be approximately constant (and equivalent to log(2) for all alkyl chain salts).[91] As a general rule for ionic surfactants, the cmc is halved with the addition of a single methylene unit to an alkyl chain up to a length of 16 carbons. For nonionic surfactants the decrease is even more pronounced, with the decrease being approximately one third its original value with the addition of a methylene group.[90] Branching of the alkyl chain has a small effect on the cmc while the addition of a second alkyl chain to the surfactant has a more pronounced effect. The addition of a

methylene group to the main alkyl chain follows the behavior described by Equation 2.1.1-3. The addition of a methylene group to the secondary alkyl chain is observed to also decrease the cmc; however, not to the same degree as for the main alkyl chain. Tanford suggests that the effect is approximately 60% of that observed for addition to the main alkyl chain.[20]

An important factor to consider when discussing surfactants is the effect that additives (other than electrolytes, which have been discussed above) have on the micellization process. Many industrial and commercial formulations use surfactants in the presence of any number of co-solutes or additives, any one of which can influence the micelle formation process through specific interactions with the surfactant molecules in solution, or by changing the nature of the solvent such that the thermodynamics of the process is altered. Organic materials which have a low miscibility with water are often solubilized, effectively, within micelles in solution, resulting in a solution with a substantial organic content. This generally results in a swelling of the micelle and often gives rise to changes in aggregate morphology. Not unexpectedly, this gives rise to changes in the energetics of the system, and the combined effect usually is to decrease the cmc of the resulting system. Organic materials which have a substantial miscibility with water (such as short-chain alcohols, glycols, and polar organic solvents) have only a minor effect when present under dilute conditions. The major effect of such additives is a reduction of the dielectric constant of water resulting in decreased electrostatic interactions between head groups and thus a decrease in the cmc. At high concentrations these additives can be considered co-solvents and as a result the solvent properties of the system will change. This can result in a decrease in the energy requirements of the transfer of the hydrophobic tails from the micelle to the bulk solution, thus increasing

the cmc. The addition of longer chain alcohols generally causes a decrease in the cmc, and is attributed to the surface activity of such molecules, i.e., a preferential adsorption at interfaces, and a strong desire to form mixed micelles.

The effect of variations in temperature is remarkably different when considering ionic as opposed to non-ionic surfactants. Ionic surfactants exhibit a minimum in the cmc as a function of temperature, typically in the broad range of 0-70°C. This behavior is reflective of the competing effect that an increase in temperature has on the hydrophilic and hydrophobic portions of the molecule. As the temperature is increased, a decrease in the hydration of the head group occurs. This results in a loss of energetic factors favoring solvation of the molecule as opposed to micelle formation, thus enhancing the tendency for micelle formation. In contrast to this, the weakening of water structure that accompanies a temperature increase gives rise to a decrease in the hydrophobic hydration of the alkyl tail, increasing its solubility. This serves to impede micelle formation and the relative magnitude of these two effects determines whether an increase or a decrease in the cmc will be observed.

The temperature dependence of the cmc for polyoxyethylene non-ionic surfactants is dominated by the hydrogen bonding interactions which occur between water and the ethylene oxide segments. As with all materials which rely on hydrogen bonding for solubilization in aqueous solutions, these surfactants show an inverse temperature/solubility relationship. As a result the cmc is observed to decrease with increasing temperature. If the temperature is increased high enough the so-called "cloud point" of the surfactant is reached. Phase

separation occurs into an aqueous phase and one containing a high fraction of surfactant. Similar behavior has been observed for the PEO-PPO-PPO triblock copolymers; however, the situation is further complicated by a strong dependence of the cmc on the PEO/PPO mass ratio within the polymer.

2.1.2 Mean aggregation number

Another important property of micelle formation is the mean aggregation number which provides direct information about the general size and shape of the aggregates formed by amphiphiles in solution, and how these properties are related to the molecular structure of the amphiphile.[93] The mean aggregation number refers to the number of surfactant monomers that, on average, assemble to form a supermolecular structure, i.e., a micelle. The most common shape of micellar aggregates in solution is spherical, and hence these are the most extensively studied. As mentioned previously the main driving force for the self-assembly of surfactant monomers into micelles is to minimize the hydrocarbon-water contacts in solution. For this reason, the lower limit of the number of surfactant monomers that form a micelle is dictated by the minimum number that must come together to effectively shield one another from contact with water.[20] The very fact that discrete aggregates, typically containing on the order of 100 monomers or less, are observed in solution implies that there must exist a force which opposes aggregate growth, or otherwise phase separation would be the eventual result. In ionic surfactants electrostatic repulsion between the ionic head groups at the micellar surface provides the major contribution to this opposing force. In the case of non-ionic surfactants steric effects as well as a preference for the hydration of the head group oppose micelle formation.[20] Micelle formation therefore represents a cooperative process whereby a

number of surfactant monomers come together through a compromise of opposing forces. It is important to note that micelles are not "monodisperse" in nature, i.e., they do not have a uniform size of a fixed number of monomers. Rather there exists a distribution of aggregate sizes from which the average number of monomers contained in a micelle is taken as the mean aggregation number, N_{agg}.

The effect that internal (such as the structure of the hydrophilic and hydrophobic moeties) and external (temperature, pressure, additives) influences have on the size and dispersity of micelles in solution often makes it difficult to place any significance on reported values of the mean aggregation number. Nevertheless some generalizations can be made:[91]

- as the length of the hydrocarbon chain is increased in a homologous series of surfactants, N_{agg} is observed to increase,
- a decrease in the "hydrophilicity" of the head group (i.e., greater counterion binding for ionics, or a reduction of the polyoxyethylene segment in non-ionics) leads to an increase in N_{agg},
- external factors, such as increased electrolyte concentration, which serve to reduce the "hydrophilicity" of the head group, will increase N_{agg}, and
- an increase in temperature results in small decreases in N_{agg} for ionic surfactants and significantly large increases for non-ionic surfactants (the latter is due primarily to the cloud-point phenomenon introduced previously).

As well, the effect of organic additives such as short chain alcohols, which are solubilized predominantly in the aqueous phase as opposed to the micellar phase, have been observed to increase or decrease N_{agg} for ionic surfactants depending upon the alcohol concentration.[90] Longer chain alcohols such as pentanol and hexanol, which are only moderately soluble in water, partition between the aqueous and micellar phases and are observed to increase N_{agg} at low alcohol concentrations. Alcohols (and other organic additives) with low water solubility are almost entirely solubilized in the interior of the micelle, and are generally

observed to cause an increase in N_{agg}. This may be due to a co-micellization phenomenon in which the actual number of surfactant molecules in the aggregate decreases (a likely case for longer chain alcohols), or due to a swelling of the hydrophobic core of the aggregate which would in turn lead to a decrease in repulsion between head groups and an increase in N_{agg}.

2.1.3 Micelle structure and shape

It is well known that the structure and shape of amphiphilic aggregates is often directly related to the application of the amphiphile in various systems.[93] An understanding of aggregation behavior such that predictions of aggregate size and shape can be made is therefore one of the critical aspects of continued research into micellar systems. If one recalls the various contributions to the Gibbs energy of micelle formation (c.f. §2.1) it is obvious that the molecular composition of the amphiphile will play a dominant role in determining the structure of the aggregate formed. It is generally accepted that aggregates formed from ionic surfactants near the cmc will be spherical in nature just above the cmc. This is similar to the model proposed in 1936 by Hartley, in which the hydrocarbon tails comprise the core of the aggregate and the head groups and bound counterions are situated at the micellar surface in what is known as the Stern layer. The degree of micelle ionization (α) is a measure of the number of counterions which are dissociated from the micelle and can be found in the electrical double layer which surrounds the micelle, termed the Gouy-Chapman layer.[90] Typically the degree of ionization is in the range of 0.2 – 0.5 implying that, correspondingly, anywhere from 80 - 50% of the counterions are bound in the Stern layer of the micelle.

Basic geometry places some limitations on the configuration of the aggregates adopted by surfactants in solution. The volume (in $Å^3$) of the hydrocarbon core of a micelle can be estimated according to[20]

$$V_{core} = m(27.4 + 26.9n_C') \qquad 2.1.3\text{-}1$$

where m is the number of hydrocarbon chains comprising the core of the micelle (m will be equivalent to N_{agg} for traditional single tail surfactants, and equivalent to $2N_{agg}$ for gemini or dialkyl surfactants), and n_C' is the number of carbon atoms of the chain which are located in the micellar core. Since it is not reasonable to allow for vacant space in the center of the micelle, the radial dimension is restricted to the fully extended length of a hydrocarbon chain which can be obtained (in Å) from[20]

$$l_{max} = (1.54 + 1.265n_C') \qquad 2.1.3\text{-}2$$

For a spherical micelle this will be equivalent to the radius of the micelle. For a surfactant having a hydrocarbon chain length of 12, Equations 2.1.3-1 and 2 would predict a mean aggregation number of 56. It is well established that many surfactants have aggregation numbers larger than this in the absence of any additives. This is due, in part, to the existence of an optimal head group area which satisfies the restrictions imposed by the principle of opposing forces outlined above. This implies that there is a tendency to form aggregates such that the surface area to volume ratio remains constant, which can only be achieved by changes in aggregate structure. The shape of micellar aggregates in solution can effectively be predicted by the surfactant packing parameter, P, according to[16]

$$P = V_{hc} / a_0 l_{hc} \qquad 2.1.3\text{-}3$$

where V_{hc} is the volume of the hydrocarbon tail of the surfactant (Equation 2.1.3-1), a_0 is the optimal head group area, and l_{hc} is the length of the hydrocarbon chain (Equation 2.1.3-2).

Aggregate shapes predicted by the packing parameter are: P = 1/3, spherical; P = 1/2 cylindrical or rodlike; P = 1, bilayers; and P > 1 inverted micelles.[16] For molecules with packing parameters lying between 1/3 and 1/2 or between 1/2 and 1, the molecules may assemble into highly symmetrical aggregates which are slightly different from that for the optimal condition (i.e., ellipsoidal for molecules with P slightly larger than 1/3).[19]

2.2 Models of Micelle Formation

Two models have gained general acceptance for use in describing the micelle formation process and thereby allow for the relation of macroscopic equilibrium thermodynamic measurements to molecular processes. They are the pseudo-phase separation model[94-97], which treats micelles as a separate phase formed at and above the cmc, and the mass-action model[96,98-101], which considers surfactant monomer in solution to be in equilibrium with micelles of a fixed size above the cmc. An extension of the mass-action model is the multiple equilibria model[69,102], which considers the formation of aggregates of various sizes, accounting for the observed polydispersity in aggregation numbers. However, this introduces a large number of variables into any analysis of experimental data making it difficult to apply. The pseudo-phase separation model has been shown to account for, at least semi-quantitatively, the observed concentration dependence of apparent molar properties and has been useful in deriving thermodynamic functions of micellization using both apparent and partial molar properties. The main criticism of this model is that calculated values often show substantial deviation from experimental values for some properties, particularly if the transition from monomer to micelle formation occurs over a broad concentration range. Nevertheless, because of the simplicity of its application, the

pseudo-phase model is widely used to model thermodynamic data, particularly for long-chain surfactants having low cmc values.[102] The mass action model allows for modeling of thermodynamic properties over a broader concentration range, i.e., pre-micellar range as opposed to the pseudo-phase model which is applicable only in the post-micellar range. As well, prediction of aggregation numbers can be made from the mass action model, and it has been more successfully applied to short-chain surfactants.

2.2.1 Pseudo-phase separation model

As stated above, the pseudo-phase separation model considers the formation of micelles to constitute the formation of a separate phase. An underlying argument for this assumption is that the activity of the monomer surfactant remains constant above the cmc, as is seen very often in surface tension measurements by the near constant value of the surface tension. The cmc can therefore be considered as the solubility limit of the monomeric species. This has been the major source of criticism for the pseudo-phase model as a number of measurements have shown that the activity of the monomer surfactant decreases above the cmc.

At equilibrium, the chemical potential of the surfactant in the monomer and micellar forms (μ_S and μ_M, respectively) are equivalent, i.e.,

$$\mu_S = \mu_M \qquad 2.2.1\text{-}1$$

The chemical potential of the monomeric surfactant is given by

$$\mu_S = \mu_S^o + RT \ln x_S \qquad 2.2.1\text{-}2$$

where μ^o_S is the standard state chemical potential of the monomer surfactant, and x_S is the mole fraction of monomers. Note that activities have been neglected since the assumption of

ideality is a reasonable one for the dilute conditions generally observed for surfactants. Because the micelles are assumed to be in their standard states $\mu_M = \mu^o_M$ and the standard Gibbs energy change due to micelle formation, ΔG^o_{mic}, is given by

$$\begin{aligned} \Delta G^o_{mic} &= \mu^o_M - \mu^o_S \\ &= \mu_M - \mu_S + RT \ln x_S \\ &= RT \ln x_S \end{aligned} \qquad 2.2.1\text{-}3$$

If we recall that the cmc can be considered to be the solubility limit of the free monomer, then $x_S = x_{cmc}$ and we obtain

$$\Delta G^o_{mic} = RT \ln x_{cmc} \qquad 2.2.1\text{-}4$$

where x_{cmc} is given by

$$x_{cmc} = \frac{n_S}{n_S + n_{H_2O}} \approx \frac{n_S}{n_{H_2O}} \qquad 2.2.1\text{-}5$$

since n_S is typically much less than n_{H_2O}. Converting into concentration units, one obtains

$$\Delta G^o_{mic} = RT[\ln cmc - \ln 55.1] \qquad 2.2.1\text{-}6$$

where 55.1 is the molar concentration of water at 25°C. The above treatment does not consider the case of ionic surfactants, for which one must take into consideration the transfer of a portion of counterions into the micellar phase, such that Equation 2.2.1-3 becomes

$$\Delta G^o_{mic} = RT \ln x_S + (1-\alpha) RT \ln x_C \qquad 2.2.1\text{-}7$$

where α is the degree of micelle ionization, and x_C is the mole fraction of bound counterions. Equation 2.2.1-7, with appropriate substitution, for a 1:1 ionic surfactant reduces to

$$\begin{aligned} \Delta G^o_{mic} &= (2-\alpha) RT \ln x_{cmc} \\ &= (2-\alpha) RT[\ln cmc - \ln 55.1] \end{aligned} \qquad 2.2.1\text{-}8$$

For the gemini surfactants, which dissociate into 3 ionic species the term (2-α) is replaced by (3-2α).

The enthalpy of micellization can be determined directly from the variation of the Gibbs energy, or more specifically the cmc, with temperature according to

$$\Delta H^{\circ}_{mic} = -RT^2\left(\frac{\partial \ln x_{cmc}}{\partial T}\right) \qquad 2.2.1\text{-}9$$

for nonionic surfactants. For ionic surfactants a term of including α must be included to account for the counterion binding. Alternatively, the enthalpy change can be determined experimentally using calorimetric methods. Direct measurement of the thermodynamic properties is generally preferable since Equation 2.2.1-9 assumes that there is no variation in the properties of the micelle with a corresponding variation in temperature, i.e., the only variation is in the relative concentrations of monomers and micelles in the solution. This is obviously an oversimplification, and it is well established in the literature that changes in physical parameters, such as the temperature and pressure, impact the size and shape of the micelle, the polydispersity of the aggregates, and the degree of micelle ionization. Typically the agreement between ΔH°_{mic} values obtained from variations of the cmc as a function of temperature agree poorly with those obtained from direct calorimetric measurement for ionic surfactants, with better agreement obtained for nonionic surfactants.[88] Also, no information regarding the thermodynamic properties of the surfactant in its monomeric and micellized state can be obtained from application of Equation 2.2.1-9, whereas such information is readily available from direct measurement of the property of interest. Regardless of the

manner in which $\Delta H°_{mic}$ is determined, the entropy of micellization generally is determined from $\Delta G°_{mic}$ and $\Delta H°_{mic}$ in the usual manner.

The volume change due to micelle formation can also be determined in two ways, the first is from the pressure derivative of the Gibbs energy in a manner analogous to that used for the enthalpy

$$\Delta V°_{mic} = RT\left(\frac{\partial \ln x_{cmc}}{\partial P}\right) \qquad 2.2.1\text{-}10$$

where again a factor of containing α should be included to account for counterion binding in the case of ionic surfactants. The above discussion with respect to the usefulness of such an approach is also applicable here and therefore direct measurement of the volume property is preferred. Apparent molar volumes for aqueous solutions are easily determined from experimental measurements of density (c.f. §3.2.2). The partial molar volume, $\overline{V}_S$, of a solute in solution is related to the apparent molar volume, $V_{\phi,S}$, according to

$$\overline{V}_S = V_{\phi,S} + m_S\left(\frac{\partial V_{\phi,S}}{\partial m_S}\right)_{T,P} = \frac{d\left(m_S V_{\phi,S}\right)}{dm_S} \approx \frac{\Delta\left(m_S V_{\phi,S}\right)}{\Delta m_S} \qquad 2.2.1\text{-}11$$

where m_S is the molality. It can be seen that, in the limit of zero concentration, the apparent molar volume becomes equivalent to the standard partial molar volume. Assuming a pseudo-phase separation model, the apparent molar volume for the surfactant above the cmc can be fit to[94,95,97]

$$V_{\phi,S} = V_{\phi,M} - \frac{CMC}{m_S}\Delta V_{mic} \qquad 2.2.1\text{-}12$$

where $V_{\phi,M}$ is the apparent molar volume of the surfactant in the micellar state, and ΔV_{mic} is the volume change due to micelle formation. The apparent molar volume for the monomer surfactant at the cmc can be taken as the difference between $V_{\phi,M}$ and ΔV_{mic} and for dilute concentrations is approximately equivalent to the standard partial molar volume for the monomer surfactant, $V°_S$. As stated previously it can be seen that more information can be obtained from direct measurement of the thermodynamic property as opposed to measuring variations in the cmc as a function of temperature and pressure and relating these to the appropriate property. It will be seen below that additional information regarding the system is available from thermodynamic studies, with application of the more complex mass action model.

2.2.2 Mass action model

The mass action model is a more appropriate description of the micellar process as it considers the surfactant monomer and micelles to be in equilibrium with one another, i.e.,

$$nS \xleftrightarrow{K_M} M \qquad 2.2.2\text{-}1$$

where M refers to a micelle comprised of n surfactant monomers. The equilibrium constant for the micelle formation process, K_M, is given by

$$K_M = \frac{x_M}{x_S^n} \qquad 2.2.2\text{-}2$$

where x_M and x_S are the mol fractions of micelles and monomers, respectively. The molar Gibbs energy due to micelle formation is calculated in the usual manner from

$$\Delta G^\circ_{mic} = -\frac{RT}{n}\ln K_M = \frac{RT}{n}[n \ln x_S - \ln x_M] \qquad 2.2.2\text{-}3$$

To obtain an expression for $\Delta G°_{mic}$ as a function of the cmc, one must then relate K_M to the cmc. A number of methods have been employed to do this, all of which are dependent upon the definition of the cmc used. For example, Moroi[88] has derived an expression for K_M as a function of the cmc based upon the strict definition of the cmc given by Philips[89], while Desnoyers et al.[99,102] have derived an expression based upon the concentration at which the fraction of surfactant in the monomer form shows an inflection ($\partial^2\alpha_0/\partial m^2 = 0$, where α_0 is the monomer fraction, and m is the surfactant molality). Regardless of which definition is used for the cmc, the resulting expression for $\Delta G°_{mic}$ is usually a function of both the cmc and the aggregation number for the micelles formed. When N_{agg} is large, the expressions reduce to Equation 2.2.1-4, or in the case of ionic surfactants, Equation 2.2.1-8.

As in the case of the psuedo-phase model, other thermodynamic properties can be derived from expressions of $\Delta G°_{mic}$ and can be studied through variations of the cmc with temperature and pressure. The resulting expressions are generally more complex than those obtained from the pseudo-phase separation model, and may not be applicable if N_{agg} also varies as a function of temperature or pressure, as is often the case. Desnoyers et al. have derived general expressions for experimentally determined thermodynamic properties as a function of surfactant concentration based upon the mass action model.[99,102] For volumes V_ϕ is given by (for ionic surfactants)

$$V_\phi = \alpha_0[V^0 + A_V\sqrt{\alpha_0 m} + B_V\alpha_0 m] + (1-\alpha_0)[V^M + (1-\alpha_0)C_V m] \qquad 2.2.2\text{-}4$$

where α_0 is the fraction of surfactant monomer in the aqueous phase, A_V is the Debye-Hückel limiting slope, V^0 is the partial molar volume of the surfactant at infinite dilution, V^M is the

partial molar volume for the surfactant in the micellar form, and B_V and C_V are the pair-wise interaction terms for surfactant monomers and micelles, respectively. The volume change due to micelle formation, ΔV_M, is calculated from V^0 and V^M according to

$$\Delta V_M = V^M - V^0 - A_V\sqrt{\alpha_0 m} - B_V\alpha_0 m \qquad 2.2.2\text{-}6$$

Therefore, it is obvious that a detailed thermodynamic study can provide not only information about the thermodynamic property under investigation in both the monomer and micellar states, but also information regarding the size of the aggregates formed as well as information regarding intermolecular and interaggregate interactions. The main limitation of this model is the requirement of a considerable amount of experimental data over the entire surfactant concentration range (i.e. premicellar, transition, and postmicellar regions). Due to instrumental limitations, this requirement can be difficult to fulfill, particularly for the premicellar region, for those surfactants having low cmc values. As a result, the mass-action model is more appropriately applied to surfactants having short alkyl chains which have reasonably high values of the cmc.

2.3 Characteristics of surfactant – polymer aggregate formation

As introduced in §1.5, the interaction of surfactants with polymers occurs through a balance of forces similar to that observed for micelle formation in aqueous solution. The interaction process is characterized, typically, by two critical concentrations, the CAC and C_2, which correspond to the concentration at which mixed aggregates begin to form, and the concentration where free micelles begin to form, respectively. Due to the similarities between the complex formation process and micelle formation, many of the observed effects

of variation in the temperature, pressure, solution composition, and surfactant structure seen in micelle formation are also observed in the case of mixed surfactant-polymer systems. In the latter case one must also be cognizant of influences due to the structure and conformation of the polymer, factors which were introduced in Chapter 1.

Recall that the effect of an increase in temperature is to induce complex behavior with respect to the cmc of ionic surfactants, due to the competing effects on the hydrophilic and hydrophobic portions of the surfactant molecule. In the case of surfactant-polymer aggregate formation, an increase in temperature is generally observed to increase the CAC as the formation of a surfactant-polymer complex is inhibited by the increased solubility of the polymer.[6] However, it should be noted that for hydrophilic polymers, which do not interact well with cationic surfactant in particular, an increase in temperature can induce an interaction when none is observed at low temperatures.[103]

The addition of added salt has an effect similar to that observed in micelle formation, specifically, increases in electrolyte concentration serves to decrease the CAC. Murata et al. have shown for the polyvinyl pyrrolidone/SDS system that the log of the CAC decreases linearly as a function of the log of the sodium ion concentration. Interestingly, the slope of this plot was found to be identical to that for a plot of log cmc as a function of log[Na^+].[104] It is noted that increased electrolyte concentration has only a negligible effect on C_2, which combined with the decrease in the CAC, serves to increase the binding ratio of surfactant to polymer.[6]

With respect to the structure of the surfactant, it is not surprising that, analogous to observations of the cmc, an increase in the length of the alkyl chain serves to decrease the CAC in a linear fashion, similar to Equation 2.1.1-3. Arai et al.[105] have shown that the Gibbs energy change per methylene group for the transfer of an alkyl chain into a surfactant-polymer complex is comparable to that for the transfer into a micelle. This points to the relative similarities of the respective aggregation processes. The main impact that surfactant structure has on surfactant-polymer interactions has already been alluded to in Chapter 1, i.e., the importance of the surfactant head group. The most significant observation is the relative strengths of the interaction of polymers with anionic versus cationic surfactants. Cationic surfactants in general have been confirmed to show a much weaker interaction with neutral polymers as compared to anionic surfactants of similar chain lengths (see reference 77 and references therein). The most accepted explanation for this phenomenon is the role played by steric hindrance, due to the larger head groups of the cationic surfactants, which effectively restricts access to the polymer. This mechanism has been modeled by Nagaragan[76,106] and Ruckenstein[107,108] in thermodynamic models proposed for the surfactant-polymer interaction. A criticism of this explanation is that weak interactions are also observed for cationic surfactants with small head groups, such as primary alkylammonium halide surfactants, for which steric hindrances are expected to be less.[77] Obviously, steric considerations is not the only contributing factor, and other explanations deal primarily with the way in which anionic and cationic surfactants interact with the hydration shell of the polymer. As a final note with respect to surfactant structure it is generally observed that no interaction occurs between nonionic surfactants and polymers in aqueous solution; however, the possibility of interactions between nonionic surfactants and

hydrophobically modified polymers remains to be investigated. It is likely that interactions similar to mixed micelle formation may occur, analogous to those observed between ionic surfactants and hydrophobically modified polymers.

The interaction of surfactants with polymers is observed to be independent of the polymer molar mass, provided the molar mass is above a minimum value. However, the lower limit of the molar mass differs for different polymer systems. The CAC is also observed to be relatively insensitive to increases in polymer concentration, while C_2 increases linearly with polymer concentration. Finally, as mentioned in §1.5, the hydrophobicity of the polymer plays a significant role in the interaction, with more hydrophobic polymers showing a stronger interaction, i.e., a lower CAC value.

A number of studies have focused on the surfactant aggregation number in mixed surfactant-polymer systems in order to investigate the structure of the resulting complex (see reference 109 and references therein). Generally, the aggregation number is observed to decrease, relative to those for the aqueous surfactant; however, the effect is concentration dependent. As the surfactant concentration increases, so will the aggregation number until a value similar to that for the aqueous system is reached. Brackman has also shown that the presence of the polymer can induce morphological changes in the aggregates, where both anionic[86] and cationic[110] surfactants that form rod-like aggregates in aqueous solution are observed to form smaller, spherical aggregates in the presence of neutral polymers.

The conformation of the polymer chain is an additional structural aspect of the resulting surfactant-polymer complex and has important implications with respect to the rheological behavior of the resulting solution. Measurement of solution viscosities provides an effective method for examining conformational changes of the polymer in mixed systems. A dramatic increase in viscosity is typically observed at the CAC for surfactant-polymer systems. This is a result of the polyelectrolyte effect which occurs as ionic surfactant builds up long the polymer chain. Repulsion between the surfactant aggregates associated with the polymer chain results in a more extended conformation of the polymer chain as compared to the aqueous polymer solution, giving rise to increased viscosity.

2.4 Models of surfactant – polymer aggregate formation

Several theoretical models have been developed in an attempt to predict or explain the observed behavior of mixed surfactant-polymer systems. Many of the more recent models are refinements of the model proposed by Gilanyi and Wolfram which was the first quantitative model that could account for the strongly cooperative behavior observed in these systems.[111] The model was further developed by Nagarajan[76,106] and Ruckenstein[107,108] to account for specific contributions to the Gibbs energy of complex formation. Assuming a mass action model for the aggregation process, the Gibbs energy for the transfer of an ionic surfactant from solution into a polymer bound complex, of size m, is given by[111]

$$\Delta G^{\circ}_{m} = RT\ln[S^{-}] + RT(1-\alpha)\ln[C^{+}] - \frac{RT}{m}\ln\left(\frac{[complex]}{[P_0]-[complex]}\right) \qquad 2.4\text{-}1$$

where $[S^{-}]$, $[C^{+}]$, and [complex] are the equilibrium concentrations of surfactant, counterion and surfactant-polymer complex, respectively. $[P_0]$ represents the concentration of "active"

sites, specifically the segments of the polymer where the interaction occurs, i.e., binding sites. The total surfactant concentration, X_t, expressed as a function of monomer surfactant concentration, X_1, is given by[76,107]

$$X_t = X_1 + g(KX_1) + g_b n X_p \left[\frac{(K_b X_1)^{g_b}}{1 + (K_b X_1)^{g_b}} \right] \qquad 2.4\text{-}2$$

where X_p is the polymer concentration, n is the number of binding sites, g and g_b are the aggregation numbers of the free and polymer-bound aggregates, respectively, and K and K_b are the formation constants for free and polymer-bound aggregates, respectively. Alternatively, a pseudo-phase separation model can also be adopted for which the Gibbs energy change is given by

$$\Delta G_m^\circ = RT(2-\alpha)\ln CAC + \frac{RT}{m}\ln C_P \qquad 2.4\text{-}3$$

where C_p is the polymer concentration.

The treatments of the Gibbs energy of complex formation of Nagarajan and of Ruckenstein are quite similar and will be treated together. The Gibbs energy change for the micelle formation process in the absence of added polymer, in terms of chemical potentials, can be written as the sum of a number of contributions according to[76,107]

$$\begin{aligned} \Delta\mu_g^\circ &= \mu_g^\circ - \mu_1^\circ \qquad 2.4\text{-}4 \\ &= \Delta\mu_{HC/w}^\circ + \Delta\mu_C^\circ + \sigma(a - a_s) - kT\ln(1 - \frac{a_p}{a}) + \Delta\mu_{elect} \end{aligned}$$

The first term of Equation 2.4-4 ($\Delta\mu^\circ_{HC/W}$) accounts for the transfer of the alkyl tail from an aqueous to a liquid hydrocarbon environment. The second term is a correction factor for the first term and accounts for the decrease in conformational freedom of the alkyl chains in the

core of the micelle as a result of the polar head groups being restricted to the micelle/water interface. The third term primarily accounts for the formation of the micelle/water interface and includes contributions from residual contact between the hydrocarbon core and water. Here σ is the interfacial tension, a is the area of the surfactant molecule at the interface, and a_s is the area per surfactant molecule which is shielded from water by the head group. The fourth term accounts for steric repulsion between the head groups at the interface, where a_P is the cross-sectional area of the head group, and the fifth term accounts for electrostatic interactions. Expressions can be written which allow for the calculation of $\Delta\mu^{\circ}_{HC/W}$, $\Delta\mu^{\circ}_{C}$ and $\Delta\mu^{\circ}_{elect}$ and both Nagarajan's and Ruckenstein's treatments assume that these terms are not affected by the addition of polymer to the solution. Differences between the approaches arise in the treatment of the interfacial term. In Nagarajan's model, the interfacial term becomes $\sigma(a-a_{pol}-a_s)$, where a_{pol} is the area per surfactant molecule which is in covered by polymer and accounts for additional shielding of the aggregate core.[76] This also results in increases in steric repulsion between head groups at the interface and, therefore, an additional term is also included in the fourth term of Equation 2.4-4 to become $\ln(1-(a_P/a)-(a_{pol}/a))$. Ruckenstein's treatment varies in the way in which the effect of the polymer on the formation of the interface is handled.[77,107] Two cases are considered, the case where the head group area, a_P, is less than the cross-sectional area of the hydrocarbon chain, a_h, and the other where a_P is greater than a_h, such that

$$\begin{aligned} \text{interface term} &= (\sigma-\Delta\sigma)(a-a_p)+\sigma(a_p-a_h)+a_p\Delta\sigma_p \text{ for } a_p > a_h \\ &= (\sigma-\Delta\sigma)(a-a_p)+a_p\Delta\sigma_p \text{ for } a_p < a_h \end{aligned} \qquad 2.4\text{-}5$$

where $\Delta\sigma$ and $\Delta\sigma_p$ are the changes in interfacial tension between the hydrocarbon core and water, and between the head groups and water, respectively. This treatment therefore makes

a distinction between the effect of the polymer on the head group-water interface, and the hydrocarbon-water interface; however, in the original treatment, $\Delta\sigma$ and $\Delta\sigma_p$ were assumed to be equal. In order to account for the case of specific surfactant polymer interactions (which the above models do not consider), Ruckenstein has revised his original model and removed this restriction such the model is able to predict conditions where interactions occur between surfactants and polymers with no corresponding decrease in the cmc.[108]

The main criticism of these above treatments is that many parameters used to characterize the resulting surfactant polymer complex are difficult to evaluate, but are apparently crucial to the interaction.[77] Additionally, the treatment of electrostatic interactions, with the assumption that the polymer has no influence on these interactions, is unreasonable. The model has been further developed by Nikas and Blankschtein[2] who attempted to refine, not only the treatment of electrostatic effects (in particular to account for repulsion between polymer bound aggregates which competes with elastic restoring forces in the polymer), but also effects of solvent quality, specific surfactant polymer interactions, and polymer hydrophobicity and flexibility. Nagarajan also revised his model to account for specific surfactant polymer interactions, and also to examine interactions with surfactant aggregates other than spherical micelles, the structure most commonly assumed.[106]

It is also important to note that the above treatment assumes that conformational changes that result from the formation of the complex have no effect on the formation constant for the polymer bound aggregates, the size of the aggregates, or the availability of binding sites (K_b, g_b, and n in Equation 2.4-2). It has been noted that this assumption is reasonable for rigid

polymers, but is questionable for flexible polymers that can show significant conformational changes upon self-assembly. Diamant et al.[112] have proposed a theory which approaches the process of complex formation, not from the traditional view of the effect of the polymer on the surfactant aggregation process, but from the view of the effect of the surfactant on the properties of the polymer. In such a model the CAC is considered to be a direct result of conformational changes in the polymer, and as such this theory has been shown to account for the behavior of hydrophobically modified polymer-surfactant systems.

All the above models allow for the prediction of aggregate properties such as the CAC and the aggregation number for the polymer-bound aggregates, with refined models providing additional information regarding the number of and distance between bound aggregates, and the overall length of the resulting complex. However, the application of such models to experimental data is difficult, due to the complexity of the models and specifically, regarding the number of parameters involved. The models do generally implicate the importance of the interfacial interactions at the micelle/water interface, with recent refinements pointing to the importance of specific surfactant-polymer interactions, similar to those that may occur with hydrophobic microdomains formed by some polymers in solution.

3. EXPERIMENTAL METHODS

3.1 Materials

The Pluronics compounds used in this study were a gift from BASF and were used without further purification. The molar mass distributions have been checked using size exclusion chromatography, and the relative molar masses were estimated by acetylation of the polymer and back titration of the unreacted acetylation reagent.[64] The EO/PO mass ratios have been confirmed using ^{1}H NMR methods through comparison of the integrated intensities for resonance signals for the methyl and methine groups of the PO segment with those of the methylene units due to both the PO and EO segments. The water content was estimated by carrying out a Karl Fisher titration. It is generally accepted that the level of impurities, i.e., diblock copolymers and mono-polymers, found in triblock copolymers has little effect on the properties of the polymer, especially when one considers the effect of polydispersity in the molar mass of the copolymer. It has been shown in several studies that purification of Pluronics by hexane extraction results in no significant changes in experimental results.[113,114] Information regarding the relative molar masses, as well as the content of PEO and PPO is provided in Table 3.1-1. PEO (average molar mass 4000, BDH) and PPO (average molar masses 725 and 2000, Aldrich) were also used as provided. With respect to the nomenclature of these compounds the letter refers to the physical nature of the material with F, P, and L standing for flake, paste, and liquid, respectively. The last digit of the numeric designation refers to the percentage of PEO in the polymer, i.e., the Pluronic F108 contains 80% PEO by mass. When the digits between the letter and the last digit of the name are the same, then the polymers have the same PPO content; for example, P103 and F108 both have a PPO content of 3250 amu.

Table 3.1-1 Composition of triblock copolymers

Pluronic	Molar Mass (amu)	wt % PEO	N_{EO}	N_{PO}	PO/EO mass ratio
F68	8700	80	158	30	.25
F108	16250	80	224	56	.25
P103	4640	30	32	56	2.3

The gemini surfactants used in this study were synthesized according to procedures previously established in the literature.[14,33,45] Whenever possible starting materials were purified by vacuum distillation before reaction. With the exception of those surfactants specifically listed below, all compounds were synthesized by reflux of the appropriate α,ω-dibromoalkane with 2 molar equivalents (plus a 10% excess) of the appropriate N,N-dimethylalkylamine. The reflux was carried out in HPLC grade acetonitrile (except for the 8-3-8 and 10-3-10 surfactants, which were carried out in 2-propanol) for 24 to 48 hours. After cooling of the reaction mixture, the solid material was recovered by filtration and recrystallized from acetonitrile or a mixture of acetonitrile/ethyl acetate where appropriate. Characterization of the surfactants was confirmed using CH&N analysis, ^{1}H NMR (for the 12-3-12 surfactant) and cmc determinations. The results of the CH&N and NMR analyses are given in Appendix A. In all cases the surfactants were recrystallized, repeatedly, until no surface-active impurities were detected by surface tension analysis.

N,N'-bis(dimethyldodecyl)-1,2-ethanediammonium dibromide (12-2-12): The 12-2-12 surfactant was synthesized by reaction of 1 equivalent of N,N,N',N'-tetramethylethylenediamine (Aldrich) with 2 equivalents (plus a slight excess) of 1-bromododecane (Aldrich) in acetonitrile under reflux for 48 hrs. After cooling, a white solid was recovered by filtration and then was recrystallized from acetonitrile.

(p-Phenylenedimethylene)-bis(dimethyldodecylammonium bromide) (12-ϕ-12): The 12-ϕ-12 surfactant was synthesized by reaction of α,α'-dibromo-p-xylene (Aldrich) dissolved in THF with excess N,N-dimethyldodecylamine (Aldrich). The solution was stirred for 4 hours at room temperature, after which a white solid was recovered by filtration. The solid material was recrystallized from a chloroform/acetone mixture.

N,N'-bis(dimethyldodecyl)-1,16-hexadecanediammonium dibromide (12-16-12): 1,16-Dibromohexadecane was synthesized by reaction of 1,16-hexadecanediol (Aldrich) with N-bromosuccinimide in a solution of triphenylphosphine in dichloromethane. N-bromosuccinimide was used as a source of bromine and triphenylphosphine was used to promote -OH as a leaving group. The mixture was stirred at room temperature for 2 hours at which point excess reagents were quenched with methanol and the dibromide was isolated by dry flash chromatography. The 12-16-12 surfactant was synthesized by reaction of 2 equivalents (plus 10%) of N,N-dimethyldodecylamine with 1 equivalent of 1,16-dibromohexadecane. The mixture was refluxed in iso-propanol for 24 hours and the solvent was evaporated. The resulting solid was recrystallized from ethyl acetate.

Water used for all solutions was purified using a Millipore™ Super Q system. The polymer stock solutions were prepared on a weight percent basis. Surfactant solutions were prepared on a molarity basis except for those solutions used in the apparent molar volume and temperature studies, which were prepared on a molality basis. Conversion, where required, between the molarity and molality concentrations was carried out using experimental density data for the corresponding solution.

3.2 Theoretical Background of Methods Used in This Study

3.2.1 Surface tension

The difference in energies between those molecules located at the surface and those in the bulk phase of a liquid or solution give rise to a surface tension. When a new surface is formed work is done, and this work will be proportional to the amount of material transferred from the bulk to the surface, and therefore is proportional to the area of the new surface.[19] This can be expressed as

$$w = \gamma \Delta A \qquad 3.2.1\text{-}1$$

where the proportionality constant γ is defined as the surface tension. Thermodynamically, the surface tension represents the change in Gibbs energy brought about by a change in area at constant temperature and pressure.

$$\gamma = \left(\frac{\partial G}{\partial A}\right)_{T,P} \qquad 3.2.1\text{-}2$$

The addition of a solute to a pure liquid will bring about changes in the surface tension as a result of the modification of the intermolecular interactions occurring within the solution. This can be illustrated by considering the Gibbs adsorption isotherm

$$d\gamma = -\sum_i \Gamma_i d\mu_i \qquad 3.2.1\text{-}3$$

which is derived from the comparison of the differential of the internal energies for the surface and the bulk.[19,91] The surface excess concentration, Γ, of a component of a solution is defined as

$$\Gamma_i = \frac{n_i^s}{A} \qquad 3.2.1\text{-}4$$

where A is the surface area, and n_i^s is the number of moles of component i located at the surface. It is convenient to define the surface or interface such that the excess of one

component, the solvent, is equal to zero. For a two component system, considering the definition for chemical potential, equation 3.2.1-3 then gives

$$d\gamma = -\Gamma_2 RT d \ln a_2 \qquad 3.2.1\text{-}5$$

where a_2 is the activity of the solute and, for dilute solutions, can be replaced by C, the concentration. Therefore by measuring the surface tension as a function of the concentration, the surface excess can be determined.

Because of the amphiphilic nature of surfactants, they preferentially locate at the air/water interface in aqueous solution, with their hydrophobic tails extended into the air and the head groups solubilized at the surface. As the concentration is increased, the surface tension is observed to decrease, until the cmc is reached. Once the cmc is reached, micelles begin to form with any added material going into the formation of micelles. At this point the surface tension is observed to remain constant, and therefore surface tension is often used in determining the cmc for a given surfactant. As well, by measuring the slope of the surface tension just prior to the cmc, one can obtain a value for the surface excess concentration (in mol m^{-2}) which then can be used to determine the cross-sectional area for the surfactant molecule of the surfactant at the air/water interface, according to Equation 3.2.1-6

$$a_0 = (N_A \Gamma)^{-1} \qquad 3.2.1\text{-}6$$

where N_A is the Avogadro number. It is generally assumed that a_0 is equivalent to the area of the surfactant head group at the interface, due to the fact that the cross-sectional area of the head group will be greater than that for the hydrocarbon tail.

The surface tension property is also extremely sensitive to contamination, which makes it a powerful diagnostic for determining the purity of a surfactant.[19] A surface active impurity will also preferentially locate at the air/water interface, influencing the packing of surfactant monomers at the interface. This leads to premature micelle formation at a concentration less than the cmc of the pure surfactant. In addition the continued build-up of impurity at the surface will decrease the surface tension of the solution below that of the plateau value that would be obtained in the absence of an impurity. As more surfactant is added to the solution, the impurity becomes solubilized with the surfactant, forming a mixed aggregate, and the surface tension rises back to a value near what would be obtained for a pure (aggregated) surfactant solution. If large amounts of impurity are present in the sample, the minimum observed in the surface tension plot can be very large and extend over a broad concentration range. The absence of a minimum in the surface tension of a surfactant is therefore an excellent indication of material of a high purity, usually > 99%.

3.2.2 Apparent molar volume

The total volume of a system is comprised of contributions due to all components present in the system. The total volume of a binary solution is related to the partial molar volume, $\overline{V}_i$, of each component according to Euler's rule

$$V = n_W \overline{V}_W + n_2 \overline{V}_2 \qquad 3.2.2\text{-}1$$

where the subscript W refers to water, and 2 refers to the solute. In dilute solutions, changes in the volume of the solution occur as a result of solute-solvent and solute-solute interactions. Under these conditions $\overline{V}_2$ is the property of interest since changes observed will reflect not only the properties of the solute itself, but also interactions that occur due to the presence of a

small amount of the solute in a large amount of solvent. The most convenient concentration scale for experimental measurements in dilute aqueous solutions is molality (mols of solute per kilogram of water) since the number of moles of water is kept fixed at 55.51, independent of pressure and temperature fluctuations. The partial molar volume can then be defined as

$$\overline{V}_2 = \left(\frac{\partial V}{\partial m_2}\right)_{T,P} \qquad 3.2.2\text{-}2$$

Unfortunately, very few partial molar properties can be easily obtained directly from experimental measurements. Instead the apparent molar volume is measured. It is defined as

$$V_{\phi,2} = \frac{V - 55.51V_W^*}{m_2} \qquad 3.2.2\text{-}3$$

where V^*_W is the molar volume of pure water. The partial molar volume can be derived from the apparent molar property (at constant temperature and pressure) to give

$$\overline{V}_2 = V_{\phi,2} + m_2\left(\frac{\partial V_{\phi,2}}{\partial m_2}\right)_{T,P} \qquad 3.2.2\text{-}4$$

where it is seen that in the limit of zero concentration the apparent molar volume becomes equal to the partial molar volume at infinite dilution, $\overline{V}_2^0$, which is the standard state for solutes in solution. The apparent molar volume is calculated from experimentally determined density data according to

$$V_{\phi,2} = \frac{M_2}{d} - \frac{1000(d - d_0)}{m_2 d d_0} \qquad 3.2.2\text{-}5$$

where M_2 is the molar mass of the solute, d and d_0 are the densities of the solution and solvent (water, $d_0 = 0.997047$ g cm^{-1} at 25°C), respectively.

3.2.3 Fluorescence studies

Fluorescent probe techniques have been used in a variety of ways to study structural and dynamical aspects of surfactant aggregates in solution. The ability of surfactant aggregates to compartmentalize solutes has in part led to a number of such studies. As well, the general use of fluorescent methods to study biological systems, for which micelles and bilayers have often been considered models, has also promoted this type of investigation.[115,116] Information regarding the structure of the micelle can be obtained from studies of various photo-physical properties such as the lifetime of the excited probe, excitation and emission spectra, vibronic intensity ratios, anisotropies and quantum yields.[117-120] Quenching studies provides information regarding micellar size as well as the dynamic properties of both the micelle and of species solubilized therein.[115,116,120-125]

3.2.3.1 Time resolved fluorescence quenching

The fluorescence behavior of an excited probe in a micellar system containing quenchers will depend upon a number of factors, including the distribution and mobility of both probe and quencher molecules throughout the system. By appropriate choice of both the probe and quencher molecule, one can ensure that both are contained within the micellar phase of the solution. This, coupled with low probe concentrations, simplifies the analysis of the fluorescence decay by reducing contributions due to excimer formation and probe or quencher exchange between micelles in solution. Generally, probe concentrations are kept at levels such that the occupancy level in the micellar phase is less than 0.05%. Quencher concentrations are chosen such that the occupancy level is no greater than 1 per micelle. The

general form for the time dependent decay of an excited probe after a narrow-pulse excitation is given by[120]

$$\ln\left(\frac{I}{I_0}\right) = -A_2 t + A_3[\exp(-A_4 t) - 1] \qquad 3.2.3.1\text{-}1$$

where the parameters A_2, A_3, and A_4 depend on the quenching kinetics of the system. For the case described above (low concentrations and strongly micelle bound probe and quencher) A_2, A_3, and A_4 simplify to k_0 (the fluorescence rate constant for the unquenched probe), $\bar{n}$ (the mean quencher occupancy number per micelle), and k_q (the fluorescence quenching rate constant), respectively. The mean aggregation number then can be determined from the above parameters, obtained by a fit of Equation 3.2.3.1-1 to the experimental decay, according to

$$N_{agg} = \frac{\bar{n}([S] - CMC)}{[Q]} \qquad 3.2.3.1\text{-}2$$

where [S] is the total concentration of surfactant and [Q] is the total concentration of quencher (assumed to be equivalent to the concentration of quencher in the micellar phase).

3.2.3.2 Vibronic ratios of pyrene

Pyrene is one of a relatively few condensed aromatic molecules that exhibit vibronic fine structure in its fluorescence spectrum. The intensities of these bands are governed by (in the absence of any interactions between pyrene and solvent molecules) the relative positions of the potential energy surfaces for the excited state, and by the Frank-Condon principle.[117] The intensities of these bands show significant variation depending upon the nature of the solvent, with enhancement of forbidden vibronic bands occurring in polar solvents

possessing large permanent dipoles. This phenomena was first observed in the "Ham" bands of benzene, and has been termed the Ham effect. The intensity enhancement occurs through specific solute-solvent dipole-dipole coupling between the excited state of pyrene and the solvent.[117] In pyrene (and in other aromatic molecules which possess a minimum D_{2h} symmetry) the first singlet absorption ($S_0 \rightarrow S_1$) is forbidden and weak. The absorption and fluorescence spectra show mixed polarization due to coupling between the first excited state (S_1), which is polarized along the short axis of the molecule, and the second excited state (S_2), polarized along the long axis of the molecule. The vibronic bands of pyrene consist of allowed (b_{1g}) and forbidden (a_g) transitions. The third vibronic peak (III, 382.9 nm, see Figure 3.3.4.2-1) is strong and allowed, and shows little variation with solvent polarity. The origin (0-0) band (I, 372.4 nm, see Figure 3.3.4.2-1) is forbidden and shows significant intensity enhancement in polar solvents.

When placed in an aqueous surfactant solution below the cmc, pyrene will have a I/III vibronic intensity ratio similar to that obtained for pure water. Pyrene, due to its hydrophobic character, will preferentially locate in the interior of the micelle above the cmc and the I/III ratio will decrease correspondingly. Therefore, a plot of the vibronic ratio versus surfactant concentration will show a transition, permitting a determination of the cmc. In mixed surfactant-polymer systems, provided a cooperative interaction exists between the surfactant and the polymer, the transition will occur at the CAC rather than the cmc. Because the environment of the polymer bound aggregates is likely to be similar to that of the micelle interior (in terms of polarity), it is unlikely that the vibronic ratio would be sensitive to the onset of free micelle formation in mixed systems.

3.2.4 Equilibrium dialysis

Equilibrium dialysis experiments using ionic surfactants are frequently carried out in the presence of excess salt (0.1M) in order to eliminate the Donnan effect. This requirement can be circumvented by appropriate treatment of the experimental data in order to account for the Donnan effect.[84,126] If we consider the mass balance for the two solutions in the dialysis equilibrium (the subscript A refers to the retentate side of the equilibrium, B to the dialysate side), the electroneutrality condition requires that

$$c_P y + [12-3-12^{2+}]_A = [Br^-]_A / 2 \qquad 3.2.4\text{-}1$$

$$[12-3-12^{2+}]_B = [Br^-]_B / 2 \qquad 3.2.4\text{-}2$$

where c_p is the concentration of polymer solution in grams of polymer per liter of solution, and y is the experimental binding ratio. If we consider the equality of chemical potentials at equilibrium (approximating activities with concentration) we have

$$[12-3-12^{2+}]_A[Br^-]_A^2 = [12-3-12^{2+}]_B[Br^-]_B^2 \qquad 3.2.4\text{-}3$$

Combining Equations 3.2.4-1 to -3 gives

$$[12-3-12^{2+}]_A = \frac{[12-3-12^{2+}]_B^3}{C_A^{\,2}} \qquad 3.2.4\text{-}4$$

where

$$C_A = [12-3-12^{2+}]_A + c_p y \qquad 3.2.4\text{-}5$$

is the total concentration of 12-3-12^{2+} ions in the retentate (i.e., polymer) solution. Both C_A and [12-3-12^{2+}]$_B$ are determined directly from experiment, therefore y can be obtained from the above definitions giving

$$y = \frac{(C_A^3 - [12-3-12^{2+}]_B^3)}{c_p C_A^2} \qquad 3.2.4\text{-}6$$

It should be noted that in the above treatment the degree of dissociation for the surfactant is assumed to be complete, i.e., there is no binding of counterions to the surfactant-polymer

complex. It has been shown that the difference between results corrected only for the Donnan effect, and those corrected for both the Donnan effect and the degree of ionization for the resulting surfactant-polymer complex, is small and therefore will not be considered in the present case.[126]

3.3 Methods

3.3.1 Specific conductance

The critical micelle concentrations of the surfactants were determined from measurements of the specific conductance of the surfactant solutions. A concentrated surfactant solution was titrated into a volume of Millipore™ water and the specific conductance (κ) was measured. The critical micelle concentration was determined from the break in the slope of a plot of κ versus the surfactant concentration. The degree of counterion dissociation (or micelle ionization), α, was determined from the ratio of the slopes of the curve before and after micellization.[127,128]

Measurements of specific conductance were carried out by using a glass/platinum electrode (Tacussel) and a Wayne-Kerr Precision Component Analyzer (Model 6425) operating at 1.5 kHz. The electrode was reconditioned with platinum black as necessary from a solution of 3.0 g of platinic chloride and 0.020g of lead acetate in 100.0 mL of water. Current was provided by a milliamp power supply, with the anode and cathode being periodically switched to ensure uniform coverage of both plates of the electrode. The cell constant varied in the range of 1.111 to 1.141 cm^{-1}. Temperature of the conductance cell was

maintained, using a Haake Model F3 circulating water bath, at 25.0 ± 0.1°C unless otherwise specified.

3.3.2 Surface tension

Surface tension measurements were carried out by using a Krüss Model K10T digital tensiometer operating in ring mode. The temperature of the sample chamber was maintained to within 0.1°C using a Haake Model F3 circulating water bath. In order to conserve materials, a titration method was used in which stock solutions of the surfactants were prepared and titrated into a known volume of water. The surface tension of the resulting solution was then measured. The accuracy of this approach was verified by measurement of independently prepared solutions, the results of which were then compared to those obtained from the titration method. No significant deviations were observed between the two methods. Duplicate readings of surface tension within 0.2 mN m^{-1} were used as an indication of stability of the measurement. Critical micelle concentrations and headgroup areas were determined from a plot of the surface tension versus the logarithm of the surfactant concentration. The absence of a minimum in the plot was used as an indication of an acceptable purity of the surfactant samples.

3.3.3 Density and volume measurements

Solution densities used in the calculation of the apparent molar volume for the surfactants were obtained using a vibrating tube flow densimeter (Sodev, Model 03D). Period readings were obtained using a digital frequency meter (Fluke 7261 Universal Counter) at 100ns resolution. Temperature was maintained at 25 ± 0.001°C using a closed

loop Sodev temperature controller (Model CT-L). The flow rate of solutions through the vibrating tube assembly was controlled by the use of a peristaltic pump set at a constant rate of 0.5 mL min^{-1}. The design of the Sodev instrument has been described in the literature and will not be discussed here[129]. The estimated precision in density measurements for this instrument under these operating conditions, described above, was found to be $\pm 2 \times 10^{-6}$ g cm^{-3}.[129]

The principle behind the operation of this instrument is that the natural period of vibration of the sample tube changes proportionally to the mass of the fluid flowing through the tube. The density (d) of the fluid is related to the period (τ) of vibration through

$$d = A + B\tau^2 \qquad 3.3.3\text{-}1$$

where A and B are instrument constants. Densities of solutions are obtained experimentally by measuring the differences in period readings between the solution of interest and the solvent. The density of a solution is related to the density of the solvent through the period of vibration according to

$$d - d_o = B\left(\tau^2 - \tau_o^2\right) \qquad 3.3.2\text{-}1$$

where the subscript o refers to the solvent. The constant B is determined by measuring the period of vibration for water (d = 0.997047 g cm^{-3}) and nitrogen (d = 0.001143 g cm^{-3}, determined from the ideal gas law). To eliminate any effects of short term drift in the instrument response on the measured density values, period measurements were made in the sequence solvent-solution-solvent and by calibration of the instrument prior to each series of measurements. This is of particular importance when considering the dilute conditions, and therefore small differences in density, required due to the low cmc values of the surfactants

used in this study. Period measurements were averaged over at least six readings with the maximum variation in the period being no greater than 1 ns.

There are practical limitations of this instrument at low concentrations (< 1 mmolal), since the uncertainties associated with the density measurement contribute to large errors in calculated apparent molar volumes. In order to obtain more reliable apparent molar volume data at low concentrations, the dilatometry method was used in conjunction with the vibrating tube instrument. The design of the dilatometer was similar to that previously reported.[130,131] The inner chamber of the dilatometer was filled with a concentrated surfactant solution, and the outer with Millipore™ water. The dilatometer was thermostated in an insulated circulating water bath with the temperature for these measurements maintained at 25 ± 0.05°C. The maximum temperature fluctuation over the course of one measurement was no greater than ± 0.005°C. The initial height of the meniscus in the arm of the dilatometer was measured using a cathetometer. The barrier between chambers was then removed and the solution was allowed to re-equilibrate. The final height of the meniscus was then measured. The volume change was determined from the difference in heights and from the volume of the tubing, 2.470×10^{-3} mL cm^{-1}. The final apparent molar volume was then determined according to

$$V_{\phi,final} = V_{\phi,initial} + \frac{\Delta V}{n} \qquad 3.3.3\text{-}3$$

where $V_{\phi,\,final}$ is the apparent molar volume of the final (diluted) surfactant solution, $V_{\phi,\,initial}$ is the apparent molar volume of the concentrated surfactant solution which was determined using the vibrating tube densimeter, ΔV is the measured change in volume, and n is the number of mols of surfactant.

3.3.4 Fluorescence studies

Pyrene was used as the fluorescent probe in all studies and was recrystallized from acetone prior to use. The desired concentration of pyrene in the sample was obtained by addition of an appropriate volume of pyrene in a hexane stock solution followed by the removal of the hexane by evaporation, using a gentle flow of N_2 over the solution. The solvent (either water or aqueous block copolymer) was then added to give pyrene concentrations in the range of 5×10^{-7} to 1×10^{-6} mol L^{-1}.

3.3.4.1 Time Resolved Fluorescence Quenching

Commercially available N,N-dibutylaniline (DBA, Aldrich) was used as the fluorescent quencher without additional purification. The use of DBA as a quencher for excited pyrene in cationic surfactant systems has been previously established.[93] Due in part to its low solubility in water DBA is an appropriate choice of quencher as this reduces the possibility for exchange between micellar aggregates over the course of the decay experiment. This in turn allows for the assumption of an immobile quencher which, coupled with the assumption of an immobile probe, appropriate due to the low aqueous solubility for pyrene, simplifies the analysis of the experimental data such that the simplified form of Equation 3.2.3.1-1 can be applied. A stock solution of DBA in hexane was prepared to give the desired DBA concentration in a manner similar to that for pyrene, above. A stock surfactant solution containing pyrene and one containing both pyrene and DBA were used to prepare solutions containing the desired quencher concentration by mixing appropriate volumes of the stock solutions. Four solutions were prepared for each surfactant concentration (either in water or the appropriate polymer in water solution), one containing only pyrene, and the remaining

three solutions containing pyrene and varying amounts of DBA. Fluorescence emission from sources other than the excited probe, under the conditions used for the time-resolved measurements, were found to be negligable.

Fluorescence decay curves were obtained using the single-photon counting technique. The excitation source was a synchronously pumped, cavity-dumped, frequency-doubled DCM picosecond dye laser, excited at a wavelength of 515 nm by an Ar/Ar^+ laser. In order to avoid exciting DBA (which absorbs below 340 nm), the output of the dye laser was tuned to 680 nm which gave a frequency-doubled UV output of 340 nm. This wavelength was used to excite pyrene at a pulse frequency of 800 kHz. A digital delay generator was used to obtain a delay of 1 μs between recorded pulses. The emission of pyrene was collected at 385 nm with a 512 channel multi-channel analyzer with a minimum of 10^4 counts recorded in the peak channel. Fluorescence decay curves were observed at the magic angle (54.7°) to eliminate polarization effects and all measurements were made at room temperature (22 ± 1°C).

3.3.4.2 Vibronic Ratios of Pyrene

Measurements of pyrene fluorescence were carried out using a SPEX Fluorolog 1680 spectrometer with slit widths of 1 mm and an excitation wavelength of 335 nm. The wavelength increment was 0.5 nm and the integration time was 0.5 seconds. A sample spectrum of the pyrene emission in an aqueous 12-3-12 surfactant solution is shown in Figure 3.3.4.2-1. Solutions were prepared by titrating a concentrated stock surfactant or surfactant

polymer solution (containing pyrene) with a known volume of solvent (also containing pyrene). Spectra were collected after each addition.

Figure 3.3.4.2-1: Fluorescence emission spectrum of pyrene in aqueous solutions containing the 12-3-12 gemini surfactant in its monomer, and micellized states.

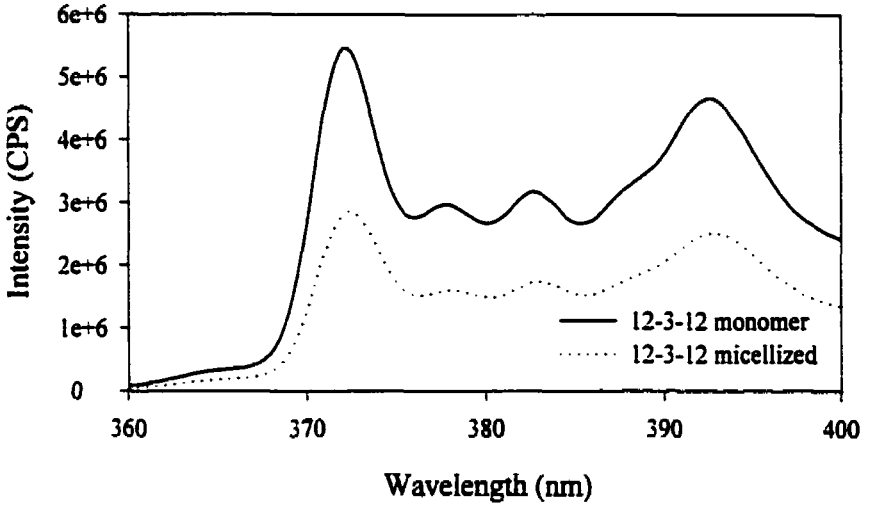

3.3.5 Proton NMR

^{1}H NMR spectra were recorded on a Bruker AM-300 NMR spectrometer operating at 300.13 MHz relative to a deuterium lock at ambient (295 K) temperature. A stock solution of surfactant, in either D_2O or the appropriate polymer/D_2O solution, was titrated into 0.500 mL of solvent in a 5 mm KIMAX NMR tube, and spectra were recorded after each addition. Sample spectra for the 12-3-12 gemini surfactant, and the triblock copolymer F108 are shown in Figures 3.3.5-1 and -2, along with the spectral assignment. The ^{1}H spectral assignment for the gemini surfactants was made based on comparison of the spectra with known spectra for the corresponding monomeric surfactant, dodecyltrimethylammonium bromide. The assignment for the triblock copolymers has previously been given in the literature.[132]

Figure 3.3.5-1 ^{1}H NMR Spectrum for the 12-3-12 gemini surfactant (in CD_3OD)

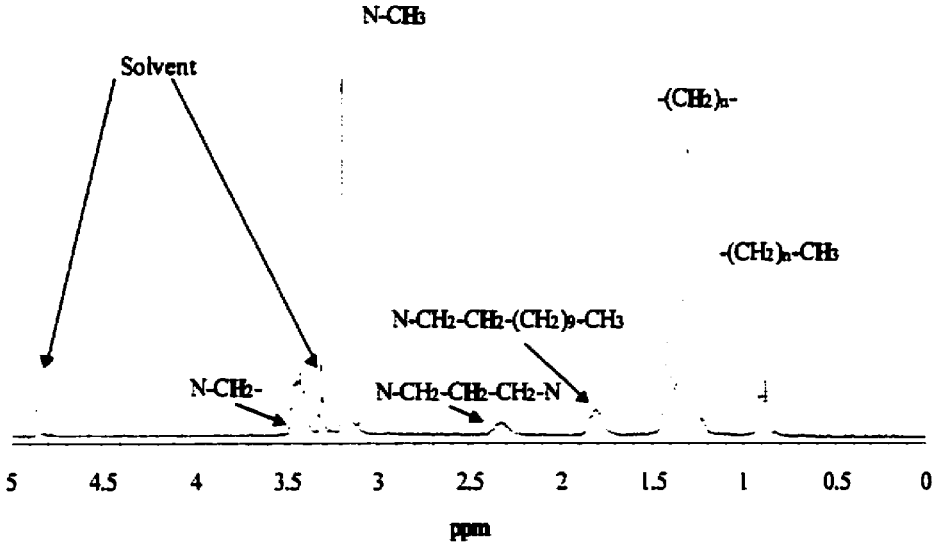

Figure 3.3.5-2 ^{1}H NMR spectrum for the triblock copolymer P103 (in D_2O)

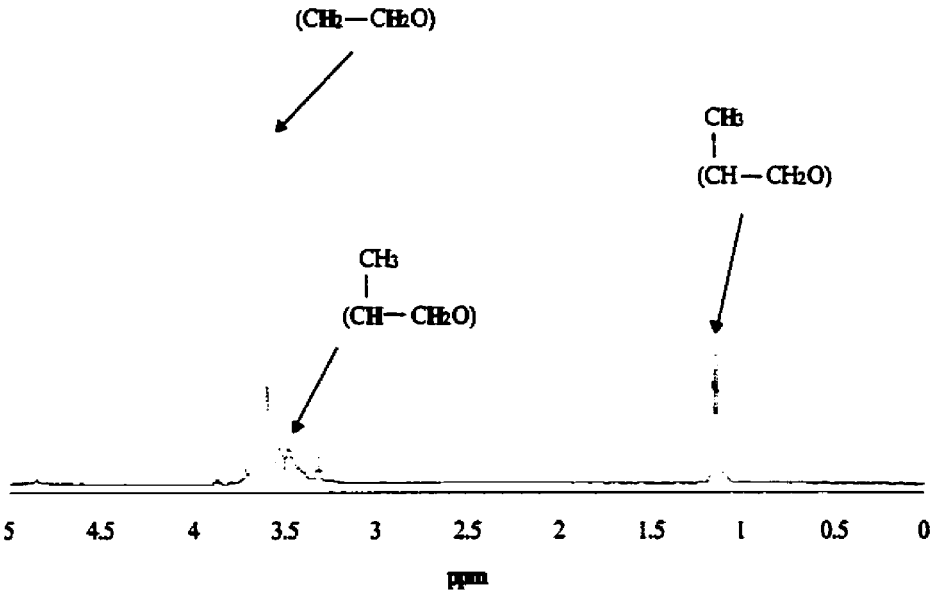

3.3.6 Equilibrium Dialysis

Equilibrium dialysis experiments were performed with the 12-3-12 surfactant in the presence of PEO, P103, F108, and F68 at various concentrations. The dialysis membrane used was a Spectra-Por 7 (Spectrum Labs) membrane, with a molecular weight cut-off of 3500. Prior to use, the tubing was rinsed with Millipore™ water and allowed to soak for a minium of 30 minutes (as per manufacturer's instructions). The dialysis cells consisted of two chambers separated by the dialysis membrane, as shown in Figure 3.3.6-1. Each chamber was filled with 2.00 mL of either surfactant or polymer solution, and the two halves were clamped together. Solutions were shaken for a minimum of 24 hrs to establish equilibrium between the surfactant and polymer solutions. The equilibrium was established from trial measurements of the solution concentrations at various times between 4 and 72 hours.

Figure 3.3.6-1: Diagram of the dialysis chamber

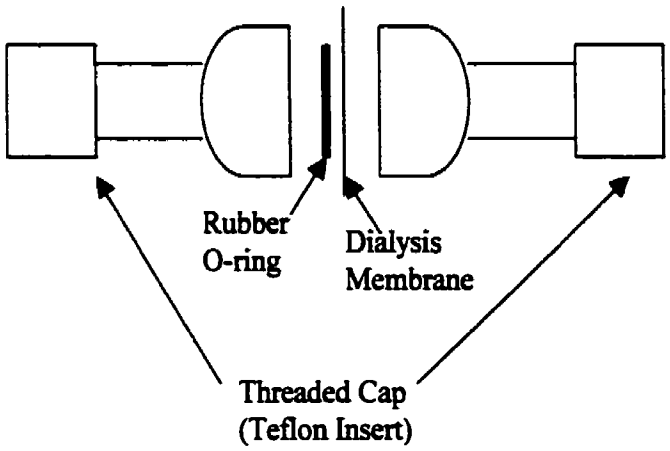

The equilibrium surfactant concentrations were determined using a complexation-photometric titration method. The cationic dye toluidine blue undergoes a metachromic shift

from blue to pink when bound to molecules containing anionic groups, such as dextran sulfate (DS). When this complex is titrated with a cationic surfactant, the surfactant preferentially binds to DS and the dye is displaced. The endpoint for the titration is seen by the reappearance of the blue color due to unbound toluidine blue.

The equivalent charge concentration (eq g^{-1}) of DS (avg. mol. weight. 5000, Sigma) was determined by titration of 200 μL of a 1.2036 g L^{-1} solution with a 1.998 × 10^{-3} molar solution of cetylpyridinium bromide (recrystallized from acetone). An average value of 5.39 ± 0.05 × 10^{-3} eq g^{-1} was obtained from 4 titrations. This value is in reasonable agreement with the charge concentration determined by Van Damme et al., 5.74 ± 0.24 × 10^{-3} eq g^{-1}, which was found to be independent of the DS molar mass over the range 8.000 – 500,000.[133] The method was validated by titrating the DS-TB complex with a gemini surfactant solution of known concentration, and results of these titrations are given in Table 3.3.6-1. No significant differences in surfactant concentration were observed. The unknown surfactant concentrations from the dialysis experiments were determined in the same manner.

Table 3.3.6-1: Determination of known 12-3-12 concentrations by the complexation-photometric titration method

Concentration (× 10^{-3} M)	Measured Conc. (× 10^{-3} M)	Average. (× 10^{-3} M)
1.003	1.05	1.02 ± 0.05
	0.986	
	0.954	
	1.08	
2.006	1.91	2.03 ± 0.09
	1.98	
	2.08	
	2.13	

4. RESULTS

4.1 Binary Surfactant – Water Systems

4.1.1 Specific Conductance Measurements

The concentration dependence of the specific conductance for the m-s-m surfactants are shown in Figures 4.1.1-1 a to d. The cmc for a surfactant was determined from the break in the conductivity vs. concentration plot by regression analysis using Sigma-Plot™ (version 4.0). The degree of micelle ionization (α) has been shown, to a first approximation, to be equivalent to the ratio of the slopes above and below the cmc and was determined in this manner.[128] Results obtained for the cmc and α for the gemini surfactants are tabulated in Table 4.1.1-1 and are in good agreement with those previously reported in the literature.[33]

Table 4.1.1-1: Critical micelle concentration (cmc) and degree of micelle ionization (α) for a series of m-s-m gemini surfactants

Surfactant	cmc ($\times 10^{-3}$ mol L^{-1})	α
8-3-8[a]	54 ± 2	0.28 ± 0.02
10-3-10	6.10 ± 0.03	0.24 ± 0.02
16-3-16[a]	0.026 ± 0.001	0.35 ± 0.02
12-2-12	0.89 ± 0.04	0.18 ± 0.02
12-3-12	0.94 ± 0.04	0.20 ± 0.02
12-4-12	1.17 ± 0.04	0.26 ± 0.02
12-6-12	1.09 ± 0.04	0.34 ± 0.02
12-8-12	0.84 ± 0.03	0.46 ± 0.04
12-10-12	0.62 ± 0.03	0.51 ± 0.06
12-12-12	0.36 ± 0.03	0.56 ± 0.08
12-16-12	0.12 ± 0.01	0.59 ± 0.08

[a] values obtained from reference 134

Two general trends are observed with respect to the cmc. The first is the usual decrease in the cmc as the length of the alkyl tail is increased for constant spacer length. While the magnitudes of the cmc are less than those for the corresponding single head group surfactants of equal alkyl chain length, the trend is the same and these results will be

Figure 4.1.1-1: Specific conductance of aqueous gemini surfactants at 25°C. Solid lines represent linear regressions of the experimental data

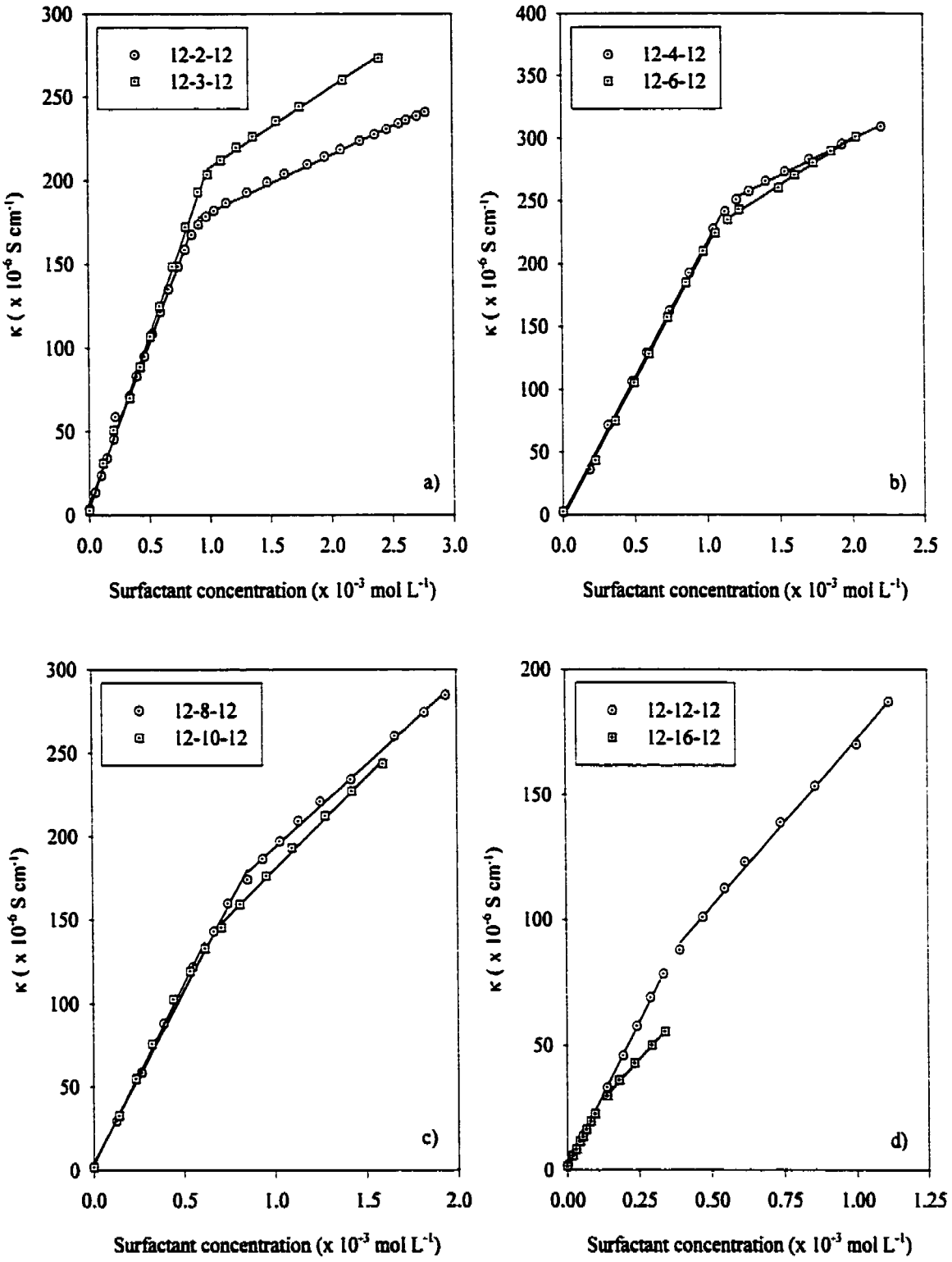

discussed further in Chapter 5. A second more complex trend is observed for those surfactants having a constant alkyl tail length and a variable spacer carbon chain length. A maximum occurs in the cmc for spacer chain lengths of 4-5 methylene units. Beyond spacer chain lengths of 8 methylene units the cmc begins to decrease in a manner expected of traditional single head group surfactants as their alkyl tail length increases.

4.1.2 Surface Tension Measurements

Surface tension vs. log concentration plots for aqueous gemini surfactant solutions are shown in Figure 4.1.2-1. As discussed in §3.2.1, the absence of a minimum in the surface tension curves indicates that the samples contain no surface active impurities. Cmcs were determined from regression analysis of the pre- and post-micellar regions of the curve and are listed in Table 4.1.2-1. Head group areas were estimated from the slope of the pre-micellar curve according to Equation 3.2.1-6 where Γ was calculated from the relation

$$\Gamma = -\frac{1}{2.30nRT}\left(\frac{d\gamma}{d\log C}\right) \qquad 4.1.2\text{-}1$$

The number of distinct species (n) which make up the surfactant and are adsorbed at the interface is three for gemini surfactants. Values of the head group area are also given in Table 4.1.2-1. Results obtained for both the cmcs and head-group areas are in good agreement with those compounds previously reported.[35] Also, the results for the cmcs obtained from surface tension measurements are in agreement with those obtained from specific conductance measurements (Table 4.1.1-1). The decrease in γ observed above the cmc has been previously noted[35] though not explained. The decrease may be due to continued variations in surfactant monomer packing at the air water interface.

Figure 4.1.2-1: Surface tension versus the logarithm of surfactant concentration (in mol L^{-1}) for a series of aqueous m-s-m gemini surfactants at 25.0°C.

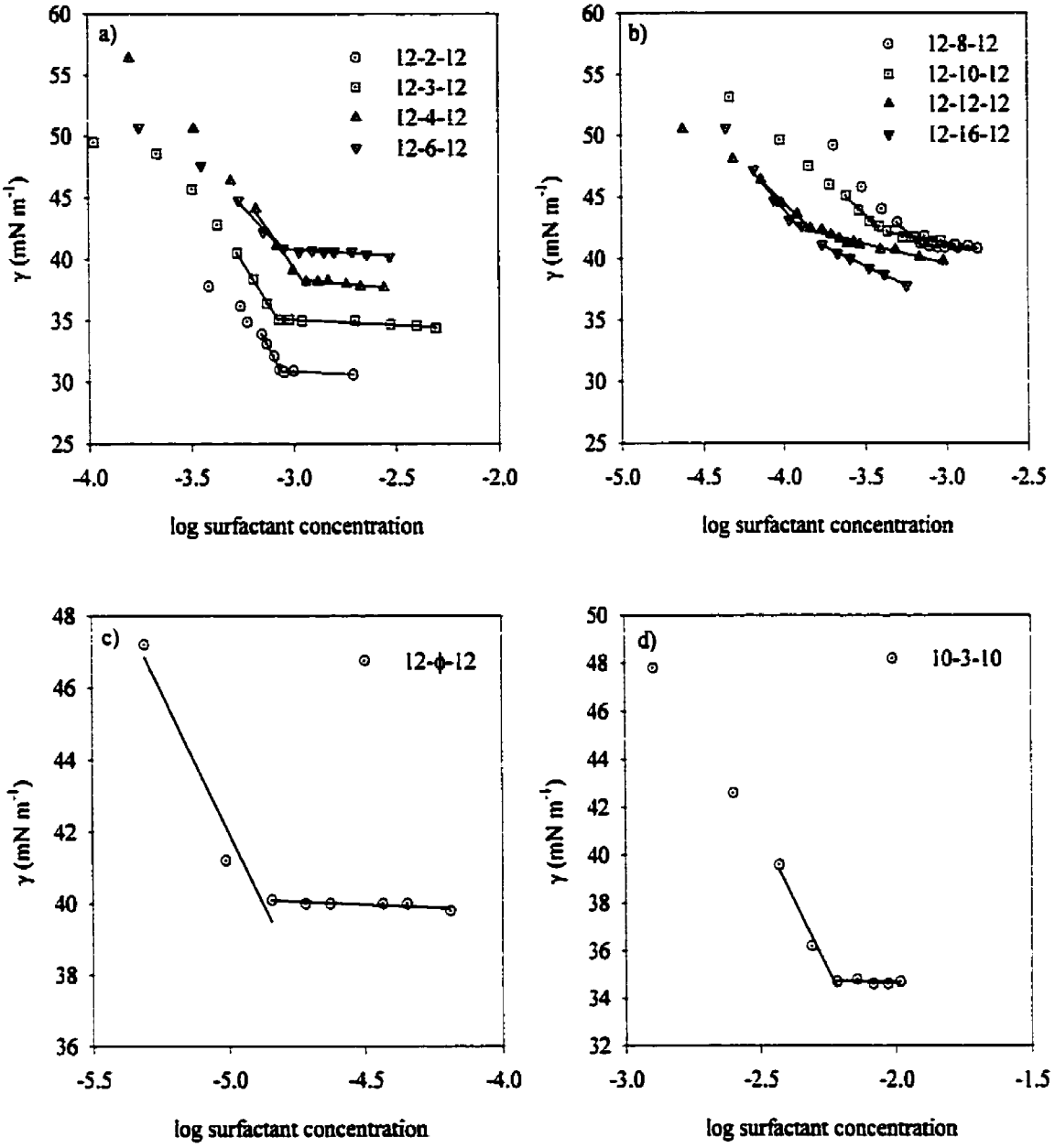

Table 4.1.2-1: Critical micelle concentrations (cmc) and head group areas (a_0) determined from surface tension measurements for a series of aqueous gemini surfactants at 25°C.

Surfactant	cmc ($\times 10^{-3}$ mol L^{-1})	a_0 (nm^2 $molecule^{-1}$)
8-3-8[a]	44 ± 2	1.56
10-3-10	6.2 ± 0.8	1.24 ± 0.06
16-3-13[a]	0.030 ± 0.002	1.21
12-2-12	0.86 ± 0.08	0.86 ± 0.05
12-3-12	0.89 ± 0.08	1.11 ± 0.04
12-4-12	1.1 ± 0.1	1.15 ± 0.09
12-6-12	0.96 ± 0.09	1.58 ± 0.08
12-8-12	0.69 ± 0.07	1.82 ± 0.07
12-10-12	0.42 ± 0.05	2.28 ± 0.08
12-12-12	0.18 ± 0.03	2.22 ± 0.08
12-16-12	0.11 ± 0.02	1.54 ± 0.09
12-ϕ-12	0.013 ± 0.003	1.8 ± 0.3

[a] values obtained from reference[134]

4.1.3 Mean Aggregation Numbers

The fluorescence decay traces of pyrene in aqueous solutions of the gemini surfactants are shown in Figures 4.1.3-1 and 4.1.3-2. The surfactant and quencher concentrations used in these studies are reported in Table D-I, along with results of the fitting procedure (k_0, k_q, and $\bar{n}$). Decay traces were fit assuming dynamic quenching of pyrene by immobile quenchers according to equation 3.2.3.1-1. Fluorescence lifetimes for pyrene ($\tau_0 = k_0^{-1}$), the average quenching rate constants (k_q), and mean aggregation numbers (N_{agg}), calculated from the quencher occupancy ($\bar{n}$) according to Equation 3.2.3.1-2, are shown in Table 4.1.3-1. It is important to note that the parallel nature of the decay traces at long times is indicative of a system where both the probe and quencher are immobile over the lifetime of the experiment. This implies that the assumptions made to obtain the reduced form of Equation 3.2.3.1-1 are valid and, therefore, it is applicable to the systems studied in this work.

Figure 4.1.3-1 Fluorescence decay curves of pyrene quenched by N,N-dibutylaniline in surfactant solutions of a) 12-2-12, b) 12-3-12, c)12-4-12, d) 12-6-12, e) 12-8-12, f) 12-10-12 at different quencher concentrations.

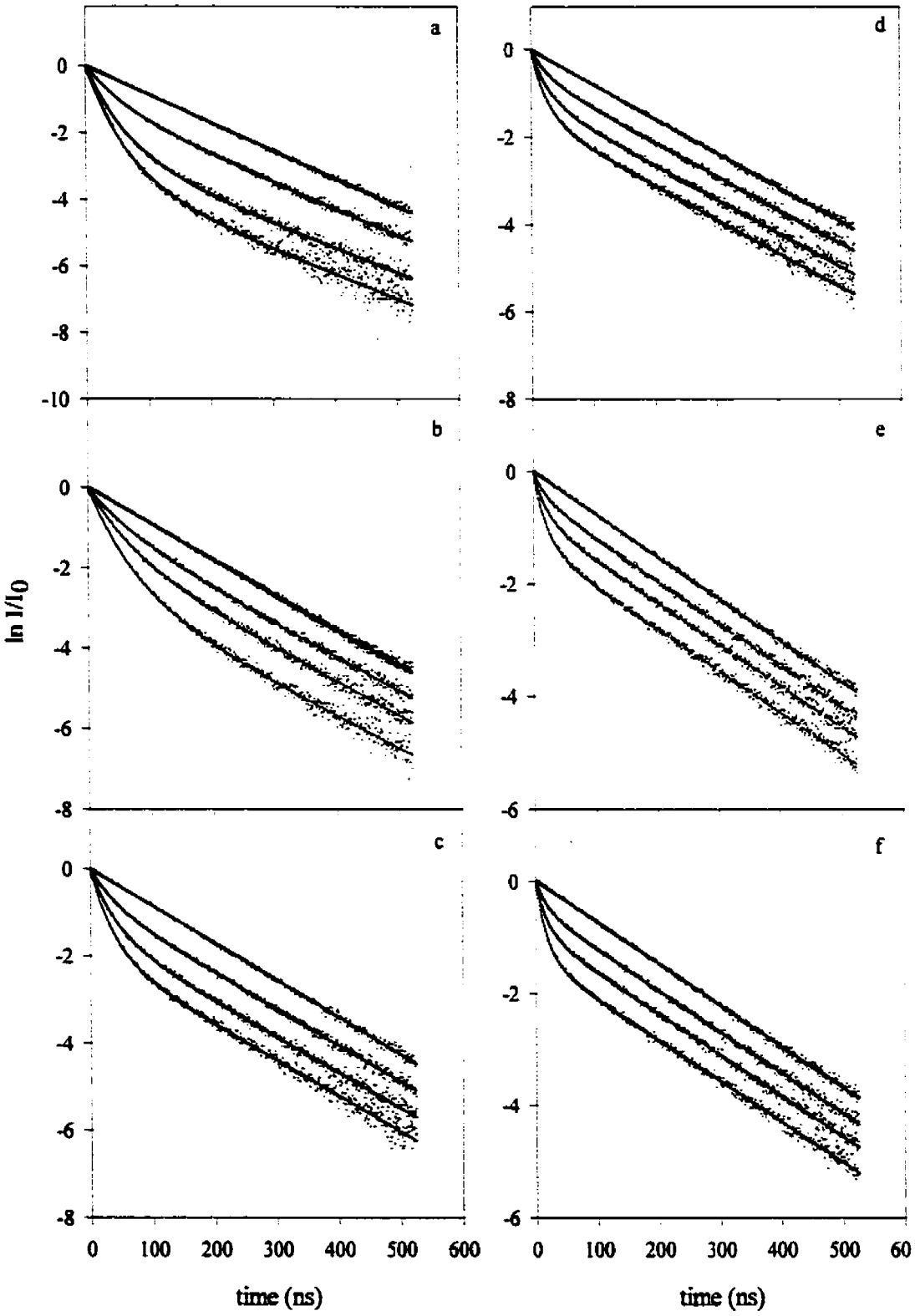

Figure 4.1.3-2: Fluorescence decay curves of pyrene in surfactant solutions of a) 12-12-12 (quenched by N,N-dibutylaniline), and b) 12-16-12 (quenched by cetylpyridinium chloride) at different quencher concentrations.

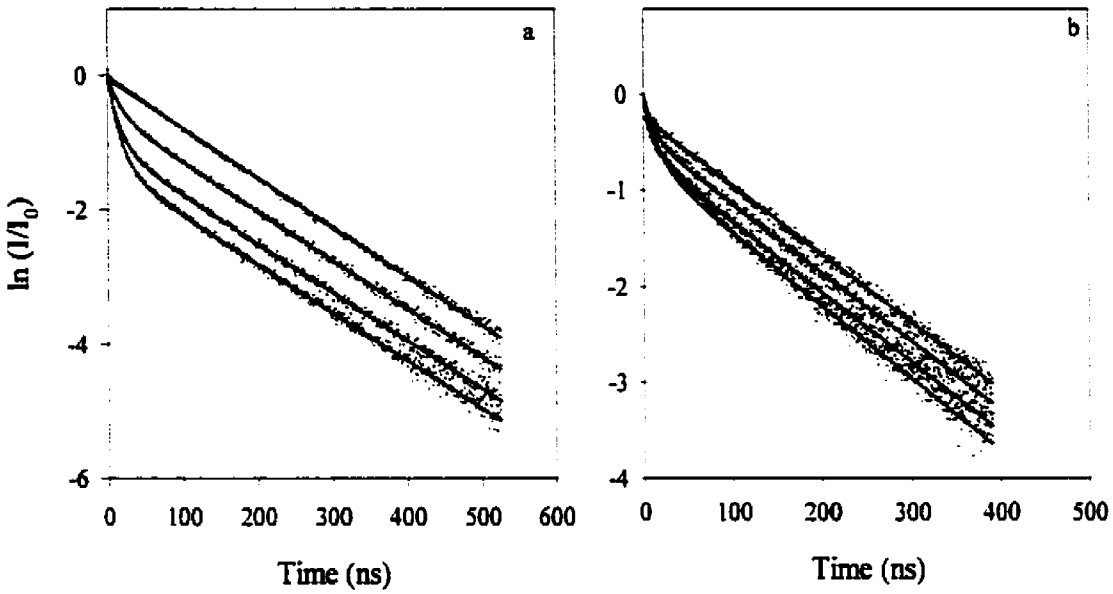

Table 4.1.3-1: Fluorescence lifetime of pyrene (τ_0), average quenching rate constant (k_q), and mean aggregation number (N_{agg}) for the m-s-m gemini surfactants

Surfactant	Surfactant Concentration (mol L^{-1})	τ_0 (ns)	k_q ($\times 10^7$ s^{-1})	N_{agg}
12-2-12	4.71×10^{-3}	119	1.4	24
12-3-12	1.06×10^{-2}	113	1.2	23
12-4-12	1.04×10^{-2}	118	2.4	30
12-6-12	1.06×10^{-2}	129	4.2	16
12-8-12	1.05×10^{-2}	134	3.4	11
12-10-12	1.03×10^{-2}	136	5.0	13
12-12-12	1.01×10^{-2}	136	5.2	22
12-16-12[a]	1.21×10^{-3}	141	7.4	51

[a] using CPyCl as quencher

4.1.4 Apparent Molar Volume Studies

Apparent molar volumes of the gemini surfactants used in this study were calculated from measurements of solution density according to Equation 3.2.2-5. Plots of V_ϕ as a function of surfactant concentration for the m-3-m series of surfactants (m=8, 10, and 12) are shown in Figure 4.1.4-1, and for the 12-s-12 (s = 2 to 10) series in Figures 4.1.4-2. Additional measurements of V_ϕ were made for the 12-3-12 and 12-6-12 surfactants using the dilatometer method in order to provide confirmation of results obtained using densimetry at very low concentrations.

Experimental data were fit to the pseudo-phase model (solid lines in Figures 4.1.4-1 and -2) according to[94]

$$V_\phi = V_{\phi,M} - \frac{CMC}{m}\Delta V_{\phi,M} \qquad 4.1.4\text{-}1$$

where $V_{\phi,M}$ is the apparent molar volume of the surfactant in the micellar phase, $\Delta V_{\phi,M}$ is the isothermal volume change due to micelle formation (based on apparent molar volume), and m is the molality of the surfactant solution. The apparent molar volume of the surfactant at the cmc, $V_{\phi,cmc}$, was obtained from the difference between $V_{\phi,M}$ and $\Delta V_{\phi,M}$. Results of the fitting procedure are listed in Table 4.1.4-1.

Simulated values for the apparent molar volumes of the 8-3-8 gemini surfactant, shown in Figure 4.1.4-1, were calculated assuming a mass action model according to[99]

$$V_\phi = \alpha_0[V^0 + A_V\sqrt{\alpha_0 m} + B_V\alpha_0 m] + (1-\alpha_0)[V^M + (1-\alpha_0)C_V m] \qquad 4.1.4\text{-}2$$

where (c.f. §2.2.2) A_V (= 9.706 cm^3 $kg^{1/2}$ $mol^{-3/2}$) is the Debye-Hückel limiting slope for apparent molar volume.[130] The value of B_V was determined from a fit of the pre-micellar data to the Debye-Hückel limiting equation and was fixed (at 6.4 cm^3 kg mol^{-2}) in the simulation program. Using a value of 15 for the mean aggregation number[134], and 0.0540 mol kg^{-1} for the cmc of 8-3-8, estimates of V^0 = 435.4 cm^3 mol^{-1}, V^M = 444.8 cm^3 mol^{-1}, were obtained. The isothermal volume change due to micelle formation (based on partial molar volume), ΔV_M, is calculated according to

$$\Delta V_M = V^M - V^0 - A_V\sqrt{\alpha_0 m} - B_V\alpha_0 m \qquad 4.1.4\text{-}3$$

giving ΔV_M = 8.3 cm^3 mol^{-1} for the above conditions.

Table 4.1.4-1: Apparent molar volumes at the cmc, and isothermal volume changes due to micelle formation for the m-s-m gemini surfactants

Surfactant	$V_{\phi,M}$ (cm^3 mol^{-1})	$\Delta V_{\phi,M}$ (cm^3 mol^{-1})	$V_{\phi,cmc}$ (cm^3 mol^{-1})
8-3-8	445.8	8.8	437.0
10-3-10[a]	514.7	11.2	503.5
16-3-16	708.1[b]	15.3	692.8[c]
12-2-12	561.0	16.2	544.8
12-3-12	579.7	12.4	567.3
12-4-12	597.7	13.5	584.2
12-6-12	631.3	13.4	617.9
12-8-12	664.3	12.5	651.8
12-10-12	697.1	14.6	682.5
12-12-12	728.8[d]	15.6	713.2[c]
12-16-12	794.3[d]	17.9	776.4[c]
12-ϕ-12	627.0[d]	10.7	616.3[c]

[a] cmc obtained from fit of volume data (0.00687 mol L^{-1})
[b] from reference 134
[c] from additivity method 2, see §5.1.4
[d] obtained from plateau region of V_ϕ curve

Figure 4.1.4-1: Apparent molar volumes of the 12-3-12 (Squares in the 12-3-12 plot correspond to data obtained from the dilatometer method), 10-3-10, and 8-3-8 gemini surfactants (squares correspond to data points simulated using the mass action model). The solid lines are fits to the pseudo-phase model.

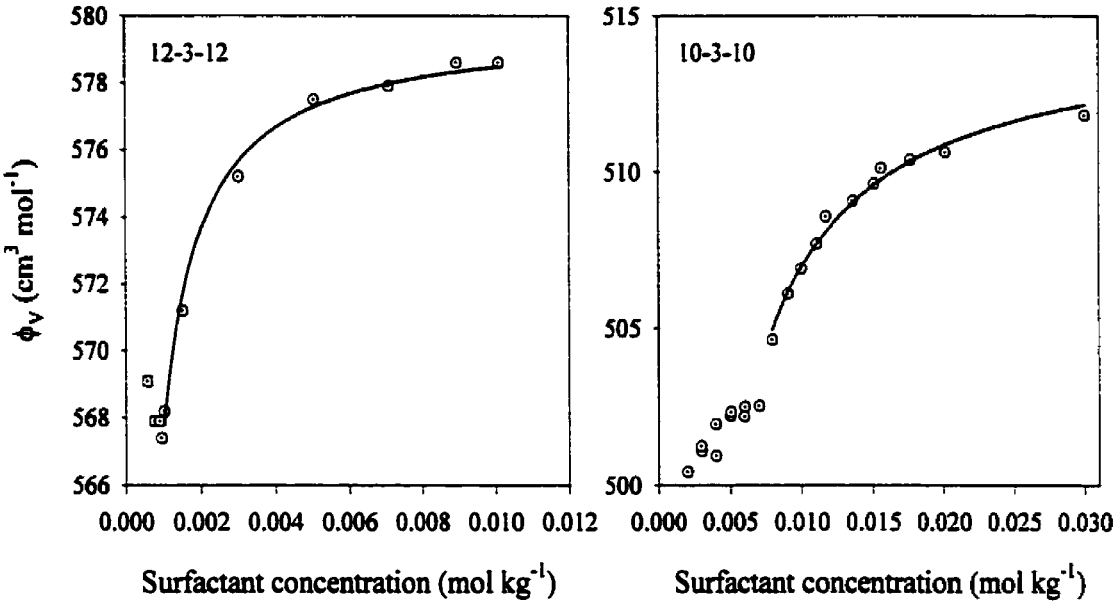

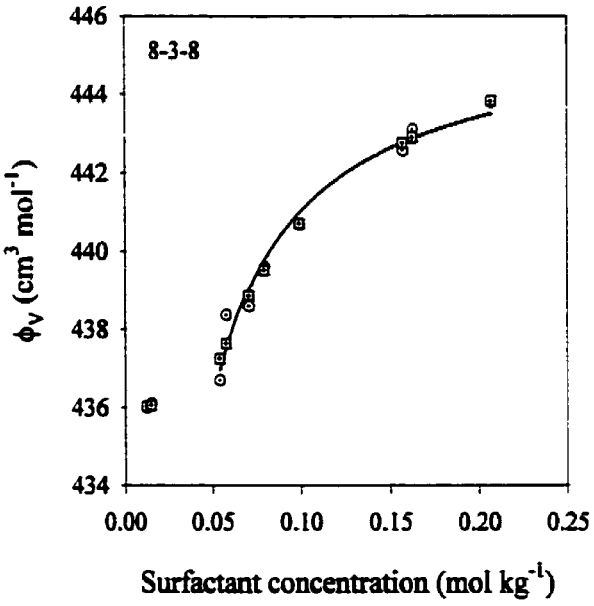

Figure 4.1.4-2: Apparent molar volumes of a) 12-2-12, b) 12-4-12, c) 12-6-12 (squares correspond to data obtained from the dilatometer method), d) 12-8-12, and e) 12-10-12 gemini surfactants. The solid lines represent fits to the pseudo-phase model.

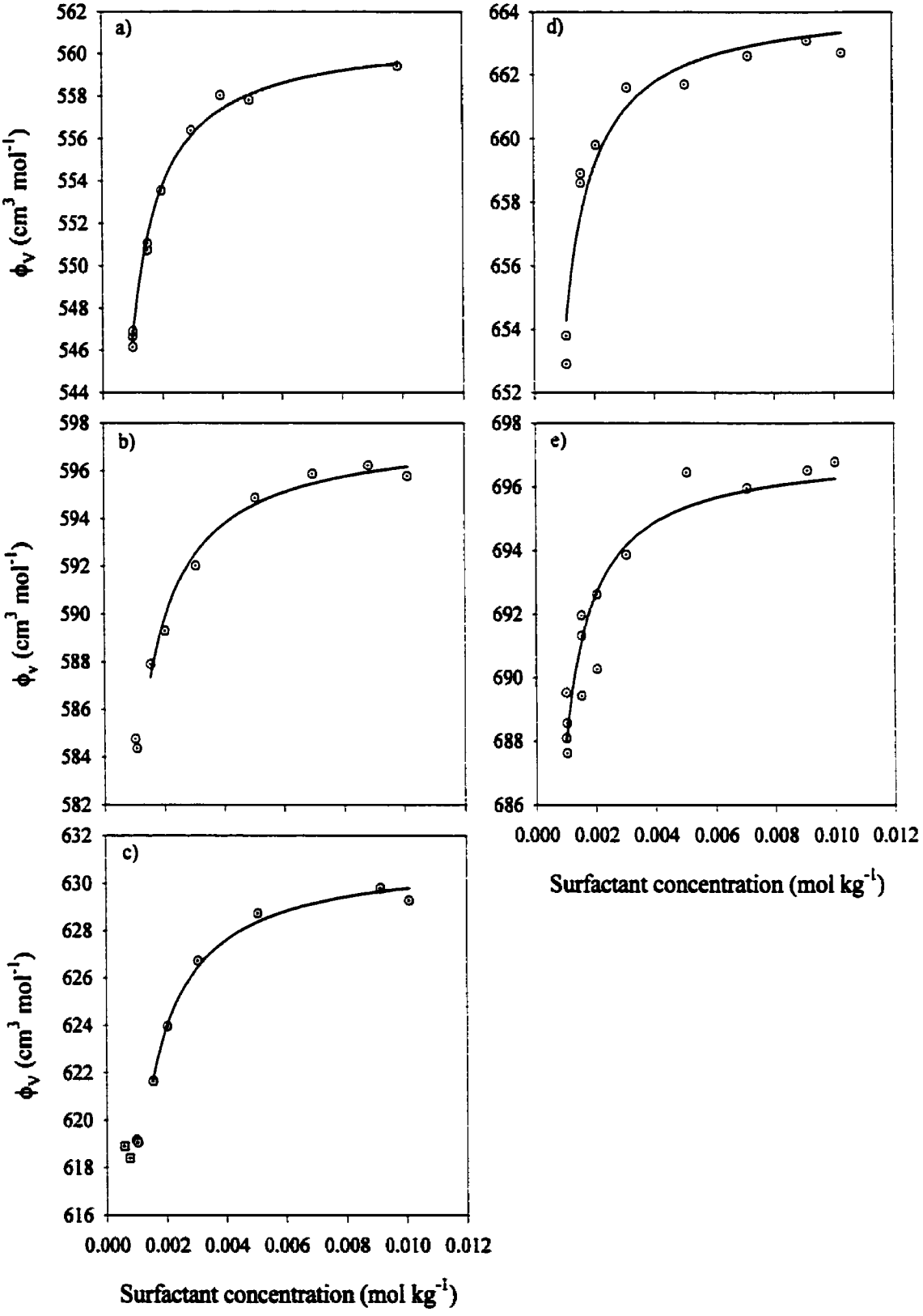

4.2 Ternary Polymer-Surfactant-Water Systems

4.2.1 Specific Conductance Studies

In order to study the effect of increased head group size on the interactions between cationic surfactants and neutral polymers, two of the gemini surfactants (12-3-12 and 12-6-12) were studied in a variety of polymer solutions at various concentrations. Figures 4.2.1-1 to 4.2.1-4 show the variation of the specific conductance as a function of surfactant concentration. It is important to note the absence of well defined breaks in the conductance profiles that would correspond to the onset of surfactant-polymer interaction (CAC) and the saturation of the polymer (C_2). Instead, one observes very broad curves which in some cases show specific conductivity values greater than those for the surfactant in aqueous solution. The broad curvature may be an indication of large degrees of polydispersity in the aggregates formed, or an indication of a binding process which differs from the usual case in which one observes evidence for well-defined CAC and C_2 values.

In some cases the aqueous polymer solution (in the absence of added surfactant) showed a specific conductance greater than that of the water being used (ca. 2 - 20 $\mu S\ cm^{-1}$ depending upon the polymer and its concentration). Similar observations have been reported previously.[135,136] In the present work this contribution was subtracted from the measured conductance for the mixed surfactant-polymer systems, as done by others.[135] It has been noted that purification of EO/PO polymeric samples by passing them through an ion exchange column reduced the specific conductance of the resulting solution; however, anomalous increases in conductance persisted.[136]

Figure 4.2.1-1: Specific conductance of a) the 12-3-12 gemini surfactant, and b) the 12-6-12 gemini surfactant in aqueous polymer solutions at 25°C.

a)

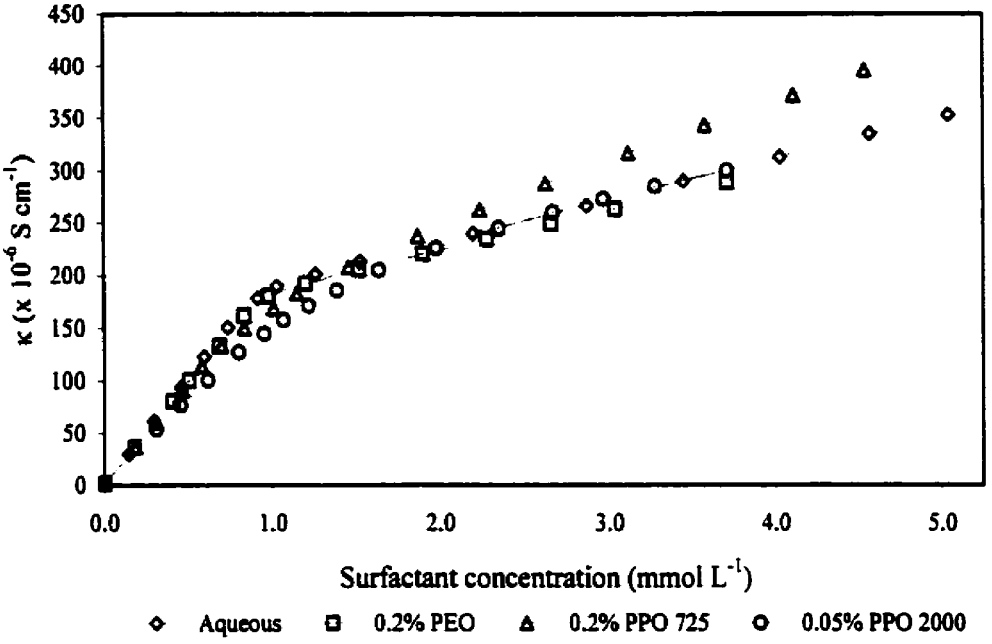

b)

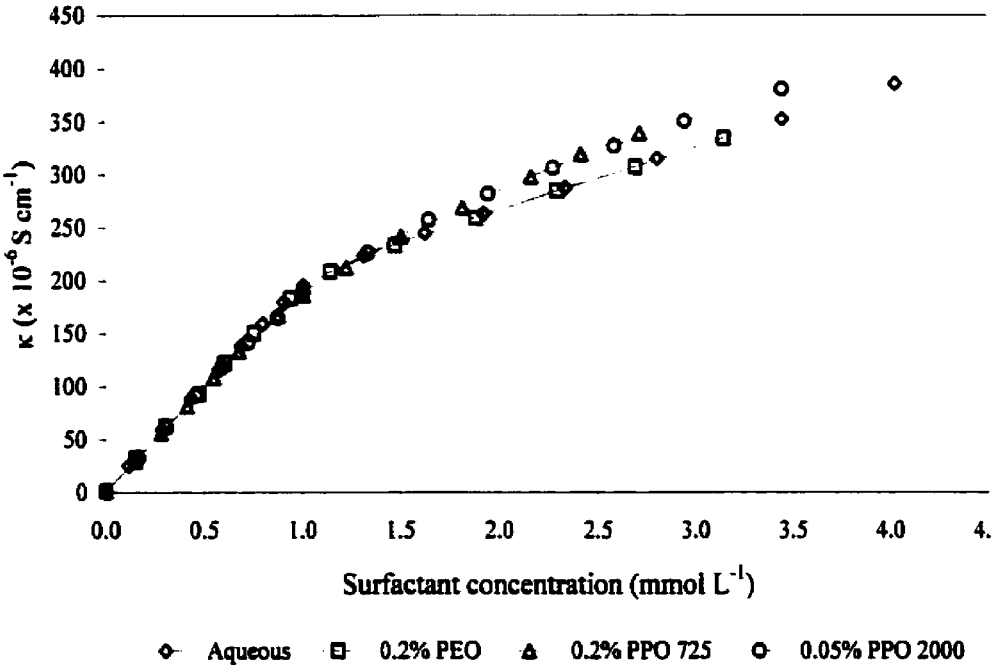

Figure 4.2.1-2: Specific conductance of a) the 12-3-12 gemini surfactant, and b) the 12-6-12 gemini surfactant in aqueous P103 solutions at 25°C.

a)

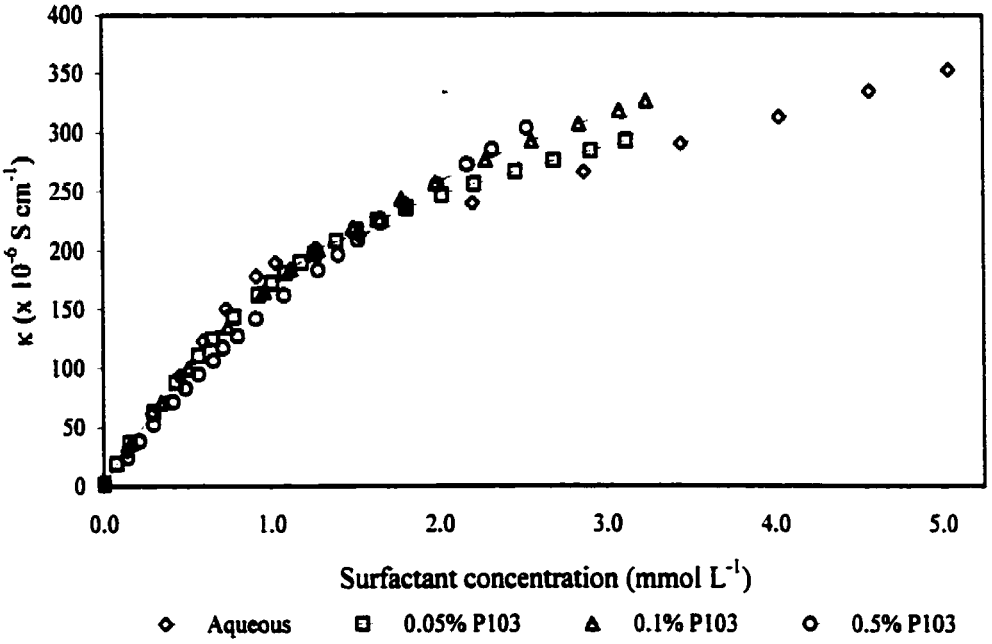

b)

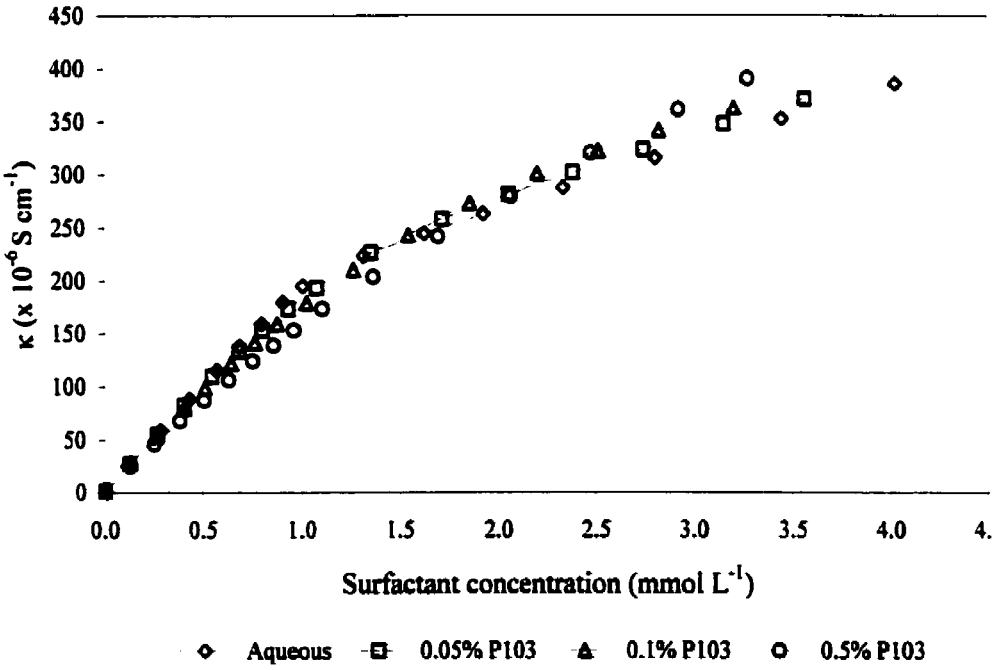

Figure 4.2.1-3: Specific conductance of a) the 12-3-12 gemini surfactant, and b) the 12-6-12 gemini surfactant in aqueous F108 solutions at 25°C.

a)

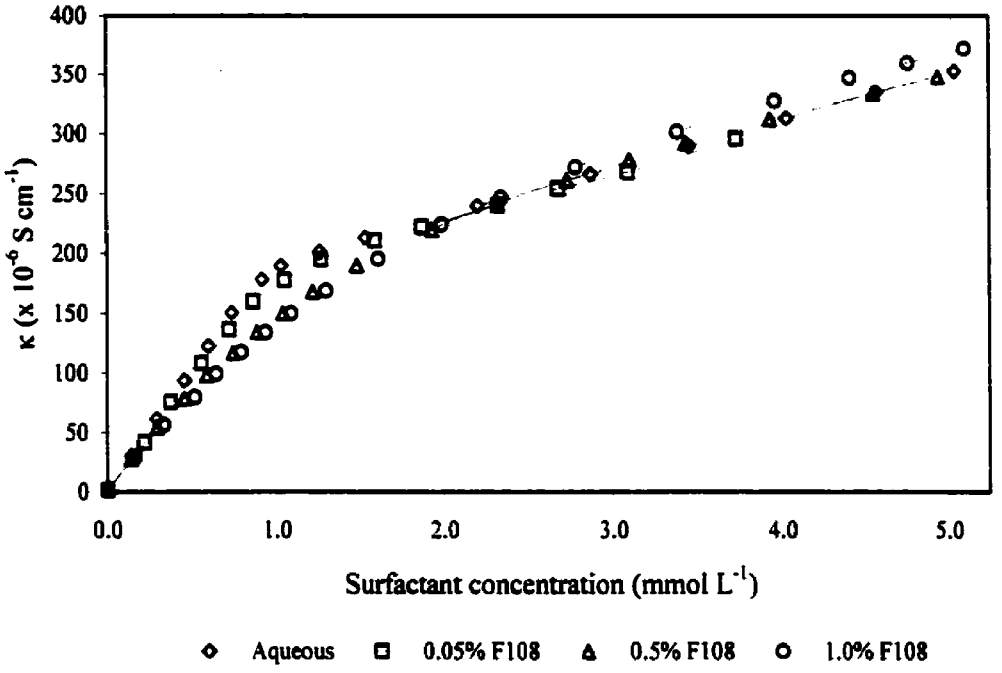

b)

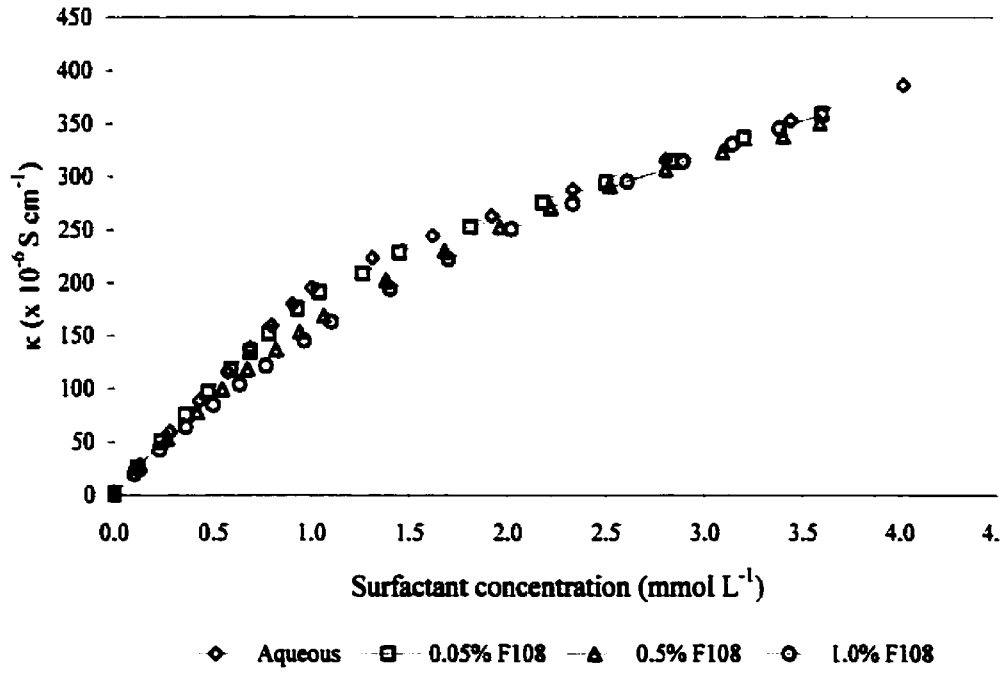

Figure 4.2.1-4: Specific conductance of a) the 12-3-12 gemini surfactant, and b) the 12-6-12 gemini surfactant in aqueous F68 solutions at 25°C.

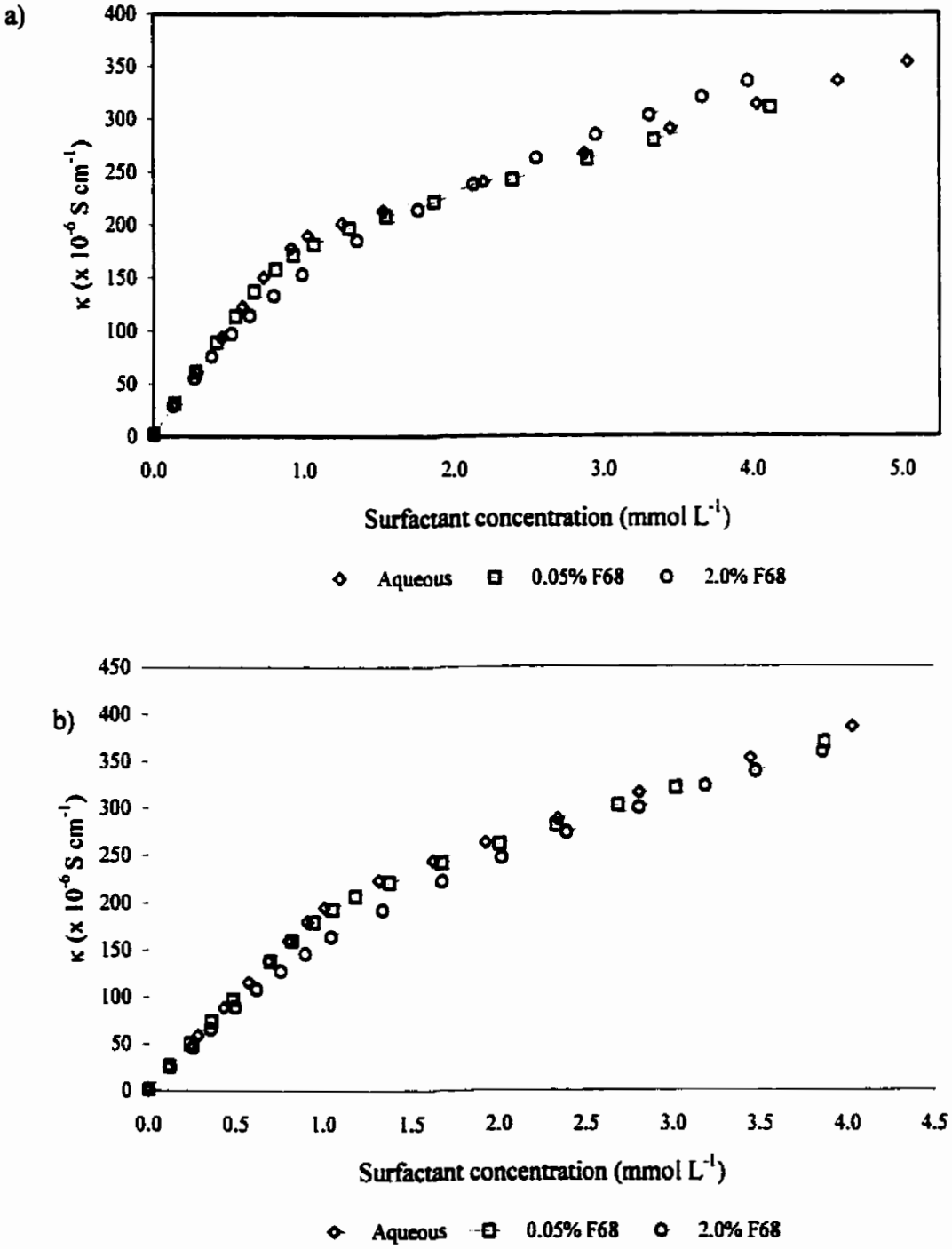

4.2.2 Surface Tension Studies

An attempt was made to study the behavior of the surface tension of the ternary surfactant-polymer-water systems. Plots of the surface tension for the 12-6-12 surfactant as a function of surfactant concentration (at fixed polymer concentration) are shown in Figure 4.2.2-1. Results obtained for PEO, PPO (M.W. 725) and the Pluronic F68 show somewhat similar behavior to that observed for the surfactant in aqueous solution. More complex results are obtained in the presence of PPO (M.W. 2000), and the Pluronic F108. The surface tension profiles are complicated by the low values for the surface tension of the aqueous polymer solutions in the absence of any added surfactant (see Table 4.2.2-1). It should be noted that attempts (by two-phase solvent extraction) to remove possible surface active impurity that may have been used during the polymer synthesis and recovery procedures did not result in any increase in the surface tension for the aqueous PPO (M.W. 2000) solution. In the case of most aqueous copolymer systems the value of the surface tension is below the plateau value for the aqueous gemini surfactant above the cmc ($\gamma_{12\text{-}6\text{-}12} \cong 40$ mN m^{-1}). As a result the addition of the gemini surfactant has only a minimal effect on the surface tension. This in turn makes it very difficult to interpret the effect of the polymer on the behavior of the surfactant. It should be noted that, as observed in the specific conductance measurements, there is no evidence to suggest a CAC or C_2 value for the ternary systems.

Table 4.2.2-1: Surface tension values for the aqueous polymer and copolymer solutions

Polymer[a]	γ (mN m^{-1})
0.2% PEO	60.4
0.2% PPO 725	43.7
0.05% PPO 2000	37.0
0.05% P103	33.1
0.05% F108	46.2
0.5% F108	39.5
0.05% F68	48.5

[a] concentration in (w/w)%

Figure 4.2.2-1: Surface tension as a function of the logarithm of the surfactant concentration (in mol L^{-1}) for the 12-6-12 gemini surfactant in aqueous polymer solutions at 25°C.

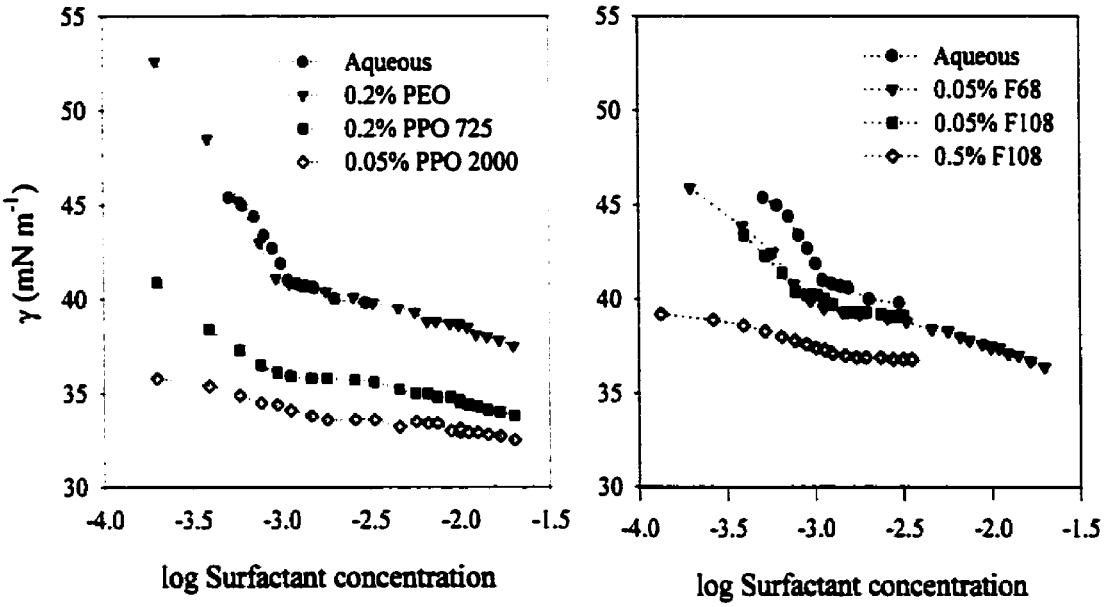

4.2.3 ^{1}H NMR

As stated previously, the chemical shift of the N-methyl protons of the gemini surfactant was measured (relative to D_2O) for several systems. Plots of the chemical shift as a function of inverse surfactant concentration for the 12-3-12 and 12-6-12 surfactants in D_2O and in various polymer solutions (in D_2O) are shown in Figures 4.2.3-1 to 4.2.3-4. D_2O was used as

a solvent for the NMR studies instead of water to minimize complications arising from solvent suppression routines. The cmc values obtained from the break in the chemical shift plots are 0.67 and 0.75 mmol L^{-1} for solutions of the 12-3-12 and 12-6-12 surfactants, respectively. These values are lower than those obtained from surface tension and conductivity measurements; however, this is primarily due to the nature of D_2O as compared to water. Decreases in the cmc have been observed from specific conductance measurements, along with corresponding increases in the aggregation number, observed from light scattering, for surfactants in D_2O as compared to water.[137] These variations have been attributed to small differences in the nature of hydrophobic interactions in water as compared to D_2O. In addition, small angle neutron scattering studies of $C_{16}TAB/D_2O$ systems have shown that the surface of the $C_{16}TAB$ micelles in D_2O are "drier" than the surface of corresponding micelles in aqueous solution.

Similar plots obtained for the ternary systems containing PEO, PPO (M.W. 725) and F68 do not show any substantial deviations from results obtained for the binary surfactant-water systems. However, the plots obtained for PPO (M.W. 2000), P103 and F108 do show deviations from the aqueous surfactant behavior at low surfactant concentrations. These deviations are similar to results obtained from conductivity measurements in that no well-defined breaks are observed in the chemical shift plots .

Figure 4.2.3-1: ^{1}H NMR chemical shifts for the N-methyl protons of the 12-3-12 gemini surfactant as a function of surfactant concentration in D_2O solutions of a) PEO, b) PPO (M.W. 725), and c) PPO (M.W. 2000).

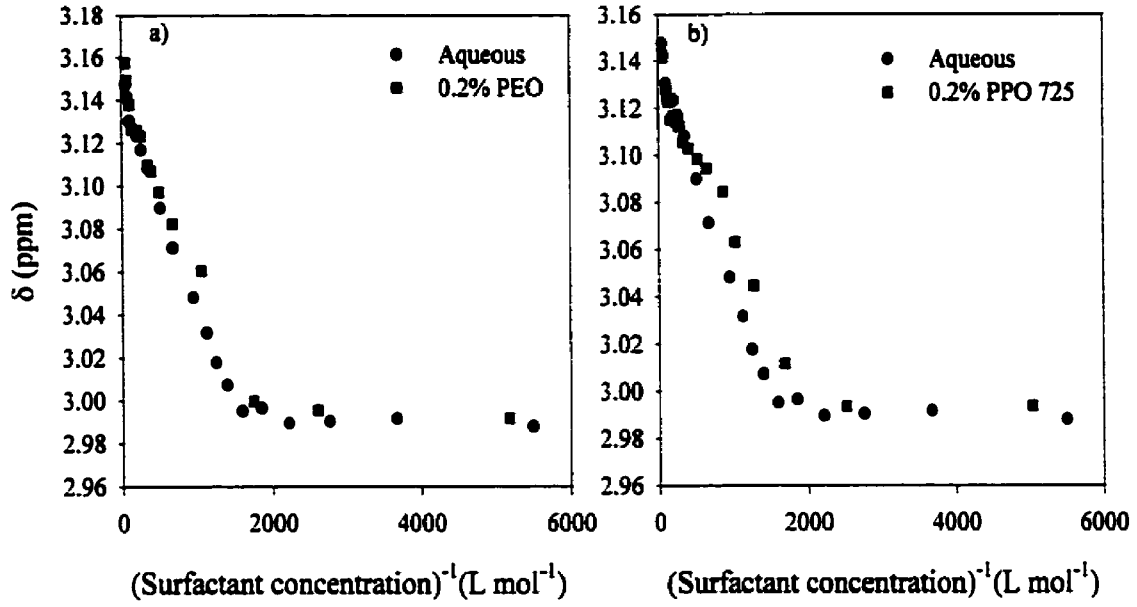

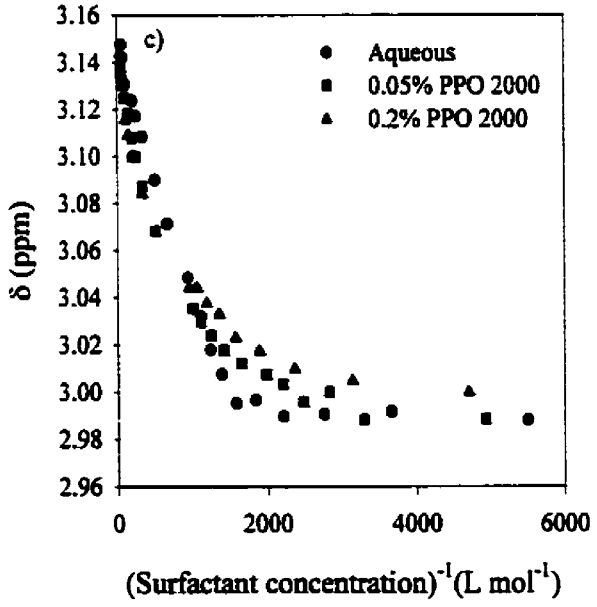

Figure 4.2.3-2: ^{1}H NMR chemical shifts for the N-methyl protons of the 12-3-12 gemini surfactant as a function of surfactant concentration in D_2O solutions of a) P103, b) F108, and c) F68.

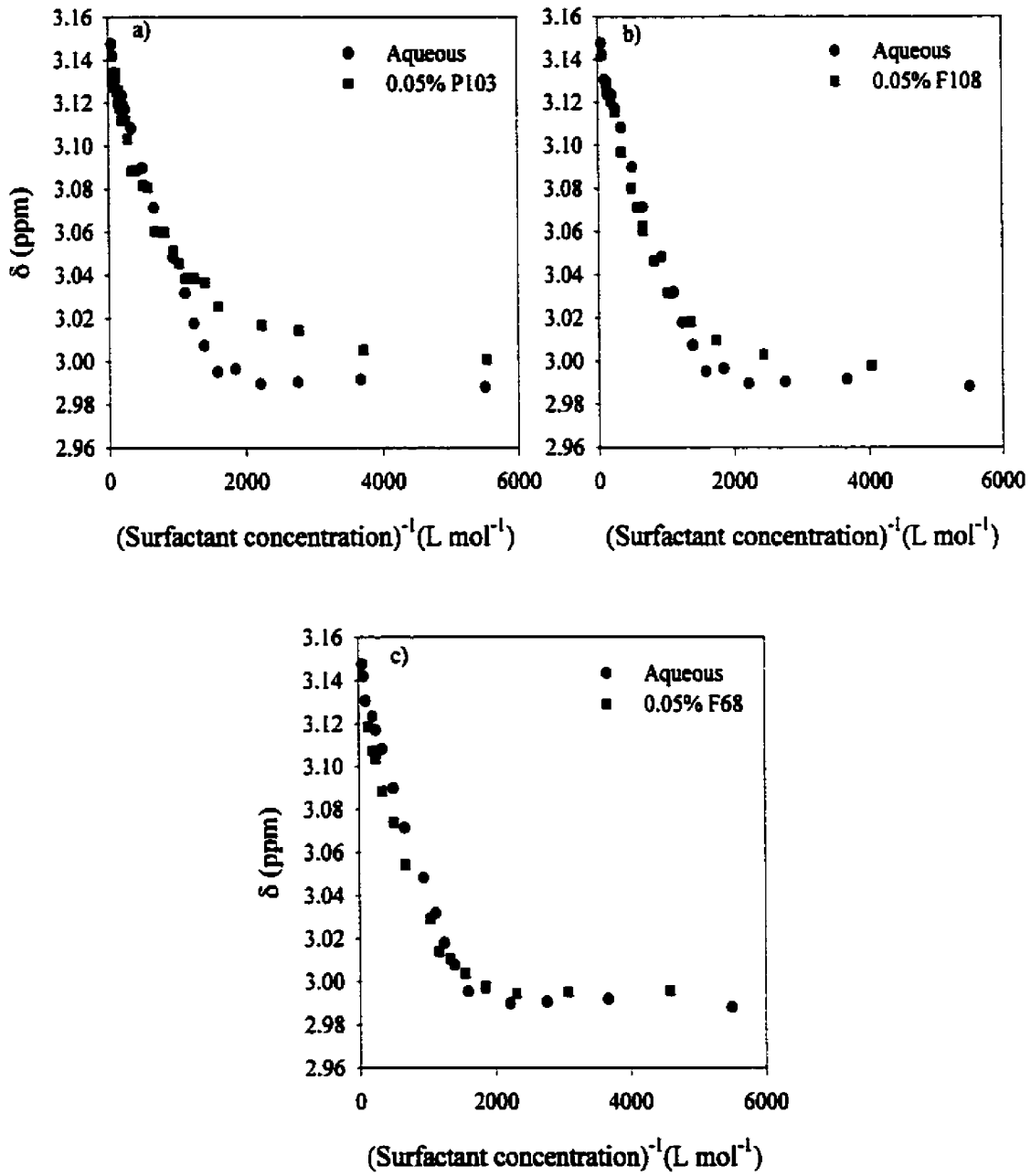

Figure 4.2.3-3: ^{1}H NMR chemical shifts for the N-methyl protons of the 12-6-12 gemini surfactant as a function of surfactant concentration in D_2O solutions of a) PEO, b) PPO (M.W. 725), and c) PPO (M.W. 2000).

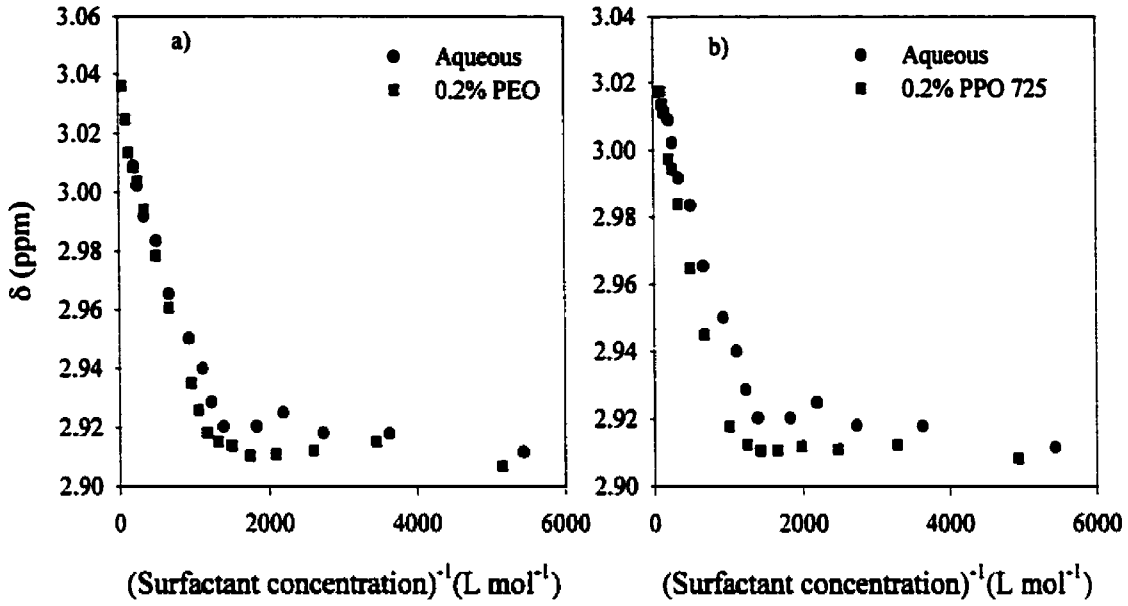

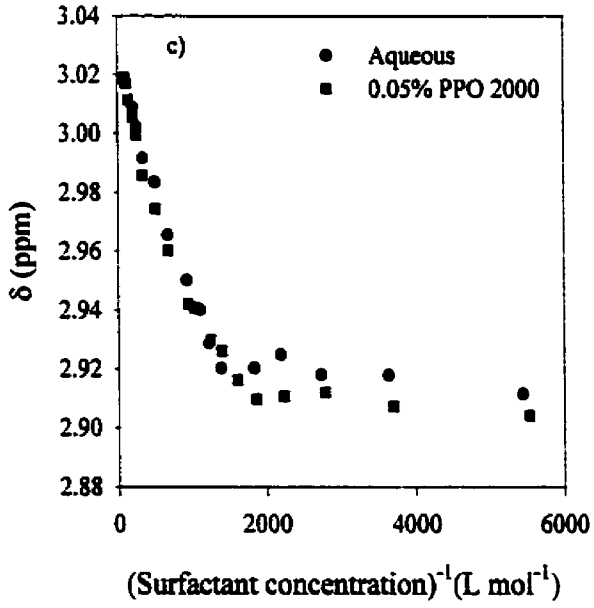

Figure 4.2.3-4: ^{1}H NMR chemical shifts for the N-methyl protons of the 12-6-12 gemini surfactant as a function of surfactant concentration in D_2O solutions of a) P103, b) F108, and c) F68.

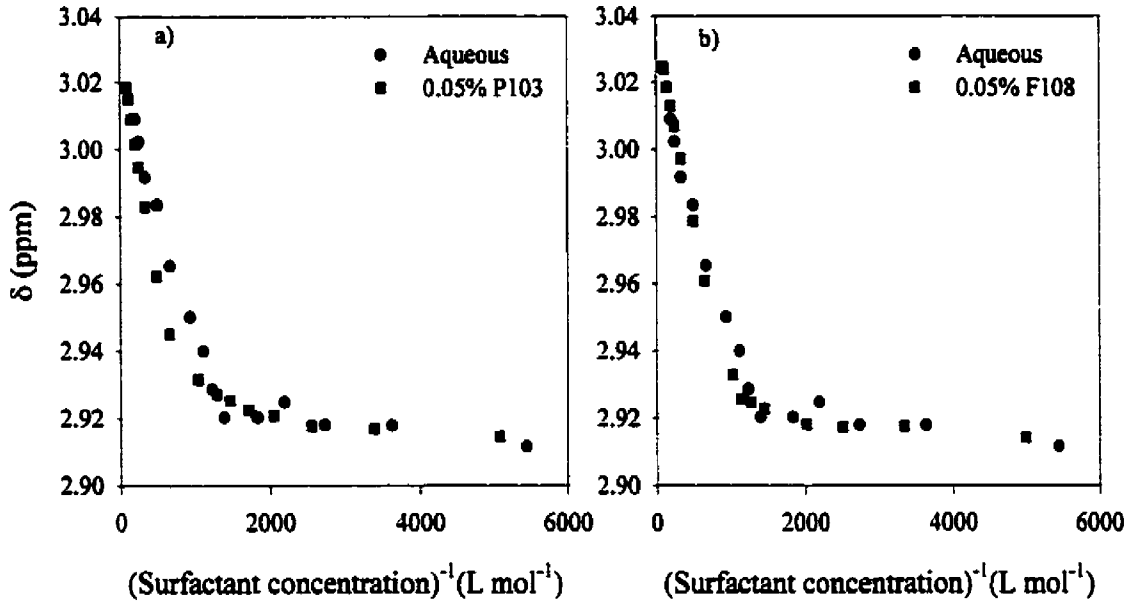

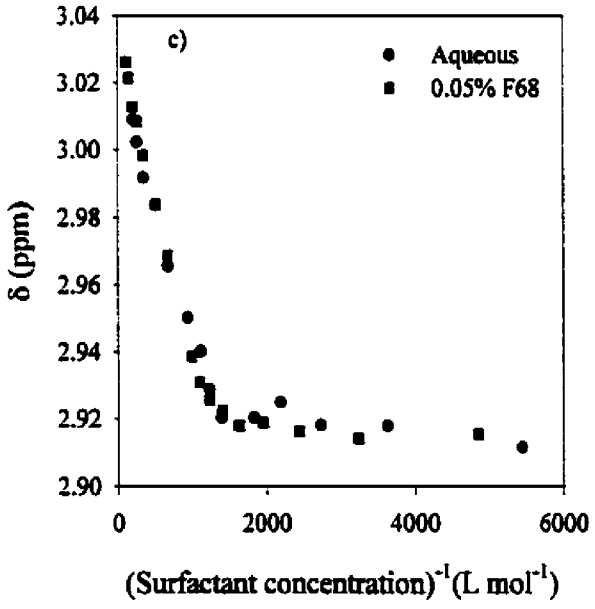

4.2.4 Fluorescence studies

4.2.4.1 Vibronic intensity ratios of pyrene

The I_1/I_3 vibronic intensity ratio of pyrene was measured in aqueous solutions of the 12-3-12 and 12-6-12 surfactant, and in ternary aqueous solutions containing polymer. The results are presented in Figures 4.2.4-1 and –2. The cmcs obtained for the 12-3-12 and 12-6-12 from this method are 0.97 mmol L^{-1} and 1.10 mmol L^{-1}, respectively, and agree well with those obtained from specific conductance (0.98 and 1.09 mmol L^{-1}) and surface tension (0.89 and 0.96 mmol L^{-1}). The value of the I_1/I_3 ratio in the micellar phase was found to be 1.42 for both surfactants. This value is somewhat lower than the value of 1.48 obtained for both surfactants in aqueous solution and close to the value of 1.41 obtained for DTAB in aqueous solution by Zana et al.[38]

Figures 4.2.4.1-1 and -2 do not indicate any significant differences between the cmc values for either surfactant in water and aqueous PEO, PPO (M.W. 725 and 2000), and F68 solutions. However, there is evidence of some interaction between the gemini surfactant micelles and these polymers as the environment sensed by pyrene is seen to decrease in polarity (with the possible exception of PPO (M.W. 725). The post-micellar I_1/I_3 values are listed in Table 4.2.4.1-1. The results for both 12-3-12 and 12-6-12 with P103 and F108 are more complex (c.f. Figures 4.2.4.1-1 and -2 b) and c)), with the results for systems containing 0.05% F108 showing clear evidence of a CAC of 0.57 and 0.72 mmol L^{-1}, for the 12-3-12 and 12-6-12 surfactants, respectively. As the concentration of F108 is increased the critical concentration appears to approach the value of the cmc for the aqueous surfactant solution (although the nature of the curve now makes a determination of the critical

Figure 4.2.4.1-1: Ratios of intensities of the first (I_1) and third (I_3) vibronic peaks for pyrene in solutions of the 12-3-12 gemini surfactant in a)PEO, PPO (M.W. 725), and PPO (M.W. 2000), b) P103, c) F108 and d) F68.

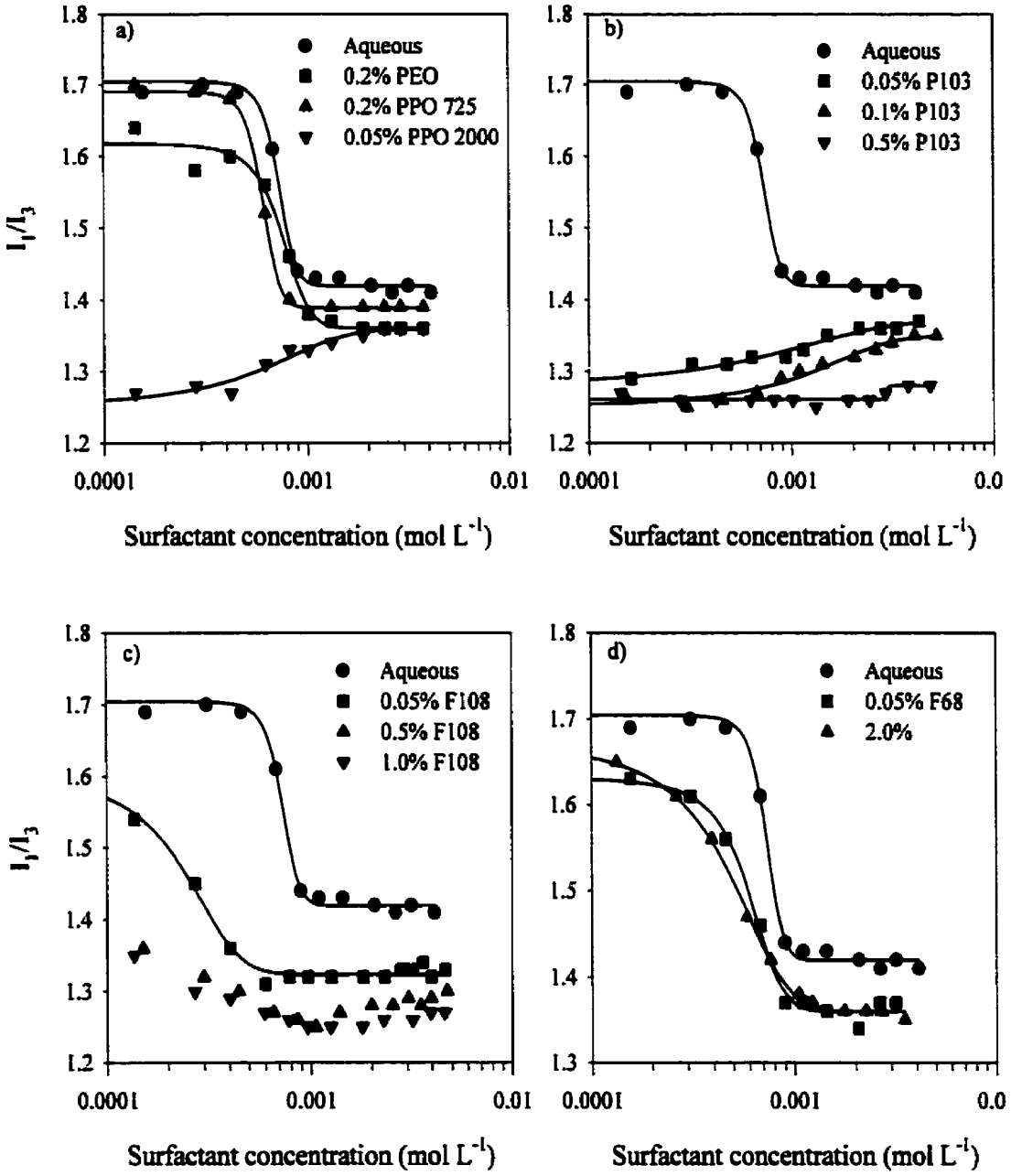

Figure 4.2.4.1-2: Ratios of intensities of the first (I_1) and third (I_3) vibronic peaks for pyrene in solutions of the 12-6-12 gemini surfactant in a)PEO, PPO (M.W. 725), and PPO (M.W. 2000), b) P103, c) F108 and d) F68.

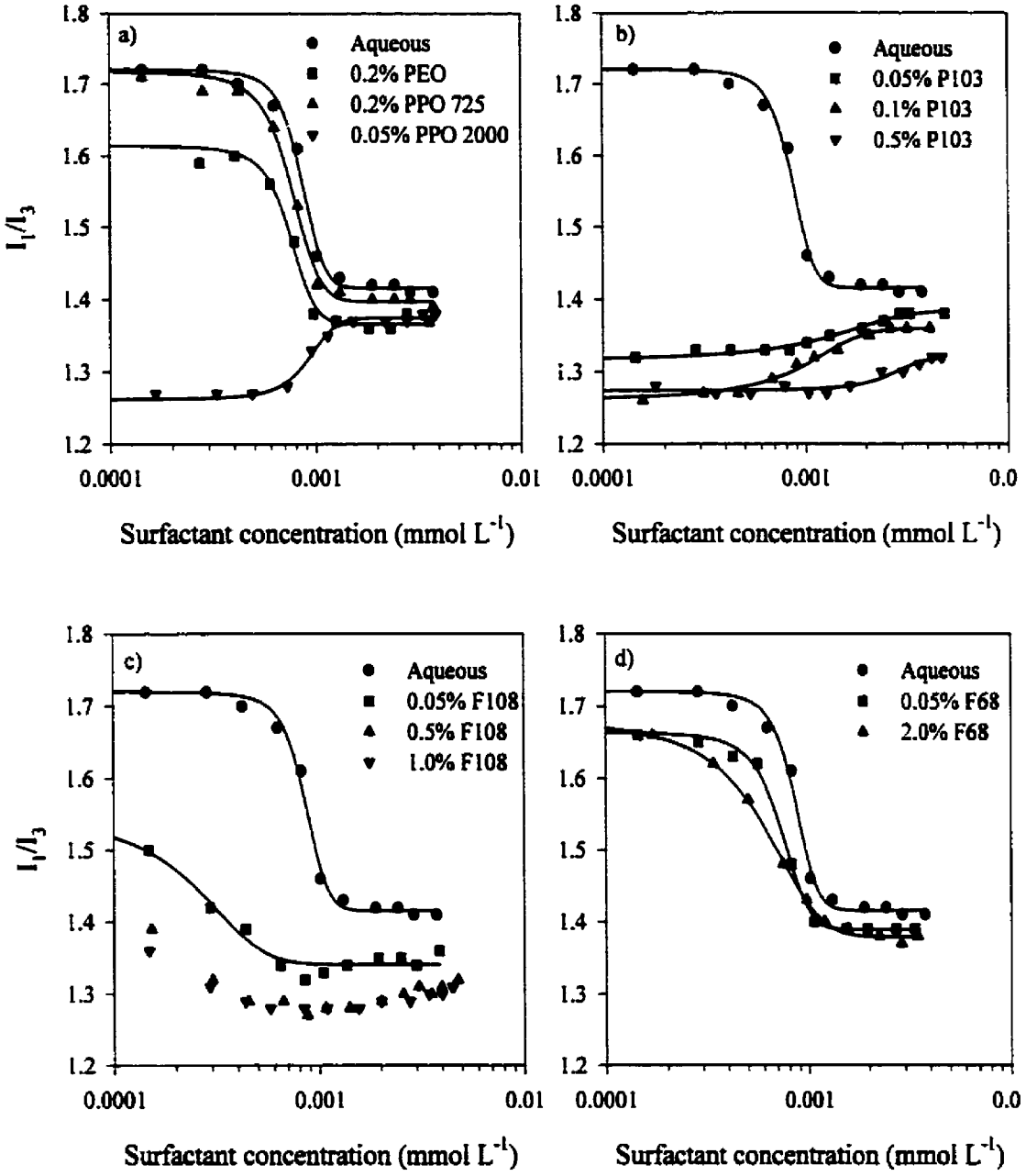

Table 4.2.4.1-1: Post-micellar values for the vibronic intensity ratio (I_1/I_3) of pyrene in aqueous mixed surfactant-polymer systems.

12-3-12		12-6-12	
Polymer	I_1/I_3	Polymer	I_1/I_3
None	1.42	None	1.42
0.2% PEO	1.36	0.2% PEO	1.37
0.2% PPO (M.W. 725)	1.39	0.2% PPO (M.W. 725)	1.40
0.05% PPO (M.W. 2000)	1.36	0.05% PPO (M.W. 2000)	1.37
0.05% P103	1.37	0.05% P103	1.38
0.1% P103	1.35	0.1% P103	1.36
0.5% P103	1.28	0.5% P103	1.32
0.05% F108	1.32	0.05% F108	1.34
0.5% F108	1.28	0.5% F108	1.32
1.0% F108	1.27	1.0% F108	1.31
0.05% F68	1.36	0.05% F68	1.39
2.0% F68	1.36	2.0% F68	1.38

concentration more difficult); however, the low value of the I_1/I_3 ratio clearly indicates an interaction between the surfactant micelles and the polymer chain. The results obtained for P103 do not indicate a CAC. However, the low initial values of I_1/I_3 for pyrene suggest that it is located in a more nonpolar region, even before micellization of the gemini surfactants starts to occur.

4.2.4.2 Mean aggregation numbers

Fluorescence decay curves were obtained for the 12-6-12 gemini surfactant in aqueous polymer solutions at various surfactant concentrations. The decay curves were fit to Equation 3.2.3.1-1 (assuming immobile probe and quencher) and values obtained for k_0, k_q, and $\bar{n}$ are given in Appendix D-II along with the surfactant and quencher concentrations studied. Mean aggregation numbers were calculated from Equation 3.2.3.1-2 using the cmc

Figure 4.2.4.2-1: Mean aggregation numbers for the 12-6-12 gemini surfactant in a) aqueous polymer, and b) aqueous Pluronic solutions.

a)

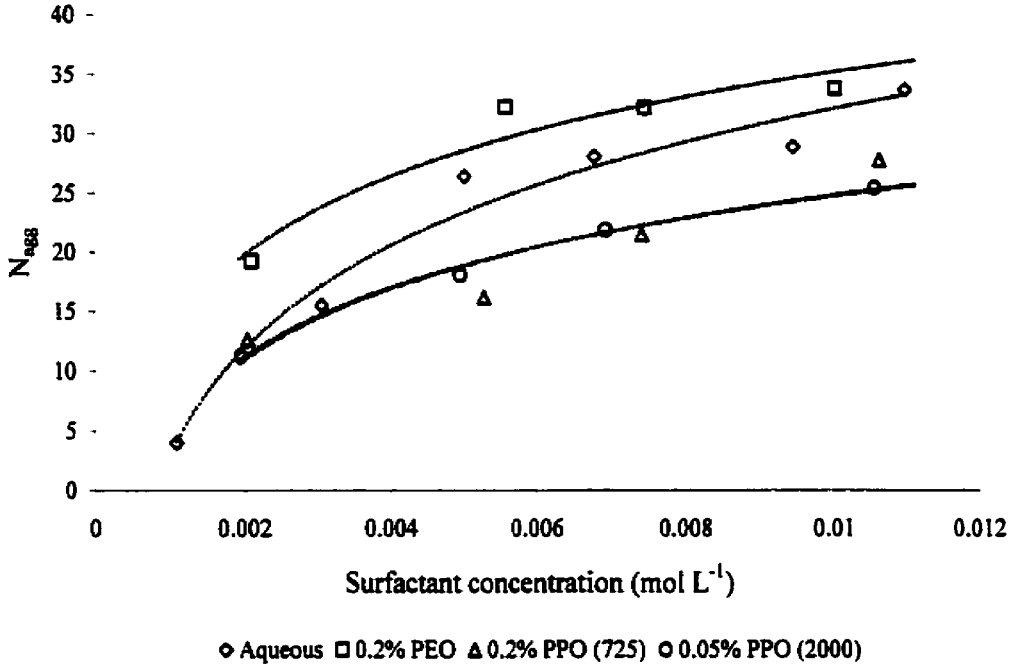

b)

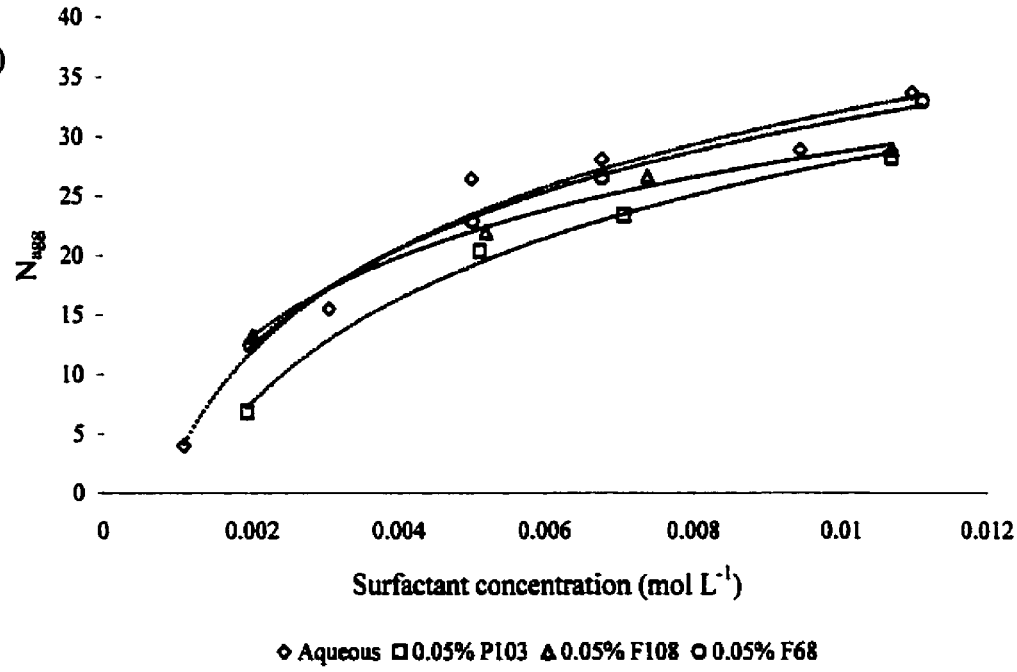

obtained for the mixed surfactant-polymer solution (c.f. Table 5.2.1-2) and are also included in Appendix D-II. Figure 4.2.4.2-1 illustrates the behavior of N_{agg} as a function of surfactant concentration, along with the effect of added polymer. It is observed that the addition of a neutral polymer to the surfactant solution of fixed concentration results, generally, in a decrease in the aggregation number of the resulting micelles in solution. The addition of PEO results in, unexpectedly, an apparent increase in the mean aggregation number of the surfactant.

4.2.5 Apparent Molar Volume Studies

4.2.5.1 Studies at 25°C

Measurements of the apparent molar volumes of the 12-3-12 and 12-6-12 gemini surfactants were made in the presence of fixed concentrations of PEO, PPO (M.W. 725 and 2000), P103, F108, and F68. Plots of the apparent molar volume as a function of surfactant concentration are shown in Figures 4.2.5.1–1 and –2. No significant differences are observed between either 12-3-12 or 12-6-12 in water and in PEO, 0.05% F108, and 0.05% F68. Increases in V_ϕ are observed for the surfactants in solutions of 0.2% PPO (M.W. 725), 0.05% PPO(M.W. 2000), P103, and higher concentrations of F108 and F68. Large and unusual deviations are observed for polymer concentrations of 2.0%. In an effort to gain further information about the reason for these deviations, studies of V_ϕ as a function of temperature were undertaken for the 12-3-12 surfactant in 2.0% P103, F108, and F68.

Figure 4.2.5.1-1: Apparent molar volume (V_ϕ) as a function of surfactant concentration for the 12-3-12 gemini surfactant in aqueous solutions of a) PEO, PPO (M.W. 725), PPO (M.W. 2000), b) P103, c) F108, and d) F68. Solid lines are fits to the pseudo-phase model, dotted lines are to assist with visualization.

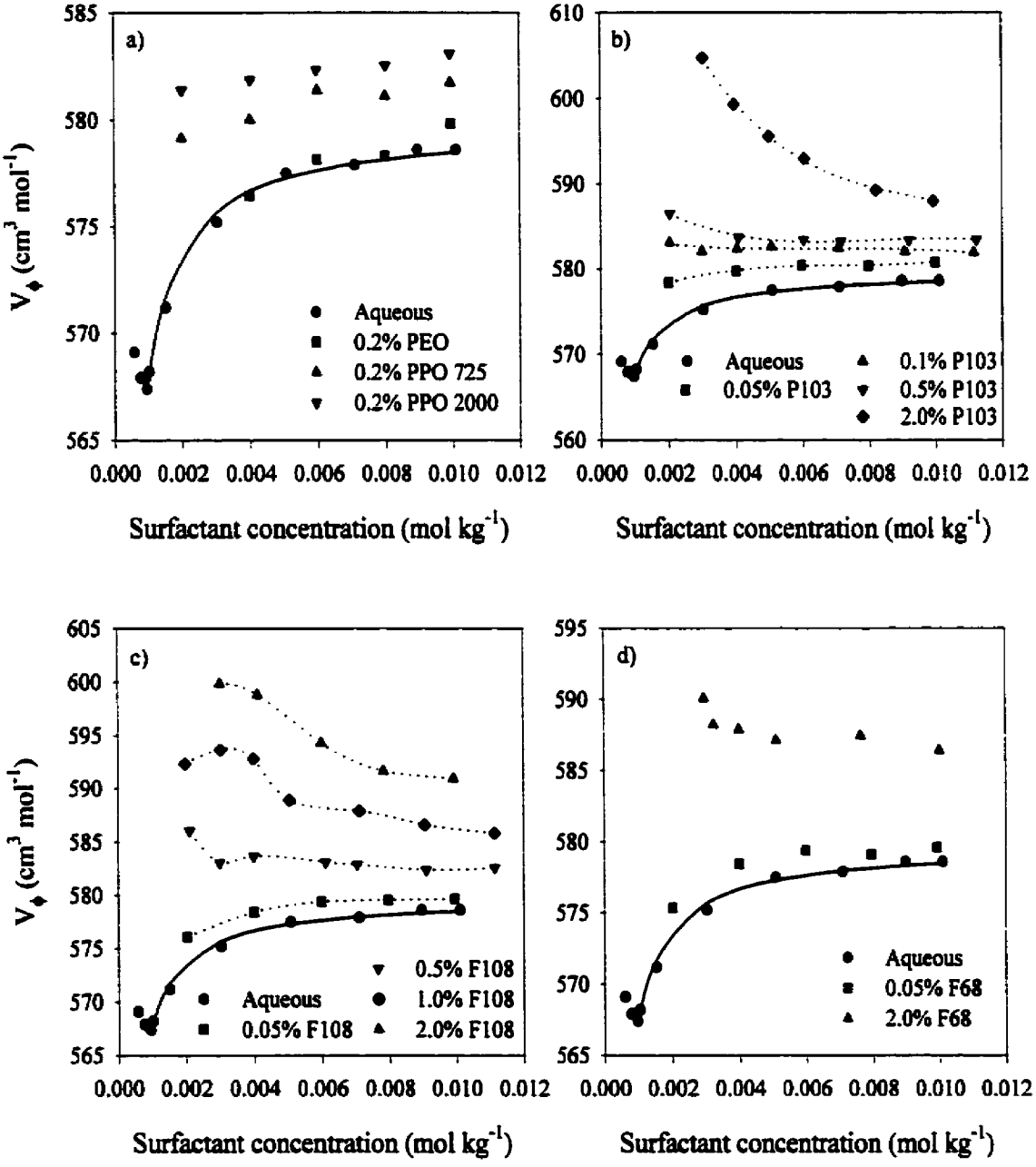

Figure 4.2.5.1-2: Apparent molar volume (V_ϕ) as a function of surfactant concentration for the 12-6-12 gemini surfactant in aqueous solutions of a) PEO, PPO (M.W. 725), PPO (M.W. 2000), b) P103, c) F108, and d) F68. Solid lines are fits to the pseudo-phase model, dotted lines are to assist with visualization.

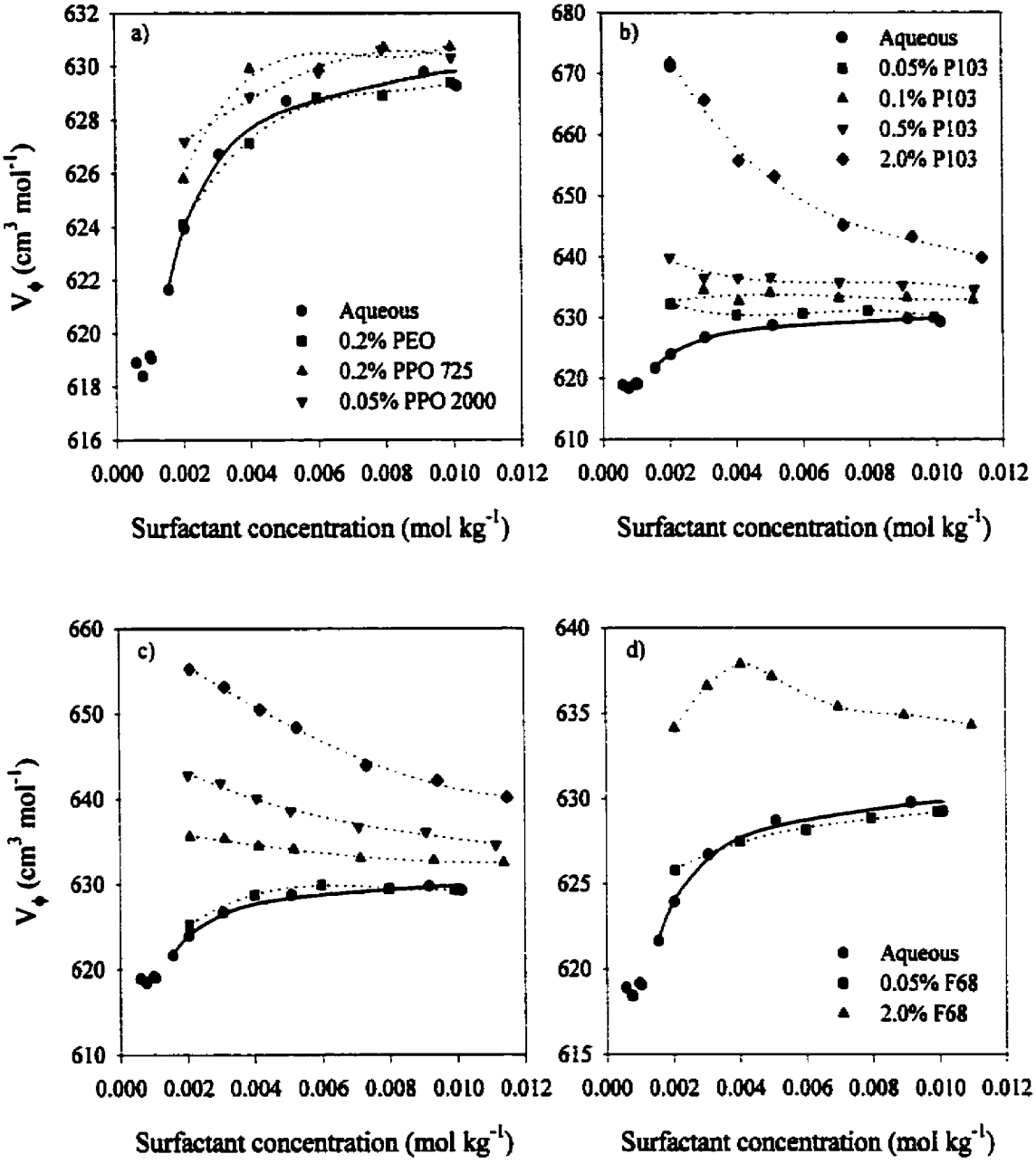

4.2.5.2 Temperature Dependent Studies

The specific conductivity and apparent molar volumes were measured at fixed surfactant and polymer concentrations as a function of temperature. Figures 4.2.5.2-1, -2, and -3 illustrate the apparent molar volume and specific conductance of the 12-3-12 gemini surfactant in 2.0% P103, 2.0% F108, and 2.0% F68, respectively.

The observed maximum in the apparent molar volume of the surfactant, as well as the transition observed in the specific conductance of the solutions, occur at the same temperature as the critical micelle temperature (cmt) for solutions of aqueous P103 and F108.[138] The Pluronic F68 does not exhibit a cmt in the temperature range studied, hence one observes no transition in either the apparent molar volume or in the specific conductance for the 12-3-12 surfactant. The cmt values for aqueous 2.0% Pluronic solutions were obtained from measurements of the apparent specific volume ($V_{\phi,specific}$, $cm^3\ g^{-1}$) according to

$$V_{\phi,specific} = \frac{1}{w}\left(\frac{1}{d} - \frac{w_0}{d_0}\right) \qquad 4.2.5.2\text{-}1$$

where w and w_0 are the weight ratio of the solute and solvent, respectively. Plots of $V_{\phi,specific}$ as a function of temperature for the 2.0% Pluronic solutions are shown in Figure 4.2.5.2-4. Cmt values obtained from $V_{\phi,specific}$ for 2.0% Pluronic solutions were; 20°C for 2.0% P103, 30°C for 2.0% F108, and no observable transition for 2.0% F68. These transitions suggest a segregation of the surfactant and polymer molecules into two types of aggregates in solution and will be discussed in more detail in §5.2.3.

Figure 4.2.5.2-1: Specific conductance (circles) and apparent molar volume (squares) as a function of temperature for the 12-3-12 gemini surfactant in aqueous 2.0% P103; a) 5 mmol kg^{-1} 12-3-12, b) 10 mmol kg^{-1} 12-3-12, c) 20 mmol kg^{-1} 12-3-12. Filled symbols are for aqueous 10 mmol kg^{-1} 12-3-12 for reference.

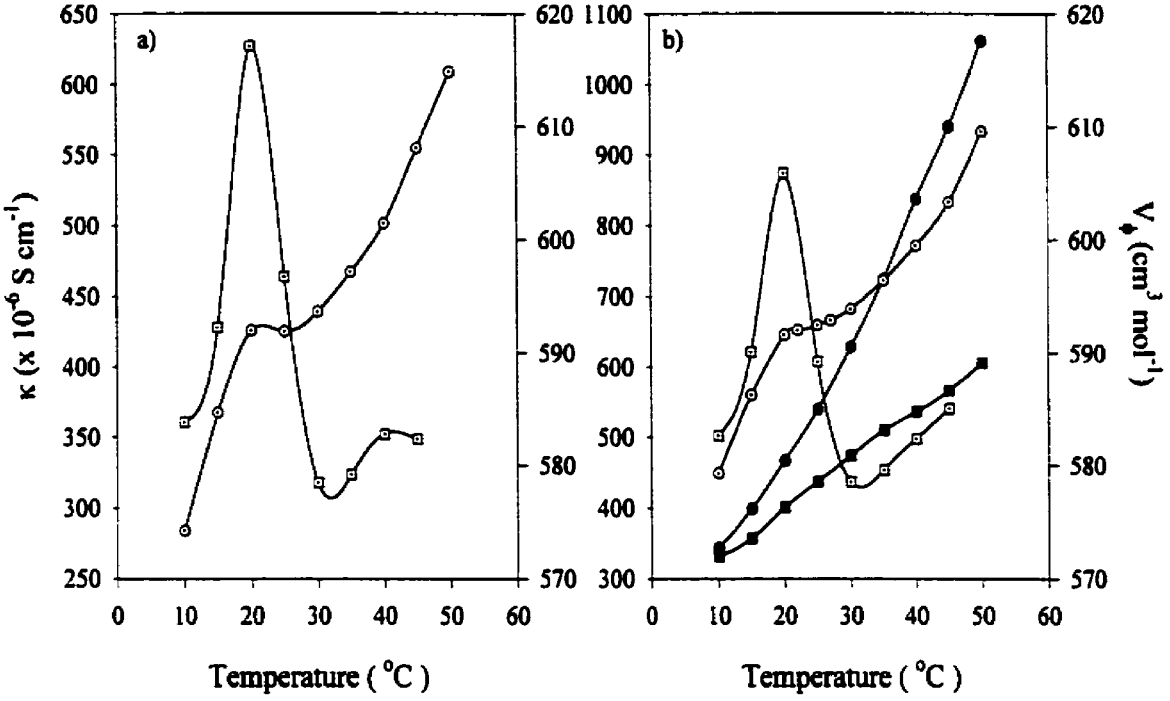

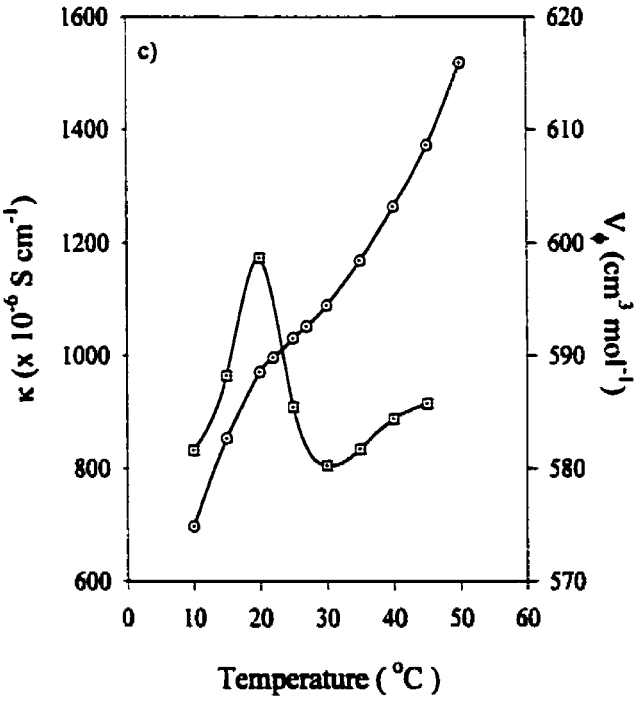

Figure 4.2.5.2-2: Specific conductance (circles) and apparent molar volume (squares) as a function of temperature for the 12-3-12 gemini surfactant in aqueous 2.0% F108; a) 5 mmol kg^{-1} 12-3-12, b) 10 mmol kg^{-1} 12-3-12, c) 20 mmol kg^{-1} 12-3-12. Filled symbols are for aqueous 10 mmol kg^{-1} 12-3-12 for reference.

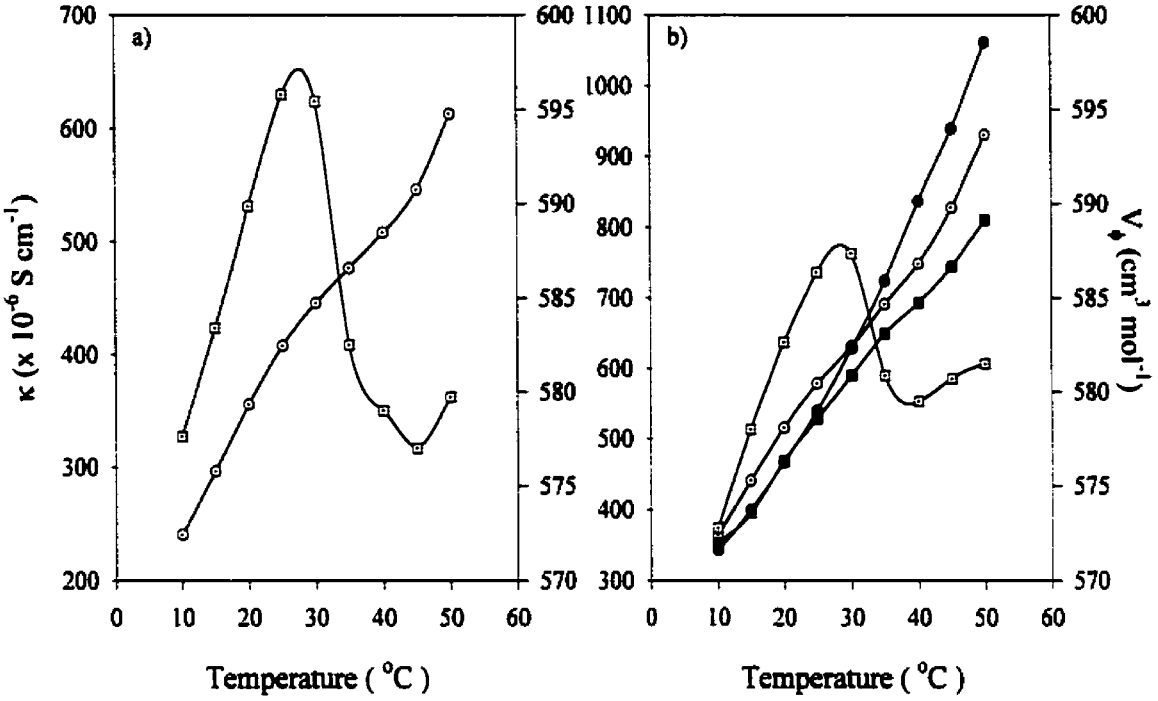

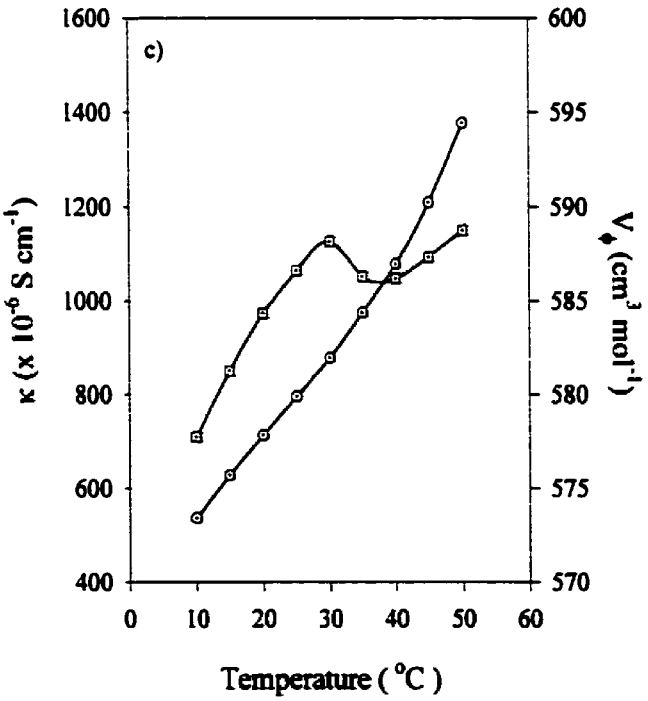

Figure 4.2.5.2-3: Specific conductance (circles) and apparent molar volume (squares) as a function of temperature for the 12-3-12 gemini surfactant in aqueous 2.0% F68; a) 5 mmol kg^{-1} 12-3-12, b) 10 mmol kg^{-1} 12-3-12, c) 20 mmol kg^{-1} 12-3-12. Filled symbols are for aqueous 10 mmol kg^{-1} 12-3-12 for reference.

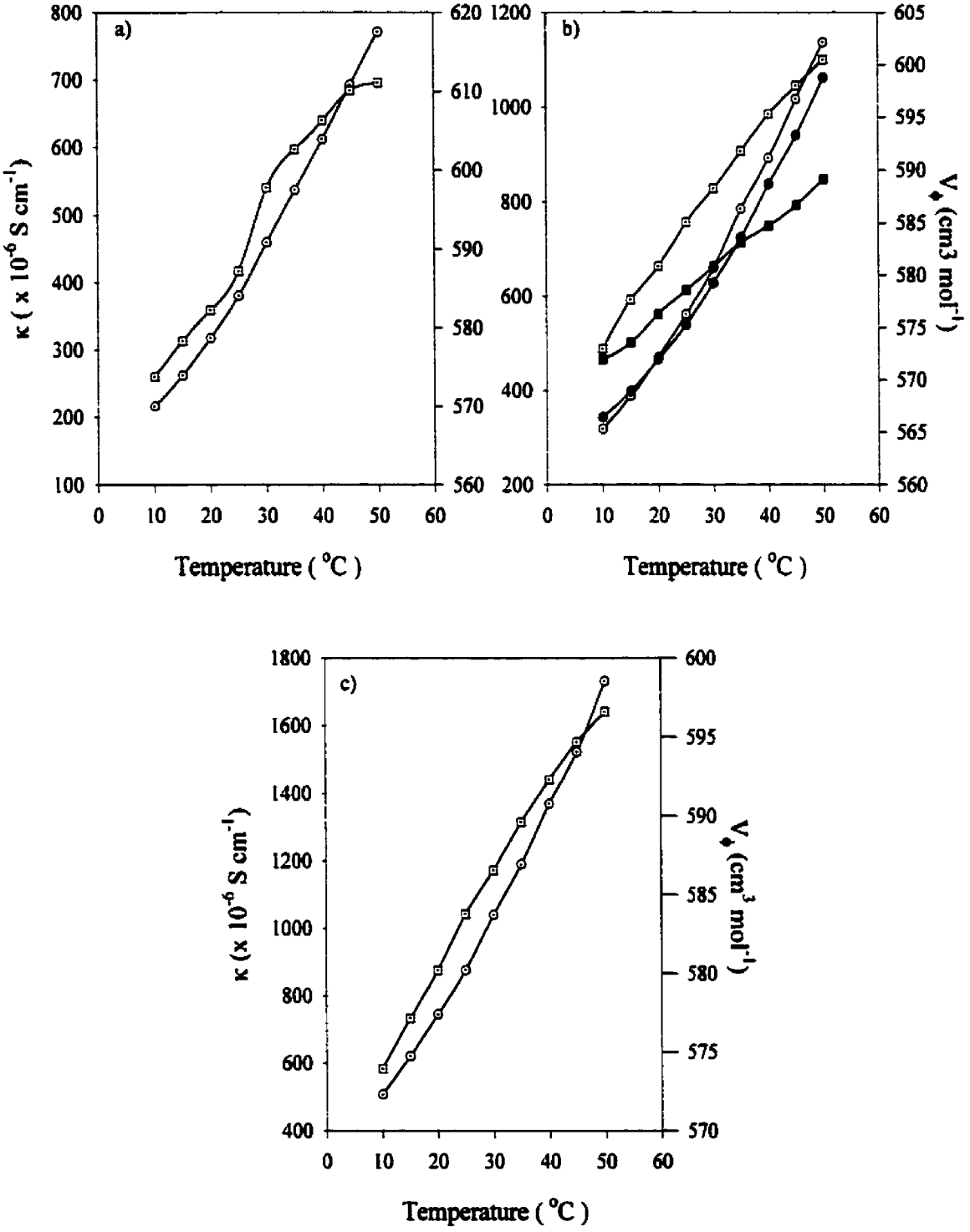

Figure 4.2.5.2-4: Apparent specific volume for aqueous 2.0% Pluronic solutions as a function of temperature.

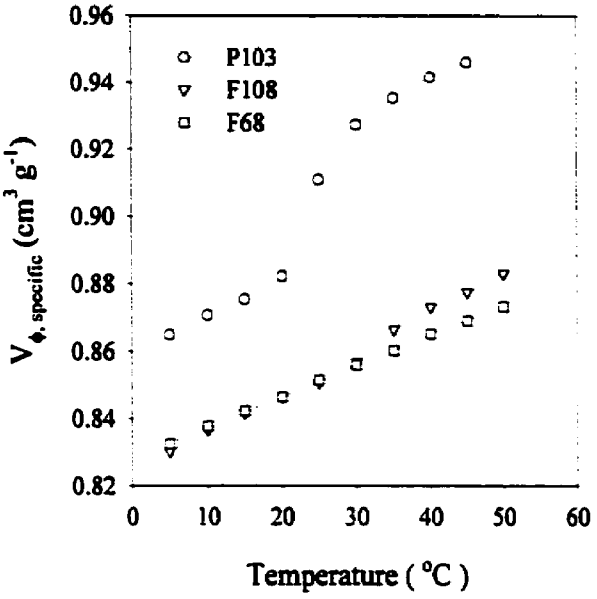

4.2.6 Equilibrium Dialysis Studies

Surfactant concentrations in both sides of the dialysis cell were determined using the colorimetric titration method described in §3.3.6. The binding ratios of surfactant to polymer, y (in mmols of surfactant per gram of polymer), were calculated according to Equation 3.2.4-6 and are plotted as a function of equilibrium surfactant concentration, $[Surfactant]_{eq}$, in Figures 4.2.6-1 to -3. The presence of the neutral Pluronics in the solutions was found to have no influence on the determination of the surfactant concentration. Because of the low molecular weight cut-off of the dialysis membrane (3500), experiments could only be performed with polymers above that molar mass, i.e., PEO, P103, F108, and F68. It was determined that no interaction occurred between the 12-3-12 surfactant and PEO and F68.

The results obtained for P103 and F108 clearly show that interactions between the gemini surfactants and the Pluronics are weak in nature, and the mechanism for the interaction is apparently different for P103 as compared to F108. A non-cooperative interaction is observed between 12-3-12 and P103 as indicated by the linear nature of the binding isotherm (below the cmc).[80,139] The interaction between F108 and the 12-3-12 gemini surfactant is more characteristic of a surfactant-polymer interaction, with no interaction observed below surfactant concentrations of approximately 0.5 mmol L^{-1}.[71,82,84,140] The dialysis results are complicated by the weak nature of the interaction and the dominance of micelle formation on the surfactant side of the dialysis chamber. A comparison of results obtained for the 12-3-12 and 12-8-12 surfactants in 0.05% P103 does show a change in the apparent interaction mechanism as the length of the spacer group is increased and the interaction begins to resemble that for the 12-3-12/F108 system.

Figure 4.2.6-1: Equilibrium dialysis results for the 12-3-12/P103 system plotted as millimoles of surfactant per gram of polymer, y, versus the equilibrium 12-3-12 concentration, $[12\text{-}3\text{-}12]_{eq}$ at 0.05%, 0.1% and 0.5% P103 concentrations.

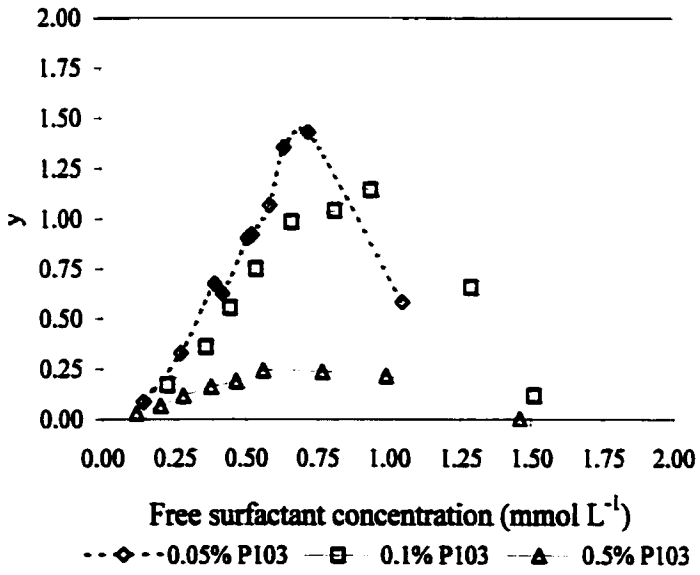

Figure 4.2.6-2: Equilibrium dialysis results for the 12-3-12/F108 system plotted as millimoles of surfactant per gram of polymer, y, versus the equilibrium 12-3-12 concentration, $[12\text{-}3\text{-}12]_{eq}$ at 0.05%, and 0.5% F108 concentrations.

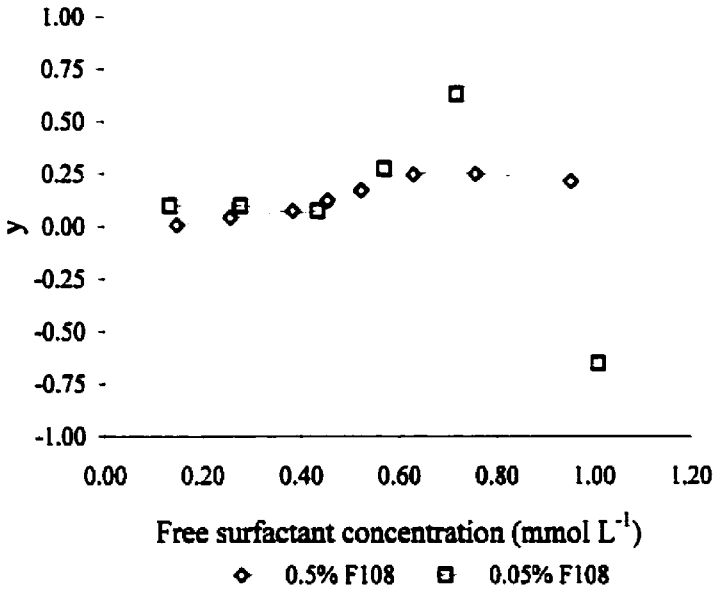

Figure 4.2.6-3: Equilibrium dialysis results for the 12-3-12/0.05% Pluronic systems plotted as millimoles of surfactant per gram of polymer, y, versus the equilibrium 12-3-12 concentration, $[12\text{-}3\text{-}12]_{eq}$. Also included are results for the 12-8-12/0.05% P103 system for comparison.

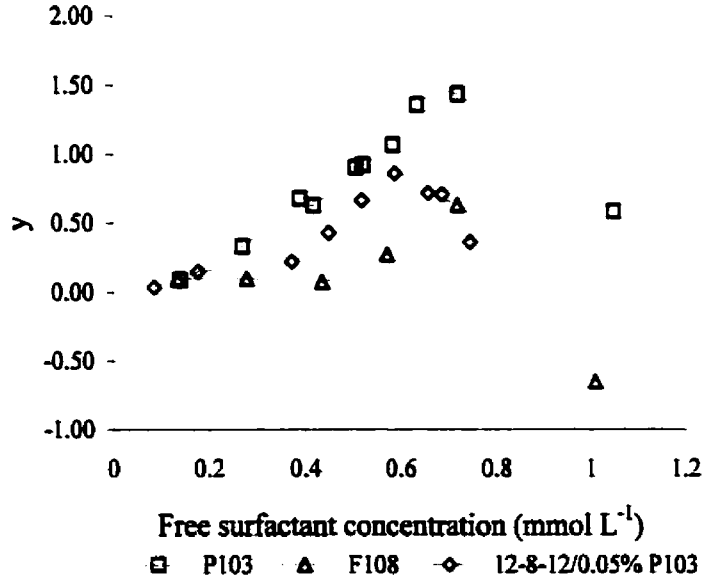

5. DISCUSSION

5.1 Binary surfactant – water systems

The study of the binary gemini surfactant systems was undertaken for two main reasons; the first to confirm and expand upon results previously reported in the literature and, the second, to provide a firm basis of comparison for the study of the ternary surfactant-polymer systems. As a result of the second of the above considerations, studies of binary gemini surfactant systems were limited to lower concentrations than were used in some of the previously reported studies, particularly for the mean aggregation number determinations. An increase in the surfactant concentration is known to bring about changes in aggregate morphology in some surfactant systems. Generally, there is a change from spherical micelles at low concentrations to less symmetrical aggregates as the concentration is increased.

Additionally, with one exception[36], there have been no studies of the volumetric behavior of gemini surfactants in aqueous solution. Thermodynamic methods have been shown to be an effective means of studying the micellization process of surfactants in aqueous solution and can provide information regarding specific solute-solute and solute-solvent interactions. As a result, a more comprehensive volumetric study of gemini surfactants was initiated, and the results obtained are correlated with the results obtained from other experimental methods.

5.1.1 Critical micelle concentrations

cmc values obtained from both the specific conductance and surface tension measurements show good agreement. Where possible, results were compared with those previously reported and found to be in excellent agreement.[32,33,44] The cmc values for the homologous series of m-3-m gemini surfactants show (Figure 5.1.1-1) the expected linear decrease in log cmc with increased alkyl tail length. When compared with the same series of m-6-m surfactants (values for 8-6-8, and 16-6-16 from reference 33, and 10-6-10 from reference 32) and the corresponding series of mono-quaternary ammonium surfactants (values from reference 141) one sees a larger(negative) slope for the m-3-m series. If one recalls that the Gibbs energy for the transfer of a surfactant from aqueous solution to the micellar phase is related to the cmc for the gemini surfactants according to

$$\Delta G^0_{mic} = (3-2\alpha)RT\ln CMC \qquad 5.1.1\text{-}1$$

(approximating activities with concentration), then it is possible to obtain values for the free energy transfer per methylene unit, $\Delta G_{mic}{}^0(CH_2)$ from the log cmc vs. n_C plots. These values are summarized in Table 5.1.1-1. Similar calculations have been reported previously by Zana et al.[33]; however, in their treatment they did not consider the ionic nature of the surfactant, and as such their values for $\Delta G°_{mic}$ will differ from the results obtained in this work by a factor of (3-2α). Both the m-3-m and m-6-m surfactant series show a larger free energy of transfer which, as will be shown later in the discussion, arises from constraints placed upon the aggregates by linking two surfactant monomers at a distance closer than the equilibrium distance between monomers in micelles formed of the corresponding mono-quaternary ammonium surfactant. This result is different from that of Zana et al.[33]

Figure 5.1.1-1: Semi-logarithmic plot of the cmc (from specific conductance) as a function of the alkyl tail length (n_C) for the aqueous gemini surfactants (s = 3 circles, s = 6, triangles). Also included are data for the corresponding alkyltrimethylammonium surfactant (squares).

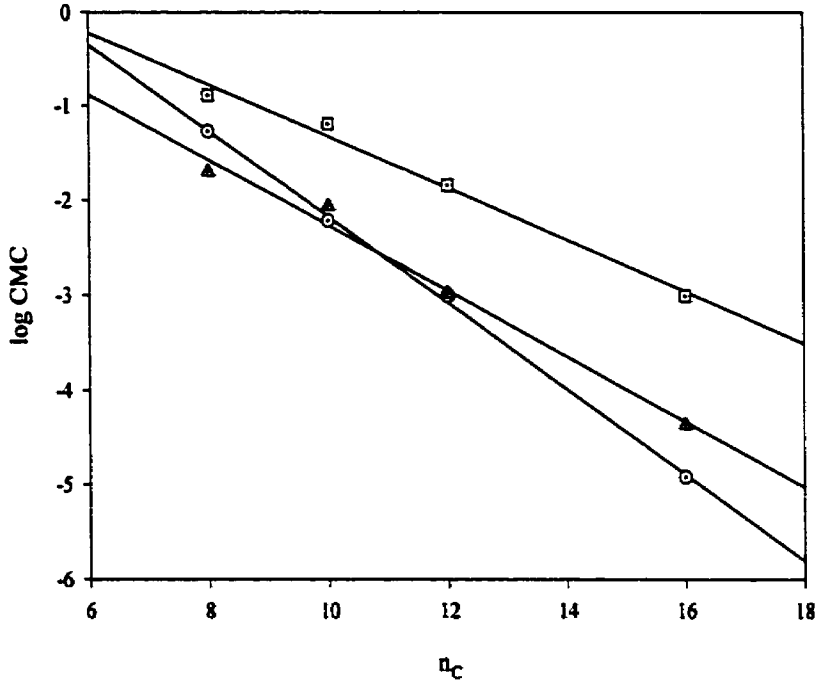

Figure 5.1.1-2: Semi-logarithmic plot of the cmc as a function of the spacer chain length (n_C) for the aqueous gemini surfactants (m = 12).

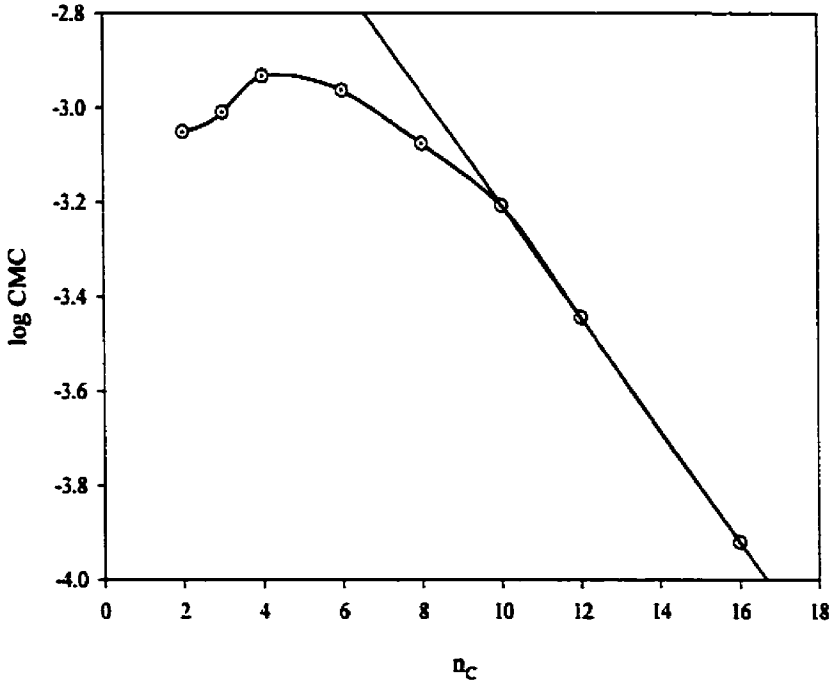

Table 5.1.1-1 Free energy of transfer per methylene unit from aqueous solution into the micellar phase for different surfactants

Surfactant series	$\Delta G_{mic}^{0}(CH_2)$ kJ mol^{-1}
C_mTAB	-3.00
m-3-m	-5.82
m-6-m	-4.58
12-s-12 (s ≥ 10)	-0.73

who found that $\Delta G_{mic}^{0}(CH_2)$ shows no significant dependence on surfactant structure. It should be noted that as the length of the spacer is increased, the Gibbs energy of transfer approaches the value for the corresponding series of single tail surfactants.

The observed variation of the cmc with increasing s (spacer chain length) is more unusual than that observed for increasing the alkyl tail at a fixed value of s (Figure 5.1.1-2), in that it does not vary in a linear fashion. The cmc is observed to increase for spacers of $2 \leq s \leq 4$ followed by a decrease in cmc for longer spacers. Only for spacers ≥ 10 methylene units in length does the cmc begin to decrease in the linear fashion associated with the increasing length of the alkyl tail of a traditional single tail - single head group surfactant. Similar behavior has been observed with the alkyldimethyldodecyl ammonium bromide surfactants, $C_{12}H_{25}(C_{m'}H_{2m'+1})\text{-}N^{+}(CH_3)_2Br^{-}$, which show a gradual decrease in cmc for m' = 1 – 3, after which the cmc decreases in a linear fashion with increasing m'.[127] The linear decrease of the cmc was attributed to the incorporation of the second alkyl chain into the core of the micelle.

While there is general agreement amongst authors that the linear decrease in log cmc for large s occurs for reasons described above,[32,33,59] the observed maximum in the log cmc plot

has yet to be satisfactorily explained. It has been suggested that the increase in the cmc arises from conformational effects in the spacer as s is increased.[33] A preferential *cis* conformation (with respect to the alkyl tails) or the monomers in solution would allow for some contact between the alkyl tails thus increasing the value for ΔG^0_{mic}, which would result in a larger value for the cmc. Alternative arguments consider the location of the spacer group to be restricted (except for the cases of large s) to the surface of the micelle. Under these conditions a longer spacer will affect the packing of the spacer at the micelle surface, thus impeding micelle formation to a degree and resulting in an increase in the cmc.[59] Results obtained in this study from determinations of the head-group area, mean aggregation number and isothermal volume change upon micelle formation suggest that the latter argument is more likely to be the case. These results will be discussed in detail in §5.1.2, 5.1.3, and 5.1.4, respectively.

5.1.2 Head-group areas

A plot of the head group area for the 12-s-12 series of surfactants as a function of the number of carbon atoms in the spacer chain reveals that the head group area goes through a maximum at approximately s = 10, as shown in Figure 5.1.2-1. The maximum has been attributed by previous authors[35] to the conformation of the spacer chain at the air-water interface. For short spacer chains, $s \leq 10$, the spacer is thought to lie fully extended along the air-water interface. As the length of the spacer is increased, it becomes flexible enough so that it can reduce the unfavorable hydrocarbon-water contacts by extending into the air, as depicted in Figure 5.1.2-2.

Figure 5.1.2-1 Head group areas, calculated from Equation 3.2.1-6, as a function of the carbon number for the spacer chain for the 12-s-12 series (O), and as a function of the alkyl tail length for the m-3-m series (□).

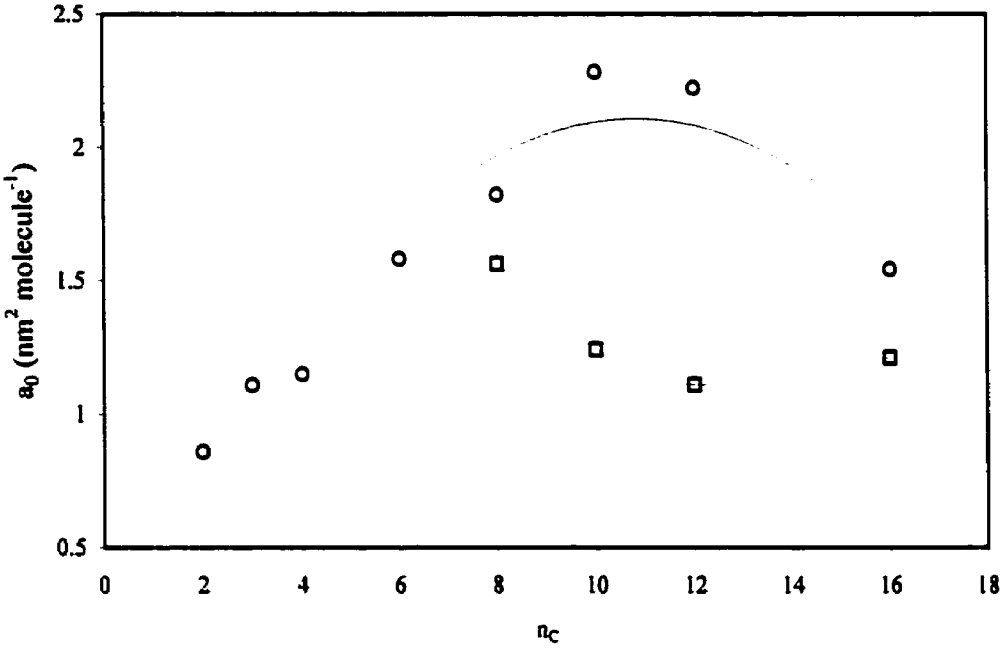

Figure 5.1.2-2: Schematic of the spacer chain conformation for the gemini surfactants at the air water interface.

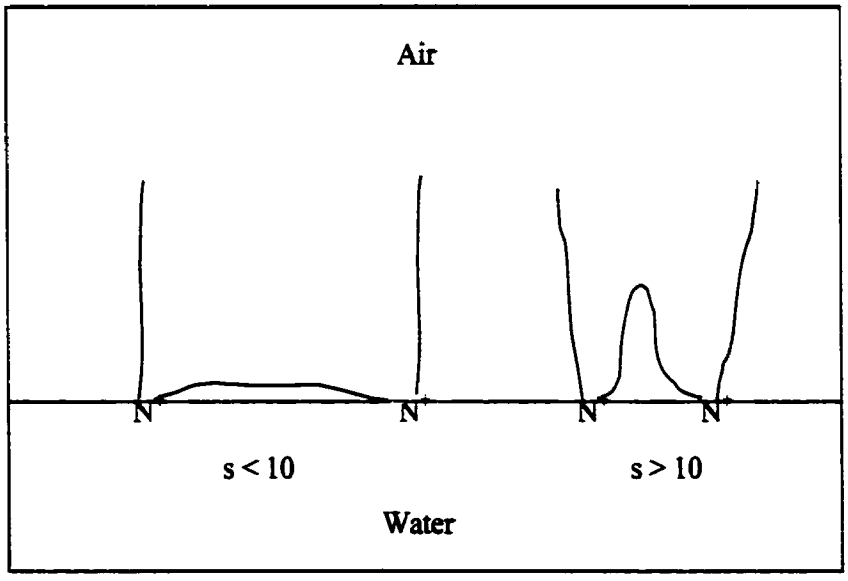

The morphology of the spacer group at the air-water interface, and the implications this has for the aggregate formation process in the bulk solution, have been discussed in some detail from both an experimental and theoretical view-point. Alami et al. have considered the principal driving force for the folding of the spacer group into the air side of the interface to be the increased hydrophobicity of the spacer group for $s \geq 10$.[35] As observed in Figure 5.1.2-1, the maximum occurs over a narrow range of s values and this is attributed to the rapid increase (by approximately a factor of 3 per methylene group) of the partition coefficient of an alkyl group between air and water. However, the results of a theoretical study suggest that the hydrophobicity of the spacer is not so important when considering the observed behavior of the spacer at the air-water interface, rather the specific hydrophilic-hydrophobic interactions between surfactant monomers and the length, flexibility and composition of the spacer chain are the determining factors.[50,51] Unfortunately, there have been no experimental studies that have confirmed Diamant et al.'s hypothesis. As a result, spacer chain hydrophobicity in combination with electrostatic repulsion between the cationic centers of the surfactant molecule are the generally accepted explanations for the observed variation in head group areas for the 12-s-12 series of gemini surfactants.

It is important to note that the absolute magnitude of the head group area is not likely to be the same at the micelle-water interface as compared to the air-water interface, particularly in light of the difference between the planar air-water and the curved micelle-water interface. Nevertheless, trends observed in the head group areas obtained from surface tension measurements are likely to be observed at the micelle-water interface. To this end, Menger et al.[59] and De et al.[48] have rationalized the conformation of the spacer chain, i.e., fully

extended or folded, in terms of the equilibrium separation between the charged ammonium centers in the gemini surfactant head group. Menger et al. determined from MM2 calculations that the energy minimized separation for the 18-s-18 series of surfactants (s = 3, 4, 5) is less than the equilibrium separation between head groups in CTAB micelles (7.9 Å). This provides additional evidence that the spacer will lie fully extended at the micelle-water interface until its length is larger than this equilibrium separation. For the 16-s-16 series of surfactants (s = 5, 6, 8, 10, 12) the equilibrium separations determined by De. et al. from small angle neutron scattering (SANS) data seem somewhat large. They predict that the spacer should begin to fold into the micellar core for s = 5, which is not consistent with either Menger's calculations or with experimental observations from surface tension measurements.

The head group area obtained for the 12-ϕ-12 surfactant (1.8 nm^2 $molecule^{-1}$) lies close to the value obtained for the 12-8-12 surfactant (1.82 nm^2 $molecule^{-1}$). If one considers that the benzene ring can be approximated, generally, as being equivalent to 3 – 3.5 methylene units in length, then the *p*-xylyl spacer is equivalent to approximately 5 – 5.5 methylene units. The larger head group area obtained for the *p*-xylyl spacer as compared to an alkyl spacer of similar length may reflect the fact that the aryl spacer is less hydrophobic (due to interactions between water and the pi electron ring of the xylyl group) than the corresponding alkyl spacer, as is expected.[142] Alternatively, the discrepancy may be an indication of differences in the packing arrangement of the corresponding surfactants at the air-water interface, consistent with the theories presented above. The trend in the head group area with increasing length of the alkyl spacers, combined with the result obtained for the *p*-xylyl spacer, indicate that the spacer only begins to be incorporated into the core of the micelle at

longer spacer lengths, consistent with the results obtained from specific conductance. The implication of this result is that efforts to investigate the effect of rigidity in the spacer on the micellization properties of gemini surfactants will likely prove fruitful only for spacer groups whose overall length is greater than that for an equivalent alkyl chain of 8 - 10 methylene units in length.

The data for the m-3-m series has been previously explained in terms of the manner in which the alkyl tails remove themselves from the water surface at the air water interface. It has been suggested that longer, more flexible tails may give rise to increases in the head group area as they collapse or tilt towards the water surface.[134] While this theory can explain the observed increase in the head group area for the 16-3-16 surfactant as compared to the 12-3-12 surfactant, it does not explain the higher values for the 8-3-8 and 10-3-10 surfactants, which from the above reasoning should be lower than that for the 12-3-12 surfactant. The high value for the head group area obtained for the 8-3-8 surfactant was attributed to the hygroscopic nature of the 8-3-8 surfactant, which served as an indication that the hydrocarbon tails of this surfactant are easily wetted.[134] This could give rise to an apparent increase in the head group area for such a case. It is important to note that activities were not considered in the above treatment and, while such an assumption is reasonable for surfactants having a low cmc ($\approx$ 1 mM or less), it is less reasonable for the 8-3-8 and 10-3-10 surfactants which have cmcs of 54 and 6.10 mM, respectively. Calculations of head group areas using activity instead of concentration (assuming application of the Debye-Hückel limiting law to estimate the activity coefficient) were made and the results are given in Table 5.1.2-1.[142] The use of the Debye-Hückel limiting law for the m = 8 and s = 3 gemini

compound, which has a relatively large cmc, is only to provide a basis for comparison with other surfactants in each series. An extended form of the law should be applied but the absence of fitting parameters for this salt precluded its use. It can be seen from Table 5.1.2-1 that the inclusion of activities in the calculation of the head group areas dramatically lowers the head group area for the 8-3-8 and 10-3-10 surfactants, bringing the results in line with the expected behavior described above. The inclusion of activities was observed to have no effect on the location of the maximum in the head group area as a function of spacer chain length for the 12-s-12 series of surfactants.

Table 5.1.2-1: Head group areas calculated with (a) and without (b) consideration of activities for the m-3-m series of gemini surfactants.

Surfactant	a_0^a (nm^2 $molecule^{-1}$)	a_0^b (nm^2 $molecule^{-1}$)
8-3-8[c]	1.56	0.83
10-3-10	1.24	0.97
12-3-12	1.15	1.10
16-3-16[c]	1.21	1.02

[c] based upon data from reference 134

5.1.3 Mean aggregation numbers

A plot of the mean aggregation numbers from Table 4.1.3-1 as a function of spacer chain length for the 12-s-12 series of surfactants shows a broad minimum is observed at $s \approx 8$, (Figure 5.1.3-1). Comparison of the results obtained in this work with those obtained previously by Danino et al.[37] for the 12-s-12 surfactants is difficult due to the way in which their data is presented. In their studies, measurements were made at a number of concentrations, all of which are greater than the concentrations used in this work. A general observation is that, for all of the surfactants studied, the aggregation numbers extrapolate to values between 20 and 25 at low surfactant concentration as s varies from 10 to 3. These

Figure 5.1.3-1: Mean aggregation numbers (N_{agg}) for the 12-s-12 series (O), and the m-3-m series of gemini surfactants (□).

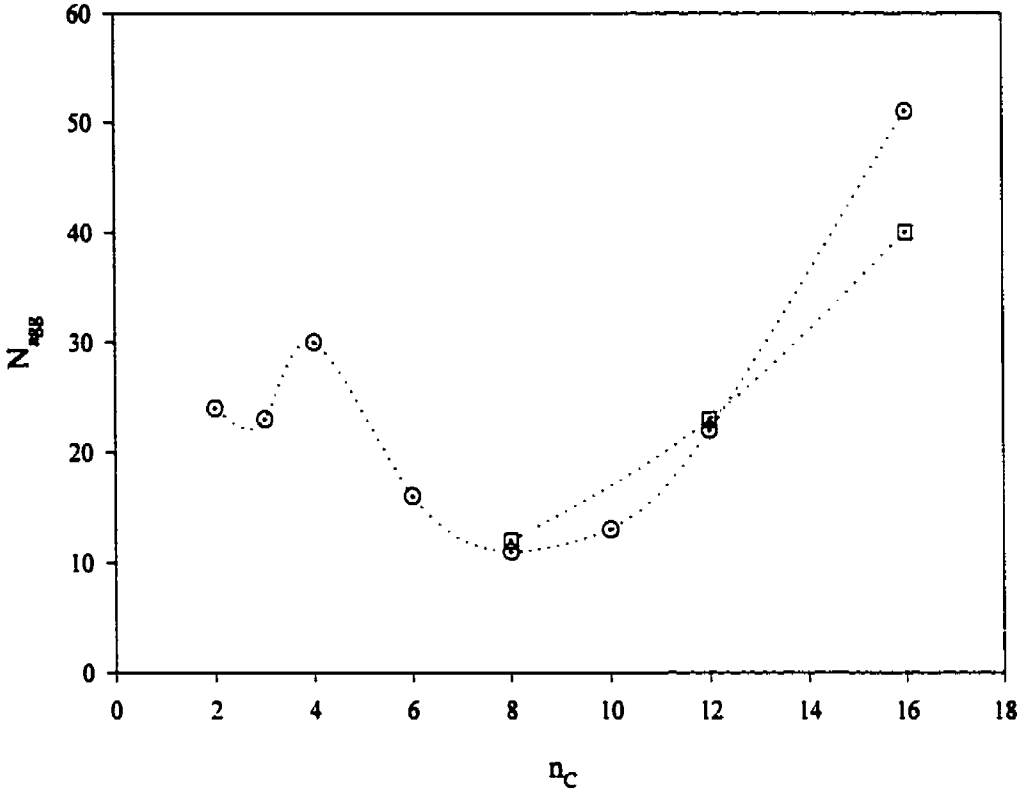

values correspond to approximately 40-50 dodecyl chains per micelle, a value which was found to be in agreement with results obtained for the corresponding alkyldimethyl-dodecylammonium bromide surfactants. As well, it was noted[37] that the results obtained are in good agreement with the value of the aggregation number (N_{agg} = 55) predicted by Tanford[16,20] for dodecyl chain surfactants independent of the type or nature of the surfactant head group. However, these results are not in agreement with results obtained in this work, for which the aggregation number is observed to decrease to a value of 11 for the 12-8-12 surfactant.

The appearance of a minimum in the mean aggregation number at s = 8 has previously been observed by De et al. They obtained aggregation numbers for the 16-s-16 series of

surfactants at 50mM surfactant concentrations, well above the cmc for these surfactants, from SANS measurements.[48] The minimum in the aggregation number was rationalized in terms of the aggregates becoming more spherical in nature (less ellipsoidal) as the length of the spacer was increased. Also, similar to results obtained in this work, the aggregation numbers for the s = 8, 10, and 12 of the 16-s-16 series of surfactants were found to be well below the value of 95 predicted by Tanford's equations for hexadecyl chain surfactants.[48]

If one considers the argument made that the spacer lies fully extended at the surface of the micelle, then the surface area available at the micelle-water interface to an additional surfactant molecule decreases as the length of the spacer is increased. This means that in order to maintain a spherical aggregate as the length of the spacer chain is increased, i.e., an increase in the head group area, then geometry requires that the aggregation number decrease in order to maintain a spherical structure. Once the spacer becomes longer than the equilibrium distance between corresponding monomer surfactants at the micelle-water interface, and flexible enough to fold into the core of the micelle it will fold into the core of the micelle. This will in turn give rise to increases in the aggregation number, particularly if the spacer group is long enough so as to act as an additional alkyl tail resulting in vesicle formation.

The values obtained for the aggregation numbers of the m-3-m series of surfactants are consistent with those obtained for the corresponding single head group surfactants as shown in Table 5.1.3-1. The observed increase in consistent with that predicted by Tanford's equations and the micelles formed at low concentrations appear to be spherical in nature for

all values of m. It should be noted here that these results do not agree with previous observations of thread-like morphologies for the aggregates formed by gemini surfactants having alkyl spacer chains of 2 or 3 methylene units in length.[27,37,48] However, results from studies previously reported have generally been for systems at significantly higher surfactant concentrations, which can result in morphological changes.

Table 5.1.3-1: Mean aggregation numbers for the m-3-m gemini and C_mTAB surfactants

Gemini Surfactants			C_mTAB Surfactants	
Surfactant	N_{agg}	Chains/micelle	Surfactant	N_{agg}
8-3-8[a]	12	24	C_8TAB[b]	23
12-3-12	23	46	$C_{12}TAB$[b]	57
16-3-16[a]	40	80	$C_{16}TAB$[c]	83

[a] from reference 134
[b] from reference 143
[c] from reference 144

5.1.4 Apparent molar volumes

A comparison of the results of the fit of the experimental apparent molar volume (AMV) data for the 8-3-8 gemini surfactant to both the pseudo-phase separation model and the mass action model show good agreement. The values of the isothermal volume change due to micelle formation are 8.8 $cm^3\ mol^{-1}$ and 8.3 $cm^3\ mol^{-1}$, respectively. The observed difference between the values of V^0 and $V_{\phi,cmc}$ (435.4 and 437.0 $cm^3\ mol^{-1}$, respectively) is consistent with the relatively high value of the cmc. The surfactant is expected to follow Debye-Hückel behavior for dilute electrolyte solutions below the cmc and therefore the apparent molar volume will increase in the pre-micellar region according to

$$V_\phi = V^0 + A_V m^{1/2} + B_V m + \ldots \qquad 5.1.4\text{-}1$$

where A_V and B_V have been defined previously in §2.2.2. The difference between V^M (mass action model) and $V_{\phi,M}$ (pseudo phase model) values (444.8 and 445.8 $cm^3\ mol^{-1}$,

respectively) is small, though outside the error for experimentally determined data points at high surfactant concentrations (± 0.02 cm^3 mol^{-1}). This may be due to the neglect of consideration of interactions between micelles in the psuedo-phase separation model. However, it is important to note that to simplify the simulation procedure, the parameter C_V in Equation 4.1.4-2 which accounts for interactions between micelles in the mass action model, was fixed at 1.0 cm^3 kg mol^{-2} and may not accurately represent interactions between micelles above the cmc.

Due to the low values of the cmc for the remaining surfactants, experimental data were fit only to the pseudo-phase separation model. Experimental data for the 12-12-12 and 12-16-12 compounds could not be fit to the pseudo-phase model due to a lack of experimental data in the concentration range cmc to 1×10^{-3} mol kg^{-1}. As a result, $V_{\phi,M}$ was obtained from the plateau region of the apparent molar volume curve, and $V_{\phi,cmc}$ was obtained from the additivity method described below. The isothermal volume change due to micelle formation, $\Delta V_{\phi,M}$, for these two surfactants was then estimated as the difference between $V_{\phi,M}$ and $V_{\phi,cmc}$. For the 12-2-12 to 12-10-12 surfactants, $V_{\phi,cmc}$ was calculated from values of $V_{\phi,M}$ and $\Delta V_{\phi,M}$ obtained from the fit to experimental data. As a result of the low values of the cmcs for the 12-s-12 series, $V_{\phi,cmc}$ can be assumed approximately equal to V^0 and the values of $V_{\phi,cmc}$ compare well with values of V^0 calculated using additivity methods described below.

The apparent molar volume of the surfactant at infinite dilution, $V^0 \approx V_{\phi,cmc}$, can be estimated using additivity methods. Two methods have been applied, the first proposed by

Frindi et al.[36] was applied previously to the 8-6-8 gemini surfactant, and the second, developed in this study[142], is based upon group contribution data from Gianni et al.[145] The first method (hereafter referred to as method 1) considers the partial molar volume of the gemini monomer as consisting of contributions from the corresponding mono-quaternary surfactant $V^0(C_nTAB, n = 8, 10, 12, or 16)$ and the partial molar volume contributions from the appropriate number of methylene groups ($V^0(CH_2)$ = 15.8 cm^3 mol^{-1}[145]) and hydrogen atoms ($V^0(H)$ = 10.7 cm^3 mol^{-1}[36]) according to the relation

$$V^0(m-s-m) = 2\times V^0(C_mTAB) - 2\times V^0(H) + (s-2)\times V^0(CH_2) \qquad 5.1.4\text{-}2$$

The values of V^0 for C_8TAB (225.1 cm^3 mol^{-1}), $C_{10}TAB$ (256.9 cm^3 mol^{-1}), and $C_{12}TAB$ (288.4 cm^3 mol^{-1}) were previously reported.[143] V^0 for $C_{16}TAB$ was calculated by adding the contribution due to four additional methylene units (4×15.8 cm^3 mol^{-1}) to the value of V^0 for $C_{12}TAB$, giving 351.6 cm^3 mol^{-1}.

The additivity method developed in this study (hereafter referred to as method 2) uses as input data the partial molar volume of the bolaform cation that corresponds to the head group of the surfactant and adds the contributions of the alkyl tails according to[142]

$$V^0_{(m-s-m)} = V^0_{((CH_3)_3N^+(CH_2)_sN^+(CH_3)_3)} + 2\times(m-1)V^0_{(CH_2)} + 2\times V^0_{Br^-} \qquad 5.1.4\text{-}3$$

where $V^0_{Br^-}$ = 30.9 cm^3 mol^{-1}.[146] Values of V^0 for the bolaform electrolytes were obtained from Gianni et al.[145] and are experimentally determined values, except for the s = 2, and s = 12 ions. The partial molar volume for the s = 2 bolaform was calculated by taking the value for the ethylenediamine cation (33.37 cm^3 mol^{-1}[145]), subtracting contributions for the $-NH_3^+$ groups (2 × 0.80 cm^3 mol^{-1}[145]), and adding the contributions for the $-N^+(CH_3)_3$ groups (2 ×

51.67 cm^3 mol^{-1}[145]) to obtain a value of 135.1 cm^3 mol^{-1}. The value for the s = 12 ion was obtained by adding the contribution of two $-CH_2$ groups (2 × 15.8 cm^3 mol^{-1}) to the value for the s = 10 ion (272.2 cm^3 mol^{-1}) to obtain a value of 303.8 cm^3 mol^{-1}. Finally, an estimate of the value of the contribution for the $(CH_3)_3N^+-CH_2-C_6H_4-CH_2-N^+(CH_3)_3$ ion was obtained by subtracting the contribution of four methylene units from the value of V^0 for the s = 6 bolaform cation and adding the contribution of the aromatic ring (equal to 62.4 cm^3 mol^{-1}[145]). The value of 206.9 cm^3 mol^{-1} was then used in Equation 5.1.4-3 to obtain V^0 for the 12-ϕ-12 gemini. The results of the additivity calculations are presented in Table 5.1.4-1 along with values of the apparent molar volume at the cmc obtained from fits of the experimental data to the pseudo-phase model.

Table 5.1.4-1: Additivity and experimental volume data for a series of m-s-m gemini surfactants

Chain Length	Spacer Length	V^o Method 1	V^o Method 2	$V_{\phi,cmc}$ Experiment
8	3	444.6	440.0	437.0
10	3	508.2	503.2	503.5
12	2	555.4	544.5	544.8
12	3	571.2	566.4	567.3
12	4	587.0	583.0	584.2
12	6	618.6	617.1	617.9
12	8	650.2	652.7	651.8
12	10	681.8	681.6	682.5
12	12	713.4	713.2	
12	16	777.0	776.4	
12	ϕ		616.3	

The above results clearly indicate that the additivity method based on partial molar volumes of the corresponding single tail (C_nTAB) surfactants is not appropriate for those surfactants possessing short spacer groups (s < 6). Significantly better agreement is obtained between experimental results and values calculated using the additivity method developed in this study. This is not surprising as Gianni et al. reported that poor agreement was obtained

between calculated and experimental partial molar volumes for molecules containing two functional groups[145], such as two quaternary ammonium groups separated by short alkyl chains. This is the case for the bolaform electrolytes and the gemini surfactants. Additivity models assume that each group in the molecule interacts independently with the solvent. Clearly this assumption does not hold for $-CH_2-$ groups adjacent to quaternary ammonium centers which show negative deviations in volume up to the β-carbon.[145] In bifunctional molecules this effect is magnified due to the overlap of the regions of influence arising from the substituents, particularly for small values of s, and the contribution for a $-CH_2-$ group would be expected to have a volume smaller than 15.8 $cm^3\ mol^{-1}$ in some instances. Therefore, by considering the volume contribution due to the bolaform cation as opposed to calculating a contribution for the spacer based upon the contribution due to a single $-CH_2-$ group, it is not surprising that one obtains better agreement with experimental results. In addition, since the additivity method proposed here does not consider the effect of the ammonium centers on the methyl groups, which are effectively relocated to the ω position of the alkyl chains, the underestimation for the volume contribution of these methyl groups may compensate for the overestimation of the $-CH_2-$ groups α to the ammonium centers in the alkyl tails.

Figure 5.1.4-1 illustrates $\Delta V_{\phi,M}$ as a function of the spacer chain length for the 12-s-12 series of surfactants. It exhibits a broad minimum for surfactants with spacers between s = 3 and 8. This minimum may be due to conformational changes in the spacer, as discussed previously to explain the observed maximum in the cmc as a function of spacer chain length. A preferential *cis* conformation for gemini surfactant monomers in solution, in which

Figure 5.1.4-1: $\Delta V_{\phi,M}$ as a function of number of carbon atoms in the alkyl spacer for a series of 12-s-12 gemini surfactants (▲).Also included is $\Delta V_{\phi,M}$ as a function of carbon number in the alkyl chains of m-3-m gemini surfactants (●) and the corresponding n-alkyltrimethylammonium surfactants (■).

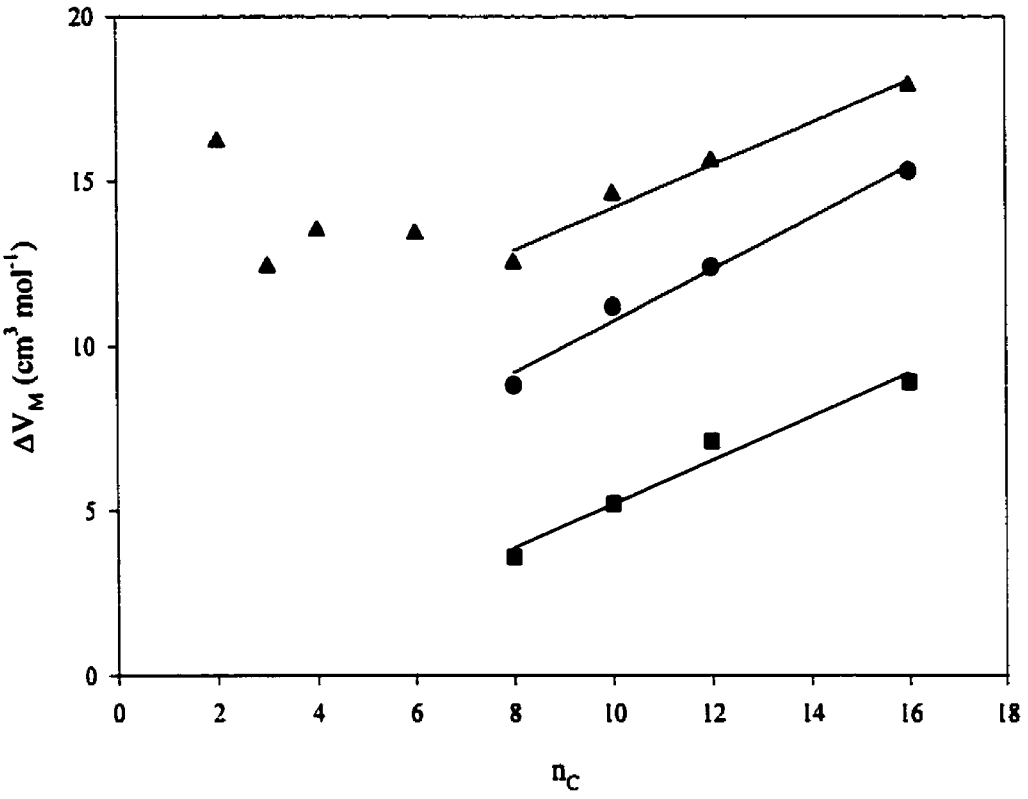

there is contact between the two C_mH_{2m+1} chains, would affect the solvation of the monomer surfactant. Consequently, the overall changes in solvation as the surfactant enters the micellar form may be diminished, resulting in a decreased $\Delta V_{\phi,M}$. The large value of $\Delta V_{\phi,M}$ for the 12-2-12 surfactant as compared to the 12-3-12 surfactant may be indicative of this fact since it has been established that, in the crystalline state, the 12-2-12 surfactant exists in a *trans* configuration (with respect to the alkyl tails) while the 12-3-12 surfactant adopts a *cis* conformation.[52] The near constant value of $\Delta V_{\phi,M}$ for s = 3 – 8 (within ± 1.1 cm^3 mol^{-1}) serves to provide additional confirmation for the argument made by Menger et al.[59] that shorter spacers, due to a lack of flexibility, will be confined to the surface of the micelle, thus

impeding micellization as a result of packing constraints at the micellar surface. This also provides an alternative explanation for the moderate increase in the cmc observed for this spacer range since, due to packing considerations, a restriction of the spacer to the micellar surface will impede micelle formation.

It is interesting to note that the value of $\Delta V_{\phi,M}$ for the 12-ϕ-12 (10.7 cm^3 mol^{-1}) does not correlate well with the values obtained for the 12-s-12 series. The slightly lower value of $\Delta V_{\phi,M}$ is consistent with the reduced hydrophobicity of this spacer resulting in differences in the solvation of the *p*-xylyl spacer as compared to the alkyl spacer. This was mentioned in §5.1.2 as a possible explanation for the high value of the head group area relative to similar length alkyl spacers. Alternatively, the observed difference in $\Delta V_{\phi,M}$ may be due to a poor estimate of V^0 for the gemini using the additivity method. Unfortunately, without experimental volume data for either the 12-ϕ-12 surfactant in the pre-micellar region (which cannot be obtained due to instrument limitations) or for the corresponding bolaform cation, the correct interpretation remains elusive.

As shown in Figure 5.1.4-1, values of $\Delta V_{\phi,M}$ begin to increase with increasing s beyond s $\cong$ 8, corresponding to approximately the same spacer length that a decrease in the head group area occurs. As well, it is the region where the cmc decreases linearly with increasing spacer length. It has been shown previously[147] for a homologous series of C_nTAB surfactants that the partial molar volume change due to micelle formation behaves in a linear fashion according to

$$\Delta V_M = \Delta V_{ion} + \Delta V_{CH_2} n_C \qquad 5.1.4\text{-}4$$

where ΔV_{ion} and ΔV_{CH_2} are the contributions of an ionic head group and a methylene group, respectively. This can be explained by the fact that as the length of the hydrocarbon chain is increased the volume fraction of the hydrophobic core in the micelle also increases. Applying a similar analysis to the observed changes in $\Delta V_{\phi,M}$ with increasing spacer length for the gemini surfactants ($s \geq 8$), one finds that the volume contribution per methylene group added to the spacer is 0.65 ± 0.07 cm^3 mol^{-1}. This compares well with the value of 0.66 ± 0.08 cm^3 mol^{-1} obtained for the n-alkyltrimethylammonium bromide series of surfactants (n = 8 – 16). These results further confirm that the spacer is incorporated into the micellar core for longer spacer lengths.

It is important to point out that the results obtained from the thermodynamic study of the volumetric behavior of the gemini surfactants are consistent with the results obtained for the cmcs and head group areas. If one considers that the calculated values of $\Delta V_{\phi,M}$ reflect processes occurring in the micellar phase (a reasonable assumption since the additivity volumes give good estimates of the premicellar surfactant volumes), then $\Delta V_{\phi,M}$ will be sensitive to changes in aggregate structure. If one considers the surfactant parameter[148,149] introduced in §2.1.3, which relates the shape of the micellar aggregates formed in solution to molecular structure, then the minimum in $\Delta V_{\phi,M}$ and the observed maximum in head group area are consistent with aggregate morphologies as seen from cryo-TEM observations[37]. It is interesting to note that if one considers only the volume contribution due to the alkyl tails for the 12-s-12 series of gemini surfactants (obtained from Tanford's equation, c.f. Equation 2.1.3-1) the morphology of the aggregate predicted from the surfactant parameter (see Table 5.1.4-2), for the surfactants with longer spacer groups, does not agree with experimental

observations of vesicle formation, for s > 12.[37,39] One therefore must consider that the volume of the hydrophobic portion of the molecule can no longer be predicted by Tanford's equation, as evidenced by the increasing values of $\Delta V_{\phi,M}$ with increasing s for the 12-s-12 series of surfactants. These results, as well as the observed linear decrease of log cmc with increasing s for s > 8, provide confirmation that the spacer group is incorporated into the core of the micelle, resulting in structural changes in the micellar aggregates formed.

Table 5.1.4-2: Calculated values for the surfactant parameter, P, for the 12-s-12 series of gemini surfactants.

Surfactant	Surfactant Tail Volume[a] (nm^3/molecule)	Surfactant Tail Length[b] (nm)	Head group area (nm^2/molecule)	P[c]	Predicted Shape
12-2-12	0.700	1.672	0.86	0.49	cylindrical
12-3-12	0.700	1.672	1.11	0.38	ellipsoidal
12-4-12	0.700	1.672	1.15	0.36	ellipsoidal
12-6-12	0.700	1.672	1.58	0.26	spherical
12-8-12	0.700	1.672	1.82	0.23	spherical
12-10-12	0.700	1.672	2.28	0.18	spherical
12-12-12	0.700	1.672	2.22	0.19	spherical
12-16-12	0.700	1.672	1.54	0.27	spherical

[a] from Equation 2.1.3-1
[b] from Equation 2.1.3-2
[c] from Equation 2.1.3-3

Figure 5.1.4-1 also illustrates $\Delta V_{\phi,M}$ for the series of m-3-m surfactants, along with those for the corresponding C_mTAB surfactants. The observed values are larger (approximately double) for the gemini surfactants as compared to the corresponding single head group surfactant, indicative of the larger volume fraction for the hydrocarbon portion of the molecule. As observed for long spacer chains with the 12-s-12 series of surfactants, the m-3-m gemini surfactants also exhibit a linear behavior of $\Delta V_{\phi,M}$ with alkyl tail length (m), similar to that observed for the C_mTAB surfactants. The contribution to $\Delta V_{\phi,M}$ per methylene

group for the m-3-m surfactants is 0.78 ± 0.07 cm^3 mol^{-1} (as compared to 0.66 ± 0.08 cm^3 mol^{-1} for the C_mTAB surfactants) and the contribution due to the ionic head group is 2.9 ± 0.9 cm^3 mol^{-1} (as compared to −1.4 ± 0.9 cm^3 mol^{-1} for the C_mTAB surfactants). The results suggest that the addition of a methylene group to each of the alkyl chains in the m-3-m surfactant series has an effect comparable to that of the addition of a methylene group to the alkyl chain of a traditional surfactant. This is somewhat surprising as one would intuitively expect that, by increasing the length of both alkyl chains in a gemini surfactant, the effective increase in the volume fraction of the hydrophobic core of the micelle would be approximately twice that observed for a traditional mono-quaternary ammonium surfactant. It may be the case that intramolecular interactions between the alkyl tails of the gemini decrease the magnitude of ΔV_{CH_2} as compared to that for traditional surfactants, again providing additional evidence for a *cis* conformation for the surfactant monomer in solution. The larger contribution due to the ionic head groups is simply a reflection of the increased size of the head group for the gemini surfactants as compared to the corresponding mono-quaternary ammonium surfactant.

5.2 Ternary Surfactant-Polymer-Water Systems

The results obtained for the ternary water-surfactant-polymer systems indicate, generally, the subtleties of the interactions occurring in these systems. Small variations are observed in the properties studied, which (with the exception of NMR) are all macroscopic in nature and thus cannot provide information regarding specific molecular interactions. Nevertheless, some important conclusions can be drawn from the experimental data regarding the interaction hypothesized to occur between the gemini surfactants and the polymers studied in this work. The discussion of the experimental results for the ternary systems will be divided into two main sections; 1) the results for the gemini surfactants with the parent PEO and PPO polymers, and 2) the results obtained for the gemini surfactants with the triblock copolymers. It is important to recall that PEO and PPO were chosen as polymers of interest as they are constituent components of the triblock copolymers. Therefore, any interaction observed to occur between the gemini surfactants and PEO or PPO provides a conceptual framework from which one can consider the more complicated gemini surfactant-triblock copolymer systems.

As well, the results obtained for the ternary surfactant-copolymer systems first will be discussed in terms of studies at 25°C, and secondly, studies as a function of temperature. The studies at 25°C were carried out to evaluate the effect of varied copolymer concentrations on the aggregation process. The results of these studies, particularly the results obtained from apparent molar volume measurements, indicated that the morphology of the copolymer itself, specifically self-aggregated or monomeric, may influence the

interaction. As a result of these observations temperature dependent studies were carried out, in order that the effect of the self-assembly process of the copolymer could be evaluated.

5.2.1 Interactions between gemini surfactants and traditional polymers at 25°C

5.2.1.1 Specific conductance studies

Contrary to the general behavior of surfactant-polymer mixed systems outlined in Chapters 1 and 2, the results of the specific conductance for the mixed surfactant-polymer systems studied in this work do not show well defined break points corresponding to the onset of surfactant-polymer interaction (CAC) and the formation of free micelles (C_2). This is not to say that there is no evidence of interaction, indeed the decrease in the specific conductance for the mixed surfactant-polymer systems relative to the aqueous surfactant system, as shown in Figures 4.2.1-1 to -4, is in itself evidence of an interaction. Specific conductivity curves as a function of increasing surfactant concentration having a broad curvature have been found to be typical of surfactant-polymer systems in which the surfactant shows an interaction with the polymer.[6,73,103,135,136,150,151] Generally, the curved nature of the specific conductance profile observed for the mixed systems is a result of a higher degree of micelle ionization for polymer bound aggregates. As such, determinations of a CAC and C_2 are difficult.[103] The CAC is usually taken as the point where the conductivity curve for the mixed system first deviates from that for the aqueous surfactant, alone, and C_2 is taken as the concentration where the two curves again become coincident. A close examination of the curves obtained for the traditional polymers (see Figures 4.2.1-1 to –3) reveals that such a treatment is not feasible for the systems in this study. This is especially true when one considers the ratio of the molar concentration of the

surfactant (at its cmc) to polymer, as given in Table 5.2.1.1-1. Examining the experimental data obtained for the ternary systems in light of these ratios, it is observed that those systems having the lowest ratio show the largest deviation in the measured solution property, indicative of "stronger" interactions. This would preclude the formation of polymer bound aggregates in the traditional sense.

Table 5.2.1.1-1: Surfactant to polymer molar ratios for the polymer concentrations used in this study

Polymer	Polymer Concentration (w/w%)	[Polymer] (mol L^{-1})	cmc/[P] 12-3-12	cmc/[P] 12-6-12
P103	0.05	1.1×10^{-4}	8.5	9.5
	0.1	2.2×10^{-4}	4.3	4.8
	0.5	1.1×10^{-3}	0.9	1.0
	2.0	4.4×10^{-3}	0.2	0.2
F108	0.05	3.1×10^{-5}	30.3	33.9
	0.5	3.1×10^{-4}	3.0	3.4
	1.0	6.2×10^{-4}	1.5	1.7
	2.0	1.3×10^{-3}	0.7	0.8
PEO	0.2	5.0×10^{-4}	1.9	2.1
PPO 725	0.2	2.7×10^{-3}	0.3	0.4
PPO 2000	0.05	2.5×10^{-4}	3.8	4.2
F68	2.0	2.3×10^{-3}	0.4	0.5

The first point of interest in considering the specific conductance profiles is that both the 12-3-12 and 12-6-12 surfactants behave quite similarly in aqueous polymer solutions. Neither surfactant shows any indication of interaction with PEO, while for the lower molar mass PPO polymer, both surfactants exhibit an unusual increase in the specific conductance for the mixed solution at higher surfactant concentrations. The 12-3-12 surfactant shows a more characteristic interaction with PPO (M.W. 2000), although in the absence of well defined breaks. There appears to be no differentiation between the interaction of PPO (M.W. 2000) and PPO (M.W. 725) with the 12-6-12 surfactant with both compounds

showing an unusual increase in specific conductance. The interaction becomes somewhat clearer by examining the relative specific conductance, κ'/κ, where κ' is the specific conductance of the solution containing both surfactant and polymer, and κ is the specific conductance of the corresponding surfactant solution.[151] Figures 5.2.1.1-1 a) and b) illustrate the effect of PEO and the two molar mass homologues of PPO on the conductance of the 12-3-12 and 12-6-12 surfactant, respectively. No interaction is observed between either 12-3-12 or 12-6-12 and PEO, as would be expected based upon previous studies of cationic surfactant-neutral polymer systems. The interaction of the 12-3-12 surfactant with the polymer shows up very clearly for the 12-3-12/PPO (M.W. 2000), system with an immediate reduction in the specific conductance relative to the conductance of the binary surfactant system. A minimum is observed to occur at a concentration approximately equivalent to the cmc for the binary system after which the conductance returns to a value equivalent to that for the binary surfactant system. The interaction between the 12-3-12 surfactant with the lower molar mass PPO is markedly different. Here the relative specific conductance shows a much smaller minimum at a concentration corresponding to the cmc for the binary aqueous 12-3-12 system after which there is an increase in the conductance to values *greater* than those for the binary case. Similar behavior is observed for the 12-6-12 surfactant with PPO polymers having different molar masses, with no apparent differentiation in the interaction with respect to the two polymers. Two important points can be made here; the first is that the cmc is clearly implicated as the critical concentration in the mixed surfactant-polymer system and, the second, is that there is an apparent differentiation in the interaction with respect to the size of the gemini surfactant head group. Table 5.2.1.1-2 gives values for the cmc and the degree of micelle ionization (α)

Figure 5.2.1.1-1: Relative specific conductance as a function of surfactant concentration for a) the 12-3-12 gemini surfactant, and b) the 12-6-12 gemini surfactant in aqueous polymer solutions at 25°C.

a)

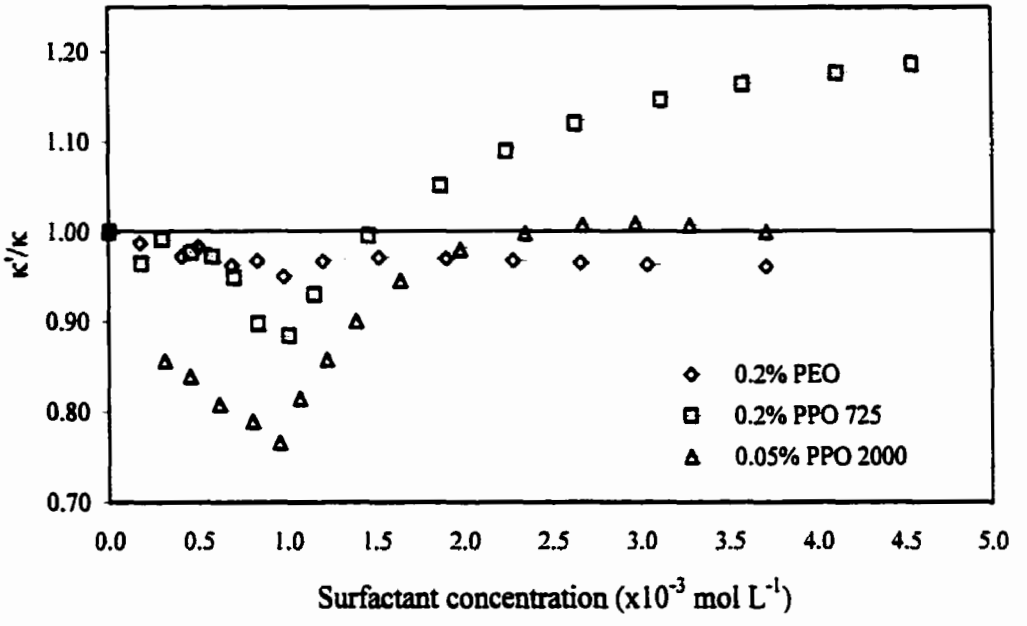

b)

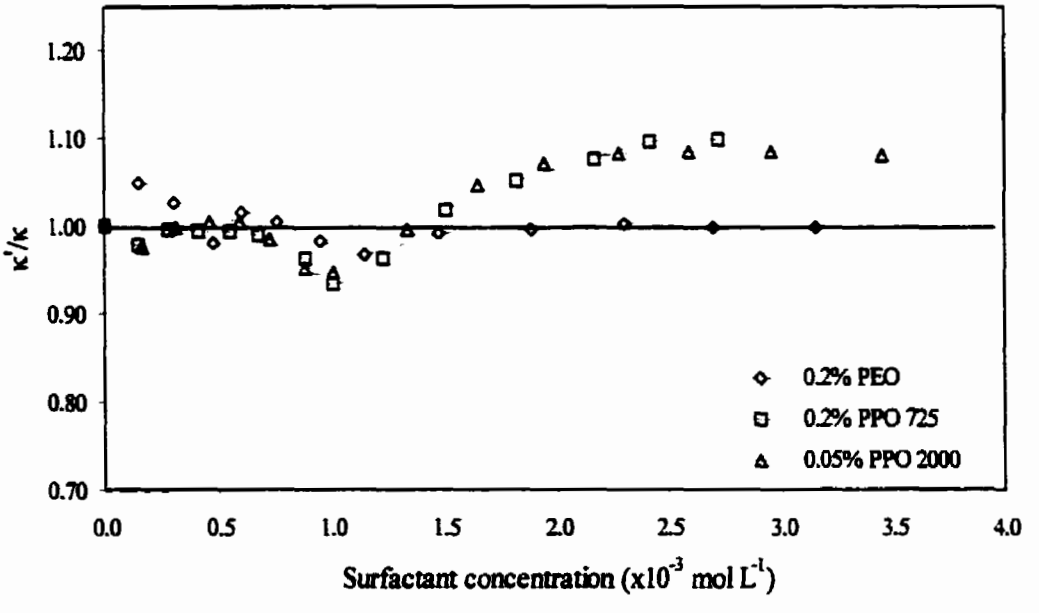

for the mixed surfactant-polymer system obtained from regression analysis of the specific conductance curves, in the same manner as for the conductivity curves for the aqueous surfactant systems (§4.1.1). The observed increase in the cmc for the case of PPO 2000 is consistent with an enhanced solubility of the surfactant monomer, likely through hydrophobic interactions between the polymer and the tails of the surfactant.

Table 5.2.1.1-2: cmc and α values for the 12-3-12 and 12-6-12 surfactants in aqueous polymer solutions.

Polymer	Polymer Concentration[a]	12-3-12		12-6-12	
		cmc[b]	α	cmc[b]	α
Aqueous		0.94	0.20	1.05	0.34
PEO	0.2	0.94	0.20	1.03	0.32
PPO 725	0.2	0.93	0.35	1.07	0.46
PPO 2000	0.05	1.23	0.31	1.17	0.40
P103	0	0.94	0.20	1.05	0.32
	0.05	1.07	0.26	1.21	0.36
	0.1	1.17	0.35	1.29	0.41
	0.5	0.96	0.63	1.11	0.64
F108	0	0.94	0.20	1.05	0.32
	0.05	0.96	0.23	1.03	0.35
	0.5	1.28	0.27	1.31	0.40
	1.0	1.4	0.33	1.27	0.51
F68	0.05	0.92	0.22	1.03	0.33
	2.0	0.99	0.34	1.16	0.42

[a] in weight %
[b] in mmol L^{-1}

Increases in the specific conductance of a surfactant in an aqueous solution of a neutral polymer, similar to that observed for PPO with the gemini surfactants, have been previously observed in studies of anionic surfactants with neutral polymers.[6,136] This has generally been attributed to a release of counterions into solution, as seen from the increased values in the degree of micelle ionization, similar to the phenomenon observed for the addition of the

lower alcohols to micellar solutions.[136,152] Alternatively the increase in conductance may be due to a dissociation of surfactant monomer from the micelle as will be discussed in §5.2.1.2 and 5.2.2.3. It is likely that above the cmc, the interaction of the surfactant micelles with the neutral polymers is similar to that for lower alcohols, i.e., the interaction is restricted to the surface or palisade layer of the micelle.

5.2.1.2 Fluorescence studies

Examining the vibronic ratios of pyrene in the mixed systems provides additional evidence for the type of interaction discussed above. In Figures 4.2.4-1a) and –2a) it is seen that there is no evidence of a CAC, rather the cmc is again observed to be the critical concentration of the system. The addition of PPO (M.W. 2000) shifts the cmc to slightly higher values, consistent with the results obtained from conductance measurements. For the higher molar mass polymers, PEO (M.W. 4000) and PPO (M.W. 2000) there is a decrease in the polarity of the micellar aggregates for both 12-3-12 and 12-6-12, as sensed by pyrene (c.f. Table 4.2.4-1). It is interesting to note that the interaction of PEO with the micellar aggregates in solution is not observed in terms of changes in α, but clearly the change in polarity is similar to that obtained for PPO (M.W. 2000). The observed decrease in polarity is consistent with an interaction of the polymer with the palisade layer of the micellar aggregates which would result in a displacement of water by polymer. Indeed it is believed, based upon results for the I_1/I_3 ratio in various micellar systems, that pyrene locates in the palisade layer[117-120] and, as such, would be sensitive to such changes. The low value for the I_1/I_3 ratio of PPO (M.W. 2000) in the absence of added surfactant is indicative of hydrophobic microdomains formed by the polymer in solution; however, one must be careful

of this tentative explanation in that the formation of such microdomains may be induced by the addition of the probe molecule (pyrene) itself, and may not exist in its absence. The existence of such microdomains would result in the enhanced solubility of the surfactant monomer and hence the increase in the cmc hypothesized from the specific conductance results above.

The decrease in the mean aggregation number of the surfactant observed in Figure 4.2.4.2-1 for the mixed 12-6-12 gemini surfactant-PPO systems is consistent with observations for previously studied surfactant polymer systems.[6,7,109,153] As in the case of SDS, the decrease in the mean aggregation number observed for the 12-6-12 surfactant becomes larger as the hydrophobicity of the polymer is increased. This observation is also consistent with theoretical models where it is predicted that the size of the polymer bound micelle will be determined by, in part, the magnitude of the steric repulsions between surfactant head groups at the micelle-water interface, which will be increased as larger amounts of polymer (i.e., greater hydrophobicity) interact with the micelles.[2] This increase in steric repulsion results in smaller aggregation numbers, which decrease with increasing polymer hydrophobicity. It is important to note that this reduction will occur regardless of whether or not a cooperative interaction occurs. Specifically, for the interaction model described above for the gemini surfactant-polymer systems, a replacement of the hydration water around the surfactant head groups by polymer at the micelle-water interface will also result in increased steric repulsions, and a decrease in the aggregation number.

5.2.1.3 NMR studies

The ^{1}H NMR chemical shift data, shown in Figures 4.2.3-1 and -3, for the binary gemini surfactant systems (D_2O as solvent) above the cmc can be analyzed, assuming the pseudo-phase model for micelle formation, according to

$$\delta_{obs} = \delta_M - \frac{CMC}{C_S}\Delta\delta \qquad 5.2.1\text{-}1$$

where δ_{obs} is the measured chemical shift, δ_M is the chemical shift for surfactant in the micellar phase, $\Delta\delta = (\delta_M - \delta_F)$ with δ_F being the chemical shift for the monomeric surfactant, and C_S is the surfactant concentration. The values for δ_M, $\Delta\delta$, and the cmc for the gemini surfactants in binary solution are given in Table 5.2.1-3.

Table 5.2.1.3-1: cmc, δ_M, and $\Delta\delta$ values for the gemini surfactants in D_2O and in D_2O-polymer solutions obtained from a fit to the pseudo-phase model.

		12-3-12			12-6-12		
Polymer	[Polymer] (w/w%)	cmc (mmol L^{-1})	δ_M (ppm)	$\Delta\delta$	cmc (mmol L^{-1})	δ_M (ppm)	$\Delta\delta$
Aqueous		0.67	3.140	0.146	0.75	3.019	0.097
PEO	0.2	0.59	3.145	0.146	0.84	3.026	0.113
PPO 725	0.2	0.57	3.149	0.144	0.98	3.017	0.104
PPO 2000	0.05	1.04	3.140	0.143	0.75	3.020	0.105
P103	0.05	0.83	3.129	0.105	1.29	3.028	0.102
F108	0.05	0.92	3.140	0.124	0.94	3.033	0.110
F68	0.05	0.76	3.126	0.130	0.84	3.033	0.114

The observed variations in the N-methyl chemical shifts for the 12-3-12 and 12-6-12 surfactants in solutions of PEO, PPO (M.W. 725) and PPO (M.W. 2000) in D_2O generally support the above hypothesis. Unfortunately, due to the small variations observed in chemical shift, i.e., < 0.2 ppm, coupled with the difference in the nature of D_2O as compared to water, this support is only qualitative. Nevertheless, it can be seen from Figures 4.2.3-1

and -3 that there is little deviation of the cmc observed between the aqueous gemini surfactants and the ternary water-surfactant-PEO and PPO (M.W. 725) solutions. Application of the pseudo-phase model allows for a determination of the cmc, δ_M, and $\Delta\delta$; however, the assumption that the chemical shift remains constant below the cmc no longer appears to be valid. This is consistent with proposed interactions between surfactant monomers and polymers in solution when the surfactant monomer is found in an environment with slightly greater hydrophobic character. As seen for the specific conductance results, there appears to be some differentiation between the interaction of the 12-3-12 or the 12-6-12 surfactants with PPO (M.W. 2000). It is seen that for the 12-3-12 surfactant the chemical shift curve (Figure 4.2.3-1c) broadens with the addition of PPO (M.W. 2000) with no distinct breaks being observed. This results in a high degree of error associated with the parameters obtained from the pseudo-phase approach. In contrast, the 12-6-12 surfactant (Figure 4.2.3-3c) shows a distinct critical concentration approximately equivalent to that observed for the aqueous surfactant solution. These observations, combined with those from conductance measurements, provide additional evidence of an enhanced interaction between the 12-3-12 surfactant and neutral polymers as compared to the 12-6-12 surfactant. This reflects, possibly, the importance of the surfactant head group size in surfactant-polymer interactions. However, it is important to note that this observed differentiation may be a result of the conformation of the surfactant monomers in solution. A preferential *cis* conformation for the alkyl tails of the 12-3-12, as introduced in §5.1, may enhance hydrophobic interactions with PPO (M.W. 2000) beyond those that occur with the 12-6-12 surfactant.

5.2.1.4 Apparent molar volume studies

The observed increases in the apparent molar volume for both the 12-3-12 and 12-6-12 surfactants in aqueous solutions of PPO (Figures 4.2.5-1a and -2a) strongly suggest an interaction between the surfactant micelles and neutral polymer in aqueous solution. While the results are somewhat consistent with results obtained for volumetric studies of anionic surfactant-polymer systems,[154,155] the results bear a greater similarity to results obtained for mixed surfactant-alcohol systems (especially for the gemini surfactant-Pluronic systems discussed below).[156-158] From the interaction model of the gemini surfactants with PEO and PPO introduced in the above discussion, one would expect the apparent molar volume of the gemini surfactant in the mixed system to be nearly equivalent to its volume in aqueous solution below the cmc. This would be similar to results obtained for the C_{12}TAB surfactant in aqueous solutions of ethoxylated butanols.[143] Because of the experimental limitations mentioned in Chapter 3, confirmation of this was not possible; however, in light of the results obtained from the various methods described above this is a reasonable assumption.

A useful quantity for discussing the volumetric behavior of a component of a ternary system is the transfer volume. For the transfer of a surfactant from aqueous solution (W) to a solution containing polymer (W+P), the transfer volume is obtained as

$$\Delta V_{\phi,S}(W \rightarrow W+P) = V_{\phi,S}(W+P) - V_{\phi,S}(W) \qquad 5.2.1\text{-}2$$

where $V_{\phi,S}$ (W+P) and $V_{\phi,S}$ (W) are the apparent molar volumes of the surfactant in the ternary system, in which water and the polymer are taken as a mixed solvent, and in water, respectively. The transfer volumes for the mixed gemini surfactant-PEO/PPO systems, shown in Figure 5.2.1.4-1, were obtained from experimentally determined apparent molar

volumes and apparent molar volumes for the corresponding binary surfactant solution estimated from the pseudo-phase model using the parameters given in Table 4.1.4-1. The transfer volumes for the surfactant from aqueous solution to a solution containing an additive can be fit, assuming a mass action model for the distribution of the additive between the aqueous and micellar phases, according to[156,158]

$$\Delta V_{\phi,S}(W \rightarrow W+P) = (V_b - V_f)\frac{m_b}{m_S} \qquad 5.2.1\text{-}3$$

where V_b and V_f are the standard partial molar volumes of an additive in the micellar and aqueous phases, respectively, and m_b is the concentration of additive bound in the micellar phase. The latter is related to the total concentration of additive in solution, the concentration of micelles present in solution (i.e., the surfactant concentration) and the distribution constant for the additive between the aqueous and micellar phases. As the focus of this work was the influence of the polymer on the properties of the surfactant in solution, a detailed volumetric study of the polymer was not undertaken, and as a result V_b, V_f, and the distribution constants are not known, precluding a fit of the transfer volumes. Nevertheless, the similarity of the curves obtained to those for the C_{12}TAB-alcohol systems is remarkable and provides strong evidence that PEO and PPO interact with the gemini surfactants in a manner analogous to that for surfactants and alcohols in aqueous solution.

To summarize, an interaction between gemini surfactants and PPO is observed in aqueous solution using a variety of experimental methods. The general observation is that this interaction is not comparable to that observed traditionally between anionic surfactants and neutral polymers. Instead there is a decided lack of cooperative behavior between the

Figure 5.2.1.4-1: Transfer volumes from water to aqueous solutions of PEO and PPO as a function of surfactant concentration for a) the 12-3-12 gemini surfactant and b) the 12-6-12 gemini surfactant at 25°C.

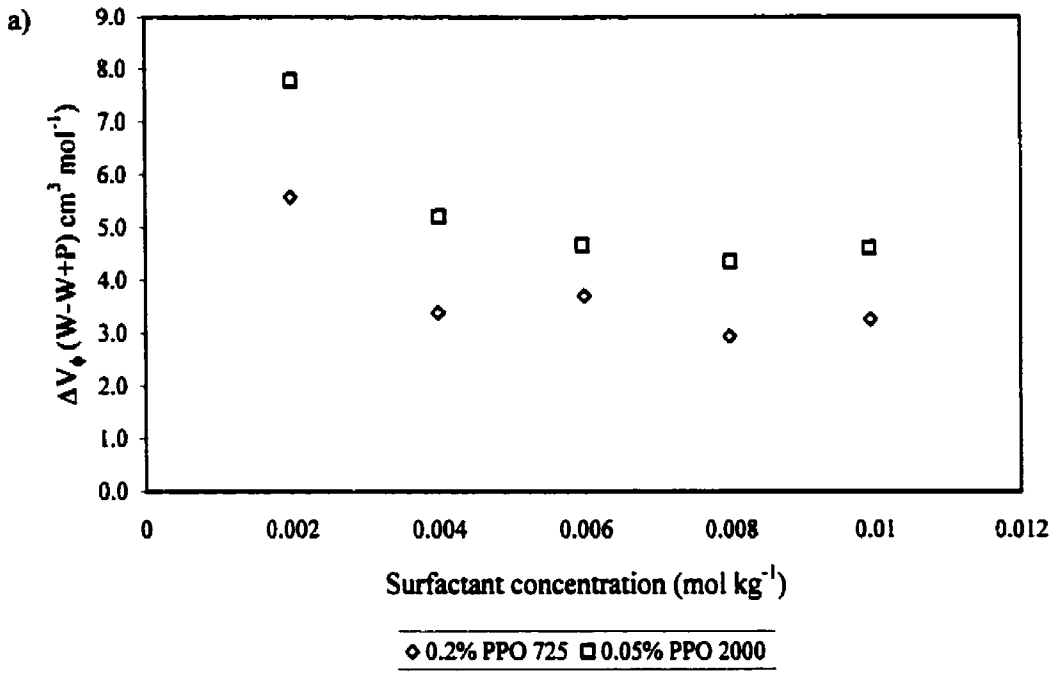

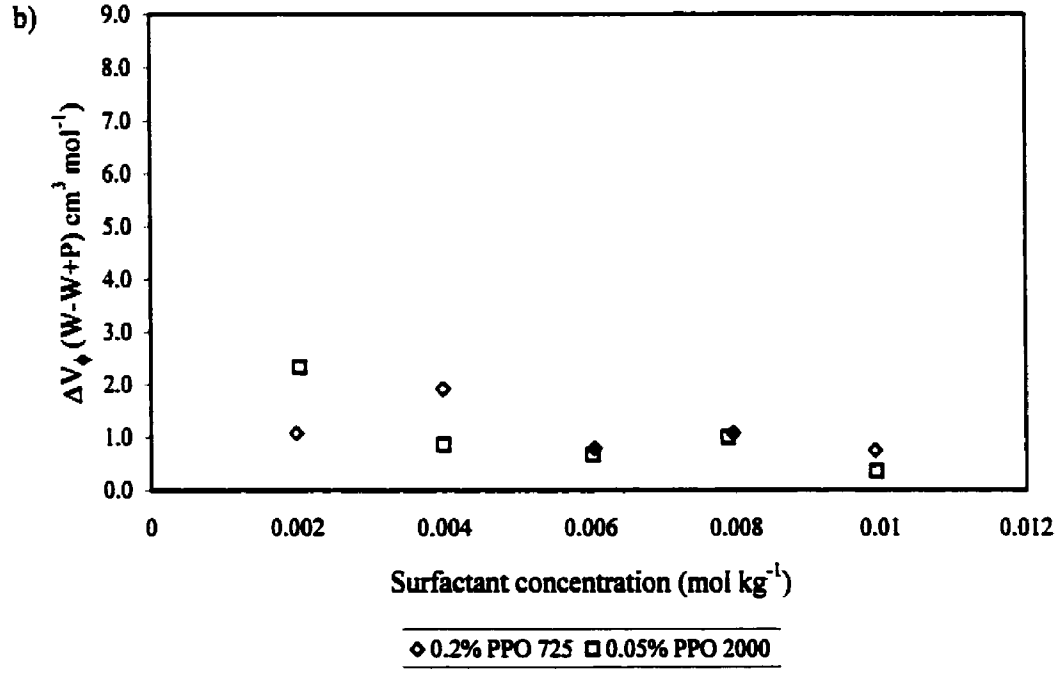

surfactant and polymer, rather the solubility of the monomer surfactant is increased due to the presence of PPO, thus increasing the cmc. Interactions between surfactant micelles and PPO are indicated above the cmc and can be seen from the observed increases in the degree of micelle ionization, the decrease in the mean aggregation number, as well as from the decrease in the I_1/I_3 ratio of pyrene and the increase in the apparent molar volume for the surfactant. The interaction above the cmc most likely results from a solubilization of the polymer at or near the surface of the surfactant micelle, resulting in a displacement of hydration water from the surface of the micelle. Such an interaction is consistent with the above observations and is depicted, schematically, in Figure 5.2.1.4-2, where the surfactant charge and counterions have been excluded for simplicity.

Figure 5.2.1.4-2: Schematic of the proposed model of the gemini-surfactant-neutral polymer interaction, for surfactant concentrations above the cmc.

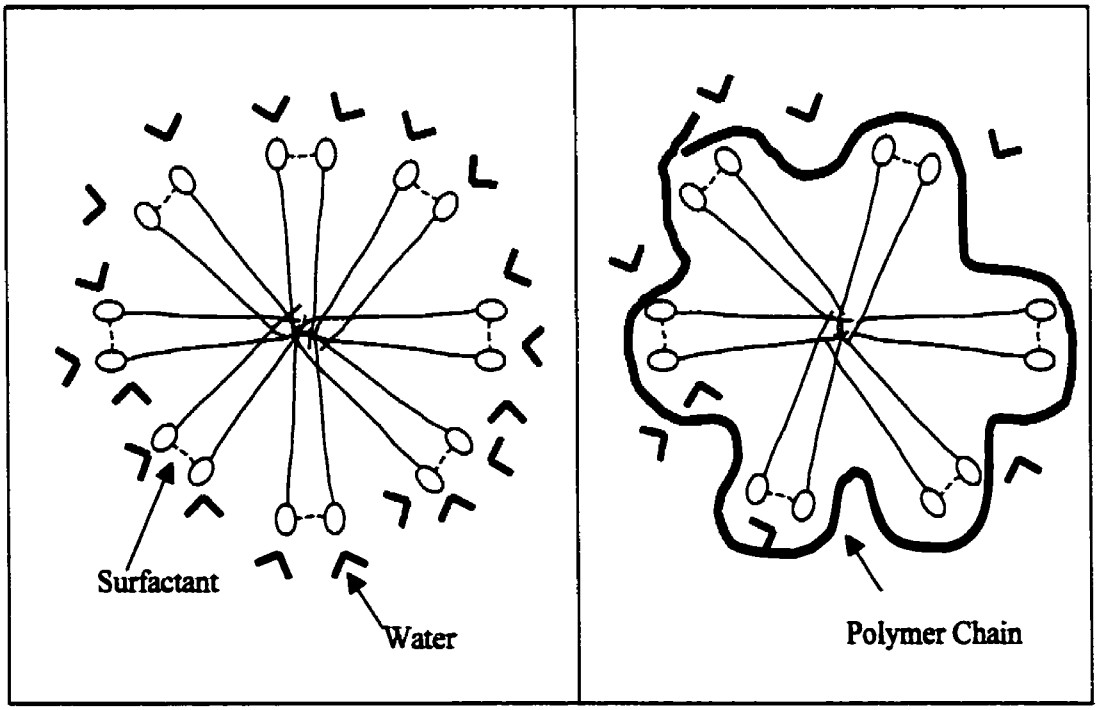

Regular micelle Mixed surfactant-polymer micelle

5.2.2 Interactions between gemini surfactants and triblock copolymers at 25°C

Prior to discussing the results obtained for the ternary water, gemini surfactant, and P103, F108 and F68 systems, it is relevant to consider the state in which one would find the binary triblock copolymer systems at the concentrations used in this study. The Pluronic F68 has been found to have a cmc at 25°C of 190 g dm^{-3} or approximately 19% (w/w) obtained from a dye solubilization method.[60] Therefore at all concentrations used in this study F68 should be found in its monomeric form in solution. The Pluronic F108 has been determined to have a cmc of 4.5%, using a dye solubilization method.[60] However, Alexandridis et al. have determined the cmc to be approximately 2.2% for F108 using surface tension. This implies that the 0.05% concentration of F108 used in this work will almost certainly be in its monomeric form in solution; however, there is a possibility that premicellar aggregation may occur at the 0.5% and 1.0% concentrations.[66] For the Pluronic P103, dye solubilization gives a cmc of 0.07%[60] while surface tension gives a value of approximately 0.1%.[66] Therefore, at 25°C 0.05% P103 should be in its monomeric form and in micellar form for concentrations of 0.1% and 0.5%. It is important to note that light scattering measurements of 5% P103 at temperatures below the cmt (i.e., below 15-20°C) show large hydrodynamic radii, corresponding to large clusters.[138] As a result there is the possibility that a similar loose network of molecules may exist even at the low 0.05% concentration at 25°C, which is well above the cmt for P103.

In addition to the aggregation state of the copolymer, one should also remain aware of the concentration of the surfactant and the importance of the cmc of the binary surfactant-water system, particularly in light of the results obtained for systems containing PPO. For

surfactant concentrations below the cmc any interaction will involve an interaction of surfactant monomer with the Pluronic copolymer, while above the cmc the interaction is likely to be similar to that described in §5.2.1, specifically, an interaction of copolymer monomers with the surface or palisade layer of the gemini surfactant micelles.

5.2.2.1 Specific conductance studies at 25°C

As observed for the 12-3-12 and 12-6-12 surfactants in aqueous PPO solutions, the specific conductance profiles show a broad curvature with the addition of Pluronics block copolymers. There is minimal differentiation with respect to surfactant head group size but more significant differences are observed with respect to the Pluronic that is added to the surfactant solution. In the case of P103, interactions between the block copolymer and the surfactant are observed for all concentrations of P103 investigated. Plotting the relative specific conductance as a function of surfactant concentration (see Figure 5.2.2.1-1), a broad minimum is observed, approximately centered on the cmc obtained for the binary surfactant solution. As in the case of PPO, an increase in specific conductance above the cmc is observed, with the increase being proportional to the concentration of P103 added to the system. For the gemini surfactant-F108 systems no significant interaction is observed at 0.05% with values of the cmc of 0.96 and 1.03 mmol L^{-1} for the 12-3-12 and the 12-6-12 surfactants, respectively, falling within the experimental error obtained for the cmcs for the aqueous surfactant systems. Similar results were obtained for the gemini surfactant-0.05% F68 systems, with cmcs of 0.92 and 1.03 mmol L^{-1} for the 12-3-12 and 12-6-12 surfactants, respectively. For 0.5% and 1.0% F108, as well as 2.0% F68, a broadly curved conductance profile is observed; however, the increase in the specific conductance observed for PPO

(§5.2.1.1) and P103 is either not observed or, in the case of the 12-3-12/1.0% F108 and the 12-3-12/2.0% F68 systems, is significantly less than that obtained for the P103 systems. Figures 5.2.2.1-2 and -3 illustrate the relative specific conductance for the gemini surfactants in aqueous F108 and F68, respectively. They show a broad minimum centered near the cmc of the binary surfactant system.

It should be noted that preliminary measurements of the solution viscosity for the 12-3-12/P103 system were made. An increase or decrease in bulk viscosity is known to affect the mobility of ions in solution, and as such will impact the specific conductance of ionic solutions. While the data for the gemini surfactant-triblock copolymer systems is not extensive, the results obtained suggest that variations in the bulk viscosity are minimal, with viscosities close to 1 cP, or close to the value expected for water. As such, the unusual increase in specific conductance observed for some of the systems studies is not likely a result of decreased solution viscosity.

The critical micelle concentration and degree of micelle ionization for each of the gemini surfactant-Pluronic systems are given in Table 5.2.1.1-2 along with those obtained for systems containing PEO and PPO. Figure 5.2.2.1-4 illustrates the cmc and α values as a function of concentration for the 12-3-12 and 12-6-12 surfactants in both P103 and F108. The degree of micellization is observed to increase linearly with the concentration of either P103 or F108 for both the 12-3-12 and the 12-6-12 surfactants. The increase is larger for the P103 polymer, consistent with an increased interaction with the surfactant micelles due to its greater hydrophobic character. The cmc values for the P103 systems increase with

Figure 5.2.2.1-1: Relative specific conductance for a) the 12-3-12 gemini surfactant, and b) the 12-6-12 gemini surfactant in aqueous P103 solutions at 25°C.

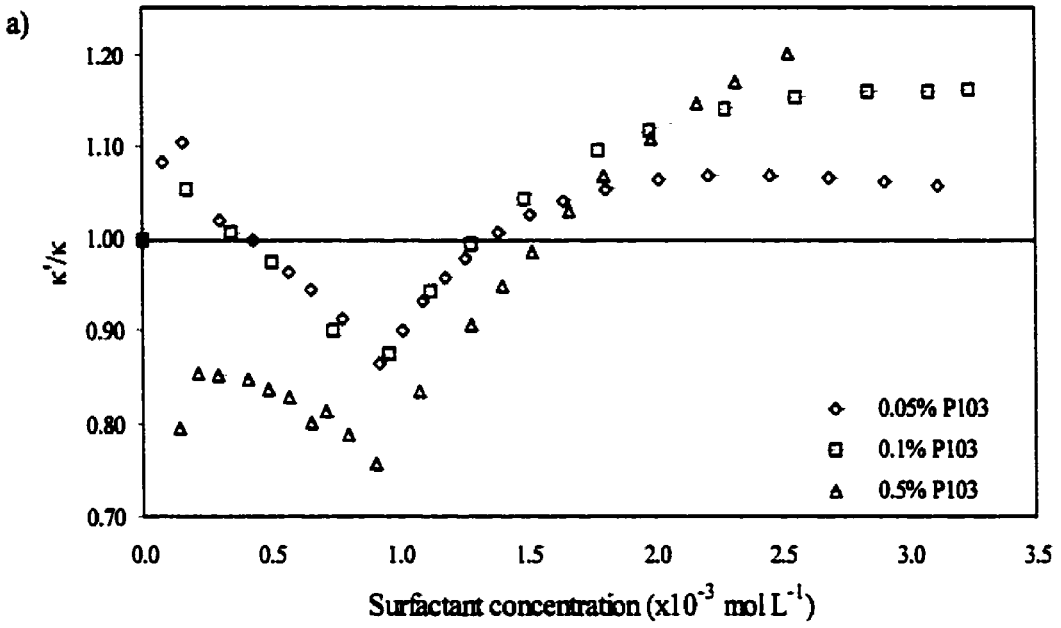

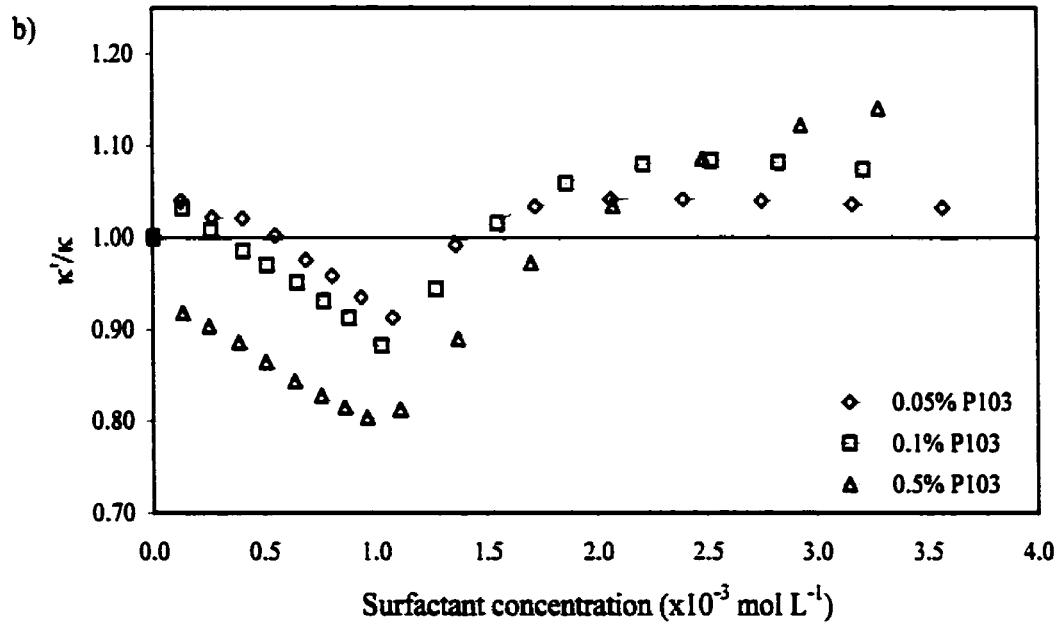

Figure 5.2.2.1-2: Relative specific conductance for a) the 12-3-12 gemini surfactant, and b) the 12-6-12 gemini surfactant in aqueous F108 solutions at 25°C.

a)

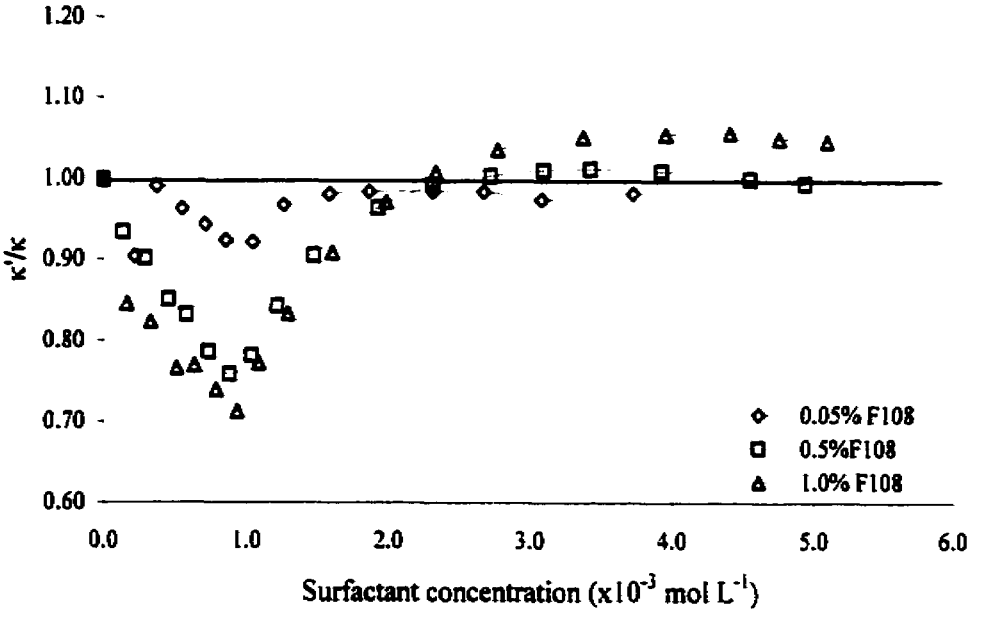

b)

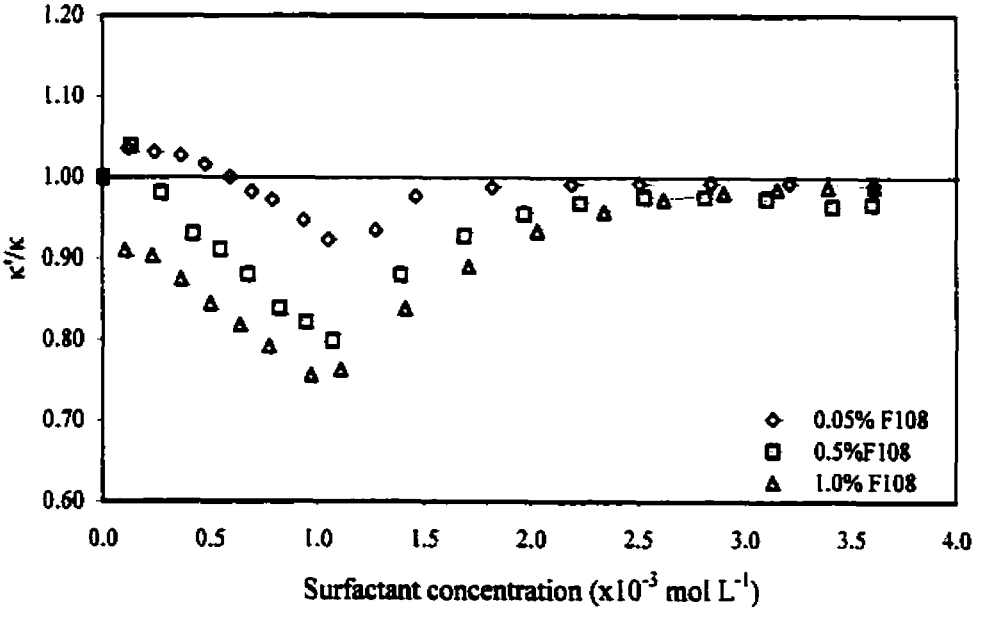

Figure 5.2.2.1-3: Relative specific conductance for a) the 12-3-12 gemini surfactant, and b) the 12-6-12 gemini surfactant in aqueous F68 solutions at 25°C.

a)

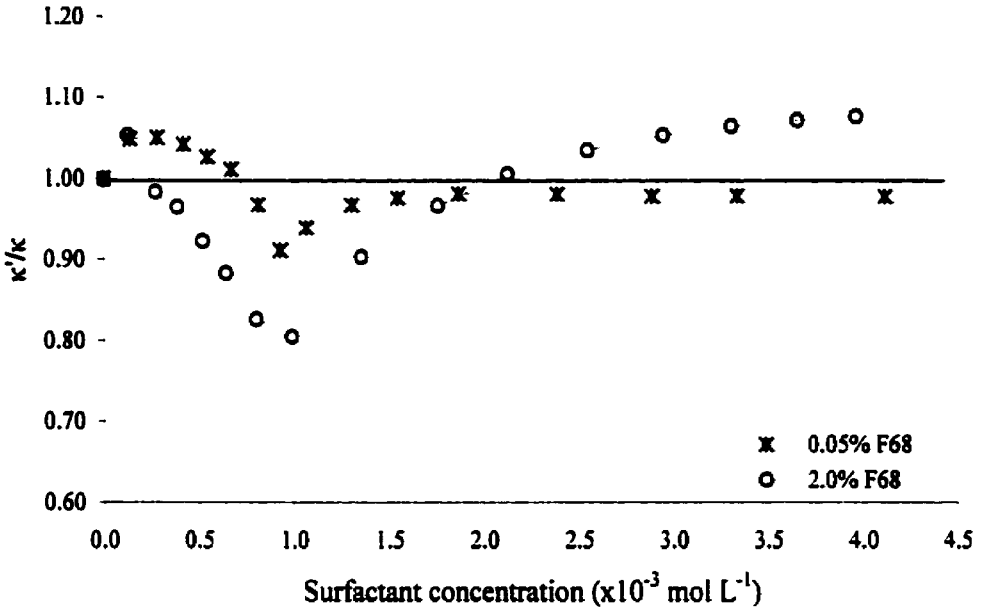

b)

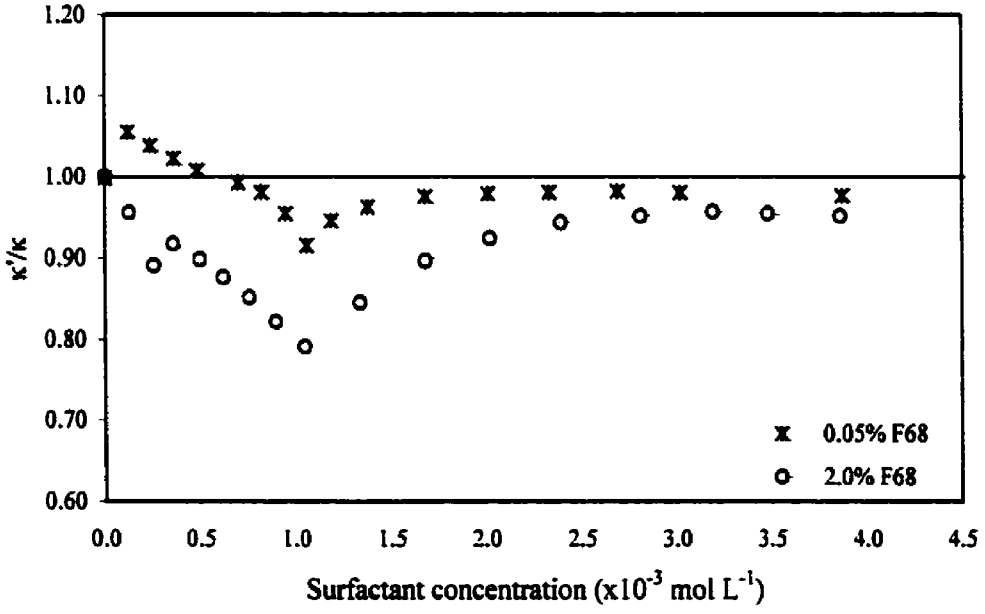

Figure 5.2.2.1-4: Degree of micelle ionization (α, ○ = P103, □ = F108) and cmc (● = P103, ■ = F108) for a) the 12-3-12 gemini surfactant, and b) the 12-6-12 gemini surfactant in aqueous copolymer solutions.

a)

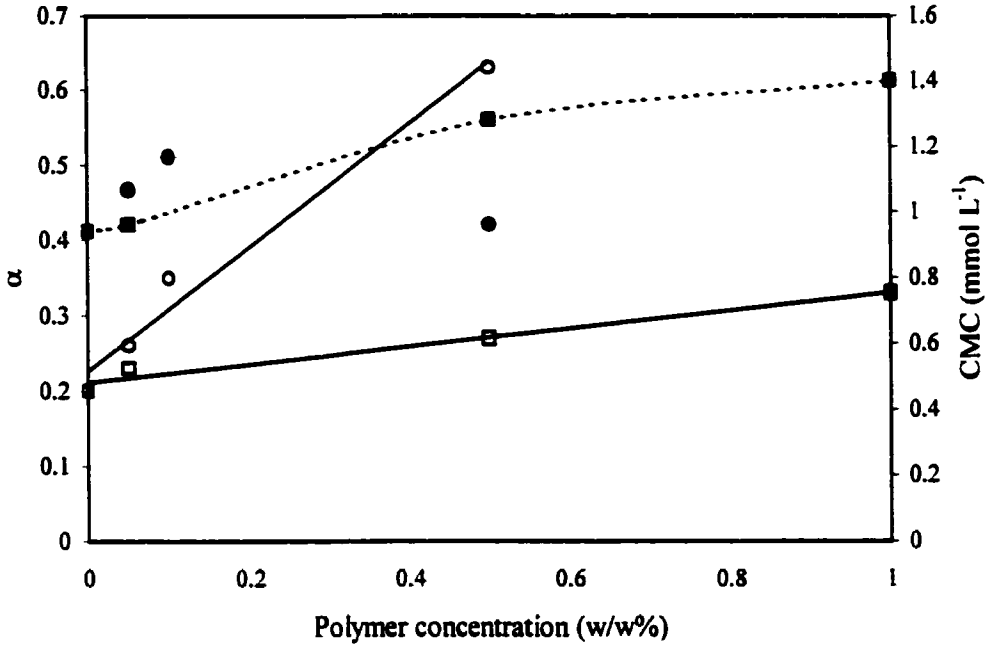

b)

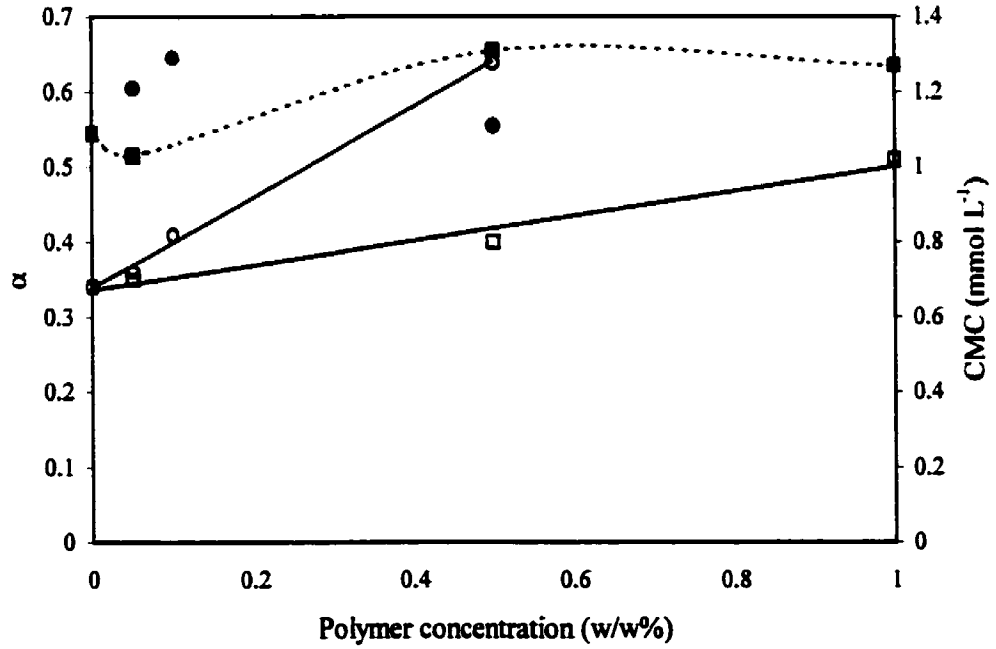

increasing P103 concentration. A maximum is observed for both the 12-3-12/P103 and 12-6-12/P103 systems at 0.1% P103, which corresponds approximately to the cmc for aqueous P103 at 25°C, i.e., ~0.07 - 0.1%. The cmc values for the 0.05% F108 systems remain unchanged with respect to the aqueous surfactant systems, within experimental error, while at higher concentrations of F108 the cmc values are also observed to increase. These observed increases in the cmc values are consistent with an increase in the surfactant monomer solubility and may result from specific interactions between the surfactant and the hydrophobic segments of the polymer, or between the surfactant and hydrophobic microdomains formed by the polymer in solution. Further to this, the observation that the cmc decreases to near its value in aqueous solution for the case of 0.5% P103 provides additional support for the above hypothesis. Above 0.07 to 0.1% P103 concentrations, self-aggregation of P103 occurs which may effectively shield the hydrophobic segment from interaction with the surfactant monomer. It is important to note that the observed variations of the cmc and α as a function of polymer concentration are not seen in systems showing a typical surfactant polymer interaction such as SDS with PEO or PVP.[153] In such systems both the cmc (or more appropriately the CAC) and α were observed to be approximately constant over a range of polymer concentrations (0.025 to 2.0%). The increase in α observed for the addition of PPO to the gemini surfactant solutions is similar to that obtained for mixed surfactant alcohol systems. This indicates that the mechanism of interaction between the gemini surfactants and the Pluronics may be similar in nature to that observed for the addition of short to medium chain alcohols to micellar solutions.[152]

5.2.2.2 NMR studies

The results obtained for ^{1}H NMR measurements qualitatively support the results obtained from conductivity measurements. Data for the surfactant-Pluronic ternary systems were analyzed assuming a pseudo-phase separation model for micelle formation, according to Equation 5.2.1-1, and values for the cmc, δ_M, and $\Delta\delta$ are presented in Table 5.2.1.3-1. As observed from specific conductance measurements, the cmc is generally observed to increase in the presence of PPO (M.W. 2000) and the Pluronics; however, due to the variation of the chemical shift below the cmc, actual determination of the cmc is difficult and is likely to be subject to significant error.

5.2.2.3 Fluorescence studies

The I_1/I_3 ratios for pyrene in the mixed surfactant-Pluronic systems also clearly indicate the absence of a CAC for the P103 systems and implicate the cmc as the point at which micelle formation occurs. As observed for PPO (M.W. 2000) in the absence of added surfactant, pyrene appears to locate in a less polar environment in P103 solutions (c.f. Figures 4.2.4.1-1 and –2a and b) since the values for the I_1/I_3 ratio are similar to those obtained for PPO (M.W. 2000), even below concentrations equivalent to the cmc of aqueous P103. This observation lends support for the presence of loose clusters of P103 polymers below the cmc, observed from light scattering measurements.[138] For the systems containing F108 more complex behavior is observed (c.f. Figures 4.2.4.1-1c and -2c). Higher concentrations of F108 indicate little variation in the cmc of the mixed solution and show no evidence to support the hypothesis of a CAC for either gemini surfactant. The higher concentrations of F108 also show evidence of pre-existing hydrophobic microdomains, as

indicated by the low values for the I_1/I_3 ratio, similar to those observed for PPO (M.W. 2000) and for P103. It is likely that these microdomains are responsible for the increase in the cmc for the gemini surfactants, observed from conductance measurements. They enhance the solubility of the gemini surfactant monomers relative to that in aqueous solution; however, one must remain aware of the possibility of the induction of aggregate formation due to the presence of the probe molecule itself. Both the 12-3-12 and the 12-6-12 surfactant in 0.05% F108 show a break in the I_1/I_3 ratio plots at approximately 0.6 mmol L^{-1} and 0.8 mmol L^{-1}, respectively. This observation is contrary to results obtained from specific conductance measurements and suggests that the mechanism of interaction between the surfactant and the Pluronics, not surprisingly, may be dependent upon the composition of the Pluronic. Additional evidence of a CAC for the 0.05% F108 systems is provided by the equilibrium dialysis results. It is seen in Figures 4.2.6-2 and -3 that little binding occurs between 12-3-12 and F108 below approximately 0.5 mmol L^{-1} surfactant concentrations. The interaction of the surfactant with F108 beings to occur above this concentration. For the 12-3-12/P103 systems the interaction is observed to occur with the addition of small amounts of surfactant and is non-cooperative in nature. Due to competition from the micellization process of the surfactants, data could not be obtained above the cmc, thus limiting the usefulness of the method. Nevertheless, evidence is provided confirming the interaction of the gemini surfactants with the Pluronics, with an apparent difference in the mechanism for P103 compared to F108. In the F68 systems no significant evidence for the presence of hydrophobic microdomains is observed (c.f. Figures 4.2.4.1-1d and -2d), and the cmc is similar to that observed for the binary system. No interaction was observed to occur between F68 (at 0.05% concentration) and the 12-3-12 surfactant from dialysis measurements.

A decrease in the I_1/I_3 ratio is observed above the cmc for all three Pluronics studied, similar to that observed with PEO and PPO. This is consistent with the interaction of micellar aggregates with the polymer chain. The magnitude of the decrease in the I_1/I_3 ratio increases with increasing Pluronic concentration indicating that the dehydration of the surfactant micelles increases with increased polymer concentration. A replacement of hydration water at the micelle-water interface by polymer results in a less polar environment in the palisade layer of the micelle, as sensed by the I_1/I_3 ratio of pyrene. This replacement of hydration water by polymer will result in a release of counterions due to combined steric and dielectric effects at the surface and in the palisade layer of the micelle, similar to the effects observed for the addition of n-alcohols to micellar solutions.[152,159] The intercalation of the polymer chain between surfactant ions serves to increase the average distance between head groups thus decreasing the surface charge density and increasing the degree of ionization. The polarity, and therefore the dielectric constant, of the palisade layer is decreased and results in increased repulsions between ionic head groups. This leads to a dissociation of a number of surfactant molecules from the micelle further decreasing the surface charge density. The observed decrease in the mean aggregation numbers, as seen in Figure 4.2.4.2-2, for both P103 and F108 support this argument. The small variations in the mean aggregation number of the gemini surfactants in aqueous copolymer solution are more consistent with such a model than with the formation of polymer bound aggregates. For example, in the case of SDS aggregation numbers are observed to decrease from 60-80 in aqueous solution to approximately 20 for PEO bound aggregates.[153]

5.2.2.4 Apparent molar volume studies at 25°C

As observed for the addition of PPO to aqueous gemini surfactant solutions, the addition of the block copolymer results in an increase in the apparent molar volume of the surfactant which, for higher Pluronic concentrations, can be quite large. The transfer volumes have been used to more effectively show this result. They are presented in Figures 5.2.2.4-1, -2, and -3 for the gemini surfactants in P103, F108, and F68, respectively. As discussed in §5.2.1.4, the transfer volumes bear remarkable similarity to those obtained for mixed C_{12}TAB-alcohol systems.[156-158] The magnitude of the maximum observed in the transfer volume vs. surfactant concentration plots increases with increasing polymer concentration. This is consistent with observations made for the mixed surfactant-alcohol systems. This is not typical of systems showing the characteristic surfactant-polymer interaction, such as the SDS/PEO or SDS/PVP systems, where the variation of the polymer concentration brings about only marginal changes in the volume behavior as a function of surfactant concentration.[154,155] It has been proposed that the lack of variation of properties, such as the cmc and α, with increased polymer concentration for the SDS/PEO and SDS/PVP systems indicates that the stoichiometric concentration of polymer does not affect the surfactant association behavior.[153] Rather it is the local concentration of polymer repeat units which is the important parameter and, provided that the total polymer concentration is low enough such that the polymer coils are not interpenetrated, little variation is therefore expected. As a result, one would also anticipate little variation in properties such as the apparent molar volume with increasing polymer concentration. The nature of the variations in the apparent molar volume for the gemini surfactants in aqueous Pluronic solutions are more indicative of

Figure 5.2.2.4-1: Transfer volumes from water to aqueous solutions of P103 as a function of surfactant concentration for a) the 12-3-12 gemini surfactant, and b) the 12-6-12 gemini surfactant at 25°C.

a)

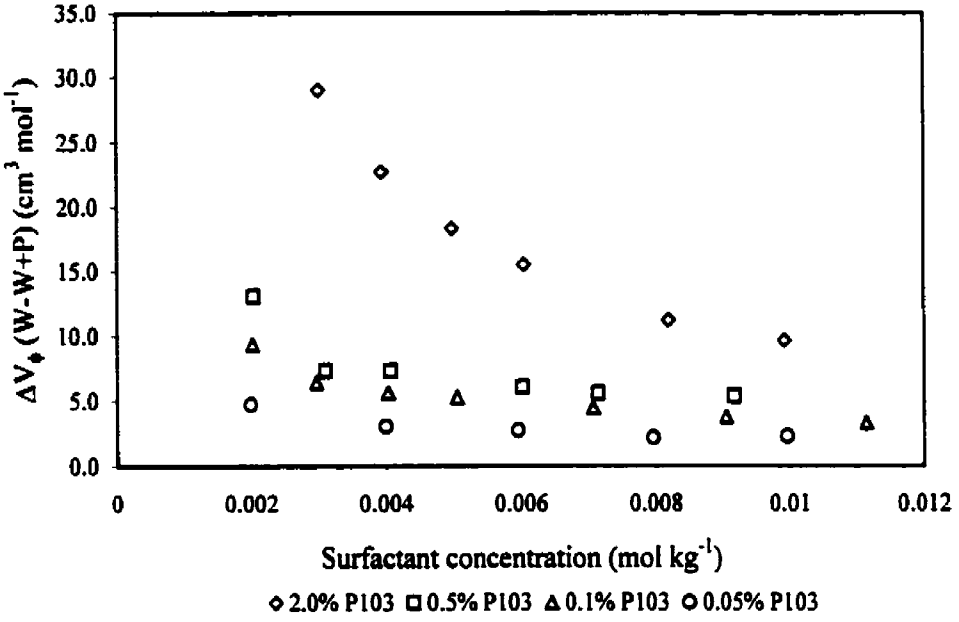

b)

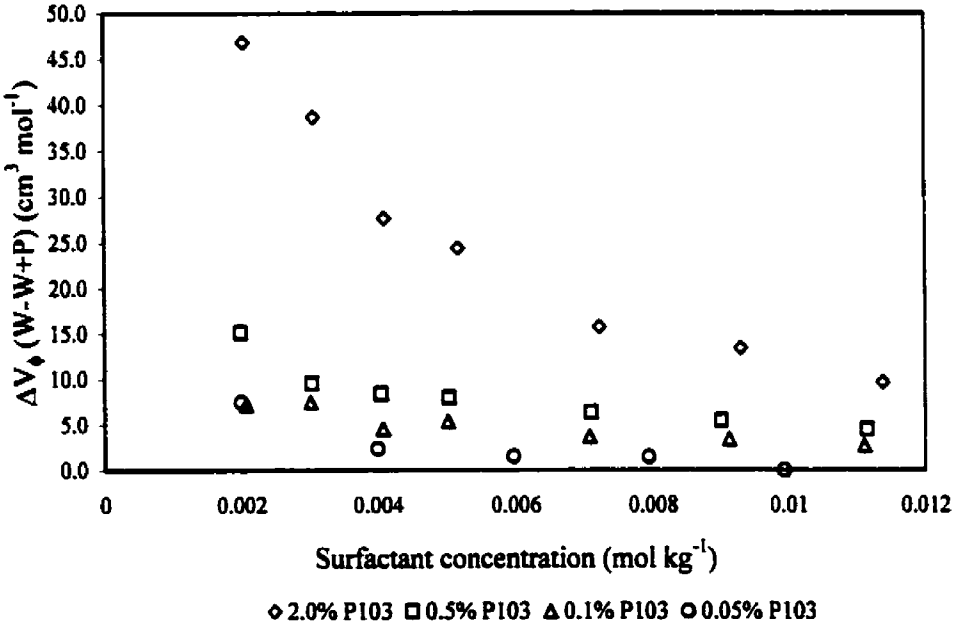

Figure 5.2.2.4-2: Transfer volumes from water to aqueous solutions of F108 as a function of surfactant concentration for a) the 12-3-12 gemini surfactant, and b) the 12-6-12 gemini surfactant at 25°C.

a)

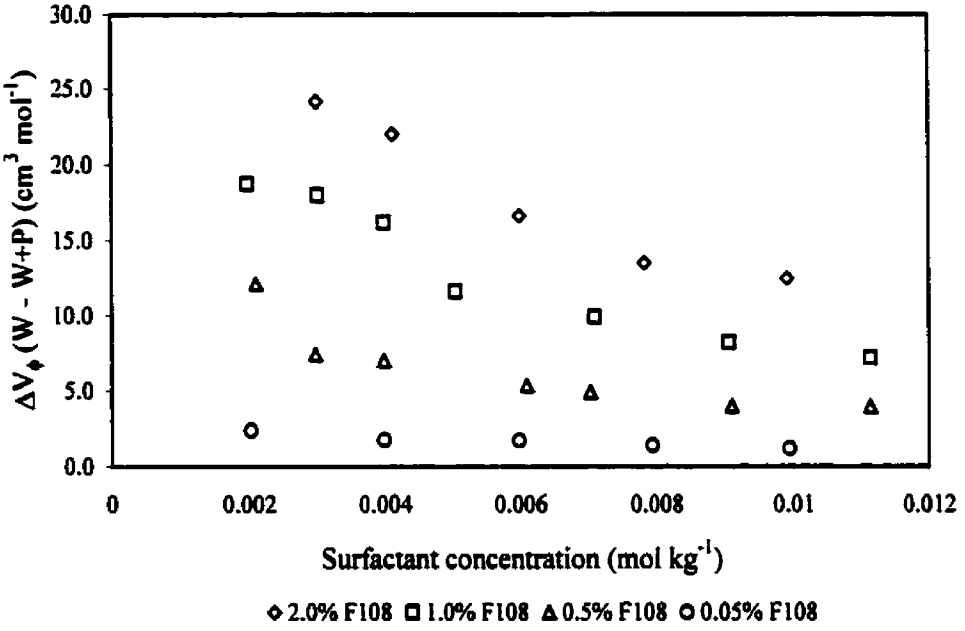

b)

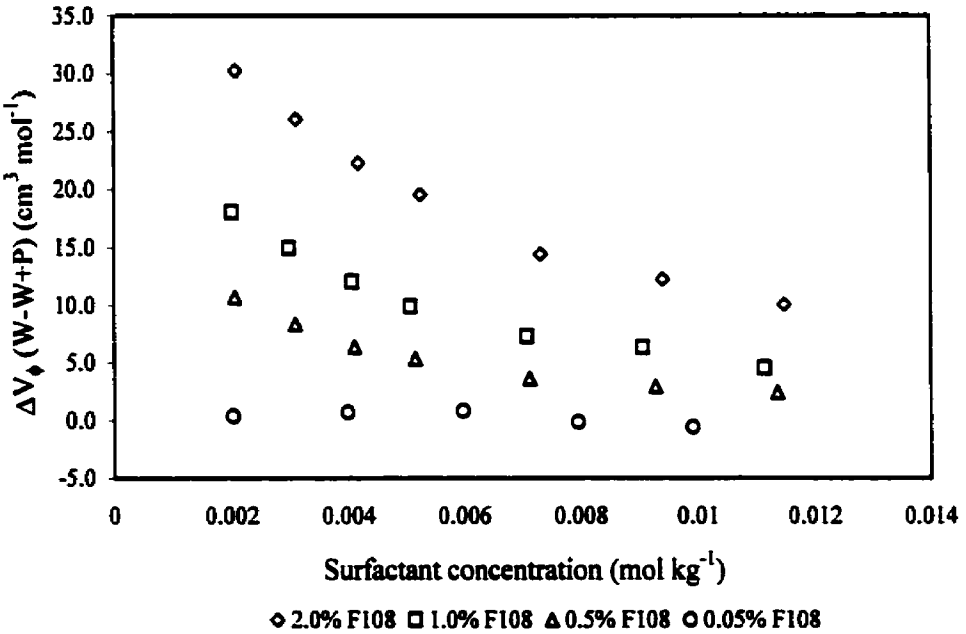

Figure 5.2.2.4-3: Transfer volumes from water to aqueous solutions of F68 as a function of surfactant concentration for a) the 12-3-12 gemini surfactant, and b) the 12-6-12 gemini surfactant at 25°C.

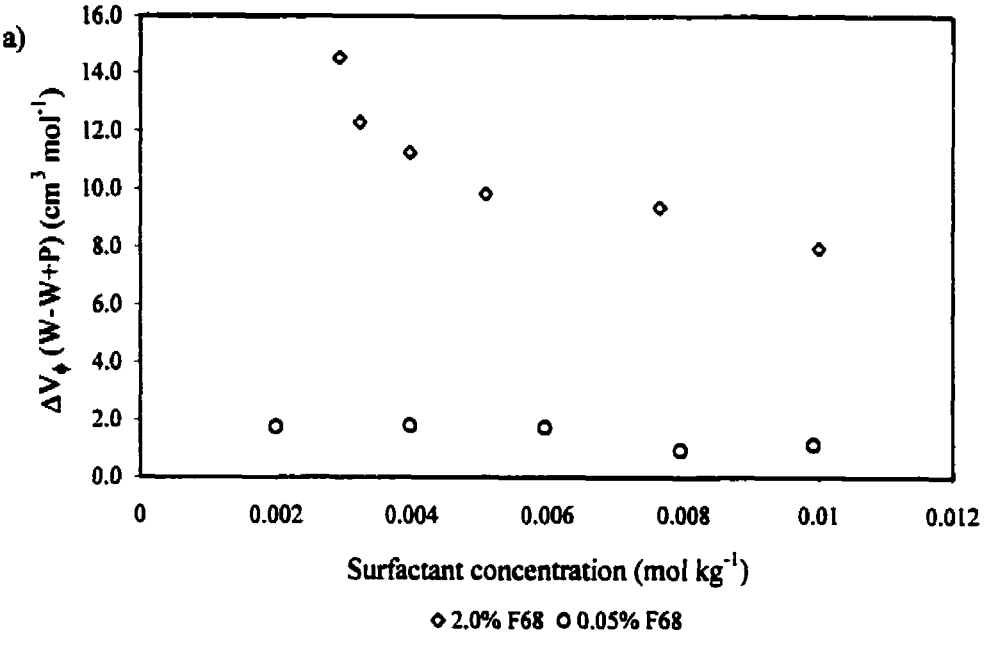

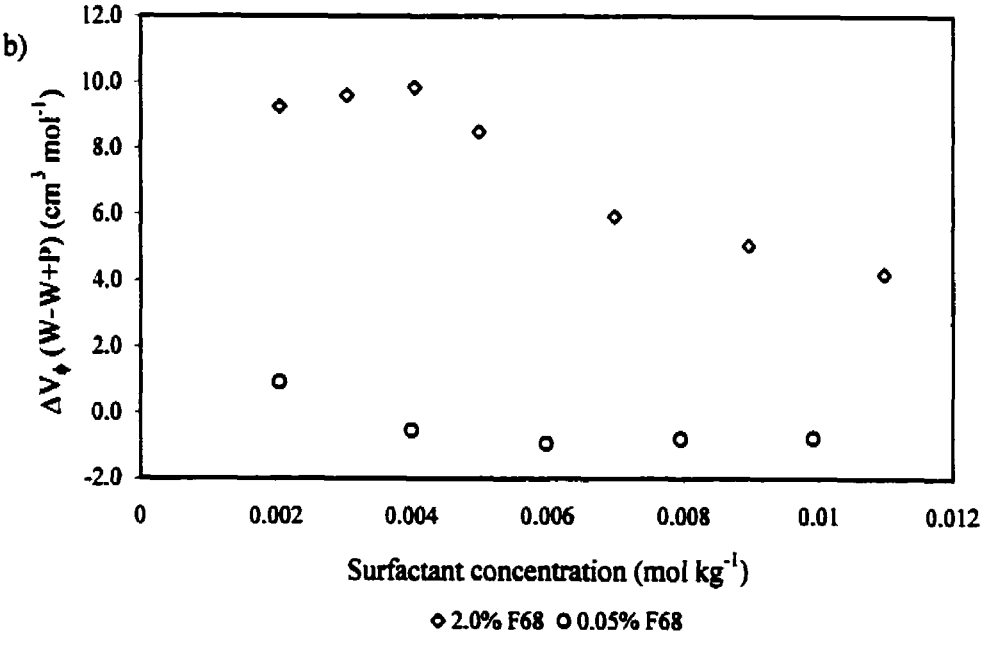

a mixed micelle formation or solubilization process as observed for the short to medium length alcohols. The trend of the transfer volume profiles for the gemini surfactant-Pluronic systems can be rationalized in a manner similar to that for the surfactant-alcohol systems by considering two concentration regions. At low concentrations, although still above the cmc, the addition of surfactant will result in an extraction of the additive from the aqueous to the micellar phase. This results in a positive contribution to $\Delta V_{\phi,S}$ due to swelling of the surfactant micelles. This swelling results in an increase of the micellar surface area, decreasing the surface charge density (resulting in the release of counterions and thus the observed increase in α) which in turn reduces the electrostriction of water. This gives rise to a positive contribution in $\Delta V_{\phi,S}$. As the concentration of surfactant is further increased, the observed decrease in $\Delta V_{\phi,S}$ results from a continuous decrease in the ratio of additive to surfactant in the resulting micelle. Recalling Equation 5.2.1-3, the expression for the transfer volume can be rewritten in terms of the total additive concentration (m_R) and the distribution constant (K_D) for the additive between the aqueous and micellar phases according to[158]

$$\Delta V_{\phi,S}(W \rightarrow W+R) = (V_b - V_f)\frac{m_R}{m_S}\frac{K_D(m_S - m_{CMC})}{1+K_D(m_S - m_{CMC})} \qquad 5.2.2.1\text{-}1$$

Equation 5.2.2.1-1 predicts a maximum in the transfer volume at a surfactant concentration $m_S = m_{cmc} + (m_{cmc}/K_D)^{1/2}$ and, as $m_S \rightarrow \infty$, $\Delta V_{\phi,S} \rightarrow 0$ and the apparent molar volume for the ternary system becomes equivalent to that for the binary surfactant system. Alternatively, the maximum observed in mixed surfactant alcohol systems has been attributed to the formation of alcohol microheterogenities that are stabilized by the addition of the surfactant.[160,161] Obviously, due to the amphiphilic nature of the Pluronic copolymers, such an explanation is highly reasonable for the gemini surfactant-Pluronic systems. Under such conditions an equilibrium between mixed aggregates (in which the additive is the dominant component)

and mixed micelles (in which the surfactant is the dominant component) can be assumed, provided the surfactant concentration is above the cmc. Therefore, at a constant additive concentration, increased surfactant concentration results in a volume excess due to the formation of mixed aggregates which diminishes as the equilibrium shifts to mixed micelle formation.

Those systems containing P103 show the largest variation in the transfer volume of the surfactants, followed by F108 and then F68. Clearly the more hydrophobic the polymer, i.e., the higher the PO/EO mass ratio, the greater the interaction observed. There appears to be an additional consideration with respect to the molar mass of the polymer as F108 shows a more significant interaction as compared to F68; however, one must remain cognizant of the fact that the size of the hydrophobic segment is reduced in F68. Since it has been established that the interaction between the gemini surfactants and the Pluronics likely occurs through the PPO segment, the effect of variation in the molar mass may result simply from this decrease.

To summarize, the data obtained for the ternary aqueous gemini surfactant-Pluronic block copolymer systems suggest that below the cmc of the surfactant, surfactant monomers are stabilized in solution, either by interaction with individual polymers, or by inducing the formation of Pluronic microheterogeneities in which the surfactant monomer can be solubilized. This results in an increase in the cmc for the surfactant. Above the cmc the interaction is remarkably similar to mixed micelle formation observed between single head group surfactants and alcohols or ethoxylated alcohols in aqueous solution. In such a case the polymer is likely solubilized at or near the surface of the micelle resulting in the observed

increase in the degree of micelle ionization (α), a decrease in the polarity as monitored by the vibronic ratio of pyrene, a decrease in aggregation number, and an increase in the transfer volume of the surfactant from aqueous to aqueous polymer solution. The interaction, based upon results obtained from the study of ternary systems containing PEO and PPO, occurs between the PPO segment of the block copolymer and the micellar surface, with the PEO segments either extending into the bulk solution or providing additional shielding of the PPO segment from water. The interactions below and above the cmc are depicted in Figure 5.2.2.4-4, where the surfactant charge and counterions have been neglected for simplicity. What remains somewhat unclear at this point is the effect that polymer self aggregation (distinguished from the pre-micellar aggregates discussed above) has on the interaction. One will recall that at P103 concentrations greater than 0.1% (i.e., greater than the cmc for P103 at 25°C), the cmc values for the gemini surfactants were observed to decrease. A discussion of this phenomenon is presented in the following section.

Figure 5.2.2.4-4: Schematic of the interaction of the gemini surfactants with triblock copolymers in aqueous solution above and below the surfactant cmc.

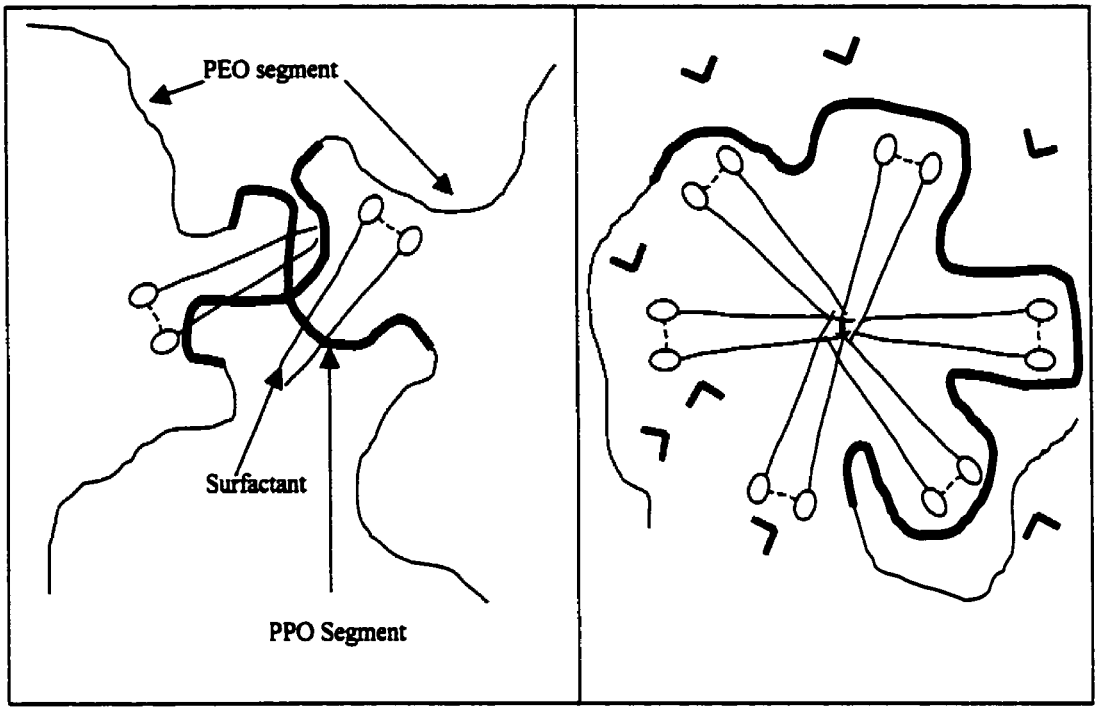

Below cmc Above cmc

5.2.3 Temperature studies of the gemini surfactant-triblock copolymer systems

The results of the study of the specific conductance and apparent molar volume behavior as a function of temperature for the mixed surfactant-Pluronic systems strongly implicate the morphology of the Pluronic as having a significant effect on the interactions occurring between the surfactant and the Pluronic in aqueous solution. As shown in Figure 4.2.5.2-4, and consistent with results reported in the literature, P103 and F108 self-assemble into micellar aggregates at temperatures of approximately 20 and 30°C, respectively, while F68 shows no evidence of micelle formation over the temperature range studied in this work.[138] Over the same temperature range, as indicated in Figures 4.2.5.2-1b, -2b, and -3b, the apparent molar volume of the surfactant in aqueous solution increases with increasing temperature in an approximately linear fashion, consistent with results obtained for single tail surfactants, reported previously.[138,162] Results from a number of studies for the C_mTAB surfactants have shown that the increase in the apparent molar volume of the monomer surfactant is larger than the increase for the surfactant in the micellar form.[162,163] This gives rise to a net decrease in the volume change due to micelle formation, most likely due to a decrease in the hydration of the ionic head group. An increase in temperature will also give rise to the observed increase in the specific conductance as the dehydration of the micellar surface will result in a decrease in the micelle aggregation number along with a corresponding release of counterions into the bulk.[88]

The results for the ternary aqueous 12-3-12/P103 and the 12-3-12/F108 systems (c.f. Figures 4.2.5.2-1 and -2) indicate for both systems that the apparent molar volume (AMV) of the surfactant, as well as the specific conductance of the solution, show a transition at a

temperature corresponding to the cmt of the Pluronic. No transition is observed for the F68 systems, consistent with the fact that 2.0% F68 solutions do not aggregate over the temperature range studied.[138] An examination of the AMV data of the surfactant (c.f. Figures 4.2.5.2-1 to -3) indicates that the magnitude of the AMV increase at the cmt of the Pluronic is greater in the presence of P103 as compared to F108. This is consistent with the results obtained at 25°C as a function of surfactant concentration which indicate a greater interaction of the surfactant with P103 than F108. Similarly, the magnitude of the maximum in the AMV decreases with increasing surfactant concentration, consistent with the results obtained for the study at 25°C. The observed increase in the apparent molar volume up to the cmt of the Pluronic is consistent with an increased swelling of the micelle (relative to that observed for an increase in temperature alone) due to increased interaction of the polymer chain with the surface or palisade layer of the micelle. The observed increase in the specific conductance of the ternary solution provides additional evidence for this type of interaction.

At the cmt significant structural changes are observed and manifest themselves as a decrease in the apparent molar volume and a break in the specific conductance versus temperature profile (in the case of 5 mmol kg^{-1} 12-3-12 in 2.0% P103 the conductance actually decreases briefly with increasing temperature). As the temperature is further increased both the apparent molar volume and the specific conductance drop to values below those obtained for the binary surfactant solutions. The implication of these results is a substantial change in the hydration of the surfactant micelles at the cmt of the Pluronic. This is likely due to the competing effects of self-aggregation of the polymer and interaction of the polymer with the surfactant aggregate. As a result of this competition, above the cmt two

distinct types of aggregates are hypothesized; surfactant dominated aggregates and Pluronic dominated aggregates, whose nature are significantly different from the pre-micellar aggregates discussed in the previous section. The micellar aggregates formed by aqueous P103 and F108 are known to be well defined aggregates which, as discussed in Chapter 1, consist of a corona of hydrated PEO and a core comprised of PPO and some hydration water. In such a complex system a number of possible interactions can exist, including;

- a continued interaction of polymer monomers with micellar aggregates,
- an interaction of surfactant monomers with polymer aggregates, possibly including a tethering of two polymer aggregates by a single surfactant monomer,
- interactions between polymer and micellar aggregates, or
- a breakdown of the surfactant micellar aggregates in favor of solubilization of the gemini surfactant in Pluronic aggregates.

Unfortunately, without knowing the actual volume behavior of the surfactant monomer as a function of temperature, conclusions drawn regarding which of the above possibilities reflect the true nature of the interaction are speculative at best. However, estimates of the infinite dilution volume of the gemini surfactant as a function of temperature can be made based upon the known volume behavior of the C_nTAB surfactants, using the additivity model proposed by Frindi et al.[36] that was introduced in §5.1.4. The standard partial molar volume of C_9TAB ($V^0(C_9TAB)$) and of a methylene group ($V^0(CH_2)$) as a function of temperature can be estimated according to[162]

$$V^0(C_9TAB) = 234.17 + 0.263 \times T \qquad 5.2.2.2\text{-}1$$

$$V^0(CH_2) = 14.66 + 0.046 \times T \qquad 5.2.2.2\text{-}2$$

where T is the temperature. It should be noted that the C_9TAB surfactant was chosen since an equation corresponding to 5.2.2.2-1 could not be found for the $C_{12}TAB$ surfactant. Values obtained from Equations 5.2.2.2-1 and -2 can be used in Equation 5.1.4-2 to obtain estimates

of the volume for the gemini surfactant in its monomer form. As the variation of $V^0(H)$ with temperature is not known, this value is assumed to be constant and will obviously introduce additional error into the estimated value. It is also important to recall the limitations of this additivity model as discussed in §5.1.4. Nevertheless, qualitatively, the volume change due to micelle formation can then be estimated as the difference between the measured apparent molar volume and the calculated volume for the monomer form. Figure 5.2.3-1 illustrates the variation in the volume change due to micelle formation as a function of temperature in aqueous solution, as well as in the 2.0% Pluronic solutions for 10 mmol kg^{-1} surfactant concentrations. While there are obviously uncertainties in the absolute magnitude of ΔV_ϕ, the trends indicate that above the cmt of the Pluronic the surfactant is found in a more hydrated environment in the presence of the Pluronic polymer than in aqueous solution alone. A comparison of the results for P103 and F108 shows that the decrease in ΔV_ϕ, relative to the aqueous surfactant solution, is greater in the presence of F108 than in P103. When one considers that the size of the corona formed by F108 will be larger than for P103, due to the increased PEO content of F108, the second and fourth of the possible interactions introduced above are implicated as interactions occurring between the Pluronic and the surfactant. Similar conclusions can be drawn by examining the difference in the specific conductivities of the surfactant (κ) in aqueous solution and in solutions containing Pluronic (κ') illustrated in Figure 5.2.3-2. Schematic representations of the proposed interaction of the gemini surfactant with the Pluronic copolymer aggregates are shown in Figure 5.2.3-3.

Figure 5.2.3-1: Volume change due to micelle formation (ΔV_M) for the 12-3-12 gemini surfactant (10 mmol L^{-1}) as a function of temperature in aqueous Pluronic solutions.

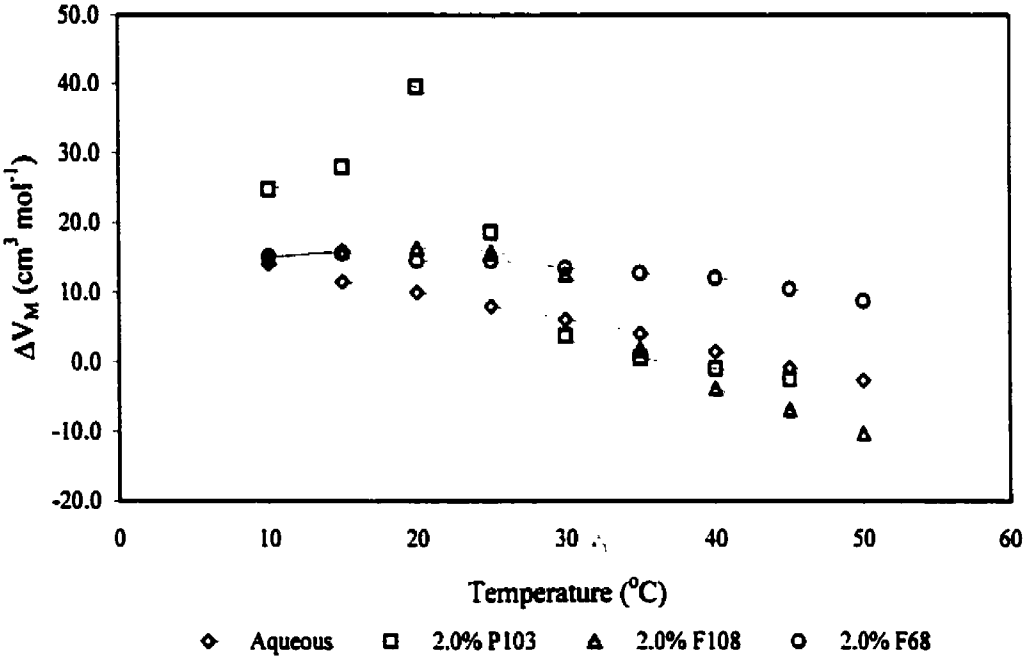

Figure 5.2.3-2: Differences in the specific conductance for the 12-3-12 gemini surfactant (10 mmol L^{-1})-Pluronic systems as a function of temperature

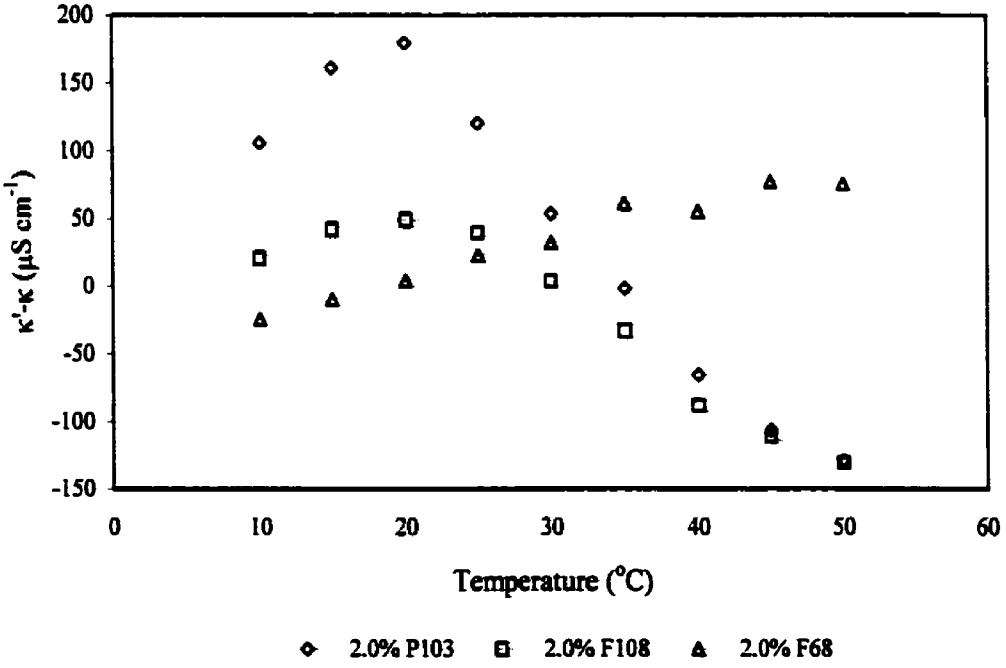

Figure 5.2.3-3: Schematic of the interaction of gemini surfactant monomers with Pluronic micelles in aqueous solution; a) two Pluronic micelles tethered by a gemini surfactant monomer, and b) gemini surfactant monomers solubilized in a Pluronic micelle

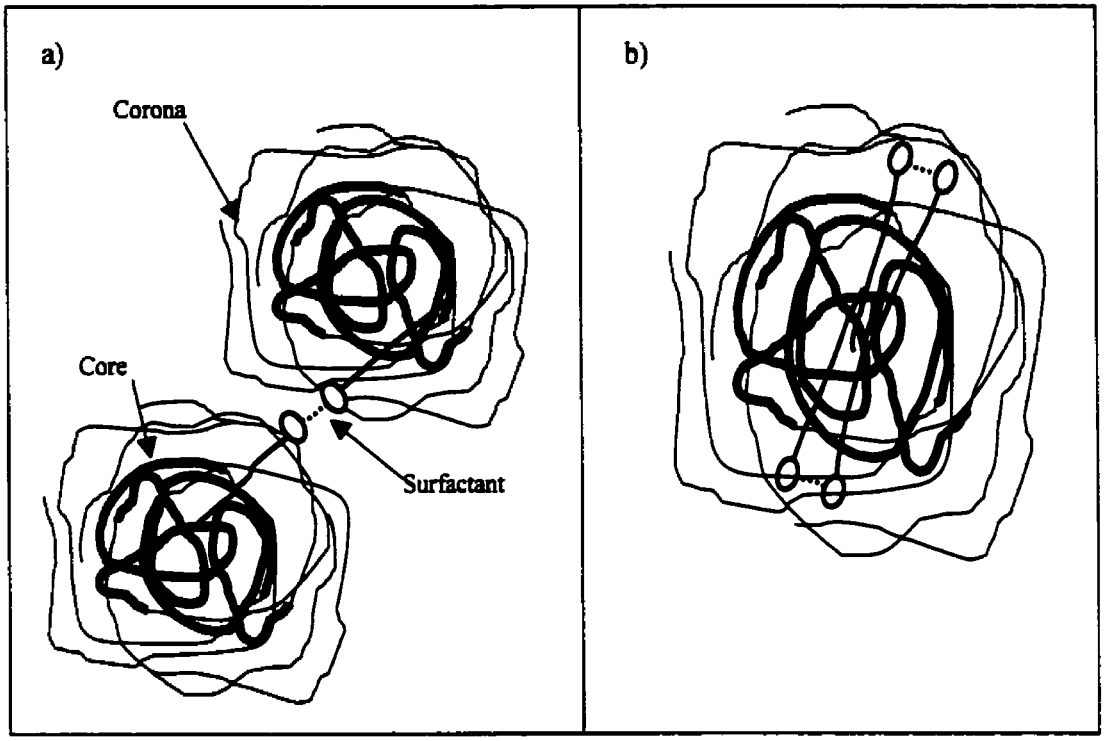

It is important to keep in mind that the above treatment is only qualitative and indicates the necessity of a complete thermodynamic study of an appropriate gemini surfactant-Pluronic system from which pre-micellar data can be obtained for the gemini surfactant. While there is no indication that the addition of the gemini surfactant has any effect on the aggregation behavior of the Pluronic from this work, specifically there is no indication of a variation in the cmt, a detailed complementary study of the specific volume for the Pluronic would provide information as to whether or not the addition of the gemini surfactant can induce or inhibit the self-aggregation of the Pluronic.

6. CONCLUSIONS AND FUTURE WORK

6.1 Concluding remarks: binary surfactant-water systems

1. The results of the specific conductance study of two series of gemini surfactants has confirmed, generally, observations previously reported in the literature. The cmc values for the gemini surfactants are observed to increase linearly with increasing alkyl tail length, in the usual manner. It is noted that, contrary to previous reports, $-\Delta G°_{mic}(CH_2)$ is larger for both the m-3-m and the m-6-m[33] series of surfactants than that obtained for the C_mTAB series of surfactants. This results from the increased tendency for micelle formation due to the increase in the size of the hydrophobic portion of the gemini surfactant molecule. Also, $-\Delta G°_{mic}(CH_2)$ is larger for the m-3-m series as compared to the m-6-m series. This result is attributed to a preferential *cis* conformation adopted by m-3-m surfactant monomers in solution. The cmc values for the 12-s-12 series of surfactants show a maximum at spacer lengths of approximately 4-5 methylene units. The cmc begins to decrease for longer spacers in a linear manner similar to that associated with the lengthening of the alkyl tail. The smaller magnitude of $-\Delta G°_{mic}(CH_2)$ indicates the incorporation of the spacer into the hydrophobic core of the micelle.

2. The mean aggregation numbers of the gemini surfactants are smaller than those previously reported; however, this is likely to be due to the low concentration region studied in this work. The variation of the mean aggregation number with increasing spacer length exhibits a minimum for a spacer 8-10 methylene units in length. This is consistent with geometrical requirements for maintaining a spherical aggregate structure. The mean

aggregation number is observed to increase with further increase in spacer length, consistent with the transition from spherical micellar aggregates to vesicles, as previously reported.[37]

3. The thermodynamic volume study of the gemini surfactants has shown that the apparent molar volumes for the gemini surfactants can be modeled, successfully, using either the mass action or pseudo-phase separation model. However because of the low values of the cmc, the pseudo-phase model is preferred.

4. Additivity schemes used for the gemini surfactants suggest that there is a preferred method to estimate thermodynamic volume properties, particularly in the case of multi-functional compounds. One based upon contributions from groups that closely resemble the head group of the surfactant has been shown to be more appropriate than previous models, particularly for surfactants possessing shorter spacer groups.

5. The observed changes in $\Delta V_{\phi,M}$ as a function of the spacer chain length are consistent with changes in the head group areas and suggest structural changes occur as the size of the spacer is varied. Results obtained in this study are consistent with previous determinations of head group areas, as well as with observations made using cryo-TEM methods. Also, the observed increase in $\Delta V_{\phi,M}$ for $s \geq 8$ is consistent with the incorporation of the spacer into the micelle core, as observed from head group area and critical micelle concentration results. Results obtained for the head group areas are in excellent agreement with those previously reported. The combined results of head group areas and apparent molar volumes suggest

that introducing rigidity into the spacer chain of the gemini surfactant likely will have an effect only for spacers longer than an equivalent of 8-10 methylene units.

6. The observed trend in the variation of $\Delta V_{\phi,M}$ with increased alkyl tail length is comparable to that observed for the corresponding monoquaternary ammonium surfactants.

6.2 Future work: binary surfactant-water systems

1. Future investigations of these systems should closely examine the effects of rigidity in the spacer group of the surfactant molecule. This rigidity may be accomplished through the introduction of unsaturations in the alkyl chain, or through the use of aromatic groups contained in the chain. However, it is crucial that the resulting length of the spacer chain be longer than 8-10 methylene units in length in order to truly evaluate the potential effect of rigidity in the spacer group. An additional experimental consideration would be to ensure that the cmc of the resulting surfactant is not so low as to complicate the study of the surfactant. Consideration should be given to choosing the length of the alkyl tails of the gemini surfactant so as to achieve this.

2. The effect of the addition of side groups such as -OH, or N-CH_3 to the spacer has been previously studied using surface tension and conductance methods.[30,31,44,45] Rosen et al. have investigated the addition of a hydroxyl group to the central carbon of the spacer chain for the 12-3-12 surfactant and observed a decrease in the cmc relative to that for the unmodified surfactant.[44] Devinsky et al. observed minimal variation in the cmc as a result of the replacement of the central methylene unit by N-CH_3 for the 12-5-12 surfactant.[30] A

complete study of the aggregation properties has not been carried out and is therefore required. Also, the effects of increasing the length of the side chain, or the number of substituents in the spacer chain should be examined.

3. It is well known that branching of the alkyl tail of a traditional single head group surfactant can result not only in a decrease in the cmc of the surfactant, but can lead to vesicle formation provided the length of the branch is sufficient. Studies should be made to examine the effect of branching in the alkyl tails of the gemini surfactant. It is possible that for shorter spacers branching may in fact lead to an increase in the cmc due to steric interactions between the surfactant molecules in the micelle, and/or increased hydrophobic interactions between the alkyl tails of a surfactant monomer brought about by the presence of bulkier groups in the alkyl tails. It is also possible that vesicle formation may be induced in gemini surfactants having shorter spacers as compared to the unmodified surfactants, where vesicles are observed to form only for long spacer groups.

4. In considering the composition of biological membranes, one observes that a major constituent of such membranes are phopholipid molecules. Because of this fact, the study of anionic gemini surfactants having phosphate head groups[27] may be of particular interest. Micelles or vesicle formed by such systems should serve as an excellent model with which to study the interaction of various types of biologically interesting molecules such as polymers, proteins, and drug molecules.

6.3 Concluding remarks: ternary surfactant-polymer-water systems

1. The conclusions which can be drawn from the study of the ternary surfactant-polymer-water systems are, due to the nature of the systems studied, somewhat speculative in nature. An immediate conclusion to be drawn from the study of the interaction of the gemini surfactants with the homopolymers PEO and PPO is that the interaction between the gemini surfactants and the Pluronic block copolymers primarily occurs through the more hydrophobic PPO segment. No detectable interaction is observed to occur between the gemini surfactants and PEO in solution.

2. The interaction that is observed to occur between the gemini surfactants and the Pluronic block copolymers is not typical of surfactant-polymer interactions. The observed variation in the cmc and degree of micelle ionization as a function of polymer concentration, along with the observed increase in the apparent molar volume of the surfactant in solutions containing Pluronic copolymers, is more typical of a process where the polymer is solubilized at or near the surface of the micelle, similar to mixed micelle formation in systems containing alcohols. It should be noted that both this interaction, as well as that usually observed, namely the formation of polymer bound aggregates, do possess some similarities. Both processes will result in a decrease in head group repulsions, leading to the observed decrease in the mean aggregation number, as well as the observed decrease in the micelle polarity, as monitored by the vibronic intensity ratio of pyrene.

2. There appears to be a minimal effect on the interaction due to variation in the surfactant head group size. Results obtained from specific conductance and NMR studies suggest that interactions are possibly promoted by the smaller 12-3-12 surfactant head group.

4. The composition of the Pluronic copolymer has a more pronounced effect on the interaction, with the more hydrophobic P103 copolymer showing the most interaction, followed by F108, and finally F68. Additionally, larger interactions are observed for higher molar mass polymers having the same PO/EO mass ratio; however, this effect potentially arises from a decrease in the size of the PPO segment in the polymer, and not specifically from a decrease in the overall molar mass.

5. The results obtained from equilibrium dialysis and fluorescence vibronic intensity ratio of pyrene studies suggest that there may be a different mechanism of interaction for P103 versus F108 at low polymer concentrations. P103 is observed to interact non-cooperatively with the 12-3-12 surfactant below the cmc, with no evidence of a CAC. F108 shows evidence for a CAC, particularly at low polymer concentrations, for the 12-3-12 surfactant of approximately 0.5 to 0.6 mmol L^{-1} in both experimental methods.

6. The aggregation state of the copolymer is observed to have a significant effect on the interaction of the gemini surfactant with the copolymer in aqueous solution. At conditions where polymer self-aggregation does not occur, specifically low concentration and low temperature, regular surfactant micelles with the polymer solubilized at or near the surface appear to be the dominant structure. Abrupt changes in structure occur at the cmt of the

copolymer. It is hypothesized that separate polymer aggregates form, as well as gemini surfactant micelles, in which there may be some solubilization of gemini surfactant monomer.

6.4 Future work: ternary surfactant-polymer-water systems

1. It is obvious from the discussion of the results of this work that a major impediment to the study of the ternary surfactant-polymer-water systems is the low values for the cmc of the gemini surfactants. This can be overcome in future studies by examining gemini surfactants with shorter alkyl tails, specifically, the 10-s-10 series of surfactants, whose cmc values are of an order of magnitude larger than those of the 12-s-12 series studied in this work.

2. A more complete thermodynamic study of the ternary systems, in turn allowing for an application of the thermodynamic models discussed in §5.2.1.4 and 5.2.2.4 is required. Studies should include an examination of the specific volume of the polymer in surfactant solution as a function of temperature to clearly probe the possibility of influencing the cmt of the Pluronic solutions by addition of gemini surfactant.

3. Future work should also be carried out to take advantage of the sensitivity of spectroscopic methods and examine the mean aggregation numbers in greater detail. Also, measurement of the rotational polarization of a probe molecule would provide information about the microviscosity of the aggregates. This may allow for some differentiation between the polymer dominated and surfactant dominated aggregates hypothesized in this work. The

possibility of introducing a fluorescent probe directly into the structure of the surfactant or the polymer molecule should be examined. This would allow for a more direct examination of the interactions occurring on the molecular level.

4. Additional binding studies should be carried out, possibly using surfactant specific electrode or titration microcalorimetric methods, which would alleviate the difficulties of determining the surfactant concentration encountered in this work. Such investigations would allow for a better understanding of the mechanism of interaction between the surfactant and Pluronic in solution. Additionally, such studies would allow for determination of the interaction of the surfactant with PPO, which was precluded in this work by the molecular weight cutoff of the dialysis membrane used.

5. A complete examination of the bulk viscosity of the ternary surfactant-polymer-water solutions is necessary to eliminate the possibility of the observed variations in the specific conductance arising from viscosity effects.

6. Provided access to an instrument having a higher field is available, a ^{13}C NMR study of the ternary systems may provide important information regarding the site of interaction of the polymer with the gemini surfactant. The requirement of a higher magnetic field than that available currently arises from the low concentrations of surfactant involved in this study. Such experiments would have required considerable machine time on the spectrometer used in this study due to the large number of scans required to obtain ^{13}C spectra. An additional advantage is that such measurements could be carried out in aqueous rather than D_2O

solution, allowing for a direct comparison of the results with results obtained from other methods.

7. Dynamic light scattering studies, which have previously been used to effectively probe copolymer systems, may provide some insight into the nature of the aggregates formed in the ternary surfactant-polymer-water systems. While the observation of micelles in aqueous solution is difficult using this method (since the resolution is on the order of 1 - 2 nm), the measured hydrodynamic radii of aggregates formed by the Pluronic copolymers used in this study are of the order of 7 nm or greater. Therefore observation of particles of this size in the ternary systems above the cmt would provide confirmation of some of the hypotheses presented in this work.

7. REFERENCES

(1) Goddard, E.D. and Ananthapadmanabhan, K.P. In *Interactions of Surfactants with Polymers and Proteins*; Goddard, E., Ananthapadmanabhan, K.P., Ed.; CRC Press, Inc.: Boca Raton, Fl., 1993.

(2) Nikas, Y.J. and Blankschtein, D., *Langmuir* **10**, 3512 (1994).

(3) Rhein, L.D., Robbins, C.R., Fernee, K. and Cantore, R., *J. Soc. Cosmet. Chem.* **37**, 125 (1986).

(4) Alli, D., Bolton, S. and Gaylord, N.S., *J. Appl. Polym. Sci.* **42**, 947 (1991).

(5) Goddard, E. In *Interactions of Surfactants with Polymers and Proteins*; Goddard, E., Ananthapadmanabhan, K.P., Ed.; CRC Press Inc.: Boca Raton, Fl., 1993.

(6) Goddard, E. In *Interactions of Surfactants with Polymers and Proteins*; Goddard, E., Ananthapadmanabhan, K.P., Ed.; CRC Press, Inc.: Boca Raton, Fl., 1993.

(7) Brackman, J.C. and Engberts, J.B.F.N., *Chem. Soc. Rev.* , 85 (1993).

(8) Brackman, J.C. and Engberts, J.B.F.N., *Langmuir* **8**, 424 (1994).

(9) Brackman, J.C. and Engberts, J.B.F.N., *Langmuir* **7**, 2097 (1991).

(10) Witte, F.M. and Engberts, J.B.F.N., *J. Org. Chem.* **52**, 4767 (1987).

(11) Cutler, R.A. and Drobeck, H.P. In *Cationic Surfactants*; Jungermann, E., Ed.; Marcel Dekker, Inc.: New York, 1970; p 527.

(12) Kastner, U. and Zana, R., *J. Colloid Int. Sci.* **218**, 468 (1999).

(13) Fredell, D.L. In *Cationic Surfactants: Analytical and Biological Evaluation*; Cross, J. and Singer, E.J., Eds.; Marcel Dekker, Inc.: New York, 1994; Vol. 53; p 31.

(14) Imam, T., Devinsky, F., Lacko, I., Mlynarcik, D. and Krasnec, L., *Pharmazie* **38**, 308 (1983).

(15) Eden, M.W. In *Nonionic Surfactants: Polyoxyalkylene Block Copolymers*; Nace, V.M., Ed.; Marcel Dekker, Inc.: New York, 1996; Vol. 60; pp 185.

(16) Israelachvili, J. *Intermolecular and Surface Forces*; Academic Press: San Diego, CA., 1991.

(17) Blokzijl, W. and Enberts, J.B.F.N., *Angew. Chem. Int. Ed. Eng.* **32**, 1545 (1993).

(18) van Oss, C.J. In *Interfacial Forces in Aqueous Media*; Marcel Dekker Inc.: New York, 1994; p 186.

(19) Evans, D.F. and Wennerstom, H. *The Colloidal Domain: Where Physics, Chemistry, Biology, and Technology Meet*; 1 ed.; VCH Publishers, Inc., 1994.

(20) Tanford, C. *The Hydrophobic Effect: Formation of Micelles and Biological Membranes*; Kreiger Publishing Company: Malabar Fl., 1991.

(21) Ben-Naim, A. *Hydrophobic Interactions*; Plenum Press: New York, 1980.

(22) Tucker, E.E., Lane, E.H. and Christian, S.D., *J. Soln. Chem.* **10**, 1 (1981).

(23) Israelachvili, J. and Pashley, P., *Nature* **300**, 341 (1982).

(24) Tsao, Y., Evans, D.F. and Wennerstrom, H., *Langmuir* **7**, 3154 (1991).

(25) Claesson, P. and Christenson, H., *J. Phys. Chem* **92**, 1650 (1992).

(26) Menger, F.M. and Littau, C.A., *J. Am. Chem. Soc.* **115**, 10083 (1993).

(27) De, S., Aswal, V.K., Goyal, P.S. and Bhattacharya, S., *Chem. Phys. Lett.* **303**, 295 (1999).

(28) Zana, R. and Levy, H., *Langmuir* **13**, 402 (1997).

(29) Zana, R., Levy, H. and Kwekat, K., *J. Colloid Int. Sci.* **197**, 370 (1998).

(30) Devinsky, F., Lacko, I., Bittererova, F. and Tomeckova, L., *J. Colloid Int. Sci.* **114**, 314 (1986).

(31) Devinsky, F., Masarova, L. and Lacko, I., *J. Colloid Int. Sci.* **105**, 235 (1985).

(32) Devinsky, F., Lacko, I. and Imam, T., *J. Colloid Int. Sci.* **143**, 336 (1991).

(33) Zana, R., Benrraou, M. and Rueff, R., *Langmuir* **7**, 1072 (1991).

(34) Alami, E., Levy, H. and Zana, R., *Langmuir* **9**, 940 (1993).

(35) Alami, E., Beinert, G., Marie, P. and Zana, R., *Langmuir* **9**, 1465 (1993).

(36) Frindi, M., Michels, B., Levy, H. and Zana, R., *Langmuir* **10**, 1140 (1994).

(37) Danino, D., Talmon, Y. and Zana, R., *Langmuir* **11**, 1448 (1995).

(38) Zana, R., In, M., Levy, H. and Duportail, G., *Langmuir* **13**, 5552 (1997).

(39) Danino, D., Talmon, Y. and Zana, R., *J. Colloid Int. Sci.* **185**, 84 (1997).

(40) Hirata, H., Hattori, N., Ishida, M., Okabayashi, H., Frusaka, M. and Zana, R., *J. Phys. Chem* **99**, 17778 (1995).

(41) Zana, R., *Curr. Opinion Colloid Interface Sci.* , 566 (1996).

(42) In, M., Bec, V., Aguerre-Chariol, O. and Zana, R., *Langmuir* **16**, 141 (2000).

(43) Schosseler, F., Anthony, O., Beinert, G. and Zana, R., *Langmuir* **11**, 3347 (1995).

(44) Song, L.D. and Rosen, M.J., *Langmuir* **12**, 1149 (1996).

(45) Rosen, M.J. and Song, L.D., *J. Colloid Int. Sci.* **179**, 261 (1996).

(46) Liu, L. and Rosen, M., *J. Colloid Int. Sci.* **179**, 454 (1996).

(47) Rosen, M. and Liu, L., *J. Am. Oil Chem. Soc.* **73**, 885 (1996).

(48) De, S., Aswal, V.K., Goyal, P.S. and Bhattacharya, S., *J. Phys. Chem* **100**, 11664 (1996).

(49) De, S., Aswal, V.K., Goyal, P.S. and Bhattacharya, S., *Journal of Physical Chemistry Part B* **101**, 5639 (1997).

(50) Diamant, H. and Andelman, D., *Langmuir* **10**, 2910 (1994).

(51) Diamant, H. and Andelman, D., *Langmuir* **11**, 3605 (1995).

(52) Hattori, N., Hirata, H., Okabayashi, H. and O'Connor, C.J., *Colloid Polym. Sci.* **277**, 306 (1999).

(53) Hattori, N., Hirata, H., Okabayashi, H. and O'Connor, C.J., *Colloid Polym. Sci.* **277**, 361 (1999).

(54) Rooycka-Rozak, B., Fisicaro, E. and Ghiossi, A., *J. Colloid Int. Sci.* **184**, 209 (1996).

(55) Chorro, C., Chorro, M., Dolladille, O., Partyka, S. and Zana, R., *J. Colloid Int. Sci.* **199**, 169 (1998).

(56) Fielden, M.L., Claesson, P.M. and Verrall, R.E., *Langmuir* **15**, 3924 (1999).

(57) Luchetti, L. and Mancini, G., *Langmuir* **16**, 161 (2000).

(58) Zana, R. In *Structure-Performance Relationships in Surfactants*; Esumi, K. and Ueno, M., Eds.; Marcel Dekker Inc.: New York, 1997; Vol. 70.

(59) Menger, F.M., Keiper, J.S. and Azov, V., *Langmuir* **16**, 2062 (2000).

(60) Chu, B. and Zhou, Z. In *Nonionic Surfactants: Polyoxyalkylene Block Copolymers*; Nace, V.M., Ed.; Marcel Dekker Inc.: New York, 1996; Vol. 60.

(61) Edens, M.W. In *Nonionic Surfactants: Polyoxyalkylene Block Copolymers*; Nace, V.M., Ed.; Marcel Dekker Inc.: New York, 1996; Vol. 60.

(62) Alexandridis, P., *Curr. Opinion Colloid Interface Sci.* **1**, 490 (1996).

(63) Alexandridis, P. and Hatton, T.A., *Colloids Surf. A* **95**, 1 (1995).

(64) Wen, X.G., Verrall, R.E. and Liu, G.J., *J. Phys. Chem. B* **103**, 2620 (1999).

(65) Wanka, G., Hoffmann, H. and Ulbricht, W., *Macromolecules* **27**, 4145 (1994).

(66) Alexandridis, P., Athanassiou, V., Fukuda, S. and Hatton, T.A., *Langmuir* **10**, 2604 (1994).

(67) Prasad, K.N., Luong, T.T., Florence, A.T., Paris, J., Vaution, C., Seiller, M. and Puisieux, F., *J. Colloid Int. Sci.* **69**, 225 (1979).

(68) Hecht, E. and Hoffmann, H., *Langmuir* **10**, 86 (1994).

(69) Jonsson, B., Lindman, B., Holmberg, K. and Kronberg, B. *Surfactants and Polymers in Aqueous Solution*; John Wiley & Sons: Chichester, 1998.

(70) *Interactions of Surfactants with Polymers and Proteins*; Goddard, E.D. and Ananthapadmanabhan, K.P., Eds.; CRC Press: Boca Raton, 1993.

(71) Goddard, E., *J. Am. Oil Chem. Soc.* **71**, 1 (1994).

(72) Breuer, M.M. and Robb, I.D., *Chem. Ind.* , 530 (1972).

(73) Jones, M.N., *J. Colloid Int. Sci.* **23**, 36 (1967).

(74) Gilanyi, T. and Wolfram, E. In *Microdomains in Polymer Solutions*; Dubin, P., Ed.; Plenum Press: New York, 1985.

(75) Cabane, B., *J. Phys. Chem* **81**, 1639 (1977).

(76) Nagarajan, R., *Colloids and Surfaces* **13**, 1 (1985).

(77) Lindman, B. and Thalberg, K. In *Interactions of Surfactants with Polymers and Proteins*; Goddard, E., Ananthapadmanabhan, K.P., Ed.; CRC Press, Inc.: Boca Raton, Fl., 1993.

(78) Hayakawa, K. and Kwak, J.C.T. In *Cationic Surfactants: Physical Chemistry*; Holland, P.M., Rubingh, D.N., Ed.; Marcel Dekker Inc., 1991; Vol. 37; pp 189.

(79) Piculell, L., Guillemet, F., Thuresson, K., Shubin, V. and Ericsson, O., *Adv. Colloid Int. Sci.* **63**, 1 (1996).

(80) Anthony, O. and Zana, R., *Langmuir* **12**, 3590 (1996).

(81) Medeiros, G. and Costa, S., *Colloids Surf. A* **119**, 141 (1996).

(82) Evertsson, H. and Holmberg, C., *Colloid Polym. Sci.* **275**, 830 (1997).

(83) Singh, S.K. and Nilsson, S., *J. Colloid Int. Sci.* **213**, 133 (1999).

(84) Holmberg, C., Nilsson, S., Singh, S.K. and Sundelof, L., *J. Phys. Chem* **96**, 871 (1992).

(85) Piculell, L., Thuresson, K. and Ericsson, O., *Faraday Disc.* **101**, 307 (1995).

(86) Brackman, J.C. and Engberts, J.B.F.N., *Langmuir* **7**, 46 (1991).

(87) Almgren, M., van Stam, J., Lindblad, C., Li, P., Stilbs, P. and Bahadur, P., *J. Phys. Chem* **95**, 5677 (1991).

(88) Moroi, Y. *Micelles: Theoretical and Applied Aspects*; Plenum Press: New York, 1992.

(89) Philips, J.N., *Trans. Far. Soc.* **51**, 561 (1955).

(90) Attwood, D. and Florence, A.T. *Surfactant Systems: Their chemistry, pharmacy and biology*; Chapman and Hall: New York, 1983.

(91) Myers, D. *Surfactant Science and Technology*; VCH Inc.: New York, 1988.

(92) Corrin, M.L. and Harkins, W.D., *J. Am. Chem. Soc.* **69**, 684 (1974).

(93) Miller, D.D. and Evans, D.F., *J. Phys. Chem* **93**, 323 (1989).

(94) Desnoyers, J.E., DeLisi, R. and Perron, G., *Pure App. Chem.* **52**, 433 (1980).

(95) Kale, K.M. and Zana, R., *J. Colloid Int. Sci.* **61**, 312 (1977).

(96) Shinoda, K. and Hutchinson, E., *J. Phys. Chem* **66**, 577 (1962).

(97) Vikingstad, E., Skange, A. and Hoiland, H., *J. Colloid Int. Sci.* **66**, 240 (1978).

(98) Caron, G., Perron, G., Lindheimer, M. and Desnoyers, J.E., *J. Colloid Int. Sci.* **106**, 324 (1985).

(99) Desnoyers, J.E., Caron, G., DeLisi, R., Roberts, D., Roux, A. and Perron, G., *J. Phys. Chem* **87**, 1397 (1983).

(100) Burchfield, T.E. and Woolley, E.M., *J. Phys. Chem* **88**, 2149 (1984).

(101) Woolley, E. and Burchfield, T.E., *J. Phys. Chem* **89**, 714 (1985).

(102) Desnoyers, J., Perron, G. and Roux, A.H. In *Surfactant Solutions: New Methods of Investigation*; Zana, R., Ed.; Marcel Dekker Inc., 1987; Vol. 22; pp 1.

(103) Anthony, O. and Zana, R., *Langmuir* **10**, 4048 (1994).

(104) Murata, M. and Arai, H., *J. Colloid Int. Sci.* **44**, 475 (1973).

(105) Arai, H., Murata, M. and Shinoda, K., *J. Colloid Int. Sci.* **37**, 223 (1971).

(106) Nagarajan, R., *J. Phys. Chem* **90**, 1980 (1989).

(107) Ruckenstein, E., Huber, G. and Hoffmann, H., *Langmuir* **3**, 382 (1987).

(108) Ruckenstein, E., *Langmuir* **15**, 8086 (1999).

(109) Winnik, F.M. In *Interactions of Surfactants with Polymers and Proteins*; Goddard, E., Ananthapadmanabhan, K.P., Ed.; CRC Press, Inc.: Boca Raton, Fl., 1993.

(110) Brackman, J.C. and Engberts, J.B.F.N., *J. Am. Chem. Soc.* **112**, 872 (1990).

(111) Gilanyi, T. and Wolfram, E., *Colloids and Surfaces* **3**, 181 (1981).

(112) Diamant, H. and Andelman, D., *Europhys. Lett.* **48**, 170 (1999).

(113) Waton, G., Michels, B. and Zana, R., *J. Colloid Int. Sci.* **212**, 593 (1999).

(114) Marinov, G., Michels, B. and Zana, R., *Langmuir* **14**, 2639 (1998).

(115) Gehlen, M.H. and De Schryver, F.C., *Chem. Rev.* **93**, 199 (1993).

(116) Zana, R. In *Surfactant Solutions: New Methods of Investigation*; Zana, R., Ed.; Marcel Dekker, Inc.: New York, 1987.

(117) Kalyanasundaram, K. and Thomas, J., *J. Am. Chem. Soc.* **99**, 2039 (1977).

(118) Nakajima, A., *Bull. Chem. Soc. Jpn.* **50**, 2473 (1977).

(119) Nakalima, A., *Photochemistry and Photobiology* **25**, 593 (1977).

(120) Kalyanasundaram, K. *Photochemistry in Microheterogeneous Systems*; Academic Press, Inc.: Orlando, 1987.

(121) van der Auweraer, M., D., J.C., Gelade, E. and De Schryver, F.C., *J. Chem. Phys.* **74**, 1140 (1981).

(122) Reekmans, S. and De Schryver, F.C. In *Frontiers in Supramolecular Organic Chemistry and Photochemistry*; Schneider, H., Durr H., Ed.; VCH Publishers, 1991.

(123) Reekmans, S., Bernik, D., Gehlen, M., van Stam, J., Van der Auweraer, M. and De Schryver, F.C., *Langmuir* **9**, 2289 (1993).

(124) Infelta, P., Gratzel, M. and Thomas, J.K., *J. Phys. Chem* **78**, 190 (1974).

(125) Tachiya, M., *J. Chem. Phys.* **76**, 340 (1982).

(126) Holmberg, C., Nilsson, S. and Sundelof, L., *Langmuir* **13**, 1392 (1997).

(127) Zana, R., *J. Colloid Int. Sci.* **78**, 330 (1980).

(128) Evans, H.C., *J. Chem. Soc.* , 579 (1956).

(129) Picker, P., Tremblay, E. and Jolcoeur, C., *J. Soln. Chem.* **3**, 377 (1974).

(130) Burns, J.A. Ph.D., University of Saskatchewan, 1973.

(131) Hepler, L.G., Stokes, J.M. and Stokes, R.H., *Trans. Far. Soc.* **61**, 20 (1965).

(132) Nivaggioli, T., Tsao, B., Alexandridis, P. and Hatton, T.A., *Langmuir* **11**, 119 (1995).

(133) Van Damme, M.-P.I., Blackwell, S.T., Murphy, W.H. and Preston, B.N., *Analytical Biochemistry* **204**, 250 (1992).

(134) Jenkins, K.M., M.Sc. Thesis, University of Saskatchewan, 2000.

(135) Francois, J., Dayantis, J. and Sabbadin, J., *European Polymer Journal* **21**, 165 (1985).

(136) Muto, S., Ino, T. and Meguro, K., *J. Am. Oil Chem. Soc.* **49**, 437 (1972).

(137) Chang, N.J. and Kaler, E.W., *J. Phys. Chem* **89**, 2996 (1986).

(138) Wen, X. Ph.D. Thesis, University of Saskatchewan, 1999.

(139) Kopperud, H.B.M., Walderhaug, H. and Hansen, F.K., *Macromol. Chem. Phys.* **200**, 1839 (1999).

(140) Evertsson, H. and Nilsson, S., *Carbohydrate Polymers* **40**, 293 (1999).

(141) Mukerjee, P. and Mysels, K. *Critical Micelle Concentrations of Aqueous Surfactant Systems*; Superintendent of Documents, U.S. Gov. Printing Office: Washington, DC., 1971; Vol. NSRDS-NBS 36.

(142) Wettig, S. and Verrall, R., *Submitted for publication* (2000).

(143) Huang, H., Ph.D. Thesis, University of Saskatchewan, 1997.

(144) Jobe, D., Verrall, R. and Skalski, B., *Langmuir* **9**, 2814 (1993).

(145) Gianni, P. and Lepori, L., *J. Soln. Chem.* **25**, 1 (1996).

(146) Verrall, R.E., Ph.D. Thesis, University of Ottawa, 1966.

(147) Kaneshina, S., Tanaka, M., Tomida, T. and Matuura, R., *J. Colloid Int. Sci.* **48**, 450 (1974).

(148) Israelachvili, J.N., Mitchell, D.J. and Ninham, B.W., *J. Chem. Soc., Faraday Trans. 2* **72**, 1525 (1976).

(149) Mitchell, D.J. and Ninham, B.W., *J. Chem. Soc., Faraday Trans. 2* **77**, 601 (1981).

(150) Zanette, D., Lima, C.F., Ruzza, A.A., Belarmino, A.T.N., Santos, S.d.F., Frescura, V.L.A., Marconi, D.M.O. and Frohner, S.J., *Colloids Surf. A* **147**, 89 (1999).

(151) Lad, K., Bahadur, A., Pandya, K. and Bahadur, P., *Indian Journal of Chemistry* **34A**, 938 (1995).

(152) Zana, R., Yiv, S., Strazielle, C. and Lianos, P., *J. Colloid Int. Sci.* **80**, 208 (1981).

(153) Zana, R., Lang, J. and Lianos, P. In *Microdomains in Polymer Solutions*; Dubin, P., Ed.; Plenum Press: New York, 1985.

(154) Perron, G., Francoeur, J., Desnoyers, J.E. and Kwak, J.C.T., *Can. J. Chem.* **65**, 990 (1987).

(155) Ballerat-Busserolles, K., Roux-Desgranges, G. and Roux, A.H., *Langmuir* **13**, 1946 (1997).

(156) De Lisi, R., Liveri, V.T., Castagnolo, M. and Inglese, A., *J. Soln. Chem.* **15**, 23 (1986).

(157) De Lisi, R., Milioto, S., Castagnolo, M. and Inglese, A., *J. Soln. Chem.* **19**, 767 (1990).

(158) De Lisi, R., Milioto, S. and Verrall, R., *J. Soln. Chem.* **19**, 97 (1990).

(159) Lianos, P. and Zana, R., *Chem. Phys. Lett.* **76**, 62 (1980).

(160) Roux, A., Hetu, D., Perron, G. and Desnoyers, J.E., *J. Soln. Chem.* **13**, 1 (1984).

(161) De Lisi, R., Genova, C., Testa, R. and Liveri, V.T., *J. Soln. Chem.* **13**, 121 (1984).

(162) De Lisi, R., Milioto, S. and Verrall, R., *J. Soln. Chem.* **19**, 665 (1990).

(163) Zielinski, R., Ikeda, S., Nomura, H. and Kato, S., *J. Chem. Soc. Farad. Trans.* **84**, 151 (1988).

8. APPENDICES

Appendix A: Characterization data for the m-s-m gemini surfactants

Table A-I: CH&N Analysis results for the gemini surfactants

Surfactant	%C cal'c	%C found	%H cal'c	%H found	%N cal'c	%N found
10-3-10	56.6	55.5	10.6	10.6	4.9	4.8
12-2-12	58.6	58.8	10.8	10.8	4.6	4.6
12-3-12	59.2	58.3	10.9	10.9	4.5	4.4
12-4-12	59.8	58.3	11.0	10.5	4.4	4.2
12-6-12	60.9	60.9	11.1	11.0	4.2	3.9
12-8-12	61.9	61.6	11.3	10.9	4.0	3.8
12-10-12	62.8	62.9	11.4	11.5	3.9	3.8
12-12-12	63.6	62.9	11.5	11.5	3.7	3.8
12-16-12	65.2	65.0	11.7	11.6	3.5	3.5
12-ϕ-12	62.6	62.3	10.2	10.0	4.1	4.4

Table A-II: ^{1}H NMR Data for the m-s-m gemini surfactants

Surfactant	Group	δ(ppm)	# of protons
10-3-10	N-CH_2-	3.61-3.23	8
	N-CH_3	3.28	12
	N-CH_2-CH_2-CH_2-N	2.60-2.45	2
	N-CH_2-CH_2-	1.68-1.52	4
	-$(CH_2)_n$-	1.25-1.00	28
	-CH_3	0.69	6
12-2-12	N-CH_2-CH_2-N	4.02	4
	N-CH_2-	3.31	4
	N-CH_3	3.26	12
	N-CH_2-CH_2-	1.85	4
	-$(CH_2)_n$-	1.43-1.30	36
	-CH_3	0.90	6
12-3-12	N-CH_2-	3.44	8
	N-CH_3	3.19	12
	N-CH_2-CH_2-CH_2-N	2.33	2
	N-CH_2-CH_2-	1.81	4
	-$(CH_2)_n$-	1.41-1.30	36
	-CH_3	0.90	6

Table A-II (con't): ^{1}H NMR Data for the m-s-m gemini surfactants

Surfactant	Group	δ(ppm)	# of protons
12-4-12	N-CH_2-CH_2- CH_2-CH_2-N	3.46	4
	N-CH_2-	3.31	4
	N-CH_3	3.12	12
	N-CH_2-CH_2-	1.87-1.80	8
	-$(CH_2)_n$-	1.40-1.30	36
	-CH_3	0.90	6
12-6-12	N-CH_2-	3.31	8
	N-CH_3	3.10	12
	N-CH_2-CH_2-	1.80	8
	-$(CH_2)_n$-	1.49-1.30	40
	-CH_3	0.91	6
12-8-12	N-CH_2-	3.31	8
	N-CH_3	3.08	12
	N-CH_2-CH_2-	1.78	8
	-$(CH_2)_n$-	1.45-1.30	44
	-CH_3	0.90	6
12-10-12	N-CH_2-	3.31	8
	N-CH_3	3.08	12
	N-CH_2-CH_2-	1.76	8
	-$(CH_2)_n$-	1.40-1.30	48
	-CH_3	0.90	6
12-12-12	N-CH_2-	3.31	8
	N-CH_3	3.08	12
	N-CH_2-CH_2-	1.75	8
	-$(CH_2)_n$-	1.39-1.30	52
	-CH_3	0.90	6
12-16-12	N-CH_2-	3.42-3.30	8
	N-CH_3	3.28	12
	N-CH_2-CH_2-	1.59-1.44	8
	-$(CH_2)_n$-	1.27-0.96	60
	-CH_3	0.74-0.65	6

Appendix B: Specific conductance data

Table B-I: Specific conductance of aqueous m-s-m gemini surfactant systems

Concentration (mol L^{-1})	κ ($\mu S\ cm^{-1}$)	Concentration (mol L^{-1})	κ ($\mu S\ cm^{-1}$)	Concentration (mol L^{-1})	κ ($\mu S\ cm^{-1}$)
10-3-10		12-2-12		12-3-12	
0.00	1.73	0.00	3.81	0.00	2.68
3.23×10^{-4}	70.60	5.15×10^{-5}	13.68	1.18×10^{-4}	31.00
7.74×10^{-4}	144.3	1.00×10^{-4}	23.61	2.03×10^{-4}	50.85
1.19×10^{-4}	241.7	1.49×10^{-4}	34.07	3.39×10^{-4}	70.02
1.52×10^{-3}	300.3	2.04×10^{-4}	45.41	4.24×10^{-4}	88.77
1.84×10^{-3}	361.1	2.71×10^{-4}	58.72	5.08×10^{-4}	106.7
2.36×10^{-3}	450.2	3.34×10^{-4}	71.33	5.85×10^{-4}	124.6
2.92×10^{-3}	554.1	3.94×10^{-4}	83.07	6.94×10^{-4}	148.6
3.47×10^{-3}	649.9	4.57×10^{-4}	95.05	8.05×10^{-4}	172.3
4.01×10^{-3}	743.0	5.25×10^{-4}	108.4	9.08×10^{-4}	193.1
4.55×10^{-3}	833.1	5.93×10^{-4}	121.4	9.87×10^{-4}	203.7
5.05×10^{-3}	914.1	6.66×10^{-4}	134.9	1.10×10^{-3}	212.2
5.61×10^{-3}	992.6	7.41×10^{-4}	148.5	1.23×10^{-3}	219.7
6.07×10^{-3}	1045	7.99×10^{-4}	158.7	1.36×10^{-3}	226.4
6.61×10^{-3}	1091	8.56×10^{-4}	167.6	1.56×10^{-3}	235.8
7.09×10^{-3}	1125	9.12×10^{-4}	173.7	1.75×10^{-3}	244.2
7.54×10^{-3}	1151	9.75×10^{-4}	178.5	2.10×10^{-3}	260.1
8.01×10^{-3}	1176	1.04×10^{-3}	182.0	2.40×10^{-3}	273.3
9.12×10^{-3}	1227	1.14×10^{-3}	186.6		
1.02×10^{-2}	1273	1.31×10^{-3}	193.0		
1.22×10^{-2}	1352	1.48×10^{-3}	199.0		
1.42×10^{-2}	1424	1.62×10^{-3}	204.0		
1.59×10^{-2}	1490	1.81×10^{-3}	209.8		
1.75×10^{-2}	1551	1.95×10^{-3}	214.4		
		2.08×10^{-3}	218.6		
		2.24×10^{-3}	223.8		
		2.36×10^{-3}	227.5		
		2.46×10^{-3}	230.6		
		2.56×10^{-3}	234.0		
		2.62×10^{-3}	236.2		
		2.71×10^{-3}	238.6		
		2.78×10^{-3}	240.8		

Table B-I(con't): Specific conductance of aqueous m-s-m gemini surfactant systems

Concentration (mol L^{-1})	κ ($\mu S\ cm^{-1}$)	Concentration (mol L^{-1})	κ ($\mu S\ cm^{-1}$)	Concentration (mol L^{-1})	κ ($\mu S\ cm^{-1}$)
12-4-12		12-8-12		12-12-12	
0.00	2.04	0.00	2.30	0.00	1.99
1.87×10^{-4}	36.29	1.27×10^{-4}	29.62	5.40×10^{-5}	13.71
3.14×10^{-4}	71.48	2.65×10^{-4}	58.53	1.39×10^{-4}	33.11
4.82×10^{-4}	106.5	3.89×10^{-4}	88.26	1.95×10^{-4}	45.79
5.84×10^{-4}	129.6	5.51×10^{-4}	121.7	2.43×10^{-4}	57.76
7.42×10^{-4}	162.4	6.67×10^{-4}	143.0	2.90×10^{-4}	69.11
8.80×10^{-4}	192.8	7.44×10^{-4}	159.8	3.36×10^{-4}	78.51
1.05×10^{-3}	227.9	8.53×10^{-4}	174.1	3.92×10^{-4}	87.92
1.13×10^{-3}	241.9	9.37×10^{-4}	186.3	4.71×10^{-4}	100.9
1.21×10^{-3}	251.3	1.03×10^{-3}	196.9	5.47×10^{-4}	112.5
1.29×10^{-3}	258.0	1.13×10^{-3}	209.3	6.17×10^{-4}	123.0
1.41×10^{-3}	266.1	1.25×10^{-3}	220.9	7.40×10^{-4}	138.9
1.54×10^{-3}	273.7	1.42×10^{-3}	234.1	8.58×10^{-4}	153.4
1.71×10^{-3}	283.4	1.66×10^{-3}	260.1	1.00×10^{-3}	170.2
1.93×10^{-3}	295.5	1.83×10^{-3}	274.3	1.12×10^{-3}	187.1
2.20×10^{-3}	309.4	1.94×10^{-3}	284.7		
12-6-12		12-10-12		12-16-12	
0.00	2.61	0.00	1.89	0.00	1.58
2.25×10^{-4}	43.55	1.40×10^{-4}	32.74	1.95×10^{-5}	5.89
3.66×10^{-4}	74.74	2.34×10^{-4}	54.82	3.07×10^{-5}	8.24
4.98×10^{-4}	105.6	3.23×10^{-4}	75.89	4.37×10^{-5}	11.49
6.01×10^{-4}	128.5	4.42×10^{-4}	102.6	5.42×10^{-5}	13.37
7.30×10^{-4}	157.3	5.36×10^{-4}	119.4	6.70×10^{-5}	16.28
8.57×10^{-4}	185.1	6.18×10^{-4}	133.0	8.23×10^{-5}	19.48
9.74×10^{-4}	210.4	7.08×10^{-4}	145.3	9.69×10^{-5}	22.41
1.06×10^{-3}	224.8	8.11×10^{-4}	159.3	1.39×10^{-4}	29.52
1.15×10^{-3}	235.4	9.57×10^{-4}	176.2	1.82×10^{-4}	35.88
1.22×10^{-3}	243.6	1.10×10^{-3}	193.0	2.35×10^{-4}	42.75
1.50×10^{-3}	260.7	1.28×10^{-3}	212.3	2.95×10^{-4}	50.01
1.61×10^{-3}	271.2	1.43×10^{-3}	227.2	3.41×10^{-4}	55.48
1.73×10^{-3}	280.8	1.60×10^{-3}	243.6		
1.86×10^{-3}	290.1				
2.03×10^{-3}	301.5				

Table B-II: Specific conductance data and specific conductance ratios for the 12-3-12 surfactant in aqueous polymer solutions

Conc. (mmol L^{-1})	κ ($\mu S\ cm^{-1}$)	κ'/κ^a	Conc. (mmol L^{-1})	κ ($\mu S\ cm^{-1}$)	κ'/κ^a
Aqueous 12-3-12			12-3-12/0.2% PEO		
0.000	1.97		0.000	1.97	1.00
0.143	30.36		0.176	36.47	0.99
0.291	61.64		0.409	80.89	0.97
0.457	93.95		0.504	100.4	0.98
0.595	123.1		0.688	133.4	0.96
0.735	150.8		0.832	161.8	0.97
0.916	178.5		0.979	180.5	0.95
1.03	190.0		1.20	192.4	0.97
1.26	201.6		1.52	205.8	0.97
1.53	213.3		1.90	220.4	0.97
2.20	240.2		2.28	234.7	0.97
2.87	266.6		2.66	249.0	0.97
3.45	290.1		3.04	263.2	0.96
4.03	312.9		3.71	288.6	0.96
4.57	335.1				
5.04	353.2				
12-3-12/0.2% PPO (M.W. 725)			12-3-12/0.05% PPO (M.W. 2000)		
0.000	1.97	1.00	0.000	1.97	1.00
0.182	36.76	0.96	0.309	54.26	0.86
0.299	60.84	0.99	0.453	77.16	0.84
0.463	91.75	0.98	0.618	100.8	0.81
0.580	114.0	0.97	0.802	127.3	0.79
0.700	133.7	0.95	0.955	144.8	0.77
0.835	150.6	0.90	1.07	157.8	0.81
1.01	169.1	0.88	1.22	171.4	0.86
1.15	183.1	0.93	1.39	186.0	0.90
1.46	208.5	1.00	1.64	204.9	0.95
1.87	237.6	1.05	1.98	225.9	0.98
2.24	262.5	1.09	2.35	244.9	1.00
2.63	287.5	1.12	2.67	260.3	1.01
3.12	316.9	1.15	2.97	272.9	1.01
3.58	343.4	1.16	3.28	285.0	1.01
4.11	372.1	1.18	3.71	300.2	1.00
4.54	395.8	1.19			

[a] κ calculated from regression analysis of the aqueous surfactant data

Table B-II(con't): Specific conductance data and specific conductance ratios for the 12-3-12 surfactant in aqueous polymer solutions

Conc. (mmol L^{-1})	κ ($\mu S\ cm^{-1}$)	κ'/κ^a	Conc. (mmol L^{-1})	κ ($\mu S\ cm^{-1}$)	κ'/κ^a
12-3-12/0.05% P103			12-3-12/0.5% P103		
0.000	1.97	1.00	0.000	1.97	1.00
0.079	19.11	1.08	0.144	24.29	0.79
0.157	36.62	1.10	0.217	38.46	0.85
0.302	63.08	1.02	0.300	52.39	0.85
0.434	87.91	1.00	0.415	71.57	0.85
0.568	110.7	0.96	0.490	83.21	0.84
0.655	124.9	0.95	0.568	95.03	0.83
0.782	143.7	0.91	0.659	106.4	0.80
0.929	162.6	0.87	0.717	117.4	0.81
1.01	172.5	0.90	0.803	127.4	0.79
1.09	181.2	0.93	0.912	142.0	0.76
1.18	189.9	0.96	1.08	162.1	0.84
1.26	197.3	0.98	1.28	183.4	0.91
1.39	207.8	1.01	1.40	196.5	0.95
1.51	216.9	1.03	1.52	208.8	0.99
1.64	225.6	1.04	1.66	223.9	1.03
1.81	235.6	1.05	1.80	238.4	1.07
2.02	246.8	1.06	1.99	255.7	1.11
2.21	256.2	1.07	2.17	272.9	1.15
2.46	266.7	1.07	2.32	285.4	1.17
2.69	276.2	1.07	2.53	303.5	1.20
2.91	284.5	1.06			
3.12	292.4	1.06			
12-3-12/0.1% P103			12-3-12/0.05% F108		
0.000	1.97	1.00	0.000	1.97	1.00
0.170	37.61	1.05	0.221	41.45	0.90
0.347	71.29	1.01	0.375	75.75	0.99
0.507	100.0	0.97	0.557	108.4	0.96
0.746	135.1	0.90	0.719	136.6	0.94
0.962	165.6	0.87	0.862	159.9	0.92
1.12	184.5	0.94	1.05	177.7	0.92
1.28	201.0	0.99	1.27	195.2	0.97
1.49	219.5	1.04	1.59	210.6	0.98
1.78	243.7	1.10	1.87	222.4	0.98
1.98	257.2	1.12	2.32	240.4	0.98
2.28	276.3	1.14	2.68	254.6	0.98
2.56	292.5	1.15	3.09	268.2	0.97
2.84	307.2	1.16	3.73	295.6	0.98
3.08	318.5	1.16			
3.24	326.5	1.16			

Table B-II(con't): Specific conductance data and specific conductance ratios for the 12-3-12 surfactant in aqueous polymer solutions

Conc. (mmol L^{-1})	κ ($\mu S\ cm^{-1}$)	κ'/κ^a	Conc. (mmol L^{-1})	κ ($\mu S\ cm^{-1}$)	κ'/κ^a
12-3-12/0.5% F108			12-3-12/1.0% F108		
0.000	1.97	1.00	0.000	1.97	1.00
0.140	27.80	0.93	0.167	29.72	0.85
0.295	54.59	0.90	0.335	56.41	0.82
0.457	78.93	0.85	0.515	79.81	0.77
0.586	98.47	0.83	0.641	99.48	0.77
0.741	117.2	0.79	0.791	117.6	0.74
0.884	134.5	0.76	0.936	134.1	0.71
1.04	150.4	0.78	1.09	150.1	0.77
1.22	168.3	0.84	1.30	169.1	0.83
1.48	190.2	0.90	1.61	195.8	0.91
1.93	220.1	0.96	1.99	224.1	0.97
2.32	242.2	0.99	2.34	247.0	1.01
2.73	261.6	1.00	2.78	272.2	1.04
3.10	278.4	1.01	3.38	301.8	1.05
3.43	292.3	1.01	3.96	327.4	1.06
3.93	311.9	1.01	4.41	347.2	1.06
4.55	333.9	1.00	4.76	359.9	1.05
4.94	347.9	0.99	5.10	372.9	1.05
12-3-12/0.05% F68			12-3-12/2.0% F68		
0.000	1.97	1.00	0.000	1.97	1.00
0.140	31.22	1.05	0.129	29.07	1.05
0.284	61.31	1.05	0.273	55.25	0.98
0.423	89.58	1.04	0.388	76.24	0.96
0.548	113.7	1.03	0.522	97.40	0.92
0.674	137.3	1.01	0.644	114.6	0.88
0.814	158.3	0.97	0.802	133.2	0.83
0.931	171.2	0.91	0.991	153.3	0.80
1.07	181.8	0.94	1.36	185.4	0.90
1.31	196.7	0.97	1.76	214.1	0.97
1.55	207.9	0.98	2.13	237.7	1.01
1.87	221.6	0.98	2.55	262.3	1.04
2.39	242.1	0.98	2.95	284.0	1.05
2.89	261.3	0.98	3.31	302.4	1.06
3.34	279.2	0.98	3.66	319.6	1.07
4.12	309.8	0.98	3.97	334.6	1.08

Table B-III: Specific conductance data and specific conductance ratios for the 12-6-12 surfactant in aqueous polymer solutions

Conc. (mmol L^{-1})	κ ($\mu S\ cm^{-1}$)	κ'/κ^a	Conc. (mmol L^{-1})	κ ($\mu S\ cm^{-1}$)	κ'/κ^a
Aqueous 12-6-12			12-3-12/0.2% PEO		
0.000	1.18		0.000	1.18	1.00
0.116	25.28		0.152	32.48	1.05
0.286	59.00		0.304	62.40	1.03
0.433	88.28		0.478	93.05	0.98
0.576	115.4		0.606	121.9	1.02
0.690	138.1		0.757	150.2	1.00
0.803	159.4		0.945	183.4	0.98
0.910	179.5		1.15	208.4	0.97
1.01	195.0		1.48	233.2	0.99
1.32	223.6		1.89	258.8	1.00
1.63	244.7		2.30	284.8	1.00
1.93	263.2		2.70	307.5	1.00
2.34	287.9		3.15	334.4	1.00
2.81	315.6				
3.45	352.9				
4.03	386.2				
12-6-12/0.2% PPO (M.W. 725)			12-6-12/0.05% PPO (M.W. 2000)		
0.000	1.18	1.00	0.000	1.18	1.00
0.148	29.54	0.98	0.165	32.75	0.98
0.282	56.21	1.00	0.310	61.92	1.00
0.414	81.79	0.99	0.462	92.15	1.00
0.551	108.5	0.99	0.593	118.0	1.00
0.680	133.1	0.99	0.729	141.8	0.98
0.881	167.5	0.96	0.880	165.2	0.95
1.01	186.1	0.93	1.01	188.7	0.95
1.23	212.5	0.96	1.34	226.0	1.00
1.51	241.5	1.02	1.65	257.2	1.05
1.82	268.7	1.05	1.95	282.1	1.07
2.17	297.9	1.08	2.28	306.5	1.08
2.42	319.6	1.10	2.59	327.5	1.09
2.72	339.8	1.10	2.95	350.8	1.09
			3.45	381.1	1.08

[a] κ calculated from regression analysis of the aqueous surfactant data

Table B-III(con't): Specific conductance data and specific conductance ratios for the 12-6-12 surfactant in aqueous polymer solutions

Conc. (mmol L^{-1})	κ ($\mu S\ cm^{-1}$)	κ'/κ^a	Conc. (mmol L^{-1})	κ ($\mu S\ cm^{-1}$)	κ'/κ^a
12-6-12/0.05% P103			12-6-12/0.5% P103		
0.000	1.18	1.00	0.000	1.18	1.00
0.128	27.31	1.04	0.135	28.51	1.03
0.270	55.30	1.02	0.264	53.34	1.01
0.405	82.25	1.02	0.408	79.97	0.99
0.552	109.6	1.00	0.514	98.90	0.97
0.690	133.1	0.98	0.649	122.1	0.95
0.808	153.0	0.96	0.769	141.4	0.93
0.939	173.3	0.94	0.883	159.0	0.91
1.08	193.2	0.91	1.03	179.2	0.88
1.36	226.3	0.99	1.27	210.5	0.94
1.72	258.1	1.03	1.55	243.2	1.02
2.06	281.1	1.04	1.86	273.1	1.06
2.39	301.7	1.04	2.21	301.0	1.08
2.75	323.4	1.04	2.52	322.3	1.08
3.16	347.6	1.04	2.83	341.6	1.08
3.57	371.6	1.03	3.21	363.3	1.07
12-6-12/0.1% P103			12-6-12/0.05% F108		
0.000	1.18	1.00	0.000	1.18	1.00
0.135	25.40	0.92	0.120	25.60	1.04
0.254	46.08	0.90	0.242	50.14	1.03
0.386	68.11	0.89	0.366	74.90	1.03
0.509	87.32	0.86	0.478	96.42	1.02
0.637	106.3	0.84	0.594	117.6	1.00
0.758	124.0	0.83	0.693	134.6	0.98
0.863	138.8	0.81	0.790	151.7	0.97
0.965	153.0	0.80	0.936	175.0	0.95
1.11	173.3	0.81	1.05	191.2	0.92
1.37	203.7	0.89	1.27	208.4	0.93
1.70	241.8	0.97	1.46	228.7	0.98
2.07	279.8	1.03	1.82	252.6	0.99
2.48	320.3	1.09	2.19	275.5	0.99
2.93	361.3	1.12	2.51	294.5	0.99
3.28	391.0	1.14	2.84	314.3	0.99
			3.21	336.3	0.99
			3.61	359.1	0.99

Table B-III(con't): Specific conductance data and specific conductance ratios for the 12-6-12 surfactant in aqueous polymer solutions

Conc. (mmol L^{-1})	κ ($\mu S\ cm^{-1}$)	κ'/κ^a	Conc. (mmol L^{-1})	κ ($\mu S\ cm^{-1}$)	κ'/κ^a
12-6-12/0.5% F108			12-6-12/1.0% F108		
0.000	1.18	1.00	0.000	1.18	1.00
0.134	28.52	1.04	0.105	19.82	0.91
0.272	53.45	0.98	0.233	42.35	0.90
0.421	77.91	0.93	0.366	63.86	0.88
0.549	99.13	0.91	0.503	84.39	0.85
0.678	118.1	0.88	0.638	103.4	0.82
0.825	136.7	0.84	0.774	121.1	0.79
0.947	153.5	0.82	0.971	144.9	0.76
1.07	168.5	0.80	1.11	162.8	0.76
1.39	202.5	0.88	1.41	194.0	0.84
1.69	230.1	0.93	1.71	222.0	0.89
1.97	252.5	0.95	2.03	250.5	0.93
2.23	271.2	0.97	2.34	274.5	0.96
2.53	290.8	0.98	2.62	295.3	0.97
2.81	307.2	0.98	2.90	314.1	0.98
3.10	323.3	0.97	3.15	330.4	0.99
3.41	337.9	0.96	3.39	345.2	0.99
3.60	350.1	0.97	3.61	358.4	0.99
12-6-12/0.05% F68			12-6-12/2.0% F68		
0.000	1.18	1.00	0.000	1.18	1.00
0.121	26.28	1.06	0.126	24.74	0.96
0.239	49.89	1.04	0.256	45.78	0.89
0.363	73.97	1.02	0.359	65.65	0.92
0.485	97.01	1.01	0.498	88.77	0.90
0.700	137.4	0.99	0.621	107.8	0.88
0.822	159.3	0.98	0.757	127.4	0.85
0.950	179.0	0.95	0.898	145.7	0.82
1.06	192.6	0.92	1.05	163.8	0.79
1.19	206.3	0.95	1.34	192.0	0.85
1.38	221.0	0.96	1.68	221.7	0.90
1.68	241.3	0.98	2.02	247.3	0.92
2.01	261.4	0.98	2.39	273.4	0.94
2.33	280.6	0.98	2.81	299.4	0.95
2.69	302.0	0.98	3.19	322.9	0.96
3.02	320.9	0.98	3.48	338.5	0.95
3.87	369.1	0.98	3.86	359.0	0.95

Table B-IV: Specific conductance data as a function of temperature for the 12-3-12 surfactant in aqueous polymer solutions

Temp. (°C)	κ (μS cm^{-1})	Temp. (°C)	κ (μS cm^{-1})	Temp. (°C)	κ (μS cm^{-1})	Temp. (°C)	κ (μS cm^{-1})
Aqueous 12-3-12		12-3-12/2.0% P103		12-3-12/2.0% F108		12-3-12/2.0% F68	
		4.977 mmol kg^{-1}		5.300 mmol kg^{-1}		5.112 mmol kg^{-1}	
		10.0	283.9	10.0	240.5	10.0	196.4
		15.0	367.5	15.0	296.2	15.0	238.6
		20.0	426.1	20.0	355.4	20.0	289.0
		25.0	425.5	25.0	408.0	25.0	345.9
		30.0	439.3	30.0	445.8	30.0	418.0
		35.0	467.6	35.0	476.6	35.0	488.8
		40.0	501.7	40.0	508.0	40.0	556.3
		45.0	554.8	45.0	545.9	45.0	629.9
		50.0	609.2	50.0	612.9	50.0	701.2
10.29 mmol kg^{-1}		9.955 mmol kg^{-1}		10.75 mmol kg^{-1}		10.02 mmol kg^{-1}	
10.0	343.0	10.0	448.6	10.0	363.6	10.0	318.5
15.0	398.8	15.0	560.0	15.0	440.9	15.0	389.0
20.0	466.5	20.0	645.8	20.0	515.7	20.0	470.6
25.0	539.4	22.0	652.6	25.0	578.7	25.0	562.1
30.0	628.7	25.0	659.6	30.0	631.7	30.0	660.7
35.0	724.4	27.0	666.3	35.0	691.6	35.0	785.4
40.0	837.3	30.0	682.3	40.0	748.7	40.0	892.0
45.0	939.6	35.0	722.5	45.0	827.8	45.0	1016.8
50.0	1061.7	40.0	772.0	50.0	930.9	50.0	1136.9
		45.0	833.3				
		50.0	932.6				
		19.91 mmol kg^{-1}		20.09 mmol kg^{-1}		20.24 mmol kg^{-1}	
		10.0	697.4	10.0	536.6	10.0	507.5
		15.0	853.3	15.0	628.1	15.0	621.2
		20.0	970.9	20.0	713.0	20.0	745.0
		22.0	996.2	25.0	795.7	25.0	877.1
		25.0	1030.5	30.0	878.1	30.0	1039.8
		27.0	1051.6	35.0	974.7	35.0	1190.5
		30.0	1088.5	40.0	1078.2	40.0	1369.5
		35.0	1168.6	45.0	1208.9	45.0	1522.8
		40.0	1264.3	50.0	1376.1	50.0	1731.4
		45.0	1372.0				
		50.0	1518.0				

Appendix C: Surface tension data

Table C-1: Surface tension data for the aqueous gemini surfactants

Concentration (mol L^{-1})	γ (mN m^{-1})	Concentration (mol L^{-1})	γ (mN m^{-1})	Concentration (mol L^{-1})	γ (mN m^{-1})
10-3-10		12-2-12		12-3-12	
1.27×10^{-3}	47.8	3.85×10^{-4}	37.8	1.07×10^{-4}	49.5
2.51×10^{-3}	42.6	5.52×10^{-4}	36.2	2.14×10^{-4}	48.6
3.72×10^{-3}	39.6	5.94×10^{-4}	34.9	3.20×10^{-4}	45.7
4.89×10^{-3}	36.2	7.00×10^{-4}	33.9	4.26×10^{-4}	42.8
6.04×10^{-3}	34.7	7.40×10^{-4}	33.1	5.32×10^{-4}	40.5
7.14×10^{-3}	34.8	8.02×10^{-4}	32.1	6.37×10^{-4}	38.4
8.24×10^{-3}	34.6	8.53×10^{-4}	31.0	7.41×10^{-4}	36.4
9.31×10^{-3}	34.6	8.93×10^{-4}	30.8	8.46×10^{-4}	35.1
1.04×10^{-2}	34.7	9.98×10^{-4}	30.9	9.50×10^{-4}	35.1
		1.96×10^{-3}	30.6	1.10×10^{-3}	35.0
				2.01×10^{-3}	35.0
				2.99×10^{-3}	34.7
				3.98×10^{-3}	34.6
				4.93×10^{-3}	34.4
12-4-12		12-6-12		12-8-12	
1.58×10^{-4}	56.4	1.76×10^{-4}	50.7	2.02×10^{-4}	49.2
3.27×10^{-4}	50.6	3.56×10^{-4}	47.6	3.02×10^{-4}	45.8
4.96×10^{-4}	46.4	5.41×10^{-4}	44.8	4.01×10^{-4}	44.0
6.59×10^{-4}	44.1	7.15×10^{-4}	42.2	5.01×10^{-4}	42.9
8.29×10^{-4}	41.1	8.94×10^{-4}	40.9	6.01×10^{-4}	41.7
9.92×10^{-4}	39.1	1.07×10^{-3}	40.6	6.95×10^{-4}	41.2
1.15×10^{-3}	38.2	1.24×10^{-3}	40.7	7.92×10^{-4}	41.0
1.32×10^{-3}	38.2	1.42×10^{-3}	40.6	8.86×10^{-4}	40.9
1.49×10^{-3}	38.3	1.59×10^{-3}	40.6	9.81×10^{-4}	40.9
1.82×10^{-3}	38.0	1.95×10^{-3}	40.6	1.17×10^{-3}	40.9
2.14×10^{-3}	37.8	2.30×10^{-3}	40.4	1.36×10^{-3}	41.0
2.77×10^{-3}	37.7	2.96×10^{-3}	40.2	1.55×10^{-3}	40.8

Table C-1(con't): Surface tension data for the aqueous gemini surfactants

Concentration (mol L^{-1})	γ (mN m^{-1})	Concentration (mol L^{-1})	γ (mN m^{-1})	Concentration (mol L^{-1})	γ (mN m^{-1})
12-10-12		12-12-12		12-16-12	
4.66×10^{-5}	53.1	2.38×10^{-5}	50.5	4.40×10^{-5}	50.6
9.55×10^{-5}	49.6	4.87×10^{-5}	48.1	6.56×10^{-5}	47.2
1.43×10^{-4}	47.5	7.28×10^{-5}	46.4	8.73×10^{-5}	44.7
1.92×10^{-4}	46.0	9.75×10^{-5}	44.5	1.09×10^{-4}	43.1
2.42×10^{-4}	45.1	1.22×10^{-4}	43.6	1.30×10^{-4}	42.6
2.90×10^{-4}	43.9	1.47×10^{-4}	42.4	1.72×10^{-4}	41.1
3.38×10^{-4}	43.0	1.72×10^{-4}	42.3	2.14×10^{-4}	40.4
3.87×10^{-4}	42.6	1.96×10^{-4}	41.9	2.55×10^{-4}	40.0
4.35×10^{-4}	42.2	2.20×10^{-4}	41.6	3.36×10^{-4}	39.2
5.40×10^{-4}	41.7	2.45×10^{-4}	41.2	4.15×10^{-4}	38.7
6.38×10^{-4}	41.7	2.69×10^{-4}	41.3	5.66×10^{-4}	37.8
7.35×10^{-4}	41.8	2.93×10^{-4}	41.1		
8.33×10^{-4}	41.3	3.93×10^{-4}	40.7		
9.29×10^{-4}	41.4	4.88×10^{-4}	40.7		
1.13×10^{-3}	41.1	6.82×10^{-4}	40.1		
		9.58×10^{-4}	39.8		
12-ϕ-12					
4.91×10^{-6}	47.2				
9.73×10^{-6}	41.2				
1.44×10^{-5}	40.1				
1.91×10^{-5}	40.0				
2.36×10^{-5}	40.0				
3.67×10^{-5}	40.0				
4.50×10^{-5}	40.0				
6.46×10^{-5}	39.8				

Table C-II: Surface tension data for the 12-6-12 gemini surfactant in aqueous polymer solutions

Concentration (mol L^{-1})	γ (mN m^{-1})	Concentration (mol L^{-1})	γ (mN m^{-1})	Concentration (mol L^{-1})	γ (mN m^{-1})
0.2% PEO		0.2% PPO (M.W. 725)		0.2% PPO (M.W. 2000)	
1.96×10^{-4}	52.6	1.98×10^{-4}	40.9	1.99×10^{-4}	35.8
3.87×10^{-4}	48.5	3.92×10^{-4}	38.4	3.93×10^{-4}	35.4
5.75×10^{-4}	45.2	5.82×10^{-4}	37.3	5.84×10^{-4}	34.9
7.58×10^{-4}	43.0	7.69×10^{-4}	36.5	7.71×10^{-4}	34.5
9.40×10^{-4}	41.1	9.51×10^{-4}	36.1	9.55×10^{-4}	34.4
1.12×10^{-3}	40.8	1.13×10^{-3}	35.9	1.14×10^{-3}	34.1
1.29×10^{-3}	40.7	1.48×10^{-3}	35.8	1.49×10^{-3}	33.8
1.80×10^{-3}	40.4	1.82×10^{-3}	35.8	1.82×10^{-3}	33.6
2.57×10^{-3}	40.1	2.61×10^{-3}	35.7	2.62×10^{-3}	33.6
3.29×10^{-3}	39.8	3.33×10^{-3}	35.6	3.34×10^{-3}	33.6
4.56×10^{-3}	39.5	4.61×10^{-3}	35.2	4.63×10^{-3}	33.2
5.64×10^{-3}	39.3	5.71×10^{-3}	35.0	5.73×10^{-3}	33.5
6.58×10^{-3}	38.8	6.66×10^{-3}	35.0	6.68×10^{-3}	33.4
7.41×10^{-3}	38.8	7.49×10^{-3}	34.8	7.52×10^{-3}	33.4
8.78×10^{-3}	38.7	8.88×10^{-3}	34.8	8.91×10^{-3}	33.0
9.88×10^{-3}	38.7	9.99×10^{-3}	34.6	1.00×10^{-2}	32.9
1.10×10^{-2}	38.5	1.11×10^{-2}	34.4	1.11×10^{-2}	32.9
1.23×10^{-2}	38.1	1.25×10^{-2}	34.3	1.25×10^{-2}	32.9
1.41×10^{-2}	38.0	1.43×10^{-2}	34.1	1.43×10^{-2}	32.8
1.65×10^{-2}	37.8	1.67×10^{-2}	34.0	1.67×10^{-2}	32.7
1.98×10^{-2}	37.5	2.00×10^{-2}	33.8	2.01×10^{-2}	32.5

Table C-II(con't): Surface tension data for the 12-6-12 gemini surfactant in aqueous polymer solutions

Concentration (mol L^{-1})	γ (mN m^{-1})	Concentration (mol L^{-1})	γ (mN m^{-1})	Concentration (mol L^{-1})	γ (mN m^{-1})
0.05% F108		0.5% F108		0.05% F68	
3.95×10^{-4}	43.4	1.33×10^{-4}	39.2	1.95×10^{-4}	45.9
5.23×10^{-4}	42.3	2.63×10^{-4}	38.9	3.87×10^{-4}	43.9
6.49×10^{-4}	41.4	3.92×10^{-4}	38.6	5.74×10^{-4}	42.5
7.74×10^{-4}	40.4	5.20×10^{-4}	38.3	7.59×10^{-4}	40.8
8.97×10^{-4}	40.2	6.45×10^{-4}	38.0	9.39×10^{-4}	39.9
1.02×10^{-3}	40.2	7.70×10^{-4}	37.8	1.12×10^{-3}	39.5
1.13×10^{-3}	40.0	8.92×10^{-4}	37.6	1.43×10^{-3}	39.3
1.26×10^{-3}	39.7	1.01×10^{-3}	37.4	1.79×10^{-3}	39.2
1.49×10^{-3}	39.3	1.13×10^{-3}	37.3	2.57×10^{-3}	39.0
1.72×10^{-3}	39.3	1.25×10^{-3}	37.1	3.29×10^{-3}	38.8
1.94×10^{-3}	39.3	1.48×10^{-3}	37.0	4.55×10^{-3}	38.4
2.37×10^{-3}	39.2	1.71×10^{-3}	36.9	5.63×10^{-3}	38.3
2.78×10^{-3}	39.1	1.93×10^{-3}	36.9	6.58×10^{-3}	38.0
3.16×10^{-3}	39.1	2.35×10^{-3}	36.9	7.39×10^{-3}	37.8
		2.76×10^{-3}	36.8	8.76×10^{-3}	37.6
		3.15×10^{-3}	36.8	9.86×10^{-3}	37.4
		3.52×10^{-3}	36.8	9.86×10^{-3}	37.5
				1.10×10^{-2}	37.4
				1.23×10^{-2}	37.1
				1.41×10^{-2}	37.0
				1.64×10^{-2}	36.7
				1.97×10^{-2}	36.4

Appendix D: Fluorescence data

Table D-1: Fitting parameters (according to Equation 3.2.3.1-1) for the experimental fluorescence decay curves, and mean aggregation numbers (according to Equation 3.2.3.1-2) for the aqueous gemini surfactants

[Surfactant] (mol L^{-1})	[Quencher] (mol L^{-1})	k_0 (sec^{-1})	$\bar{n}$	k_q (sec^{-1})	N_{agg}
		12-2-12			
4.71×10^{-3}	0.00	8.39×10^{6}	-	-	-
	1.82×10^{-4}	7.93×10^{6}	1.11	1.4×10^{7}	23
	3.63×10^{-4}	7.35×10^{6}	2.52	1.4×10^{7}	27
	5.45×10^{-4}	7.46×10^{6}	3.27	1.5×10^{7}	23
		12-3-12			
1.06×10^{-2}	0.00	8.86×10^{6}	-	-	-
	3.33×10^{-4}	8.26×10^{6}	0.882	1.2×10^{7}	26
	6.65×10^{-4}	8.20×10^{6}	1.437	1.3×10^{7}	21
	9.98×10^{-4}	7.69×10^{6}	2.343	1.2×10^{7}	23
		12-4-12			
1.04×10^{-2}	0.00	8.49×10^{6}	-	-	-
	2.18×10^{-4}	8.32×10^{6}	0.74	2.3×10^{7}	31
	4.35×10^{-4}	8.16×10^{6}	1.42	2.3×10^{7}	30
	6.53×10^{-4}	8.20×10^{6}	1.95	2.5×10^{7}	28
		12-6-12			
1.06×10^{-2}	0.00	7.76×10^{6}	-	-	-
	3.30×10^{-4}	7.46×10^{6}	0.60	4.1×10^{7}	17
	6.59×10^{-4}	7.39×10^{6}	1.11	4.2×10^{7}	16
	9.89×10^{-4}	7.40×10^{6}	1.56	4.4×10^{7}	15
		12-8-12			
1.05×10^{-2}	0.00	7.47×10^{6}	-	-	-
	3.73×10^{-4}	7.63×10^{6}	0.46	3.2×10^{7}	12
	7.47×10^{-4}	7.67×10^{6}	0.85	3.4×10^{7}	11
	1.12×10^{-4}	7.71×10^{6}	1.32	3.6×10^{7}	11
		12-10-12			
1.03×10^{-2}	0.00	7.37×10^{6}	-	-	-
	3.57×10^{-4}	7.30×10^{6}	0.51	4.7×10^{7}	14
	7.13×10^{-4}	7.30×10^{6}	0.92	5.1×10^{7}	12
	1.07×10^{-3}	7.24×10^{6}	1.40	5.1×10^{7}	13

Table D-1(con't): Fitting parameters (according to Equation 3.2.1-1) for the experimental fluorescence decay curves, and mean aggregation numbers (according to Equation 3.2.3.1-2) for the aqueous gemini surfactants

[Surfactant] (mol L^{-1})	[Quencher] (mol L^{-1})	k_0 (sec^{-1})	$\bar{n}$	k_q (sec^{-1})	N_{agg}
		12-12-12			
1.01×10^{-2}	0.00	7.33×10^{6}	-	-	-
	2.32×10^{-4}	7.25×10^{6}	0.57	5.0×10^{7}	24
	4.64×10^{-4}	7.22×10^{6}	1.06	5.5×10^{7}	22
	6.96×10^{-4}	7.19×10^{6}	1.37	5.0×10^{7}	19
		12-16-12[a]			
1.21×10^{-3}	0.00	7.11×10^{6}	-	-	-
	8.47×10^{-6}	7.15×10^{6}	0.42	8.3×10^{7}	55
	1.23×10^{-5}	7.31×10^{6}	0.59	7.9×10^{7}	53
	1.70×10^{-5}	7.60×10^{6}	0.68	5.9×10^{7}	44

[a] using CPyCl as quencher

Table D-II: Fitting parameters (according to Equation 3.2.3.1-1) for the experimental fluorescence decay curves, and mean aggregation numbers (according to Equation 3.2.3.1-2) for the 12-6-12 gemini surfactant in aqueous polymer solution.

[Surfactant] (mol L^{-1})	[Quencher] (mol L^{-1})	k_0 ($\times 10^6$ sec^{-1})	$\bar{n}$	k_q ($\times 10^7$ sec^{-1})	N_{agg}
		Aqueous 12-6-12			
1.081×10^{-3}	0.00	8.87			
	1.69×10^{-6}	7.69	0.327	1.1	6
	3.37×10^{-6}	7.81	0.389	1.6	4
	5.06×10^{-6}	7.82	0.494	2.1	3
3.056×10^{-3}	0.00	8.48			
	4.33×10^{-5}	8.00	0.341	2.9	16
	8.63×10^{-5}	8.00	0.599	3.3	14
	1.30×10^{-4}	8.04	1.094	4.0	17
5.014×10^{-3}	0.00	8.83			
	7.02×10^{-5}	8.16	0.453	4.3	26
	1.40×10^{-4}	8.17	0.840	4.5	24
	2.10×10^{-4}	8.26	1.596	5.0	30
6.787×10^{-3}	0.00	8.75			
	1.02×10^{-4}	8.17	0.555	4.2	31
	2.02×10^{-4}	8.23	0.853	4.2	24
	3.04×10^{-4}	8.37	1.525	4.8	29
9.463×10^{-3}	0.00	8.75			
	1.49×10^{-4}	8.33	0.522	4.7	30
	2.97×10^{-4}	8.32	0.970	4.1	28
	4.45×10^{-4}	8.27	1.568	4.2	30
1.099×10^{-2}	0.00	9.00			
	1.75×10^{-4}	8.22	0.660	3.9	38
	3.49×10^{-4}	8.42	1.104	4.6	31
	5.23×10^{-4}	8.42	1.691	4.5	32

Table D-II(con't): Fitting parameters (according to Equation 3.2.1-1) for the experimental fluorescence decay curves, and mean aggregation numbers (according to Equation 3.2.3.1-2) for the gemini surfactants in aqueous polymer solution.

[Surfactant] (mol L^{-1})	[Quencher] (mol L^{-1})	k_0 ($\times 10^6$ sec^{-1})	$\bar{n}$	k_q ($\times 10^7$ sec^{-1})	N_{agg}
		12-6-12/0.2% PEO			
2.106×10^{-3}	0.00	7.89			
	2.95×10^{-5}	7.94	0.444	5.9	16
	5.87×10^{-5}	7.86	1.085	7.3	20
	8.82×10^{-5}	7.88	1.780	6.6	22
5.590×10^{-3}	0.00	8.02			
	1.08×10^{-4}	7.98	1.075	8.1	45
	2.16×10^{-4}	8.10	1.585	8.0	34
	3.24×10^{-4}	8.05	2.194	6.1	31
7.461×10^{-3}	0.00	8.12			
	1.50×10^{-4}	8.10	1.112	9.0	48
	3.00×10^{-4}	8.09	1.608	7.4	35
	4.50×10^{-4}	8.09	2.089	5.6	30
1.003×10^{-2}	0.00	8.14			
	2.08×10^{-4}	8.14	1.032	8.0	45
	4.15×10^{-4}	8.13	1.603	7.0	35
	6.24×10^{-4}	8.08	2.273	5.5	33
1.539×10^{-2}	0.00	8.15			
	3.29×10^{-4}	8.20	1.065	7.9	46
	6.57×10^{-4}	8.22	1.767	6.0	39
	9.86×10^{-4}			8.4	
		12-6-12/0.2% PPO (M.W. 725)			
2.051×10^{-3}	0.00	7.42			
	2.83×10^{-5}	7.30	0.326	2.9	11
	5.64×10^{-5}	7.33	0.742	5.0	13
	8.46×10^{-5}	7.36	1.175	5.1	14
5.278×10^{-3}	0.00	7.83			
	1.01×10^{-4}	7.78	0.348	4.1	14
	2.02×10^{-4}	7.74	0.804	4.9	17
	3.03×10^{-4}	7.77	1.240	5.1	17

Table D-II(con't): Fitting parameters (according to Equation 3.2.1-1) for the experimental fluorescence decay curves, and mean aggregation numbers (according to Equation 3.2.3.1-2) for the gemini surfactants in aqueous polymer solution.

[Surfactant] (mol L^{-1})	[Quencher] (mol L^{-1})	k_0 ($\times 10^6$ sec^{-1})	$\bar{n}$	k_q ($\times 10^7$ sec^{-1})	N_{agg}
		12-6-12/0.2% PPO (M.W. 725)			
7.414×10^{-3}	0.00	7.90			
	1.49×10^{-4}	7.80	0.487	4.1	21
	2.98×10^{-4}	7.79	1.005	5.2	21
	4.47×10^{-4}	7.98	1.569	5.4	22
1.063×10^{-2}	0.00	8.04			
	2.22×10^{-4}	7.95	0.668	4.8	29
	4.42×10^{-4}	7.93	1.272	5.3	27
	6.64×10^{-4}	7.90	1.874	4.8	27
1.503×10^{-2}	0.00	8.10			
	3.21×10^{-4}	8.07	0.643	5.0	28
	6.41×10^{-4}	8.12	1.219	5.8	27
	9.62×10^{-4}	8.15	1.907	5.2	28
		12-6-12/0.05% PPO (M.W. 2000)			
1.958×10^{-3}	0.00	7.11			
	2.16×10^{-5}	7.03	0.230	2.9	11
	4.30×10^{-5}	6.97	0.497	4.6	12
	6.46×10^{-5}	7.04	0.670	4.5	11
4.952×10^{-3}	0.00	7.80			
	8.92×10^{-5}	7.74	0.462	4.2	21
	1.78×10^{-4}	7.72	0.754	4.8	17
	2.67×10^{-4}	7.80	1.078	4.7	16
6.928×10^{-3}	0.00	7.99			
	1.34×10^{-4}	7.89	0.553	4.7	25
	2.67×10^{-4}	7.81	0.907	4.3	20
	4.0×10^{-4}	7.91	1.358	4.6	20
1.05×10^{-2}	0.00	8.18			
	2.16×10^{-4}	8.14	0.605	4.7	27
	4.30×10^{-4}	7.99	1.046	4.5	23
	6.46×10^{-4}	8.08	1.727	4.5	26

Table D-II(con't): Fitting parameters (according to Equation 3.2.1-1) for the experimental fluorescence decay curves, and mean aggregation numbers (according to Equation 3.2.3.1-2) for the gemini surfactants in aqueous polymer solution.

[Surfactant] (mol L^{-1})	[Quencher] (mol L^{-1})	k_0 ($\times 10^6$ sec^{-1})	$\bar{n}$	k_q ($\times 10^7$ sec^{-1})	N_{agg}
		12-6-12/0.2% PPO (M.W. 2000)			
1.504×10^{-2}	0.00	8.21			
	3.17×10^{-4}	8.26	0.615	4.6	27
	6.32×10^{-4}	8.18	1.134	4.7	25
	9.50×10^{-4}	8.25	1.995	4.3	30
		12-6-12/0.05% P103			
1.941×10^{-3}	0.00	6.91			
	2.57×10^{-5}	6.84	0.217	3.7	6
	5.13×10^{-5}	6.85	0.480	5.1	7
	7.70×10^{-5}	6.74	0.785	4.7	7
5.127×10^{-3}	0.00	7.78			
	9.77×10^{-5}	7.76	0.488	4.2	20
	1.95×10^{-4}	7.73	1.081	5.2	22
	2.92×10^{-4}	7.74	1.476	5.0	20
7.076×10^{-3}	0.00	7.99			
	1.42×10^{-4}	7.88	0.597	4.3	25
	2.83×10^{-4}	7.94	1.161	5.0	24
	4.24×10^{-4}	7.91	1.529	4.6	21
1.071×10^{-2}	0.00	8.14			
	2.24×10^{-4}	8.09	0.664	4.7	28
	4.46×10^{-4}	8.19	1.337	5.3	28
	6.70×10^{-4}	8.10	1.972	5.0	28
1.498×10^{-2}	0.00	8.21			
	3.20×10^{-4}	8.34	0.674	5.0	29
	6.38×10^{-4}	8.45	1.623	5.2	35
	9.58×10^{-4}	8.20	2.043	4.6	29
		12-6-12/0.05% F108			
2.019×10^{-2}	0.00	7.48			
	2.75×10^{-5}	7.29	0.376	2.9	14
	5.48×10^{-5}	7.26	0.707	3.9	13
	8.23×10^{-5}	7.38	1.112	4.9	13

Table D-II(con't): Fitting parameters (according to Equation 3.2.1-1) for the experimental fluorescence decay curves, and mean aggregation numbers (according to Equation 3.2.3.1-2) for the gemini surfactants in aqueous polymer solution.

[Surfactant] (mol L^{-1})	[Quencher] (mol L^{-1})	k_0 ($\times 10^6$ sec^{-1})	$\bar{n}$	k_q ($\times 10^7$ sec^{-1})	N_{agg}
		12-6-12/0.05% F108			
5.212×10^{-3}	0.00	7.89			
	9.96×10^{-5}	7.87	0.528	4.7	22
	1.97×10^{-4}	7.85	1.032	5.0	22
	2.98×10^{-4}	7.94	1.563	4.8	22
7.399×10^{-3}	0.00	7.97			
	1.49×10^{-4}	7.98	0.660	5.1	28
	2.97×10^{-4}	7.91	1.194	4.9	26
	4.46×10^{-4}	8.02	1.823	5.0	26
1.071×10^{-2}	0.00	8.09			
	2.24×10^{-4}	8.04	0.720	4.6	31
	4.46×10^{-4}	8.02	1.196	4.5	26
	6.70×10^{-4}	8.24	2.052	4.9	30
1.507×10^{-2}	0.00	8.12			
	3.17×10^{-4}	8.07	0.923	5.2	41
	6.32×10^{-4}	8.15	1.649	4.8	37
	9.50×10^{-4}	8.19	2.423	4.4	36
		12-6-12/0.05% F68			
1.986×10^{-3}	0.00	7.55			
	2.68×10^{-5}	7.39	0.390	2.8	12
	5.34×10^{-5}	7.40	0.809	4.3	13
	8.02×10^{-5}	7.38	1.234	4.4	13
5.027×10^{-3}	0.00	7.85			
	9.54×10^{-5}	7.80	0.578	4.2	23
	1.90×10^{-4}	7.75	1.086	4.7	22
	2.86×10^{-4}	7.90	1.708	4.8	23
6.790×10^{-3}	0.00	8.02			
	1.35×10^{-4}	8.01	0.624	5.0	26
	2.69×10^{-4}	7.88	1.402	4.9	29
	4.03×10^{-4}	8.05	1.723	4.9	24

Table D-II(con't): Fitting parameters (according to Equation 3.2.1-1) for the experimental fluorescence decay curves, and mean aggregation numbers (according to Equation 3.2.3.1-2) for the gemini surfactants in aqueous polymer solution.

[Surfactant] (mol L^{-1})	[Quencher] (mol L^{-1})	k_0 ($\times 10^6$ sec^{-1})	$\bar{n}$	k_q ($\times 10^7$ sec^{-1})	N_{agg}
		12-6-12/0.05% F68			
1.114×10^{-2}	0.00	8.12			
	2.33×10^{-4}	8.04	0.766	4.8	33
	4.65×10^{-4}	7.98	1.721	4.6	37
	6.99×10^{-4}	7.99	2.039	4.6	29
1.506×10^{-2}	0.00	8.21			
	3.22×10^{-4}	8.10	0.734	4.3	32
	6.42×10^{-4}	8.10	1.506	5.1	33
	9.64×10^{-4}	8.25	2.530	4.4	36

Table D-III: Vibronic intensity ratios of pyrene for the 12-3-12 and 12-6-12 gemini surfactants in aqueous polymer solutions

Conc. (mol L^{-1})	I_1/I_3	Conc. (mol L^{-1})	I_1/I_3	Conc. (mol L^{-1})	I_1/I_3	Conc. (mol L^{-1})	I_1/I_3
				12-3-12			
Aqueous		0.2% PEO		0.2% PPO 725		0.05% PPO 2000	
0	1.73	0	1.63	0	1.68	0	1.25
0.000156	1.69	0.000143	1.64	0.000143	1.70	0.000143	1.27
0.000309	1.70	0.000283	1.58	0.000283	1.69	0.000283	1.28
0.000459	1.69	0.000420	1.60	0.000420	1.68	0.000421	1.27
0.000679	1.61	0.000621	1.56	0.000621	1.52	0.000622	1.31
0.000893	1.44	0.000817	1.46	0.000816	1.40	0.000817	1.33
0.00110	1.43	0.00101	1.38	0.00101	1.38	0.00101	1.33
0.00143	1.43	0.00131	1.37	0.00131	1.39	0.00131	1.34
0.00206	1.42	0.00188	1.36	0.00188	1.39	0.00188	1.35
0.00263	1.41	0.00241	1.36	0.00240	1.39	0.00241	1.36
0.00315	1.42	0.00289	1.36	0.00288	1.39	0.00289	1.36
0.00409	1.41	0.00374	1.36	0.00374	1.39	0.00374	1.36

Table D-III(con't): Vibronic intensity ratios of pyrene for the 12-3-12 and 12-6-12 gemini surfactants in aqueous polymer solutions

Conc. (mol L^{-1})	I_1/I_3	Conc. (mol L^{-1})	I_1/I_3	Conc. (mol L^{-1})	I_1/I_3	Conc. (mol L^{-1})	I_1/I_3
			12-3-12				
0.05% P103		0.1% P103		0.5% P103		0.05% F108	
0	1.28	0	1.26	0	1.27	0	1.61
0.000162	1.29	0.000154	1.26	0.000143	1.27	0.000137	1.54
0.000322	1.31	0.000305	1.25	0.000283	1.26	0.000271	1.45
0.000478	1.31	0.000453	1.26	0.000421	1.26	0.000403	1.36
0.000631	1.32	0.000670	1.27	0.000623	1.26	0.000596	1.31
0.000929	1.32	0.000881	1.29	0.000818	1.26	0.000783	1.32
0.00114	1.33	0.00109	1.30	0.00101	1.26	0.000966	1.32
0.00149	1.35	0.00141	1.31	0.00131	1.25	0.00126	1.32
0.00214	1.36	0.00203	1.32	0.00189	1.26	0.00181	1.32
0.00274	1.36	0.00259	1.33	0.00241	1.26	0.00231	1.32
0.00328	1.36	0.00311	1.34	0.00289	1.27	0.00278	1.33
0.00425	1.37	0.00403	1.35	0.00375	1.28	0.00319	1.33
		0.00519	1.35	0.00482	1.28	0.00359	1.34
						0.00395	1.32
						0.00461	1.33
0.5% F108		1.0% F108		0.05% F68		2.0% F68	
0	1.55	0	1.56	0	1.63	0	1.67
0.000151	1.36	0.000136	1.35	0.000156	1.631	0.000133	1.65
0.000298	1.32	0.000269	1.30	0.000309	1.61	0.000263	1.61
0.000443	1.30	0.000401	1.29	0.000458	1.56	0.000391	1.56
0.000655	1.27	0.000592	1.27	0.000678	1.46	0.000578	1.47
0.000862	1.26	0.000779	1.26	0.000891	1.37	0.00076	1.42
0.00106	1.25	0.00096	1.25	0.001100	1.37	0.00105	1.38
0.00138	1.27	0.00125	1.25	0.00143	1.36	0.00122	1.37
0.00199	1.28	0.00179	1.25	0.00205	1.34	0.00175	1.36
0.00254	1.28	0.00229	1.26	0.00262	1.37	0.00224	1.36
0.00304	1.29	0.00318	1.26	0.00315	1.37	0.00268	1.36
0.00351	1.28	0.00393	1.27			0.00348	1.35
0.00395	1.29	0.00459	1.27				
0.00472	1.30						

Table D-III(con't): Vibronic intensity ratios of pyrene for the 12-3-12 and 12-6-12 gemini surfactants in aqueous polymer solutions

Conc. (mol L^{-1})	I_1/I_3	Conc. (mol L^{-1})	I_1/I_3	Conc. (mol L^{-1})	I_1/I_3	Conc. (mol L^{-1})	I_1/I_3
			12-6-12				
Aqueous		0.2% PEO		0.2% PPO 725		0.05% PPO 2000	
0	1.74	0	1.64	0	1.75	0	1.25
0.000143	1.72	0.000272	1.59	0.000143	1.71	0.000165	1.27
0.000283	1.72	0.000404	1.60	0.000283	1.69	0.000327	1.27
0.000421	1.70	0.000597	1.56	0.000421	1.69	0.000486	1.27
0.000622	1.67	0.000785	1.48	0.000622	1.64	0.000719	1.28
0.000817	1.61	0.000967	1.38	0.000817	1.53	0.000945	1.33
0.00101	1.46	0.00126	1.37	0.00101	1.42	0.00114	1.35
0.00131	1.43	0.00181	1.36	0.00131	1.41	0.00152	1.37
0.00188	1.42	0.00231	1.36	0.00188	1.40	0.00218	1.37
0.00241	1.42	0.00277	1.38	0.00241	1.40	0.00278	1.37
0.00289	1.41	0.00359	1.37	0.00289	1.40	0.00334	1.38
0.00374	1.41			0.00374	1.39	0.00385	1.38
0.05% P103		0.1% P103		0.5% P103		0.05% F108	
0	1.31	0	1.27	0	1.28	0	1.55
0.000144	1.32	0.000156	1.26	0.00018	1.28	0.000148	1.5
0.000285	1.33	0.000310	1.27	0.000356	1.27	0.000292	1.42
0.000423	1.33	0.000460	1.27	0.000528	1.27	0.000434	1.39
0.000626	1.33	0.000680	1.29	0.000781	1.28	0.000642	1.34
0.000823	1.33	0.000894	1.31	0.00103	1.27	0.000844	1.32
0.00101	1.34	0.00110	1.32	0.00127	1.27	0.00104	1.33
0.00132	1.35	0.00144	1.33	0.00165	1.28	0.00136	1.34
0.00190	1.36	0.00206	1.35	0.00237	1.30	0.00194	1.35
0.00242	1.37	0.00263	1.36	0.00302	1.30	0.00249	1.35
0.00291	1.38	0.00316	1.36	0.00363	1.31	0.00298	1.34
0.00327	1.38	0.00410	1.36	0.00419	1.32	0.00387	1.36
0.00485	1.38			0.00470	1.32		

Table D-III(con't): Vibronic intensity ratios of pyrene for the 12-3-12 and 12-6-12 gemini surfactants in aqueous polymer solutions

Conc. (mol L^{-1})	I_1/I_3	Conc. (mol L^{-1})	I_1/I_3	Conc. (mol L^{-1})	I_1/I_3	Conc. (mol L^{-1})	I_1/I_3
0.5% F108		1.0% F108		0.05% F68		2.0% F68	
0	1.54	0	1.51	0	1.68	0	1.68
0.000152	1.39	0.000148	1.36	0.000144	1.66	0.00017	1.66
0.000301	1.32	0.000292	1.31	0.000285	1.65	0.000337	1.62
0.000447	1.29	0.000433	1.29	0.000422	1.63	0.000501	1.57
0.000661	1.29	0.000571	1.28	0.000557	1.62	0.000740	1.48
0.000869	1.27	0.000837	1.28	0.000816	1.48	0.000973	1.43
0.00107	1.28	0.00109	1.28	0.00106	1.4	0.00120	1.40
0.00140	1.28	0.00156	1.28	0.00153	1.39	0.00156	1.39
0.00200	1.29	0.00200	1.29	0.00195	1.39	0.00224	1.38
0.00256	1.30	0.00277	1.29	0.0027	1.39	0.00287	1.37
0.00307	1.31	0.00343	1.30	0.00334	1.39	0.00344	1.38
0.00354	1.30	0.00400	1.30				
0.00398	1.31	0.00450	1.31				
0.00477	1.32						

Appendix E: ^{1}H NMR chemical shift data

Table E-I: ^{1}H NMR chemical shift data (of the N-methyl surfactant protons) for the 12-3-12 gemini surfactant in aqueous polymer solutions

Conc. (mol L^{-1})	δ (ppm)	Conc. (mol L^{-1})	δ (ppm)	Conc. (mol L^{-1})	δ (ppm)	Conc. (mol L^{-1})	δ (ppm)
Aqueous		0.2% PEO		0.2% PPO 725		0.05% PPO 2000	
9.14×10^{-5}	2.985	1.93×10^{-4}	2.992	1.99×10^{-4}	2.994	1.02×10^{-4}	2.996
1.82×10^{-4}	2.988	3.85×10^{-4}	2.995	3.98×10^{-4}	2.994	2.03×10^{-4}	2.988
2.73×10^{-4}	2.992	5.76×10^{-4}	3.000	5.96×10^{-4}	3.012	3.04×10^{-4}	2.988
3.63×10^{-4}	2.990	9.56×10^{-4}	3.061	7.93×10^{-4}	3.045	3.54×10^{-4}	3.000
4.53×10^{-4}	2.990	1.52×10^{-3}	3.082	9.89×10^{-4}	3.063	4.04×10^{-4}	2.996
5.43×10^{-4}	2.996	2.07×10^{-3}	3.097	1.18×10^{-3}	3.084	4.54×10^{-4}	3.003
6.32×10^{-4}	2.995	2.63×10^{-3}	3.107	1.57×10^{-3}	3.094	5.04×10^{-4}	3.007
7.21×10^{-4}	3.007	2.99×10^{-3}	3.110	1.96×10^{-3}	3.099	6.04×10^{-4}	3.012
8.09×10^{-4}	3.018	4.07×10^{-3}	3.123	2.53×10^{-3}	3.103	7.03×10^{-4}	3.017
8.98×10^{-4}	3.032	5.12×10^{-3}	3.126	3.10×10^{-3}	3.106	8.02×10^{-4}	3.024
1.07×10^{-3}	3.048	7.48×10^{-3}	3.127	3.66×10^{-3}	3.113	9.00×10^{-4}	3.030
1.51×10^{-3}	3.071	1.00×10^{-2}	3.138	4.03×10^{-3}	3.114	9.98×10^{-4}	3.035
2.01×10^{-3}	3.090	1.58×10^{-2}	3.150	4.58×10^{-3}	3.117	1.96×10^{-3}	3.068
2.99×10^{-3}	3.108	2.09×10^{-2}	3.158	5.11×10^{-3}	3.117	2.97×10^{-3}	3.087
4.01×10^{-3}	3.117			6.01×10^{-3}	3.115	4.03×10^{-3}	3.100
5.05×10^{-3}	3.124			7.06×10^{-3}	3.123	5.04×10^{-3}	3.108
1.00×10^{-2}	3.131			8.08×10^{-3}	3.123	7.02×10^{-3}	3.118
1.53×10^{-2}	3.142			9.08×10^{-3}	3.128	9.85×10^{-3}	3.125
2.01×10^{-2}	3.148			1.01×10^{-2}	3.129	1.56×10^{-2}	3.131
				1.52×10^{-2}	3.142	2.06×10^{-2}	3.137
				2.06×10^{-2}	3.146		

Table E-I(con't): ^{1}H NMR chemical shift data (of the N-methyl surfactant protons) for the 12-3-12 gemini surfactant in aqueous polymer solutions

Conc. (mol L^{-1})	δ (ppm)	Conc. (mol L^{-1})	δ (ppm)	Conc. (mol L^{-1})	δ (ppm)	Conc. (mol L^{-1})	δ (ppm)
0.2% PPO 2000		0.05% P103		0.05% F108		0.05% F68	
1.07×10^{-4}	2.997	1.81×10^{-4}	3.001	2.48×10^{-4}	2.998	2.18×10^{-4}	2.996
2.13×10^{-4}	3.000	2.70×10^{-4}	3.005	4.12×10^{-4}	3.003	3.26×10^{-4}	2.995
3.19×10^{-4}	3.005	3.60×10^{-4}	3.014	5.75×10^{-4}	3.010	4.34×10^{-4}	2.994
4.24×10^{-4}	3.010	4.49×10^{-4}	3.017	7.36×10^{-4}	3.018	5.41×10^{-4}	2.998
5.29×10^{-4}	3.017	6.26×10^{-4}	3.025	9.76×10^{-4}	3.032	6.48×10^{-4}	3.004
6.34×10^{-4}	3.023	7.14×10^{-4}	3.037	1.21×10^{-3}	3.046	7.55×10^{-4}	3.010
7.38×10^{-4}	3.033	8.02×10^{-4}	3.039	1.52×10^{-3}	3.062	8.61×10^{-4}	3.014
8.42×10^{-4}	3.037	8.89×10^{-4}	3.038	1.52×10^{-3}	3.060	9.67×10^{-4}	3.029
9.45×10^{-4}	3.044	9.76×10^{-4}	3.046	1.75×10^{-3}	3.071	1.49×10^{-3}	3.054
1.05×10^{-3}	3.044	1.06×10^{-3}	3.051	2.06×10^{-3}	3.080	2.00×10^{-3}	3.074
3.02×10^{-3}	3.084	1.23×10^{-3}	3.060	2.97×10^{-3}	3.097	3.00×10^{-3}	3.088
5.03×10^{-3}	3.100	1.49×10^{-3}	3.060	4.02×10^{-3}	3.115	4.05×10^{-3}	3.103
7.05×10^{-3}	3.109	1.74×10^{-3}	3.081	5.03×10^{-3}	3.121	5.06×10^{-3}	3.107
9.05×10^{-3}	3.116	1.99×10^{-3}	3.082	6.02×10^{-3}	3.123	7.54×10^{-3}	3.119
1.53×10^{-2}	3.130	2.49×10^{-3}	3.089	7.12×10^{-3}	3.124		
2.00×10^{-2}	3.135	2.97×10^{-3}	3.089	8.06×10^{-3}	3.129		
2.47×10^{-2}	3.144	3.51×10^{-3}	3.103				
		4.04×10^{-3}	3.112				
		4.57×10^{-3}	3.118				
		5.0×10^{-3}	3.112				
		5.50×10^{-3}	3.123				
		5.98×10^{-3}	3.118				
		6.52×10^{-3}	3.126				
		7.04×10^{-3}	3.120				
		7.56×10^{-3}	3.125				
		8.91×10^{-3}	3.134				
		1.02×10^{-2}	3.128				
		1.15×10^{-2}	3.128				
		1.28×10^{-2}	3.134				
		1.40×10^{-2}	3.130				
		1.51×10^{-2}	3.134				

Table E-II: ^{1}H NMR chemical shift data (of the N-methyl surfactant protons) for the 12-6-12 gemini surfactant in aqueous polymer solutions

Conc. (mol L^{-1})	δ (ppm)	Conc. (mol L^{-1})	δ (ppm)	Conc. (mol L^{-1})	δ (ppm)	Conc. (mol L^{-1})	δ (ppm)
Aqueous		0.2% PEO		0.2% PPO 725		0.05% PPO 2000	
1.84×10^{-4}	2.911	1.94×10^{-4}	2.907	2.03×10^{-4}	2.908	1.81×10^{-4}	2.904
2.76×10^{-4}	2.918	2.90×10^{-4}	2.915	3.05×10^{-4}	2.912	2.71×10^{-4}	2.907
3.67×10^{-4}	2.918	3.86×10^{-4}	2.912	4.05×10^{-4}	2.911	3.60×10^{-4}	2.912
4.58×10^{-4}	2.925	4.81×10^{-4}	2.911	5.06×10^{-4}	2.912	4.49×10^{-4}	2.911
5.48×10^{-4}	2.920	5.76×10^{-4}	2.910	6.05×10^{-4}	2.911	5.38×10^{-4}	2.910
7.23×10^{-4}	2.920	6.71×10^{-4}	2.914	7.05×10^{-4}	2.911	6.23×10^{-4}	2.916
8.17×10^{-4}	2.929	7.65×10^{-4}	2.915	8.04×10^{-4}	2.912	7.15×10^{-4}	2.926
9.06×10^{-4}	2.940	8.59×10^{-4}	2.918	1.00×10^{-3}	2.918	8.02×10^{-4}	2.930
1.08×10^{-3}	2.950	9.53×10^{-4}	2.926	1.49×10^{-3}	2.945	9.76×10^{-4}	2.941
1.51×10^{-3}	2.965	1.05×10^{-3}	2.935	2.06×10^{-3}	2.965	1.06×10^{-3}	2.942
2.03×10^{-3}	2.984	1.51×10^{-3}	2.961	3.07×10^{-3}	2.984	1.49×10^{-3}	2.960
3.02×10^{-3}	2.992	2.05×10^{-3}	2.978	4.04×10^{-3}	2.994	1.99×10^{-3}	2.974
4.05×10^{-3}	3.002	3.01×10^{-3}	2.994	5.06×10^{-3}	2.997	3.05×10^{-3}	2.986
5.03×10^{-3}	3.009	4.01×10^{-3}	3.004	7.04×10^{-3}	3.011	4.05×10^{-3}	3.000
		5.05×10^{-3}	3.009	9.00×10^{-3}	3.014	5.00×10^{-3}	3.005
				1.10×10^{-2}	3.017	7.05×10^{-3}	3.011
						9.07×10^{-3}	3.017
						1.10×10^{-2}	3.019
0.2% PPO 2000		0.05% P103		0.05% F108		0.05% F68	
1.81×10^{-4}	2.904	1.97×10^{-4}	2.914	2.01×10^{-4}	2.914	2.07×10^{-4}	2.915
2.71×10^{-4}	2.907	2.95×10^{-4}	2.917	3.00×10^{-4}	2.917	3.09×10^{-4}	2.914
3.60×10^{-4}	2.912	3.92×10^{-4}	2.918	4.00×10^{-4}	2.917	4.12×10^{-4}	2.916
4.49×10^{-4}	2.911	4.89×10^{-4}	2.921	4.98×10^{-4}	2.918	5.14×10^{-4}	2.919
5.38×10^{-4}	2.910	5.86×10^{-4}	2.922	6.95×10^{-4}	2.923	6.15×10^{-4}	2.918
6.23×10^{-4}	2.916	6.82×10^{-4}	2.925	7.93×10^{-4}	2.925	7.16×10^{-4}	2.922
7.15×10^{-4}	2.926	7.78×10^{-4}	2.927	8.90×10^{-4}	2.926	8.17×10^{-4}	2.926
8.02×10^{-4}	2.930	9.68×10^{-4}	2.932	9.87×10^{-4}	2.933	9.17×10^{-4}	2.931
9.76×10^{-4}	2.941	1.53×10^{-3}	2.945	1.56×10^{-3}	2.961	1.02×10^{-3}	2.939
1.06×10^{-3}	2.942	2.08×10^{-3}	2.962	2.03×10^{-3}	2.979	1.51×10^{-3}	2.969
1.49×10^{-3}	2.960	3.06×10^{-3}	2.983	3.03×10^{-3}	2.997	2.00×10^{-3}	2.984
1.99×10^{-3}	2.974	4.08×10^{-3}	2.995	4.07×10^{-3}	3.007	3.03×10^{-3}	2.998
3.05×10^{-3}	2.986	5.05×10^{-3}	3.002	5.07×10^{-3}	3.013	4.02×10^{-3}	3.008
4.05×10^{-3}	3.000	7.03×10^{-3}	3.009	7.02×10^{-3}	3.019	5.06×10^{-3}	3.013
5.00×10^{-3}	3.005	9.04×10^{-3}	3.015	9.08×10^{-3}	3.024	7.00×10^{-3}	3.021
7.05×10^{-3}	3.011	1.10×10^{-2}	3.019	1.10×10^{-2}	3.025	9.00×10^{-3}	3.026
9.07×10^{-3}	3.017						
1.10×10^{-2}	3.019						

Appendix F: Density and apparent molar volume data

Table F-I: Density and apparent molar volume data for the aqueous gemini surfactant systems[†]

molality (mol kg^{-1})	d[a] (g cm^{-3})	V_ϕ (cm^3 mol^{-1})	molality (mol kg^{-1})	d[a] (g cm^{-3})	V_ϕ (cm^3 mol^{-1})
	8-3-8			10-3-10	
1.247×10^{-2} [b]	0.997212	436.0 ± 0.2	2.0160×10^{-3}	0.997233	496.29 ± 1.99
1.514×10^{-2} [b]	0.998286	436.1	2.9825×10^{-3}	0.997294	501.23
5.399×10^{-2} [b]	1.001300	436.7	3.9830×10^{-3}	0.997364	501.94
7.059×10^{-2} [b]	1.003130	438.6	5.0487×10^{-3}	0.997439	502.33
7.922×10^{-2} [b]	1.003202	439.6	6.0419×10^{-3}	0.997509	502.49
1.6280×10^{-1} [b]	1.008359	443.1	7.0477×10^{-3}	0.997581	502.53
2.0727×10^{-1} [b]	1.011053	443.8 ± 0.01	9.0712×10^{-3}	0.997693	506.11
5.7640×10^{-2}	1.001538	438.37 ± 0.07	1.1050×10^{-2}	0.997809	507.71
9.9331×10^{-2}	1.004370	440.69	1.5091×10^{-2}	0.998047	509.62
1.5712×10^{-1}	1.007991	442.56 ± 0.03	2.0185×10^{-2}	0.998329	511.70
			2.5342×10^{-2}	0.998629	512.33
			3.0017×10^{-2}	0.998925	511.82 ± 0.14
	12-2-12			12-3-12	
9.9514×10^{-4}	0.997145	546.16 ± 4.03	5.800×10^{-4} [c]		569.1 ± 1.8
9.9514×10^{-4}	0.997145	546.64	7.660×10^{-4} [c]		567.9 ± 1.5
9.9898×10^{-4}	0.997145	546.91	9.1485×10^{-4}	0.997133	567.61 ± 4.93
9.9898×10^{-4}	0.997145	546.91	9.1485×10^{-4}	0.997132	568.13
1.4998×10^{-3}	0.997174	550.76	9.4877×10^{-4}	0.997136	566.85
1.4998×10^{-3}	0.997173	551.07	9.4877×10^{-4}	0.997135	567.85
1.9677×10^{-3}	0.997199	553.54	1.0191×10^{-3}	0.997138	568.91
2.9739×10^{-3}	0.997254	556.38	1.0191×10^{-3}	0.997139	567.51
3.9667×10^{-3}	0.997307	558.04	1.5152×10^{-3}	0.997165	571.17
4.9391×10^{-3}	0.997365	557.82	3.0110×10^{-3}	0.997242	575.16
9.8829×10^{-3}	0.997639	559.40 ± 0.41	5.0669×10^{-3}	0.997344	577.53
			7.0838×10^{-3}	0.997448	577.86
			8.9558×10^{-3}	0.997540	578.57
			1.0096×10^{-2}	0.997599	578.61 ± 0.40

[a] $d_0 = 0.997047$ g cm^{-3}

[b] data from reference 134

[c] from dilatometer method

[†] low concentration volume data should correctly be reported only to 3 significant figures; however, 5 have been reported for consistency in the data tables.

Table F-I(con't): Density and apparent molar volume data for the aqueous gemini surfactant systems

molality (mol kg^{-1})	d[a] (g cm^{-3})	V_ϕ (cm^3 mol^{-1})	molality (mol kg^{-1})	d[a] (g cm^{-3})	V_ϕ (cm^3 mol^{-1})
	12-4-12			12-6-12	
1.0175×10^{-3}	0.997136	584.74 ± 3.95	5.790×10^{-4} [c]		618.9 ± 1.8
1.0175×10^{-3}	0.997136	584.74	7.590×10^{-4} [c]		618.4 ± 1.4
1.0663×10^{-3}	0.997139	584.35	9.8145×10^{-4}	0.997128	618.44 ± 4.09
1.0663×10^{-3}	0.997139	584.35	9.8145×10^{-4}	0.997127	619.89
1.5223×10^{-3}	0.997163	587.06	1.0237×10^{-3}	0.997130	618.81
1.5223×10^{-3}	0.997160	588.63	1.0237×10^{-3}	0.997130	619.28
2.0146×10^{-3}	0.997187	589.29	1.5371×10^{-3}	0.997154	621.64
3.0538×10^{-3}	0.997236	592.02	2.0204×10^{-3}	0.997174	623.95
5.0551×10^{-3}	0.997327	594.86	3.0540×10^{-3}	0.997216	626.71
6.9706×10^{-3}	0.997415	595.87	5.0739×10^{-3}	0.997299	628.72
8.8193×10^{-3}	0.997502	596.22	9.1493×10^{-3}	0.997468	629.79
1.0121×10^{-2}	0.997569	595.78 ± 0.40	1.0104×10^{-2}	0.997514	629.27 ± 0.40
	12-8-12			12-10-12	
1.0421×10^{-3}	0.997125	652.93 ± 3.85	1.0116×10^{-3}	0.997117	687.62 ± 3.97
1.0421×10^{-3}	0.997124	653.84	1.0116×10^{-3}	0.997116	688.56
1.5433×10^{-3}	0.997140	658.62	9.8827×10^{-4}	0.997114	689.53
1.5433×10^{-3}	0.997140	658.92	9.8827×10^{-4}	0.997115	688.09
2.0654×10^{-3}	0.997160	659.83	1.5030×10^{-3}	0.997132	691.33
3.1065×10^{-3}	0.997197	661.60	1.5030×10^{-3}	0.997131	691.96
5.0465×10^{-3}	0.997273	661.72	2.0279×10^{-3}	0.997149	692.62
7.1495×10^{-3}	0.997349	662.63	2.0279×10^{-3}	0.997154	690.27
9.1265×10^{-3}	0.997419	663.11	3.0234×10^{-3}	0.997182	693.87
1.0288×10^{-2}	0.997467	662.73 ± 0.39	5.0418×10^{-3}	0.997239	696.45
			7.0565×10^{-3}	0.997308	695.96
			9.0738×10^{-3}	0.997370	696.52 ± 0.40
			1.0003×10^{-2}	0.997397	696.78

Table F-I(con't): Density and apparent molar volume data for the aqueous gemini surfactant systems

molality (mol kg^{-1})	d^a (g cm^{-3})	V_ϕ (cm^3 mol^{-1})	molality (mol kg^{-1})	d^a (g cm^{-3})	V_ϕ (cm^3 mol^{-1})
	12-12-12			12-6-12	
4.236×10^{-3}	0.997204	726.75 ± 0.95	1.0131×10^{-3}	0.997110	779.15 ± 3.96
5.982×10^{-3}	0.997252	727.61	1.0131×10^{-3}	0.997111	777.74
8.061×10^{-3}	0.997300	729.26	1.0131×10^{-3}	0.997113	776.33
1.027×10^{-2}	0.997365	728.87	1.5021×10^{-3}	0.997122	782.07
1.551×10^{-2}	0.997513	728.76	1.5021×10^{-3}	0.997121	783.02
2.090×10^{-2}	0.997662	728.78 ± 0.19	1.5021×10^{-3}	0.997122	782.07
			1.9955×10^{-3}	0.997132	784.80
	12-ϕ-12		1.9955×10^{-3}	0.997130	785.76
4.98E-04	0.997109	623	1.9955×10^{-3}	0.997133	784.56
4.98E-04	0.997108	626	2.5248×10^{-3}	0.997142	786.84
4.98E-04	0.997106	630	2.9957×10^{-3}	0.997152	787.83
4.98E-04	0.997107	627	3.4955×10^{-3}	0.997150	792.03
			4.0003×10^{-3}	0.997157	792.93
			5.0874×10^{-3}	0.997172	794.30± 0.79

Table F-II: Density, apparent molar volume, and transfer volume data for the 12-3-12 gemini surfactant in aqueous polymer solutions[†]

molality (mol kg^{-1})	d (g cm^{-3})	V_ϕ^a	ΔV_ϕ^a	molality (mol kg^{-1})	d (g cm^{-3})	V_ϕ^a	ΔV_ϕ^a
0.2% PEO; d_0 = 0.997404				0.2% PPO (M.W. 725); d_0 = 0.997243			
0.0039770	0.997619	576.45		0.0019885	0.997346	579.16	5.6
0.0059796	0.997716	578.15		0.0039952	0.997445	580.04	3.4
0.0079680	0.997818	578.32		0.0059891	0.997538	581.38	3.7
0.0099445	0.997905	579.84		0.0079836	0.997637	581.12	2.9
				0.0099348	0.997727	581.74	3.3
0.05% PPO (M.W. 2000); d_0 = 0.997112				0.05% P103; d_0 = 0.997134			
0.0019974	0.997211	581.40	7.8	0.0019915	0.997239	578.36	4.8
0.0040101	0.997308	581.87	5.2	0.0039925	0.997338	579.73	3.1
0.0059654	0.997400	582.32	4.7	0.0059591	0.997433	580.41	2.7
0.0079935	0.997496	582.54	4.4	0.0079609	0.997534	580.34	2.2
0.0099245	0.997583	583.09	4.6	0.0099649	0.997630	580.76	2.3
0.1% P103; d_0 = 0.997207				0.5% P103; d_0 = 0.997600			
0.0020212	0.997696	582.80	9.4	0.0020322	0.997688	586.81	13.1
0.0029746	0.997744	581.78	6.4	0.0031122	0.997747	583.15	7.4
0.0040261	0.997794	582.07	5.7	0.0040656	0.997788	584.06	7.4
0.0050485	0.997842	582.33	5.3	0.0060204	0.997880	583.76	6.1
0.0070700	0.997940	582.17	4.5	0.0071420	0.997933	583.59	5.6
0.0090510	0.998037	581.84	3.8	0.0091750	0.998026	583.74	5.4
0.011138	0.998140	581.63	3.3	0.011226	0.998120	583.80	5.2
2.0% P103; d_0 = 0.998816				0.05% F108; d_0 = 0.997147			
0.0030152	0.998891	604.71	29.0	0.0020230	0.997257	576.10	2.4
0.0039431	0.998935	599.35	22.7	0.0039841	0.997355	578.42	1.8
0.0049792	0.998984	595.60	18.3	0.0059804	0.997453	579.38	1.7
0.0060442	0.999035	593.21	15.5	0.0079346	0.997551	579.56	1.4
0.0081910	0.999143	589.43	11.2	0.0099370	0.997652	579.65	1.2
0.0099189	0.999224	588.13	9.7				
0.5% F108; d_0 = 0.997870				1.0% F108; d_0 = 0.998763			
0.0021030	0.997962	586.04	12.1	0.0019776	0.998837	592.27	18.8
0.0029759	0.998010	583.04	7.4	0.0030122	0.998871	593.60	18.0
0.0039856	0.998055	583.66	7.0	0.0039869	0.998910	592.76	16.2
0.0061001	0.998156	583.07	5.4	0.0050435	0.998968	588.84	11.6
0.0070334	0.998201	582.88	4.9	0.0071019	0.999059	587.82	9.9
0.0091005	0.998303	582.37	4.0	0.0090588	0.999151	586.49	8.2
0.011129	0.998397	582.56	4.0	0.011129	0.999248	585.71	7.2

[†] low concentration volume data should correctly be reported only to 3 significant figures; however, 5 have been reported for consistency in the data tables.

Table F-II(con't): Density, apparent molar volume, and transfer volume data for the 12-3-12 gemini surfactant in aqueous polymer solutions

molality (mol kg^{-1})	d ($g\ cm^{-3}$)	V_ϕ[a]	ΔV_ϕ[a]	molality (mol kg^{-1})	d ($g\ cm^{-3}$)	V_ϕ[a]	ΔV_ϕ[a]
2.0% F108; d_0 = 1.000147				0.05% F68; d_0 = 0.997151			
0.0029968	1.000233	599.81	24.2	0.0019955	0.997261	575.35	1.7
0.0041159	1.000270	598.77	22.0	0.0039774	0.997358	578.45	1.8
0.0059921	1.000352	594.29	16.6	0.0059633	0.997456	579.39	1.7
0.0078189	1.000435	591.63	13.5	0.0079402	0.997559	579.11	0.9
0.0099079	1.000518	590.93	12.5	0.0099213	0.997655	579.61	1.1
2.0% F68; d_0 = 1.000106							
0.0029340	1.000219	590.09	14.5				
0.0032281	1.000236	588.22	12.3				
0.0039802	1.000268	587.89	11.3				
0.0050922	1.000317	587.14	9.8				
0.0076380	1.000425	586.63	9.4				
0.010000	1.000532	585.80	8.0				

[a] units of $cm^3\ mol^{-1}$

Table F-III: Density, apparent molar volume, and transfer volume data for the 12-6-12 gemini surfactant in aqueous polymer solutions

molality (mol kg^{-1})	d ($g\ cm^{-3}$)	V_ϕ[a]	ΔV_ϕ[a]	molality (mol kg^{-1})	d ($g\ cm^{-3}$)	V_ϕ[a]	ΔV_ϕ[a]
0.2% PEO; d_0 = 0.997403				0.2% PPO (M.W. 725); d_0 = 0.997258			
0.0019881	0.997499	624.10		0.0019943	0.997352	625.80	1.1
0.0039850	0.997584	627.13		0.0039886	0.997429	629.92	1.9
0.0059728	0.997664	628.83		0.0060542	0.997517	629.93	0.8
0.0079122	0.997748	628.91		0.0079605	0.997591	630.73	1.1
0.0099328	0.997831	629.39		0.0099285	0.997673	630.73	0.8
0.05% PPO (M.W. 2000); d_0 = 0.997122				0.05% P103; d_0 = 0.997136			
0.0020402	0.997215	627.19	2.3	0.0020013	0.997217	632.25	7.5
0.0039921	0.997297	628.87	0.9	0.0039907	0.997305	630.39	2.4
0.0060318	0.997381	629.79	0.7	0.0059680	0.997388	630.61	1.5
0.0078891	0.997454	630.64	1.0	0.0079440	0.997467	631.10	1.5
0.0099465	0.997543	630.33	0.4	0.0099332	0.997560	629.98	0.0
0.1% P103; d_0 = 0.997190				0.5% P103; d_0 = 0.997596			
0.0020695	0.997275	632.16	7.2	0.0019927	0.997661	639.86	15.2
0.0030181	0.997306	634.45	7.5	0.0030332	0.997705	636.54	9.6
0.0040659	0.997354	632.66	4.6	0.0040389	0.997741	636.46	8.4
0.0050081	0.997384	634.06	5.4	0.0050274	0.997776	636.67	8.0
0.0070756	0.997470	633.14	3.7	0.0070985	0.997856	635.80	6.3
0.0091277	0.997550	633.28	3.4	0.0090056	0.997929	635.31	5.5
0.0111073	0.997632	632.83	2.7	0.0111431	0.998016	634.63	4.5

Table F-III(con't): Density, apparent molar volume, and transfer volume data for the 12-6-12 gemini surfactant in aqueous polymer solutions

molality (mol kg^{-1})	d (g cm^{-3})	V_ϕ[a]	ΔV_ϕ[a]	molality (mol kg^{-1})	d (g cm^{-3})	V_ϕ[a]	ΔV_ϕ[a]
2.0% P103; d_0 = 0.998954				0.05% F108; d_0 = 0.997139			
0.0020393	0.998953	671.69	46.8	0.0020259	0.997236	625.21	0.4
0.0030684	0.998971	665.70	38.7	0.0039890	0.997315	628.70	0.7
0.0040881	0.999018	655.78	27.7	0.0059743	0.997395	629.93	0.8
0.0051609	0.999048	653.19	24.4	0.0079615	0.997483	629.50	-0.2
0.0072195	0.999143	645.22	15.7	0.0099175	0.997568	629.38	-0.6
0.0092964	0.999215	643.31	13.4				
0.011378	0.999312	639.84	9.7				
0.5% F108; d_0 = 0.997829				1.0% F108; d_0 = 0.998515			
0.0020574	0.997905	635.61	10.7	0.0020102	0.998573	642.80	18.0
0.0030969	0.997943	635.40	8.3	0.0029876	0.998604	641.87	15.0
0.0041088	0.997985	634.46	6.4	0.0040631	0.998643	640.11	12.0
0.0051513	0.998026	634.10	5.3	0.0050626	0.998683	638.59	9.9
0.0071300	0.998108	633.09	3.6	0.0070842	0.998763	636.73	7.3
0.0092832	0.998194	632.83	2.9	0.0090592	0.998836	636.17	6.3
0.011364	0.998279	632.56	2.4	0.011136	0.998926	634.65	4.5
2.0% F108; d_0 = 1.000152				0.05% F68; d_0 = 0.997158			
0.0020763	1.000184	655.22	30.2	0.0020419	0.997254	625.80	0.9
0.0031155	1.000207	653.14	26.1	0.0040001	0.997339	627.49	-0.5
0.0041782	1.000237	650.47	22.3	0.0059771	0.997425	628.17	-0.9
0.0052464	1.000269	648.35	19.6	0.0079465	0.997507	628.86	-0.8
0.0073187	1.000347	643.93	14.4	0.0099172	0.997589	629.22	-0.8
0.0094068	1.000419	642.16	12.3				
0.011475	1.000499	640.20	10.0				
2.0% F68; d_0 = 1.000114							
0.0020441	1.000189	634.13	9.3				
0.0030406	1.000218	636.57	9.6				
0.0040423	1.000247	637.89	9.8				
0.0049866	1.000281	637.15	8.5				
0.0069708	1.000360	635.36	5.9				
0.0089613	1.000433	634.89	5.1				
0.010975	1.000511	634.30	4.2				

[a] units of cm^3 mol^{-1}

Table F-IV: Density and apparent molar volume data for the 12-3-12 gemini surfactant in aqueous polymer solutions at various temperatures

Temp (°C)	d ($g\ cm^{-3}$)	d ($g\ cm^{-3}$)	V_ϕ^a	Temp (°C)	d ($g\ cm^{-3}$)	d ($g\ cm^{-3}$)	V_ϕ^a
0.005088 mol kg^{-1}/2.0% P103				0.005000 mol kg^{-1}/2.0% F108			
10.0	1.002385	1.002606	583.84	10.0	1.002903	1.003150	577.63
15.0	1.001679	1.001861	592.30	15.0	1.002206	1.002426	583.43
20.0	1.000662	1.000718	617.17	20.0	1.001226	1.001416	589.87
25.0	0.998943	0.999108	596.77	25.0	0.999999	1.000163	595.79
30.0	0.997217	0.997494	580.24	30.0	0.998491	0.998661	595.44
35.0	0.995480	0.995743	579.19	35.0	0.996718	0.996957	582.53
40.0	0.993574	0.993824	582.76	40.0	0.994795	0.995057	579.00
45.0	0.991499	0.991757	582.33	45.0	0.992708	0.992985	577.00
0.01013 mol kg^{-1}/2.0% P103				0.01013 mol kg^{-1}/2.0% F108			
10.0	1.002297	1.002749	582.63	10.0	1.002984	1.003532	572.77
15.0	1.001611	1.001991	590.08	15.0	1.002292	1.002790	577.99
20.0	1.000594	1.000807	607.24	20.0	1.001312	1.001769	582.66
25.0	0.998882	0.999285	589.23	25.0	1.000081	1.000506	586.38
30.0	0.997180	0.997701	578.54	30.0	0.998583	0.999008	587.36
35.0	0.995433	0.995952	579.59	35.0	0.996797	0.997296	580.87
40.0	0.993523	0.994025	582.32	40.0	0.994874	0.995397	579.49
45.0	0.991460	0.991946	585.04	45.0	0.992813	0.993334	580.71
				50.0	0.990559	0.991085	581.51
0.02004 mol kg^{-1}/2.0% P103				0.01999 mol kg^{-1}/2.0% F108			
10.0	1.002372	1.003280	581.61	10.0	1.002903	1.003880	577.74
15.0	1.001681	1.002465	588.22	15.0	1.002206	1.003120	581.26
20.0	1.000661	1.001248	598.67	20.0	1.001226	1.002090	584.34
25.0	0.998937	0.999806	585.42	25.0	0.999999	1.000831	586.62
30.0	0.997217	0.998206	580.24	30.0	0.998491	0.999308	588.16
35.0	0.995470	0.996449	581.71	35.0	0.996718	0.997591	586.31
40.0	0.993577	0.994524	584.38	40.0	0.994795	0.995691	586.19
45.0	0.991502	0.992444	585.75	45.0	0.992708	0.993604	587.34

Table F-IV(con't): Density and apparent molar volume data for the 12-3-12 gemini surfactant in aqueous polymer solutions at various temperatures.

Temp (°C)	d (g cm^{-3})	d (g cm^{-3})	V_ϕ[a]	Temp (°C)	d (g cm^{-3})	d (g cm^{-3})	V_ϕ[a]
	0.004998 mol kg^{-1}/2.0% F68						
10.0	1.002385	1.003227	573.74				
15.0	1.001679	1.002524	578.29				
20.0	1.000662	1.001539	582.23				
25.0	0.998943	1.000273	587.19				
30.0	0.997217	0.998760	597.77				
35.0	0.995480	0.997059	602.62				
40.0	0.993574	0.995159	606.27				
45.0	0.991499	0.993093	610.13				
50.0		0.990867	611.09				
	0.009989 mol kg^{-1}/2.0% F68				0.01012 mol kg^{-1}/Aqueous		
10.0	1.002297	1.003499	572.97	10.0	0.999700	1.000273	571.95
15.0	1.001611	1.002774	577.68	15.0	0.999100	0.999660	573.58
20.0	1.000594	1.001779	580.86	20.0	0.998204	0.998741	576.32
25.0	0.998882	1.000499	585.07	25.0	0.997047	0.997567	578.58
30.0	0.997180	0.999011	588.29	30.0	0.995648	0.996153	580.88
35.0	0.995433	0.997304	591.79	35.0	0.994032	0.994523	583.12
40.0	0.993523	0.995395	595.31	40.0	0.992215	0.992699	584.75
45.0	0.991460	0.993325	598.00	45.0	0.990212	0.990688	586.68
50.0		0.991084	600.49	50.0	0.988033	0.988496	589.15
	0.01999 mol kg^{-1}/2.0% F68						
10.0	1.002960	1.004013	573.93				
15.0	1.002279	1.003274	577.16				
20.0	1.001311	1.002256	580.21				
25.0	1.000066	1.000953	583.78				
30.0	0.998602	0.999449	586.57				
35.0	0.996921	0.997726	589.62				
40.0	0.995033	0.995807	592.31				
45.0	0.992980	0.993730	594.69				
50.0	0.990752	0.991489	596.58				

Appendix G: Equilibrium dialysis data

Table G-1: Equilibrium surfactant concentrations(in mmol L^{-1}) and binding ratios(y) for the 12-3-12 gemini surfactant in aqueous Pluronic solutions

C_i	C_{eq}[a] dialysate	C_{eq}[a] retentate	y	C_i	C_{eq}[a] dialysate	C_{eq}[a] retentate	y
	0.05% F108				0.5% F108		
0.303	0.136	0.16	0.10	0.303	0.150	0.163	0.01
0.607	0.280	0.309	0.10	0.607	0.259	0.353	0.04
0.910	0.436	0.467	0.07	0.910	0.386	0.557	0.07
1.21	0.573	0.646	0.27	1.21	0.456	0.777	0.12
1.52	0.721	0.872	0.63	1.52	0.525	1.00	0.17
1.82	1.01	0.954	-0.65	1.82	0.633	1.37	0.25
2.12	1.22	0.975	-2.37	2.12	0.759	1.45	0.25
				2.43	0.956	1.47	0.21
	0.05% P103				0.1% P103		
0.303	0.141	0.163	0.09	0.607	0.224	0.297	0.17
0.607	0.271	0.349	0.33	0.91	0.36	0.526	0.36
0.91	0.391	0.556	0.67	1.21	0.446	0.723	0.55
1.01	0.419	0.569	0.62	1.52	0.537	0.928	0.75
1.21	0.508	0.73	0.90	1.82	0.663	1.19	0.98
1.21	0.523	0.749	0.92	2.12	0.814	1.34	1.04
1.42	0.586	0.849	1.07	2.43	0.942	1.51	1.14
1.62	0.637	0.981	1.35	2.73	1.29	1.55	0.66
1.82	0.722	1.08	1.43	3.03	1.51	1.55	0.12
2.12	1.05	1.2	0.58				
	0.5% P103				12-8-12/0.05% P103		
0.303	0.117	0.189	0.03	0.193	0.087	0.097	0.04
0.607	0.199	0.388	0.07	0.385	0.178	0.214	0.15
0.91	0.279	0.636	0.12	0.771	0.374	0.430	0.22
1.21	0.377	0.882	0.16	0.930	0.450	0.552	0.43
1.52	0.466	1.04	0.19	1.16	0.520	0.678	0.66
1.82	0.560	1.31	0.24	1.35	0.590	0.796	0.86
2.12	0.767	1.41	0.24	1.35	0.660	0.830	0.72
2.43	0.992	1.51	0.22	1.54	0.688	0.856	0.71
3.03	1.460	1.46	0.00	1.54	0.747	0.843	0.36

[a] dialysate refers to the side of the dialysis chamber which does not contain polymer, retentate to the side containing polymer.